CYLINDRICAL AERIAL

RADIATION AND PROPAGATION

Thesis submitted by J.D. Cummins B.E.(Elect.) with Honours, M.Sc. (Hons.), Grad. I.E.E., University Research Scholar 1952-3 and holder of the Christchurch City Council Research Scholarship in Electrical Engineering 1954, for the degree of Doctor of Philosophy in the University of New Zealand, at Canterbury University College, Christchurch.

ACKNOWLEDGEMENTS

The author wishes to thank the University of New Zealand and the Christchurch City Council for making this work financially possible and all those members of the staff of the National School of Engineering and other Departments of Canterbury University College, Christchurch, who gave him assistance in any way during 1952-54. Especial thanks are due to the Supervisors, Professor N.M. MacElwee and Mr. B.T. Withers for their encouragement, to Mr. W.R. Andress of the Mathematics Department and Mr. N.L. Calhaem of the Electrical Engineering Department for their assistance with theoretical aspects of the subject and to the late Mr. F.M. Mantell and Mr. E.H. Martinson, Electronics Laboratory Technicians, for their assistance with equipment and experiments.

J.D. Cummins,

January, 1955.

I N D E X

SECTION 1.

INTRODUCTION.

The purpose of this thesis is to investigate the behaviour of cylindrical dipole aerials using theoretical and experimental techniques.

The important properties of a transmitting aerial which require a solution are

(i) The signal strength at a given distance for a known amount of radiated power.

(ii) The shape of the radiation pattern.

(iii) The input impedance of the aerial, so that the aerial may be matched to the source of power and thus ensure that the radiated power is a maximum.

(iv) The input impedance - frequency characteristic of the aerial, so that the performance of the aerial for broad-band communications such as television may be evaluated.

These four properties are dependent on the current distribution along the aerial. If the current distribution is known the above four properties may be evaluated. The current distribution is partially dependent on the physical arrangement and size of the conductors forming the aerial. It follows that a study of the physical arrangement and size of the elements forming the aerial will give a knowledge of the current distribution and hence the field strength and impedance properties of the aerial may be determined.

The studies presented here arose out of investigations into the behaviour of a Television Aerial at Canterbury University College, Christchurch. The carrier frequency of this aerial is 95.5 Mcps. with a composite video signal of 8 Mcps. It was decided to study wide band cylindrical dipole aerials with the television aerial as a basis for investigation.

The length of a dipole aerial for a frequency of 95.5 Mcps. is approximately 5 feet. This length imposes a large cost if a considerable number of aerials are to be tested. The possibility of using 1/5th scale models was investigated and found to be satisfactory. The possibility of constructing a model of a given electro-magnetic system arises from the linearity of Maxwell's Field Equations which describe the fields in any electromagnetic system. Provided no non-linear media or elements are used it is possible to make relative measurements and also absolute measurements by choice of scale ratios. A comparison of Maxwell's Equations for both the model and prototype systems by dimensional analysis yields the following results.[1,2]

Name of Quantity	Full Scale System	Model System
Length	ℓ	$\ell' = \frac{\ell}{p}$
Time	t	$t' = \frac{t}{p}$
Conductivity	g	$g' = pg$
Dielectric Constant	ϵ	$\epsilon' = \epsilon$
Permeability	μ	$\mu' = \mu$
Frequency	f	$f' = pf$
Impedance	Z	$Z' = Z$
Aerial Gain	G	$G' = G$

where p is the ratio of any full scale length to any corresponding model length.

If copper is used for both the model and prototype aerials the quantities g and g' are large and tend to infinity. Under these conditions the relationship $g' = pg$ is approximately true for all values of p. Hence it follows that if the physical dimensions are decreased by the scale ratio and the frequency increased by the scale ratio, the results obtained for a copper model aerial will be valid for a full scale aerial.

On the basis of the above considerations, tests were carried out over the range of frequencies i.e. 450-500 Mcps.,

for cylindrical dipole aerials. The experiments simulate a 1/5th scale model of a dipole aerial with a carrier frequency of 95.5 Mcps. and a composite video frequency 8 Mcps. wide.

The method of investigation adopted here is to treat the cylindrical aerial under the following headings.

(i) Hypothesis

(ii) Theory

(iii) Experiment and Equipment

(iv) Discussion

(v) Conclusion.

Headings (i) and (ii) are treated in Section 2, (iii) in Sections 3 and 4 and (iv) and (v) in Section 5.

The following paragraph gives a brief survey of the subjects covered in each of the following sections.

In Section 2 the cylindrical dipole aerial is treated theoretically. The results of calculations from the theoretical analyses together with the relevant graphs are also given. In Section 3 the design of equipment required for carrying out impedance and field strength experiments on cylindrical aerials is given. In Section 4 the input impedance and free space polar diagram measurements are given. The methods of measurement together with the experiments and results of these measurements are also presented. In Section 5, the theoretical and experimental results are discussed and compared. Also the effect of the physical arrangement of the aerial elements, the earth and a frequency variation on the aerials' properties are discussed. Conclusions based on these discussions are also presented.

In general each section covers the topics given in the above paragraph. In some cases parts of one section may appear in another section for reasons of continuity.

SECTION 2.

THEORY

(a) RADIATION FORMULAE[3,4,5]

In order to obtain a complete understanding of radiation phenomena, the basic equations of electromagnetic theory are required. For this reason several well known laws and expressions derived from these laws are developed in the following subsections.

(1) A Vector.

A vector is a quantity which is completely defined once its direction and magnitude are known. In cartesian co-ordinates (x,y,z) with unit vectors i,j,K in the directions x,y,z a vector $\underline{A}$ is defined by

$$\underline{A} = \underline{i}A_x + \underline{j}A_y + \underline{K}A_z$$

(2) The Product Operations of Vectors.

Definitions:

(i) The Dot Product of Two Vectors $\underline{a}$ and $\underline{b}$

$$\underline{a}.\underline{b} = |a||b| \cos \hat{ab}$$

(ii) The Vector Product of Two Vectors $\underline{a}$ and $\underline{b}$

$$\underline{a}_\wedge \underline{b} = |a||b| \sin \hat{ab}\ \underline{n}$$

where $\underline{n}$ is a unit vector perpendicular to the plane of the vectors $\underline{a}$ and $\underline{b}$.

(iii) The Scalar Triple Product of Three Vectors $\underline{a}, \underline{b}$ and $\underline{c}$.

$$\underline{a}.\underline{b}_\wedge\underline{c} = \begin{vmatrix} a_x & a_y & a_z \\ b_x & b_y & b_z \\ c_x & c_y & c_z \end{vmatrix}$$

(iv) The Vector Triple Product of Three Vectors $\underline{a}, \underline{b}$ and $\underline{c}$.

$$\underline{a}_\wedge(\underline{b}_\wedge\underline{c}) = \underline{a}.\underline{c}\,\underline{b} - \underline{a}.\underline{b}\,\underline{c}$$

(3) The Operator ∇ (Del).

The operator ∇ is defined as the following fictitious vector

$$\nabla = i\frac{\partial}{\partial x} + j\frac{\partial}{\partial y} + K\frac{\partial}{\partial z}$$

(4) **The Gradient.**

The gradient of a scalar function is the maximum space rate of change of that function and consequently is a vector. If V is a scalar function of position then in cartesian co-ordinates

$$grad V = i\frac{\partial V}{\partial x} + j\frac{\partial V}{\partial y} + k\frac{\partial V}{\partial z}$$

This function is a function of position

Now $$\nabla V = \left(i\frac{\partial}{\partial x} + j\frac{\partial}{\partial y} + k\frac{\partial}{\partial z}\right)V$$

$$= grad\, V$$

$$\therefore grad \equiv \nabla$$

(5) **The Divergence.**

The notion of the divergence of a vector arises from considering the excess of outward normal flux per unit volume as shown in the accompanying diagram of a small element of volume.

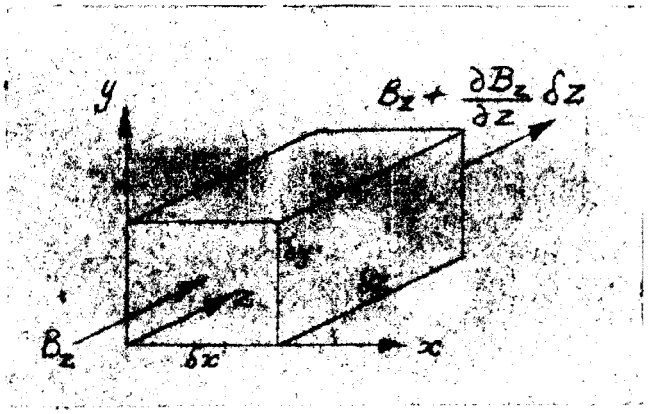

The excess of outward flux over inward flux in the Z direction.

$$= \left\{B_z + \frac{\partial B_z}{\partial z}\delta z - B_z\right\}\delta x\,\delta y = \frac{\partial B_z}{\partial z}\delta x\,\delta y\,\delta z$$

It follows that the total outward flux per unit volume

$$= \frac{\partial B_x}{\partial x} + \frac{\partial B_y}{\partial y} + \frac{\partial B_z}{\partial z}.$$

This quantity is defined as the divergence of a vector

$$div B = \frac{\partial B_x}{\partial x} + \frac{\partial B_y}{\partial y} + \frac{\partial B_z}{\partial z}$$

Also $$\nabla . B = \left(i\frac{\partial}{\partial x} + j\frac{\partial}{\partial y} + k\frac{\partial}{\partial z}\right)\cdot\left(iB_x + jB_y + kB_z\right)$$

$$= \frac{\partial B_x}{\partial x} + \frac{\partial B_y}{\partial y} + \frac{\partial B_z}{\partial z} = div B$$

$$\therefore div \equiv \nabla.$$

(6) <u>The Curl</u>.

The curl of a vector function is a vector which has the magnitude of a line integral per unit area, the orientation of the surface being such as to make this magnitude a maximum. The direction of this vector is given by a normal to the surface, where the sense is given by the right hand screw rule.

To find the curl of a vector H consider the x-component of the line integral as given by the accompanying diagram.

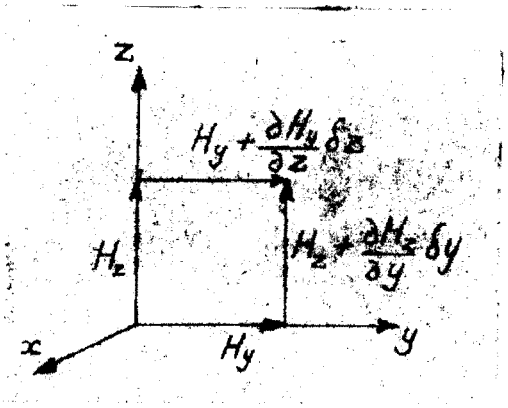

The x component of the line integral

$$= \left\{H_y - \left(H_y + \frac{\partial H_y}{\partial z}\delta z\right)\right\}\delta y - \left\{H_z - \left(H_z + \frac{\partial H_z}{\partial y}\delta y\right)\right\}\delta z$$

$$= \left\{\frac{\partial H_z}{\partial y} - \frac{\partial H_y}{\partial z}\right\}\delta y\,\delta z$$

The line integral per unit area in the x direction gives the x component of the curl

$$curl_x H = \left(\frac{\partial H_z}{\partial y} - \frac{\partial H_y}{\partial z}\right)i$$

$$\therefore curl\, H = \left(\frac{\partial H_z}{\partial y} - \frac{\partial H_y}{\partial z}\right)i + \left(\frac{\partial H_x}{\partial z} - \frac{\partial H_z}{\partial x}\right)j + \left(\frac{\partial H_y}{\partial x} - \frac{\partial H_x}{\partial y}\right)K$$

$$\because \nabla_\wedge H = \left(i\frac{\partial}{\partial x} + j\frac{\partial}{\partial y} + K\frac{\partial}{\partial z}\right)_\wedge \left(iH_x + jH_y + KH_z\right)$$

$$= \left(\frac{\partial H_z}{\partial y} - \frac{\partial H_y}{\partial z}\right)i + \left(\frac{\partial H_x}{\partial z} - \frac{\partial H_z}{\partial x}\right)j + \left(\frac{\partial H_y}{\partial x} - \frac{\partial H_x}{\partial y}\right)K$$

$$\therefore \nabla_\wedge H = curl\, H$$

$$\therefore curl \equiv \nabla_\wedge$$

(7) The Vector Operations.

There are nine possible double combinations of grad, div and curl of which four are inadmissable. These operations are gradient of a vector quantity H and the divergence or curl of a scalar quantity V. The five possible double combinations on reduction give the following formulae.

$$\text{div grad } V = \nabla.\nabla V = \nabla^2 V$$
$$\text{curl grad } V = \nabla_\wedge \nabla V = 0$$
$$\text{grad div } H = \nabla \nabla.H$$
$$\text{div curl } H = \nabla.\nabla_\wedge H = 0$$
$$\text{curl curl } H = \nabla_\wedge \nabla_\wedge H = \nabla \nabla.H - \nabla^2 H$$

The operator ∇^2 is known as Laplace's Operator

$$\nabla^2 = \nabla.\nabla = \frac{\partial^2}{\partial x^2} + \frac{\partial^2}{\partial y^2} + \frac{\partial^2}{\partial z^2}$$

and is fundamental to all wave motion phenomena.

The forms given below of general relations between scalar functions V and vector functions H and E are useful in all vector applications.

$$\text{div } (V\underline{H}) = \underline{H}.\text{grad}V + V\text{div}\underline{H}$$
$$\text{curl } (V\underline{H}) = \underline{H}_\wedge \text{grad}V + V\text{curl}\underline{H}$$
$$\text{div } (\underline{E}_\wedge \underline{H}) = \underline{H}.\text{curl}\underline{E} - \underline{E}.\text{curl}\underline{H}$$

(8) The Theorems of Gauss, Stoke and Green.

The theorems outlined below enable transformations between line, surface and volume integrals to be made for continuous functions of position which possess a derivative.

(1) Gauss' Theorem.

The derivation follows readily from the definition of a vector quantity. Consider a small element of area δa. Then for a vector field $\underline{H}$ the total contribution of the normal component of the vector over the total area is

$$\int_A \underline{n}.\underline{H}\,\delta a$$

where $\underline{n}$ is the unit vector perpendicular to the surface at any point. Again the divergence of the vector $\underline{H}$ is defined as the normal component divided by the element of volume $\delta\tau$.

Hence for a volume V enclosed by a surface area A

$$\int_V div\underline{H}\, dv = \int_A \underline{n}.\underline{H}\, da$$

The above expression is Gauss' Theorem and gives the transformation between volume and surface integrals.

(ii) Stoke's Theorem.

Consider a small element of area δa. Then the line integral round such an element of area is equal to the curl of the vector field at that point resolved in the direction of the normal. The sum of all the line integrals round each element of area gives the line integral of the surrounding boundary L since internal contributions are cancelled. Hence

$$\int_A \underline{n}.curl\underline{H}\, da = \int_L \underline{H}.d\underline{l}$$

This expression is Stoke's Theorem and enables transformations between line and area integrals to be carried out.

(iii) Green's Theorem.

Apply Gauss' Theorem to a vector which is the product of a scalar V and the gradient of a scalar grad U.

$$\int_V div\,(V\,grad U)dv = \int_A n.(V\,grad U)\,da$$
$$= \int_A V\frac{\partial U}{\partial n}\,da \qquad (1)$$

$$Now\ div\,(V\,grad\,U) = grad V.grad U + V\,div(grad U)$$
$$= grad V.grad U + V\nabla^2 U \qquad (2)$$

Substituting for (2) in (1) we obtain

$$\int_V (grad V.grad U + V\nabla^2 U)\,dv = \int_A V\frac{\partial U}{\partial n}\,da$$
$$\int_V (\nabla V.\nabla U + V\nabla^2 U)\,dv = \int_A V\frac{\partial U}{\partial n}\,da \qquad (3)$$

This is Green's Theorem of the First Form.

Let $U = V$ and $V = U$ in (3)

$$\int_V (\nabla U.\nabla V + U\nabla^2 V)\,dv = \int_A U\frac{\partial V}{\partial n}\,da \qquad (4)$$

Subtract (3) from (4) giving

$$\int_V (U\nabla^2 V - V\nabla^2 U)\,dv = \int_A \left(U\frac{\partial V}{\partial n} - V\frac{\partial U}{\partial n}\right)da \qquad (5)$$

The above expression is the symmetrical form of Green's Theorem.

(9) <u>The Generalized Orthogonal Curvilinear Co-ordinates</u>.

In most radiation problems the system of co-ordinates chosen are usually not cartesian so that general equations for transforming from cartesian to orthogonal curvilinear co-ordinates are required.

Consider a point P defined by three point functions (u,v,w) which are orthogonal in space and consider further an element of volume as shown in the accompanying diagram.

$$PA = h_1 du$$
$$PB = h_2 dv$$
$$PC = h_3 dw$$

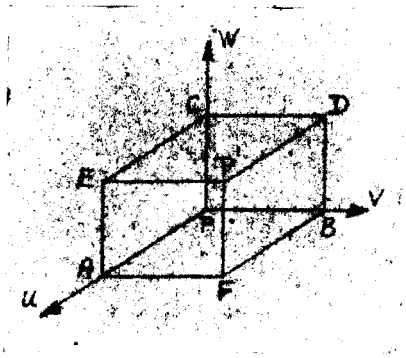

where h_1, h_2, h_3, are functions of u, v, w

Let $\delta a, \delta V$ be elements of area and volume.

$$(\delta a)_u = h_2 h_3\, dv\, dw$$
$$(\delta a)_v = h_1 h_3\, du\, dw$$
$$(\delta a)_w = h_1 h_2\, du\, dv$$
$$\delta V = h_1 h_2 h_3\, du\, dv\, dw$$

Let $\underline{a}, \underline{b}, \underline{c}$ be unit vectors in the directions u, v, w

$$\underline{PA} = h_1 du\,\underline{a}$$

$$\underline{BF} = \underline{PA} + \frac{\partial}{\partial v}(\underline{PA})\,dv$$

$$= h_1 du\,\underline{a} + \frac{\partial}{\partial v}(h_1 du\,\underline{a})\,dv$$

$$\underline{PB} = h_2 dv\,\underline{b}$$

$$\underline{AF} = \underline{PB} + \frac{\partial}{\partial u}(\underline{PB})\,du = h_2 dv\,\underline{b} + \frac{\partial}{\partial u}(h_2 dv\,\underline{b})\,du$$

Now $\underline{PA}+\underline{AF} = \underline{BF}+\underline{PB}$

$$h_1 du\underline{a} + h_2 dv\underline{b} + \frac{\partial}{\partial u}(h_2 dv\underline{b})du = h_1 du\underline{a} + \frac{\partial}{\partial v}(h_1 du\underline{a})dv + h_2 dv\underline{b}$$

$$\therefore \frac{\partial}{\partial u}(h_2\underline{b}) = \frac{\partial}{\partial v}(h_1\underline{a})$$

Take the dot product with respect to $\underline{b}$.

$$\underline{b}\cdot\left(\frac{\partial h_2}{\partial u}\underline{b} + h_2\frac{\partial \underline{b}}{\partial u}\right) = \underline{b}\cdot\left(\frac{\partial h_1}{\partial v}\underline{a} + h_1\frac{\partial \underline{a}}{\partial v}\right)$$

$\underline{b}\cdot\frac{\partial \underline{b}}{\partial u} = 0$ since $\underline{b}$ is of constant length

and $\underline{b}\perp\underline{a}$ $\therefore$ $\underline{b}\cdot\underline{a}=0$ Also $\underline{b}\cdot\underline{b}=1$

$$\therefore \frac{\partial h_2}{\partial u} = h_1\underline{b}\cdot\frac{\partial \underline{a}}{\partial v}$$

Similarly $$\frac{\partial h_3}{\partial u} = h_1\underline{c}\cdot\frac{\partial \underline{a}}{\partial w}$$

Now let the axes of (x,y,z) coincide with the axes of the curvilinear co-ordinates at P. Then

$$dx = h_1 du \qquad dy = h_2 dv \qquad dz = h_3 dw$$

If ϕ is a scalar point function

$$\frac{\partial\phi}{\partial x} = \frac{1}{h_1}\frac{\partial\phi}{\partial u} \qquad \frac{\partial\phi}{\partial y} = \frac{1}{h_2}\frac{\partial\phi}{\partial v} \qquad \frac{\partial\phi}{\partial z} = \frac{1}{h_3}\frac{\partial\phi}{\partial w}$$

Also $\underline{i},\underline{j},\underline{k}$ coincide with $\underline{a},\underline{b},\underline{c}$ and hence

$$\text{grad }\phi = \nabla\phi = \underline{i}\frac{\partial\phi}{\partial x} + \underline{j}\frac{\partial\phi}{\partial y} + \underline{k}\frac{\partial\phi}{\partial z}$$

$$= \frac{\underline{a}}{h_1}\frac{\partial\phi}{\partial u} + \frac{\underline{b}}{h_2}\frac{\partial\phi}{\partial v} + \frac{\underline{c}}{h_3}\frac{\partial\phi}{\partial w} \qquad (1)$$

The curvilinear expression for the divergence of the point function

$$H = H_1\underline{a} + H_2\underline{b} + H_3\underline{c}$$

is given as follows

$$\text{div } H = \nabla\cdot H = \underline{i}\cdot\frac{\partial H}{\partial x} + \underline{j}\cdot\frac{\partial H}{\partial y} + \underline{k}\cdot\frac{\partial H}{\partial z}$$

$$= \frac{\underline{a}}{h_1}\cdot\frac{\partial}{\partial u}(H_1\underline{a}+H_2\underline{b}+H_3\underline{c}) + \frac{\underline{b}}{h_2}\cdot\frac{\partial}{\partial v}(H_1\underline{a}+\cdots) + \frac{\underline{c}}{h_3}\cdot\frac{\partial}{\partial w}(H_1\underline{a}+\cdots)$$

Now $\underline{a}\cdot\frac{\partial \underline{a}}{\partial u} = 0$ Also $\underline{a}\perp\underline{b}\perp\underline{c}$

$\therefore$ The H_1 terms become $\frac{1}{h_1}\frac{\partial H_1}{\partial u} + \frac{H_1}{h_2}\underline{b}.\frac{\partial \underline{a}}{\partial v} + \frac{H_1}{h_3}\underline{c}.\frac{\partial \underline{a}}{\partial w}$

Also $\underline{b}.\frac{\partial \underline{a}}{\partial v} = \frac{1}{h_1}\frac{\partial h_2}{\partial u}$

$\underline{c}.\frac{\partial \underline{a}}{\partial w} = \frac{1}{h_1}\frac{\partial h_3}{\partial u}$

$\therefore$ The H_1 terms $= \frac{1}{h_1}\frac{\partial H_1}{\partial u} + \frac{H_1}{h_1 h_2}\frac{\partial h_2}{\partial u} + \frac{H_1}{h_1 h_3}\frac{\partial h_3}{\partial u}$

$= \frac{1}{h_1 h_2 h_3}\frac{\partial}{\partial u}(h_2 h_3 H_1)$

Evaluating the other two terms and summing

$$\text{div } \underline{H} = \frac{1}{h_1 h_2 h_3}\left(\frac{\partial}{\partial u}(h_2 h_3 H_1) + \frac{\partial}{\partial v}(h_3 h_1 H_2) + \frac{\partial}{\partial w}(h_1 h_2 H_3)\right) \quad (2)$$

$$\nabla^2\phi = \nabla.\nabla\phi = div\left(\frac{\underline{a}}{h_1}\frac{\partial \phi}{\partial u} + \frac{\underline{b}}{h_2}\frac{\partial \phi}{\partial v} + \frac{\underline{c}}{h_3}\frac{\partial \phi}{\partial w}\right)$$

$$= \frac{1}{h_1 h_2 h_3}\left\{\frac{\partial}{\partial u}\left(\frac{h_2 h_3}{h_1}\frac{\partial \phi}{\partial u}\right) + \frac{\partial}{\partial v}\left(\frac{h_3 h_1}{h_2}\frac{\partial \phi}{\partial v}\right) + \frac{\partial}{\partial w}\left(\frac{h_1 h_2}{h_3}\frac{\partial \phi}{\partial w}\right)\right\} \quad (3)$$

Also

$$\text{curl } H = \sum \frac{\underline{a}}{h_1} \wedge \frac{\partial}{\partial u}(H_1\underline{a} + H_2\underline{b} + H_3\underline{c})$$

$$= \frac{\underline{a}}{h_2 h_3}\left\{\frac{\partial}{\partial v}(h_3 H_3) - \frac{\partial}{\partial w}(h_2 H_2)\right\}$$

$$+ \frac{\underline{b}}{h_3 h_1}\left\{\frac{\partial}{\partial w}(h_1 H_1) - \frac{\partial}{\partial u}(h_3 H_3)\right\} + \frac{\underline{c}}{h_1 h_2}\left\{\frac{\partial}{\partial v}(h_1 H_1) - \frac{\partial}{\partial u}(h_2 H_2)\right\} \quad (4)$$

The above expressions (1) to (4) give grad div, ∇^2 and curl in orthogonal curvilinear co-ordinates.

The most important systems of curvilinear orthogonal co-ordinates used in radiation phenomena are cylindrical (ρ, ϕ, z) and spherical (r, θ, ϕ). The transformed expressions for grad, div, ∇^2 and curl in cylindrical and spherical co-ordinates are summarized below. These expressions are determined with the aid of the above formulae.

<u>Cylindrical Co-ordinates</u>.

For cylindrical co-ordinates $P(\rho, \phi, z)$

$$\text{grad}_\rho V = \frac{\partial V}{\partial \rho} \; ; \; grad_z V = \frac{\partial V}{\partial z} \; ; \; grad_\phi V = \frac{1}{\rho}\frac{\partial V}{\partial \phi}$$

$$\text{div } D = \frac{1}{\rho}\frac{\partial}{\partial \rho}(\rho D_\rho) + \frac{1}{\rho}\frac{\partial D_\phi}{\partial \phi} + \frac{\partial D_z}{\partial z}$$

$$\text{curl}_\rho E = \frac{1}{\rho}\frac{\partial E_z}{\partial \phi} - \frac{\partial E_\phi}{\partial z}$$

$$\text{curl}_z E = \frac{1}{\rho}\left\{\frac{\partial}{\partial \rho}(\rho E_\phi) - \frac{\partial E_\rho}{\partial \phi}\right\}$$

$$\text{curl}_{\phi} E = \frac{\partial E_{\rho}}{\partial z} - \frac{\partial E_z}{\partial \rho}$$

$$\nabla^2 V = \frac{1}{\rho}\frac{\partial}{\partial \rho}\left(\rho \frac{\partial V}{\partial \rho}\right) + \frac{1}{\rho^2}\frac{\partial^2 V}{\partial \phi^2} + \frac{\partial^2 V}{\partial z^2}$$

Spherical Co-ordinates.

For spherical co-ordinates $P(r, \theta, \phi)$

$$\text{grad}_r V = \frac{\partial V}{\partial r} \quad ; \quad \text{grad}_{\theta} V = \frac{1}{r}\frac{\partial V}{\partial \theta}$$

$$\text{grad}_{\phi} V = \frac{1}{r\sin\theta}\frac{\partial V}{\partial \phi}$$

$$\text{div} \quad D = \frac{1}{r^2}\frac{\partial}{\partial r}(r^2 D_r) + \frac{1}{r\sin\theta}\frac{\partial}{\partial \theta}(D_{\theta}\sin\theta) + \frac{1}{r\sin\theta}\frac{\partial D_{\phi}}{\partial \phi}$$

$$\text{curl}_r E = \frac{1}{r\sin\theta}\left\{\frac{\partial}{\partial \theta}(E_{\phi}\sin\theta) - \frac{\partial E_{\theta}}{\partial \phi}\right\}$$

$$\text{curl}_{\theta} E = \frac{1}{r\sin\theta}\frac{\partial E_r}{\partial \phi} - \frac{1}{r}\frac{\partial (rE_{\phi})}{\partial r}$$

$$\text{curl}_{\phi} E = \frac{1}{r}\left\{\frac{\partial}{\partial r}(rE_{\theta}) - \frac{\partial E_r}{\partial \theta}\right\}$$

$$\nabla^2 V = \frac{1}{r^2}\frac{\partial}{\partial r}\left(r^2 \frac{\partial V}{\partial r}\right) + \frac{1}{r^2\sin\theta}\frac{\partial}{\partial \theta}\left(\frac{\partial V}{\partial \theta}\sin\theta\right) + \frac{1}{r^2\sin^2\theta}\frac{\partial^2 V}{\partial \phi^2}$$

(10) **The Fundamental Laws.**

(1) **The Electrostatic Inverse Square Law.**

The force F between two charges is given by the well known experimental law of Coulomb

$$F = \frac{q_1 q_2}{4\pi\epsilon r^2}$$

where F = The force (Newtons)

r = The distance between the charges (Metres)

$q_1 q_2$ = The charges(Coulombs)

ϵ = The dielectric constant (Farads/metre)

If E = The electric field intensity i.e. the force on unit charge then

$$F = Eq$$

Again the work done in moving unit charge from a point at potential V to one at potential $V+\delta V$ is

$$-\delta V = E.\delta s$$

whence in the limit $E = -\frac{\partial V}{\partial s}$

$$\therefore E = -\,grad\,V$$

(ii) <u>The Electrostatic Divergence Law</u>.

Consider a number of charges $q_1 q_2 \cdots\cdots q_n$ over an area A. Let E_1 be the intensity over an element of area δa due to a charge q_1 at P_1. Then q_1 gives rise to a flux threading δa whose component normal to δa is given by

$$E_1 \delta a \cos\theta$$

where θ is the angle between E_1 and the outward drawn normal $\underline{n}$ to the surface δa.

$$\underline{E_1}.\delta a = E_1 \delta a \cos\theta = \frac{q_1}{4\pi\epsilon r^2}\delta a \cos\theta$$

$$= \frac{q_1}{4\pi\epsilon}\delta\Omega$$

where $\delta\Omega$ is the solid angle subtended by δa at P_1.

The complete solid angle subtended at P_1 is 4π. Hence the normal flux through the whole surface due to q_1 is $\frac{q_1}{\epsilon}$

Integrating the flux due to all the charges inside the surface gives

$$\int_A E.dA = \frac{q}{\epsilon}$$

where $q = q_1 + q_2 + q_3 + \cdots\cdots + q_n$

Using Gauss' Theorem we obtain

$$\text{div } E = \lim_{v \to 0} \frac{1}{v}\int_A E.dA = \frac{\rho}{\epsilon}$$

where ρ = The quantity of charge per unit volume.

Now for an isotropic medium the dielectric displacement $D = \epsilon E$

$$\therefore \text{div } D = \rho$$

(iii) <u>The Magnetostatic Inverse Square Law</u>.

The experimental law of force between magnetic poles

was discovered by Coulomb and is

$$F = \mu \frac{m_1 m_2}{4\pi r^2}$$

where

F = The force (Newtons)

r = The distance between the poles (Metres)

m_1, m_2 = The pole strengths (Webers)

μ = The permeability (Henries/metre)

Again as for the electric intensity E we have

$$H = -\text{ grad } U$$

where H = The magnetic field intensity

U = The magnetic scalar potential

(iv) <u>The Magnetostatic Divergence Law</u>.

Since it is impossible to obtain a preponderance of magnetic poles of one kind, there are no free magnetic poles. Consequently the divergence of the lines of magnetic intensity is zero

$$\text{div } H = 0$$

Also the Flux Density $B = \mu H$

$$\therefore \text{div } B = 0$$

(v) <u>Ampere's Law</u>.

Ampere's Law follows from Oersted's Experiments of 1820. Oersted found experimentally that electric current flowing along a wire was accompanied by a magnetic field and Ampere showed by experiment that a small closed circuit of current had a magnetic effect at a distant point which is proportional to the area of the circuit and to the current in the loop.

Ampere's findings show that the magnetic moment for a small element of area is $I\delta a$ where I is the current and δa the normal component of area.

By analogy with the electrostatic case the magnetic

potential at a point P distance r from an element of magnetic moment $I\delta a$ is

$$\delta U = \frac{\mu I \delta a \cos\theta}{4\pi r^2}$$

Now $\frac{\delta a \cos\theta}{r^2} = \delta\Omega$ is the solid angle subtended at P by δa.

Hence the magnetic potential U due to the complete area is proportional to the solid angle Ω subtended by the loop at P

$$\text{i.e. } U \propto I\Omega$$

The work done in taking unit pole once round the current is the difference in potential before and after the revolution

$$U_1 - U_2 \propto I((4\pi + \Omega) - \Omega) \qquad = 4\pi I$$

Also the work done is the line integral of the field intensity

$$U_2 - U_1 = \oint H.dl$$

Hence choosing the constant appropriately

$$\oint H.dl = I$$

where H = The magnetic intensity (Amps./metre)

I = The Current (Amps.)

From Stoke's Theorem

$$\text{curl } H = \lim_{A \to 0} \frac{1}{A} \oint H.dl = J$$

where J = The current density (Amps./metre^2)

(vi) **Faraday's Law.**

Faraday's Law discovered in 1831, showed that the induced e.m.f. in a secondary circuit is proportional to the time rate of change of flux in the primary circuit

$$\oint E.dl = -\frac{d}{dt}\int_A B.da$$

Again using Stoke's Theorem

$$\text{curl } E = \lim_{A \to 0} -\frac{1}{A} \int_A \frac{dB}{dt}.da = -\frac{dB}{dt}$$

$$\therefore \text{curl } E = -\dot{B}$$

(vii) <u>The Equation of Continuity</u>.

Experiments show that moving charges are equivalent to currents. In order that there is no accumulation of charge in a volume the currents flowing in and out of an element of volume must be equal. The total outward flow of current from an element of volume is div J , and this must be equal to minus the time rate of change of charge density in the volume for continuity to obtain

$$\text{i.e.} \quad \text{div } J = -\frac{\partial \rho}{\partial t}$$

(viii) <u>Summary of Laws</u>.

(i) $F = \frac{q_1 q_2}{4\pi\epsilon r^2}$ $\quad F = Eq \quad E = -\text{grad} V$

(ii) $\text{div } D = \rho \quad D = E\epsilon$

(iii) $F = \frac{\mu m_1 m_2}{4\pi r^2} \quad H = -\text{grad} U$

(iv) $\text{div } B = 0 \quad B = H\mu$

(v) $\text{curl } H = J$

(vi) $\text{curl } E = -\frac{\partial B}{\partial t}$

(vii) $\text{div } J = -\frac{\partial \rho}{\partial t}$

(ix) <u>Maxwell's Equations</u>.

Combining $\quad \text{div } J = -\dot{\rho}$

and $\quad \text{div } D = \rho$

gives $\quad \text{div } (J + \dot{D}) = 0$

Now curl H = J and div (curl H) = 0 whence we have in general curl H = J + $\dot{D}$ for the above expressions to be true.

The four fundamental equations named after Maxwell are therefore

$$\text{curl } H = J + \frac{\partial D}{\partial t}$$
$$\text{curl } E = -\frac{\partial B}{\partial t}$$
$$\text{div } D = \rho$$
$$\text{div } B = 0$$

where $J = gE \quad D = \epsilon E \quad B = \mu H$

The first of these latter equations is Ohms Law where g is in mhos/metre.

In radiation problems it is assumed that E and H vary harmonically in time, i.e. as $e^{j\omega t}$. Making this substitution in the above forms of Maxwell's Equations we obtain

$$\text{curl } H = (g + j\omega\epsilon)E$$
$$\text{curl } E = -j\omega\mu H$$
$$\text{div } (\epsilon E) = \rho$$
$$\text{div } (\mu H) = 0$$

(11) <u>The Wave Equations for E and H.</u>

$$\text{curl } H = J + \frac{\partial D}{\partial t}$$
$$\text{curl curl } H = \text{grad div } H - \nabla^2 H$$
$$= curl\, J + \frac{\partial}{\partial t}\, curl(\epsilon E)$$
$$\text{curl } E = -\frac{\partial(\mu H)}{\partial t}$$
$$\text{div } H = 0$$
$$\therefore -\nabla^2 H = \text{curl } J - \mu\epsilon \frac{\partial^2 H}{\partial t^2}$$

Let $\mu\epsilon = \frac{1}{c^2}$

$$\frac{1}{c^2}\frac{\partial^2 H}{\partial t^2} - \nabla^2 H = \text{curl } J$$

Also
$$\text{curl } E = -\mu \frac{\partial H}{\partial t}$$
$$\text{curl curl } E = \text{grad div } E - \nabla^2 E$$
$$= -\mu \frac{\partial}{\partial t} \text{curl } H$$

$$\text{div } E = \frac{\rho}{\epsilon} \qquad \text{curl } H = J + \epsilon \frac{\partial E}{\partial t}$$

$$\therefore \text{ grad } \frac{\rho}{\epsilon} - \nabla^2 E = -\mu \frac{\partial J}{\partial t} - \mu\epsilon \frac{\partial^2 E}{\partial t^2}$$

$$\therefore \frac{1}{c^2} \frac{\partial^2 E}{\partial t^2} - \nabla^2 E = -\mu \frac{\partial J}{\partial t} - \frac{1}{\epsilon} \text{grad}\rho$$

These two results are the wave equations for E and H. The waves travel with velocity equal to the velocity of light C. If the current and charge distributions are known the equations for E and H may be obtained.

(12) The Energy Theorems and Poynting's Theorem.

In an electrostatic field the work done in bringing unit charge to a point of electrostatic potential V is V joules.

If the charge density is increased by $\delta\rho$ then the work done against the whole charge system is

$$\int_{vol.} V\delta\rho\, dv$$

Also work is done by the charges in opposing $\delta\rho$. At a point of charge density ρ the potential has increased by δV and the work done is

$$\int_{vol.} \rho\delta V\, dv$$

The work done δW in bringing up the charges must be equal to the increase in field energy

$$\therefore \delta W = \frac{1}{2}\int(\rho\delta V + V\delta\rho)\, dv = \frac{1}{2}\delta\int(\rho V)\, dv$$

$$\therefore W = \frac{1}{2}\int_{vol.} \rho V\, dv$$

Now div D $= \rho \qquad D = \epsilon E$

$$V \text{ div } D = \text{div } VD - D.\text{grad}V$$

$$E = -\text{ grad } V$$

$$\therefore W = \frac{1}{2}\int_{vol.} V \,\text{div}(\epsilon E)\, dv$$

$$= \frac{1}{2}\int_{vol.} \text{div}(V\epsilon E)\, dv - \frac{1}{2}\int_{vol.} \epsilon E.\text{grad}V\, dv$$

Apply Gauss' Theorem

$$= \frac{1}{2}\int_{area} n.(V\epsilon E)\, da + \frac{1}{2}\int_{vol.} \epsilon E.E\, dv$$

The first integral in the limit is zero, hence the energy in an electrostatic field is

$$W = \frac{1}{2}\int_{vol.} \epsilon E.E\,dv = \frac{1}{2}\int_{vol.} \epsilon E^2\,dv$$

Similarly for a magnetic field

$$W = \frac{1}{2}\int_{vol.} \mu H^2\,dv$$

Hence the total field energy is

$$W = \frac{1}{2}\int_{vol.} (\mu H^2 + \epsilon E^2)\,dv$$

Now curl H = J + $\dot{D}$

$$E.\text{curl H} = E.J + E.\dot{D}$$

$$\text{curl E} = -\dot{B}$$

$$H.\text{curl E} = -H.\dot{B}$$

$$\text{div } E_{\wedge}H = H.\text{curl}E - E.\text{curl}H$$

$$= -H.\dot{B} - E.J - E.\dot{D}$$

Rearrange and integrate over a volume v bounded by a surface A and apply Gauss' Theorem

$$\int_{vol.} E.J\,dv + \int_{vol.} \frac{\partial}{\partial t}\left\{\frac{1}{2}(\epsilon E^2 + \mu H^2)\right\}dv + \int_A (E_{\wedge}H).n\,da = 0$$

The terms from the left represent

(i) the Joule loss in the system

(ii) the rate of change of electric and magnetic energies in the system

(iii) the flow of energy normal to the surface of integration.

$$P = E_{\wedge}H \quad \text{Watts/Sq. metre}$$

is defined as Poynting's Vector and it is this vector which gives rise to the radiation from aerials.

(13) <u>The Retarded Potentials</u>.

In the solution of electrodynamic problems such as the current distribution of an aerial it is convenient to

introduce two potential functions which are related to the scalar potential of electrostatics and the vector potential of magnetostatics. Both these potentials are modified to allow for the finite time of propagation of electromagnetic effects and consequently are known as Retarded Potentials.

Let B = curl A

where B = The Magnetic flux density

A = The magnetic vector potential.

From Maxwell's Equations

$$\text{div } B = 0 \qquad \text{also div curl } A = 0$$

$$\text{curl } E = -\frac{\partial B}{\partial t} = -\text{curl } \dot{A}$$

Integrating

$$E = -\dot{A} - \text{grad } V$$

where V = The scalar potential

$$\text{curl curl } A = \text{curl } B$$

$$= \mu\epsilon \frac{\partial E}{\partial t} + \mu J_i$$

where J_i = The impressed current density

$$\text{curl curl } A = \mu\epsilon \frac{\partial}{\partial t}(-\dot{A} - \text{grad } V) + \mu J_i$$

$$= \text{grad div } A - \nabla^2 A$$

$$-\mu\epsilon \ddot{A} - \mu\epsilon \text{ grad } \dot{V} + \mu J_i = \text{grad div } A - \nabla^2 A$$

$$\therefore \nabla^2 A = \mu\epsilon \ddot{A} + \text{grad}(\text{div } A + \mu\epsilon \dot{V}) - \mu J_i$$

Assume $\text{div } A + \mu\epsilon \dot{V} = 0$

This may be done without any loss in generality and is equivalent to continuity.

$$\therefore \underline{\nabla^2 A = \mu\epsilon \ddot{A} - \mu J_i} \qquad (1)$$

Again $\text{div } D = \rho$

$$\text{div}(-\dot{A} - \text{grad } V) = \frac{\rho}{\epsilon}$$

$$\text{div } A = -\mu\epsilon\dot{V}$$

$$\mu\epsilon\ddot{V} - \text{div grad } V = \frac{\rho}{\epsilon}$$

$$\underline{\nabla^2 V = \mu\epsilon\ddot{V} - \frac{\rho}{\epsilon}} \qquad (2)$$

The equations given above are the wave equations for A and V. In an electrostatic field $\ddot{V} = 0$ so that equation (2) reduces to Poisson's Equation. Further if the charge distribution throughout space is zero equation (2) reduces to Laplace's Equation.

$$\nabla^2 V = -\frac{\rho}{\epsilon} \qquad \text{Poisson's Equation.}$$

$$\nabla^2 V = 0 \qquad \text{Laplace's Equation.}$$

The solution for V is obtained by assuming simusoidal variation with time

$$\ddot{V} = -\omega^2 V \qquad \omega^2\mu\epsilon = \frac{\omega^2}{c^2} = \beta^2$$

$$\therefore (\nabla^2 + \beta^2)V = -\frac{\rho}{\epsilon} \qquad (3)$$

Use Green's Theorem of the Second Form where V and U are two scalars and v a volume bounded by a closed surface A.

Let $U = \dfrac{e^{-j\beta r}}{r}$

where r = The distance from the field point P to the element.

$$\int_{vol.} (U\nabla^2 V - V\nabla^2 U)\, dv = \int_{area} \left(U\frac{\partial V}{\partial n} - V\frac{\partial U}{\partial n}\right) da \qquad (4)$$

When $r=0$ $U\to\infty$ so that integration of a small area round P is excluded.

Operating on the defining equation for U gives

$$\nabla^2 U = -\beta^2 U$$

Substituting in the left hand side of (4) and using (3) gives

$$\int_{vol.} U(\nabla^2 V + \beta^2 V)\, dv = -\int_{vol.} \frac{\rho}{\epsilon}\,\frac{e^{-j\beta r}}{r}\, dv$$

The right hand side of (4) consists of integrations over the total surface A_1 and the surface surrounding the field point $P(x'y'z')$ A_2

$$\int_{A_2}\left(U\frac{\partial V}{\partial n}-V\frac{\partial U}{\partial n}\right)da=\int_{A_2}\left\{\frac{e^{-j\beta r}}{r}\left(-\frac{\partial V}{\partial r}\right)-V\left(-\frac{\partial}{\partial r}\frac{e^{-j\beta r}}{r}\right)\right\}da$$

$$=\int_{A_2}\left\{-\frac{e^{-j\beta r}}{r}\frac{\partial V}{\partial r}-V\frac{e^{-j\beta r}}{r^2}-j\beta\frac{Ve^{-j\beta r}}{r^2}\right\}da$$

Now $r^2d\Omega = da$

As $r\longrightarrow 0$ this integral becomes

$$\int_{A_2}-\frac{Ve^{-j\beta r}}{r^2}da=-\int_{A_2}Ve^{-j\beta r}d\Omega$$

$$=-V_p4\pi$$

Again $\int_{A_1}\left(U\frac{\partial V}{\partial n}-V\frac{\partial U}{\partial n}\right)da=\int_{A_1}\left\{\frac{e^{-j\beta r}}{r}\frac{\partial V}{\partial n}-V\frac{\partial}{\partial n}\left(\frac{e^{-j\beta r}}{r}\right)\right\}da$

Now V varies as $e^{j\omega t}$ and $\omega=\beta c$ which gives

$$=\int_{A_1}\left\{\frac{e^{j\omega(t-\frac{r}{c})}}{r}\frac{\partial V}{\partial n}-\frac{Ve^{j\omega(t-\frac{r}{c})}}{}\frac{\partial}{\partial n}\left(\frac{1}{r}\right)+j\beta V\frac{e^{j\omega(t-\frac{r}{c})}}{r}\frac{\partial r}{\partial n}\right\}da$$

By moving the surface A_1 to infinity and assuming the charge distribution is finite in area the above integral may be made equal to zero.

Finally we have by combining both sides of equation (4)

$$-\int_{vol}\frac{\rho}{\epsilon}\frac{e^{j\omega(t-\frac{r}{c})}}{r}d\upsilon=-4\pi V_p$$

$$V_p=\frac{1}{4\pi\epsilon}\int_{vol.}\frac{[\rho]}{r}d\upsilon \qquad (5)$$

Where $[\rho]$ takes into account the retarded time. If the time factor is implied as it is in most cases V_p may be expressed as

$$V_p=\frac{1}{4\pi\epsilon}\int_{vol.}\frac{\rho e^{-j\beta r}}{r}d\upsilon \qquad (6)$$

The expressions for the retarded vector potential A are obtained by analogy with equations (5) and (6).

$$A_p=\frac{\mu}{4\pi}\int_{vol.}\frac{[J_i]}{r}d\upsilon$$

$$A_p=\frac{\mu}{4\pi}\int_{vol.}\frac{J_i e^{-j\beta r}}{r}d\upsilon$$

It is worth noting that the co-ordinates of P are $(x'y'z')$ whilst the static or moving charges have co-ordinates (xyz). The above expressions are useful starting points in the solution of aerial problems.

(14) <u>The Reciprocity Theorems for Aerials</u>.

The following paragraphs show by means of the general reciprocity theorem the equivalence for both reception and transmission of the following aerial properties

(a) Impedance

(b) Polar diagram.

(i) <u>The Generalized Reciprocity Theorem</u>.

Consider two harmonic systems of impressed current densities of which J_1 is a typical element in system one and J_2 in system two.

Applying Maxwell's Equations

$$\text{curl } E_1 = -j\omega\mu H_1 \qquad curl\, H_1 = (g+j\omega\epsilon)E_1 + J_1$$

$$\text{curl } E_2 = -j\omega\mu H_2 \qquad curl\, H_2 = (g+j\omega\epsilon)E_2 + J_2$$

$$\text{div } (E_1 \wedge H_2) = H_2 . curl\, E_1 - E_1 . curl\, H_2$$

$$= -j\omega\mu H_1 . H_2 - (g+j\omega\epsilon) E_1 . E_2 - E_1 . J_2$$

Integrating over a volume v bounded by an area A and using Gauss' Theorem

$$-\int_{vol.} E_1 . J_2 \, dv = \int_V g E_1 . E_2 \, dv + j\omega \int_V (\mu H_1 . H_2 + \epsilon E_1 . E_2)\, dv + \int_A (E_1 \wedge H_2) . n \, da \qquad (1)$$

Integrating over an infinite sphere to consider all space and noting

$$E_{\theta_1} = \eta H_{\phi_1} \qquad E_{\phi_1} = -\eta H_{\theta_1}$$

where η = The intrinsic impedance of free space

$$\int_A (E_1 \wedge H_2) . n \, da = \int_A \left(-E_{\phi_1} H_{\theta_2} + H_{\phi_2} E_{\theta_1}\right) da$$

$$= \eta \int_A \left(H_{\theta_1} H_{\theta_2} + H_{\phi_1} H_{\phi_2}\right) da \qquad (2)$$

From Equations (1) and (2) interchanging suffixes 1 and 2 and equating equal parts

$$\int_{vol.} E_1 . J_2 \, dv = \int_{vol} E_2 . J_1 \, dv$$

This is the General Reciprocity Theorem.

The medium must be isotropic but not necessarily homogeneous, i.e. g, μ and ϵ must be scalar functions but need not be constant.

(ii) <u>The Equality of Impedance</u>.

Apply Thevenin's Theorem to an aerial

$$I_\ell = \frac{V}{Z + Z_\ell}$$

where I_ℓ = The load current

V = The open circuit e.m.f. across the aerial terminals.

Z = The aerial impedance

Z_ℓ = The source impedance

V is dependent on the mode of excitation but not on the aerial impedance. Hence the transmission case in which the applied e.m.f. is concentrated across the aerial terminals is a special case of excitation. As a consequence the impedance of the aerial is the same whether receiving or transmitting.

(iii) <u>The Equality of Polar Diagrams</u>.

The polar diagrams of an aerial for receiving and transmission are shown to be equal by the Reciprocity Theorem.

To find the polar diagram of an aerial A when transmitting we explore the field at a fixed long distance from A with a receiving aerial B oriented to pick up maximum signal from A. The relative strengths of the received currents are a measure of the polar diagram for transmission. By using B as the transmitter instead of A, the same relative currents are received at A as were formerly received at B.

Hence the polar diagrams for transmission and reception are identical.

The above theory has been treated in some detail because it is the basic theory from which all theoretical aerial results are developed. Without a firm understanding of these principles the results of the following sections could not have been deduced.

(b) FIELD INTENSITY RELATIONSHIPS.

(1) Introduction.[6,7]

The space around a half wavelength dipole aerial may be divided into two parts, (i) the region near the aerial and (ii) the remaining space known as the outer region. The boundary between the two regions is a sphere centre the aerial driving point and passing through the aerial ends. Consider a voltage applied across the terminals. A wave travels outwards with the electric field E lines forming concentric circles. The magnetic field is normal to the electric field and therefore consists of circles with line of centres on the dipole axis. This representation of the field is exact for a biconical aerial and approximate for a cylindrical aerial. Now, after a time $t = \ell/c$ where ℓ is the dipole half-length and c is the velocity of light, the wave reaches the boundary sphere. In the case of the field along the dipole axis a discontinuity is reached and part or all of the field will be reflected depending on the interference pattern. In the case of the equatorial plane no such discontinuity exists on the boundary sphere and the waves are radiated into the outer region without reflection and radiation is a maximum in this direction. The boundary sphere is transparent in the equatorial plane and becomes opaque along the dipole axis. The resulting field pattern has zero radiation along the dipole axis and maximum radiation in the equatorial plane.

We now consider the field in greater detail. The E lines of the principal mode fields must end on conductors and, hence, cannot exist in free space. The waves which can exist and propagate in free space are higher mode forms in which the E lines form closed loops. The wave travels outwards from the driving point to the boundary sphere. At the boundary sphere some higher order waves are reflected and some are radiated, the proportions being such that the fields at the boundary sphere are continuous. The field has a radial component which is greatest near the dipole axis and zero on the equatorial plane so that the E lines at this plane travel through the boundary surface without change. Since the radial components of the field attenuate more rapidly than the transverse components, the radial field becomes negligible in comparison with the transverse field at a large distance from the aerial. It is for this reason that the space is divided into two regions called (i) the near or Fresnel Zone, (ii) the far or Fraunhofer Zone. The boundary between the two is taken at a radius $R = \frac{8\ell^2}{\lambda}$ In the Fraunhofer Region the measurable field components are transverse and the field pattern is independent of radius whilst in the Fresnel Region the radial field is not zero and the field pattern is dependent on the radius.

The near and far fields are treated below.

(2) The Near Field.[3,8]

The relationships for the near field intensities are derived as follows.

Consider an aerial of height ℓ along the Z axis above a perfectly conducting plane earth. From the diagram the following relationships hold for any field point P .

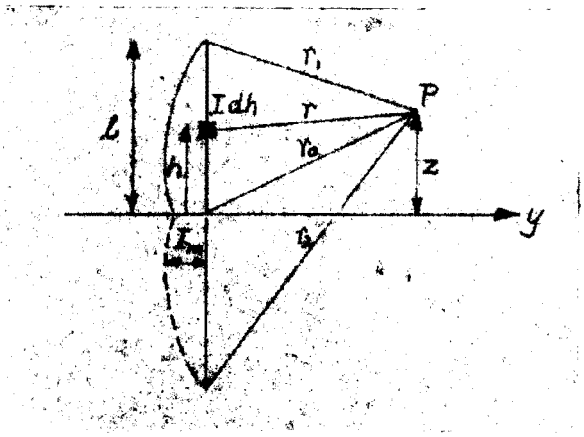

$$r = \sqrt{(z-h)^2+y^2}$$

$$r_1 = \sqrt{(z-\ell)^2+y^2}$$

$$r_2 = \sqrt{(z+\ell)^2+y^2}$$

$$r_0 = \sqrt{z^2+y^2}$$

The co-ordinates of P are (ρ,ϕ,z) in cylindrical polars. Since the aerial is symmetrical there will be no variation with change in ϕ. Let $\phi = 90^\circ$ then $\rho = y$ without any loss in generality. The current distribution for this type of aerial is unknown. The distribution along thin cylindrical antennas has been shown by Schelkunoff to be approximately simusoidal. Hence for this aerial the assumption is made that the current distribution is simusoidal.

$$I = I_m \sin\beta(\ell-h)\,e^{j\omega t} \qquad h>0$$

$$= I_m \sin\beta(\ell+h)\,e^{j\omega t} \qquad h<0$$

The vector potential at P from Maxwell's Equations is

$$dA_z = \frac{I\,dh\,e^{j(\omega t-\beta r)}}{4\pi r} \qquad (1)$$

Substituting the current in (1) and integrating along the length of the aerial and omitting the time factor

$$A_z = \frac{I_m}{4\pi}\left\{\int_0^{\ell}\frac{\sin\beta(\ell-h)e^{-j\beta r}dh}{r} + \int_{-\ell}^{0}\frac{\sin\beta(\ell+h)e^{-j\beta r}dh}{r}\right\} \qquad (2)$$

From Maxwell's Equations the magnetic flux at P in cylindrical polars is

$$H_\phi = curl_\phi A = -\frac{\partial A_z}{\partial \rho} \qquad (4)$$

Consider P in the $y-z$ plane, then (4) reduces to

$$H_\phi = -H_x = -\frac{\partial A_z}{\partial y} \qquad (5)$$

Substituting (2) in exponential form in (5) differentiating and integrating gives four terms which when summed yield the relationship for H_ϕ given below.

$$H_\phi = -\frac{I_m}{4\pi j}\left(\frac{e^{-j\beta r_1}}{y} + \frac{e^{-j\beta r_2}}{y} - \frac{2\cos\beta\ell\, e^{-j\beta r_0}}{y}\right) \qquad (9)$$

From Maxwell's Equations

$$\text{curl } H = \epsilon \frac{\partial E}{\partial t}$$

$$\therefore E = \frac{1}{j\omega\epsilon} curl\, H$$

where E = The Electric Field Intensity.

In the $y-z$ plane

$$E_z = \frac{1}{j\omega\epsilon}(curl\, H_\phi)_z = \frac{1}{j\omega\epsilon y}\frac{\partial}{\partial y}(y H_\phi) \qquad (10)$$

$$E_y = \frac{1}{j\omega\epsilon}(curl\, H_\phi)_y = \frac{-1}{j\omega\epsilon}\frac{\partial}{\partial z}(H_\phi) \qquad (11)$$

Substituting (9) in (10) the parallel component of field intensity becomes on reduction

$$E_z = -j30 I_m\left(\frac{e^{-j\beta r_1}}{r_1} + \frac{e^{-j\beta r_2}}{r_2} - \frac{2\cos\beta\ell\, e^{-j\beta r_0}}{r_0}\right) \qquad (12)$$

The three terms in the above field intensity relationship represent the spherical waves originating from the top of the aerial, its image point in the ground plane and the base of the aerial respectively. The third term is dependent on the height of the aerial.

Substituting (9) in (11) the perpendicular component of field intensity becomes

$$E_y = j30 I_m\left(\frac{z-\ell}{y}\frac{e^{-j\beta r_1}}{r_1} + \frac{z+\ell}{y}\frac{e^{-j\beta r_2}}{r_2} - \frac{2z\cos\beta\ell}{y}\frac{e^{-j\beta r_0}}{r_0}\right) \qquad (13)$$

Consider now the diagram below, consisting of a portion of a cylinder of radius r. The current distributes itself

uniformly around the circumference of the cylinder, mainly flowing on the outer surface of the cylinder.

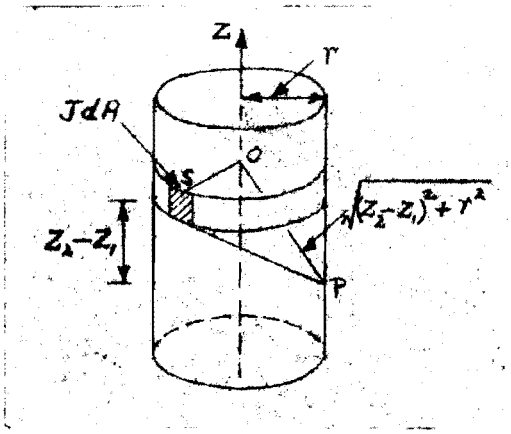

An approximation is made here that the electric field calculated from the current distribution along the cylinder would be the same as that calculated by considering the current concentrated along the axis of the cylinder.

Now $$SP \doteq \sqrt{(Z_2-Z_1)^2+2r^2}$$

$$OP = \sqrt{(Z_2-Z_1)^2+r^2}$$

If the effective radius is taken to be $\sqrt{2}\,r$ the above approximation has been shown to give results which are very close to those obtained by a rigorous analysis.

Using the above approximation we have for a field point P on the cylinder and $y=\sqrt{2}\,r$

$$\left.\begin{aligned} r_0 &= \sqrt{2r^2+Z^2} \\ r_1 &= \sqrt{2r^2+(\ell-Z)^2} \\ r_2 &= \sqrt{2r^2+(\ell+Z)^2} \end{aligned}\right\} \qquad (14)$$

From equations (12), (13) and (14) the parallel E_z and perpendicular E_y components of the near field intensity may be calculated. The following tables give the results of calculations based on these three equations. The results are only strictly true for $\frac{r}{\ell}$ ratios less than 0.02 since aerials of radii greater than this value do not support simusoidal current distributions. The results for $\frac{r}{\ell}$

ratio greater than 0.02 have been computed in order to show the trend with increase in $\frac{r}{\ell}$ ratio. Both real and imaginary field strength components are evaluated in volts/metre.

Dipole of length = λ

$\frac{z}{\ell}$	$\frac{r}{\ell}$ = 0		$\frac{r}{\ell}$ = 0.02		$\frac{r}{\ell}$ = 0.04	
	$\mathcal{R}(E_z)$	$\mathcal{I}(E_z)$	$\mathcal{R}(E_z)$	$\mathcal{I}(E_z)$	$\mathcal{R}(E_z)$	$\mathcal{I}(E_z)$
0.01	126.0	3940	125.0	1292	125	564
0.1	126.0	341	125.0	325	124	288
0.2	123.0	129.1	123.0	129	122	119
0.3	118.8	52.5	119	53	118	49
0.4	113.3	16.2	113	16.2	113	14.6
0.5	106.7	0	107	0	106	0+
0.6	99.1	-1.3	99	0+	99	0-
0.7	90.1	12.5	91	12.5	90	11
0.8	79.7	49.4	80	49	80	45
0.9	72.3	158	72.2	150	72	131
0.99	63.8	1960	63.8	636	63	312

$\mathcal{R}(E_y) = 0$

Dipole of length = λ

$\frac{z}{\ell}$	$\frac{r}{\ell}$ = 0.02	$\frac{r}{\ell}$ = 0.04
	$\mathcal{I}(E_y)$	$\mathcal{I}(E_y)$
0.01	480	107
0.05	1220	-
0.10	1280	578
0.20	1130	544
0.30	830	402
0.40	440	212
0.50	0	0
0.60	-440	-220
0.70	-835	-412
0.80	-1150	-558
0.90	-1380	-620
0.99	-935	-414

Dipole of length $= \frac{\lambda}{2}$

$\frac{z}{\ell}$	$\frac{r}{\ell} = 0$	$\frac{r}{\ell}=0.02$	$\frac{r}{\ell}=0.04$	$\frac{r}{\ell} = 0$	$\frac{r}{\ell}=0.02$	$\frac{r}{\ell}=0.04$
	$\mathcal{R}(E_z)$	$\mathcal{R}(E_z)$	$\mathcal{R}(E_z)$	$\mathcal{I}(E_z)$	$\mathcal{I}(E_z)$	$\mathcal{I}(E_z)$
0.01	80	79.9	79.9	0.02	-	-
0.1	79.9	79.9	79.4	1.3	0.4	0.5
0.2	79.2	79.2	78.6	5.1	4.9	4.2
0.3	78.2	78.2	77.9	12.0	11.7	10.7
0.4	77	77	76.5	22.4	21.8	20.6
0.5	75.5	75.4	75.0	37.7	37.0	35.1
0.6	73.5	73.5	73.0	60.6	59.5	56.1
0.7	71.3	71.1	70.6	97.6	95.4	88.4
0.8	68.6	68.6	68.3	169	161.3	141.7
0.9	65.8	65.9	65.5	375	321	236
0.99	63.5	63	62.6	3980	2180	326

$\mathcal{R}(E_y) = 0$

Dipole of length $= \frac{\lambda}{2}$

$\frac{z}{\ell}$	$\frac{r}{\ell} = 0.02$	$\frac{r}{\ell} = 0.04$
	$\mathcal{I}(E_y)$	$\mathcal{I}(E_y)$
0.01	21	12
0.1	210	109
0.2	434	216
0.3	639	317
0.4	828	409
0.5	996	490
0.6	1135	557
0.7	1250	605
0.8	1318	623
0.9	1310	575
0.99	1100	385

The following conclusions on the near field intensity may be deduced from the above tabulated results.

The parallel component E_z : The real component of the parallel field intensity component E_z is not markedly affected by changes in $\frac{r}{\ell}$ ratio for both the full- and half wavelength dipole. The curve shape is similar for both the full wave and half wave dipole but the variation

of field intensity with length is greater for the full wavelength dipole than it is for the half wavelength dipole. The imaginary component of the parallel field intensity component E_z is markedly affected near the cap for a half wavelength dipole and close to the cap and base for the full wavelength dipole. As the $\frac{r}{\ell}$ ratio is increased the field intensity decreases for both types of aerial. This reduction is to be expected since the Induction Field will have less effect for bigger diameters than for small ones. The reduction in imaginary field intensity component at the base of a half wavelength dipole is a point in its favour when comparing it with a full wavelength dipole.

The perpendicular component E_y : The real component of perpendicular component of near field intensity is substantially zero for all values of $\frac{r}{\ell}$ ratio in the range and for both types of aerial. Diagrams of the imaginary component of E_y with variation in the $\frac{r}{\ell}$ ratio are similar. The maximum value decreases with increase in $\frac{r}{\ell}$ ratio for both types of aerial. As mentioned previously this is to be expected as the Induction Field will have less effect for bigger diameter aerials. The patterns of the imaginary component of E_y for the half and full wavelength dipoles while in essence similar, show differences. The maximum field intensity for both are of the same order for equal $\frac{r}{\ell}$ ratio. At $\frac{z}{\ell} = 0$ the half wavelength dipole has zero field intensity and zero variation in field intensity, whilst the full wavelength dipole has a variation in field intensity with $\frac{r}{\ell}$ ratio. At the point $\frac{z}{\ell} = 0.5$ the full wavelength dipole has zero imaginary field intensity whilst the half wavelength dipole has a large variation in field intensity with $\frac{r}{\ell}$ ratio. The variation of field intensity near the base is smaller in the case of the half wave dipole than it is in the case of the full wavelength dipole.

The near field intensity has been treated in some detail for both half and full wavelength dipoles. It is necessary to consider now the far or distant field since a knowledge of the distant field gives a great insight into the propagation of the radiation.

(3) <u>The Far Field</u>.[8,9]

Consider the diagram given below for a dipole of length 2ℓ

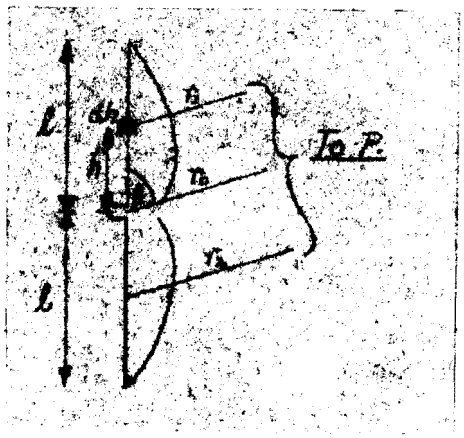

$$I = I_m \sin\beta(\ell-h)\, e^{j\omega t} \qquad h>0$$

$$= I_m \sin\beta(\ell+h)\, e^{j\omega t} \qquad h<0$$

where I_m = The maximum current

$$r_1 = r_0 - h\cos\theta \qquad r_2 = r_0 + h\cos\theta$$

The vector potential at P due to an element Idh is

$$dA_z = \frac{Idh\, e^{j(\omega t-\beta r)}}{4\pi r} = \frac{I e^{-j\beta r} dh}{4\pi r} \qquad (15)$$

The total vector potential at P is therefore from Equation (15)

$$A_z = \frac{\mu}{4\pi}\left\{\int_{-\ell}^{o}\frac{I_m \sin\beta(\ell+h)e^{-j\beta r}dh}{r} + \int_{o}^{\ell}\frac{I_m\sin\beta(\ell-h)e^{-j\beta r}dh}{r}\right\} \qquad (16)$$

Now the only field of interest is the radiation field so that it is permissible to put $r \doteq r_0$ in the denominator and $r = r_0 - h\cos\theta$ in the numerator. On making these substitutions equation (16) becomes

$$A_z = \frac{I_m e^{-j\beta r_o}}{4\pi r_o}\left\{\int_{-\ell}^{o} \sin\beta(\ell+h)e^{j\beta h\cos\theta}\,dh + \int_{o}^{\ell} \sin\beta(\ell-h)e^{j\beta h\cos\theta}\,dh\right\}$$

$$= \frac{I_m e^{-j\beta r_o}}{4\pi r_o}\int_{o}^{\ell} \sin\beta(\ell-h)\left\{e^{j\beta h\cos\theta} + e^{-j\beta h\cos\theta}\right\}dh$$

$$= \frac{I_m e^{-j\beta r_o}}{2\pi r_o \beta}\left\{\frac{\cos(\beta\ell\cos\theta) - \cos\beta\ell}{\sin^2\theta}\right\} \qquad (17)$$

Now $H_\phi = -\sin\theta \frac{\partial A_z}{\partial r}$

and $E_\theta = \eta H_\phi$

where η = The Intrinsic Impedance of Free Space = 120π ohms.

Then

$$E_\theta = \frac{j60 I_m e^{-j\beta r_o}}{r_o}\left\{\frac{\cos(\beta\ell\cos\theta) - \cos\beta\ell}{\sin\theta}\right\} \qquad (18)$$

The equation given above defines the distant field intensity in terms of the angle of elevation for free space and is shown tabulated below.

E_θ is in volts/metre at one metre for one ampere maximum current.

θ°	$\ell = \frac{\lambda}{4}$ E_θ	$\ell = \frac{\lambda}{2}$ E_θ
0	0	0
10	8.5	0.5
20	16.8	1.5
30	25.2	10.6
40	34.2	24.0
50	41.7	43.4
60	49.0	69.5
70	54.8	94.3
80	58.6	112.4
90	60.0	120.0

The following figures have been tabulated from the above equation for a half wavelength dipole resonant at 477.5 Mcps and also for the frequencies 457.5 and 497.5 Mcps.

Normalized Field Intensity E_θ

f Mcps.	457.5	477.5	497.5
θ°			
0	0.00	0.00	0.00
5	0.64	0.60	0.75
10	1.41	1.31	1.32
15	2.16	2.02	2.02
20	2.82	2.75	2.78
25	3.55	3.49	3.41
30	4.24	4.16	4.12
35	4.97	4.90	5.00
40	5.69	5.58	5.51
45	6.35	6.29	6.20
50	7.05	6.94	6.89
55	7.65	7.58	7.54
60	8.22	8.16	8.12
65	8.72	8.68	8.66
70	9.17	9.14	9.13
75	9.53	9.51	9.52
80	9.80	9.78	9.79
85	9.96	9.95	9.96
90	10.00	10.00	10.00

In comparing the relative merits of aerials as far as directivity is concerned the beam width, i.e. the angle between half power points is important. The beam width for a half wavelength dipole is 78° compared with 47° for a full wavelength dipole showing that the full wavelength dipole has greater directivity in a direction normal to the dipole. The radiation field intensity patterns are free space values and the effect of the earth for an aerial raised above the earth at some finite distance is quite marked. It is proposed to investigate the effect of the earth on field intensity diagrams in a later section. A few remarks on the general effect of the earth on polar diagrams are given here.

Consider the diagram shown below of a transmitting aerial.

Let h = The height of aerial above the ground.

Δ = The path difference between reflected and direct rays.

ϕ = The angle of elevation to the source of radiation.

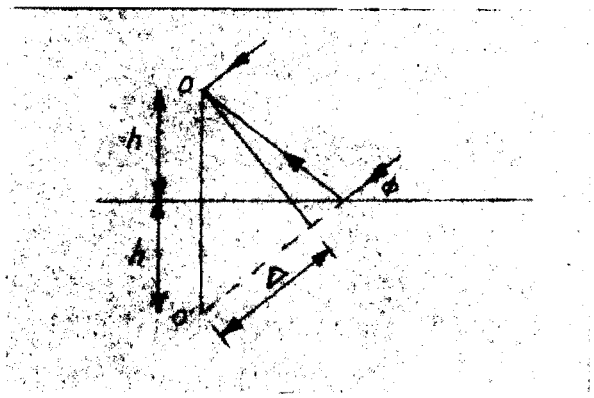

Then $\Delta = 2h\sin\phi$

Let δ = The phase delay on reflection

R = The reflection coefficient.

The field strength

$$E = E_o\left(1 + R\,e^{j(\beta\Delta+\delta)}\right)$$

For grazing incidence it will be shown that $\delta \doteq \pi$ and $R = 1$

$$\therefore E = 2E_o \sin(\beta h \sin\phi) \qquad (19)$$

The vertical polar diagram will be given by equation (19). If the free space diagram is given by $f(\phi)$ then

$$E = E_o\left(f(\phi) + f(-\phi)\,e^{j(\beta\Delta+\pi)}\right)$$

If $f(\phi)$ is symmetrical about a horizontal plane, as is the case for a dipole

$$f(\phi) = f(-\phi)$$

$$\therefore |E| = 2E_o f(\phi) \sin\left(\frac{2\pi h \sin\phi}{\lambda}\right) \qquad (20)$$

The form of equation (20) indicates that the polar diagram envelope is $f(\phi)$ but it will have a series of maxima and minima in the form of lobes. The first maximum is given approximately by

$$\sin\phi_{max_1} = \frac{\lambda}{4h}$$

The first zero

$$\sin\phi_{min_1} = \frac{\lambda}{2h}$$

The above analysis shows briefly the reasons for the lobe shaped patterns of dipoles elevated above the ground.

If a number of half wavelength sections are stacked axially, then assuming a perfect earth the radiation pattern obtained for an n -section aerial will have greater horizontal directivity than a one section aerial but at the same time break up into minor lobes will occur. Now, the field intensity for one section is exponential of the form $E = E_0 f(\epsilon)$

Consequently, for n sections the field intensity is

$$E_n = (E)^n$$

Now since $|E| \leq 1$ this means that the greater n is, the greater the horizontal directivity will be. A three stack aerial on preliminary inspection gives excellent directivity. However, the impedance characteristics will be reduced considerably so that a single element aerial may be the best type of aerial.

The following properties are the properties of the distant field in relation to half and full wavelength dipoles in summarized form. Radiation axially is zero and is a maximum in the equatorial direction for both types of aerial. The free space polar plot for a centre fed half wavelength dipole has a beam width of 78° compared with 47° for a full wavelength dipole. In the case of half wavelength dipoles which will be treated further because of their convenient physical size, increase in number of stacked dipoles reduces the aerial resistance but improves the envelope of the radiation pattern. Increase in height above the earth will have some effect upon the directivity of the aerial as well as breaking up the free space pattern into a series of several minor lobes. Since the radiation field is a distant field phenomenon it should be apparent that the radiation field patterns will be affected by only a small amount with variation in $\frac{r}{\ell}$ ratio.

It is seen that $\frac{r}{\ell}$ ratio variation has a marked effect on near field intensity but very little on distant field intensity. Also, aerial elevation has a considerable effect on the radiation pattern. It is this last phenomenon which will markedly affect the behaviour of half wavelength dipoles.

A detailed analysis of the far field pattern for which the distribution of current is not assumed to be simusoidal has been carried out and shows the following results.[9]

(i) The points where $E_\theta = 0$ for the simple simusoidal case do not occur. The zeros are rounded off.

(ii) The change in pattern shape even for thick aerials is not appreciable.

(iii) The maximum value of the minor lobes is generally increased.

(iv) The maximum value of the major lobes is generally decreased.

It follows that the field strength patterns deduced by the simple theory will yield adequate results provided it is remembered that the zeros will be rounded off.

(4) <u>The Power Received</u>.[10]

In designing a receiver to detect a known radiation it is necessary to know the amount of transmitted power picked up by the receiver. The amount of transmitted power received by a receiver is deduced below. The expression derived was used in designing a U.H.F. Receiver.

It is convenient to define the directivity as the maximum possible power gain of one aerial with respect to an isotropic source

$$g = \frac{P_o}{P} = \frac{\iint \Phi_o \, d\Omega}{\iint \Phi \, d\Omega} = \frac{4\pi}{\iint \Phi \, d\Omega} \quad \text{where } \Phi_o = \Phi_{max} = 1$$

The directivity is equal to the ratio of the maximum radiation intensity to the average radiation intensity.

The radiation intensity of a current element is proportional to $\sin^2\theta$

$$g = \frac{4\pi}{\int_0^{2\pi}\int_0^{\pi}\sin^3\theta\, d\theta\, d\phi} = \frac{3}{2}$$

The effective area of a receiving aerial is the maximum power that can be received at the terminals of the aerial from a linearly polarized wave divided by the power per unit area carried by the wave

$$A = \frac{P_{max.rec.}}{\frac{E^2}{240\pi}}$$

Assume a current element of length S parallel to the electric intensity E. Let V be the voltage induced. Then V = ES.

Let Z be the radiation impedance, that is, the impedance due to the reaction of the wave produced by the current I in the element. Let Z_ℓ be the impedance of the circuit in series with the element.

$$V = Es = (Z + Z_\ell)I$$

$$P_{rec.} = \frac{1}{2}R_\ell|I|^2 = \frac{R_\ell|Es|^2}{2|Z+Z_\ell|^2}$$

$$= \frac{R_\ell E^2 s^2}{2(R+R_\ell)^2 + 2(X+X_\ell)^2}$$

This is a maximum if $X + X_\ell = 0 \qquad R = R_\ell$

Also $R = 80\pi^2\frac{s^2}{\lambda^2}$

$$\therefore P_{max.rec.} = \frac{E^2\lambda^2}{640\pi^2}$$

This is the maximum power received and is independent of the length of the current element.

$$A = \frac{P_{max.rec.}}{\frac{E^2}{240\pi}} = \frac{3}{8}\frac{\lambda^2}{\pi}$$

If P_{tr} the power radiated by the transmitting aerial is radiated uniformly in all directions, then the power flowing per unit area at distance r is $\frac{P_{tr}}{4\pi r^2}$

If the power gain of the transmitting aerial is g_1, then the power flow at the receiving aerial is increased by a factor g_1. If the effective area of the receiving aerial is A_2 then

$$P_{rec.} = \frac{P_{tr.}}{4\pi r^2} g_1 A_2$$

Substituting for g_1 and A_2 from above we obtain

$$P_{rec.} = \frac{9}{64\pi^2} \left(\frac{\lambda}{r}\right)^2 P_{tr}$$

This relationship was used in designing the field strength measuring equipment.

(c) INPUT IMPEDANCE.

(1) The Cylindrical Aerial Problem.

The methods by which a cylindrical aerial's current distribution and impedance variation are computed are given below. Any solution of the aerial problem will be a solution of Maxwell's Equations subject to the boundary conditions imposed by the aerial and source. The solution for a centre fed dipole aerial is not as simple as the simple shape would lead one to believe. Though it is theoretically possible to obtain expressions for the field if the current distribution is known it is relatively difficult to determine the field intensity knowing the aerial shape and the exciting voltage applied to the dipole as is usually the case. In the latter circumstance the current distribution is unknown and must be determined by an approximate method. The methods by which the aerial impedance data is obtained are given below with a brief explanation of each method.

(i) The Poynting Vector Method.[8]

The method consists of integrating over a sphere at some distance from the aerial to obtain the radiated power and from an assumed or known current distribution the radiation resistance is found.

(ii) The Induced E.M.F. Method.[8]

By assuming a sinusoidal current distribution and integration of the complex Poynting vector over the aerial length the complex power is obtained giving the loop reactance and radiation resistance. The method is particularly suited to half wavelength dipoles.

(iii) The Equivalent Transmission Line Method.[8]

The aerial is treated as a lossy line, the losses being due to radiation. In order to determine the attenuation constant of the equivalent transmission line the power dissipated must be determined by methods (i) or (ii).

(iv) The Biconical Aerial Method.[11]

The method is due to S.A. Schelkunoff and is based on the idea of a biconical aerial being a transmission line of constant characteristic impedance with an abrupt discontinuity at the surface of the sphere surrounding the biconical conductors. If the cones are made narrow the thin aerial case is obtained and by taking a non-uniform characteristic impedance other aerial shapes such as cylinders may be considered. The method gives both the input reactance and resistance and allowance may be made for end cap capacitance.

(v) The Cylindrical Aerial Method.[12]

The method is due to Erik Hallen; he assumes a current distribution and obtains general expressions for the field by the use of retarded potentials. The boundary conditions imposed by the aerial are then applied and an integral equation for current is obtained. The solution of this integral equation has been reduced to sine, cosine and iterated sine and cosine integrals and from tables of these functions Hallen has evaluated input resistance and reactance versus length to wavelength ratio for varying radius to length ratios. The information obtained may also be plotted in the form of admittance diagrams making allowance for base capacitance and stub compensation relatively simple.

(vi) The Spheroidal Aerial Method.[13-18]

The solution of the aerial problem for certain symmetrical shapes such as a prolate spheroid is capable of exact calculation. The solution consists of an infinite number of free oscillation modes with coefficients chosen to satisfy the force function. The solution near resonance converges rapidly but in regions not near resonance the convergence is slow so that numerical work becomes laborious. Also the cylindrical aerial may only be solved by considering it equivalent to a thin prolate spheroid and the problem becomes one of deciding which prolate spheroid is equivalent to a cylinder of certain dimensions. Consequently, the method is not readily applicable to the solution of the cylindrical aerial problem.

The main methods of treating the cylindrical aerial problem are given above and the following subsections treat methods (i) to (v) in detail.

(2) The Radiation Resistance by Poynting's Vector.[4,19,20]

Poynting's Vector is defined as

$$\underline{P} = \underline{E} \wedge \underline{H} \qquad \text{Watts/square metre}$$

and in the case of a dipole aerial the vector reduces to

$$P = E_\theta H_\phi \quad \text{where} \quad H_\phi = \frac{1}{\eta} E_\theta$$
$$= \frac{1}{\eta} E_\theta^2 \qquad (1)$$

From subsection (b) equation (18)

$$E_\theta = \frac{j\eta I_m e^{-j\beta r_o}\{\cos(\beta \ell \cos\theta) - \cos\beta\ell\}}{2\pi r_o \sin\theta} \qquad (2)$$

Combining equations (1) and (2) and integrating through a semispherical surface of radius r_o the total radiated power will equal

$$\oint P_{av}\, dA = \frac{1}{2}\frac{1}{\eta}\frac{\eta^2 I_m^2 e^{-2j\beta r_o}}{4\pi^2 r_o^2} \int_o^{2\pi} \frac{\{\cos(\beta\ell\cos\theta) - \cos\beta\ell\}^2}{\sin^2\theta}\, dA$$

$$dA = \pi r_o \sin\theta\, r_o\, d\theta$$

$$\therefore \oint P_{av}\, dA = \frac{\eta I_m^2 e^{-2j\beta r_o}}{2\pi} I(\theta)$$

$$\text{where } I(\theta) = \int_o^{\frac{\pi}{2}} \frac{\{\cos(\beta\ell\cos\theta) - \cos\beta\ell\}^2}{\sin\theta}\, d\theta$$

Integration of the function $I(\theta)$ becomes a problem of mathematical juggling and is not here included. The power radiated is equal to $I_{eff.}^2 R_{rad.}$ where

I_{eff} = The Effective Current = $\frac{I_m}{\sqrt{2}}$

R_{rad} = The Radiation Resistance

Substituting these values and evaluating the integral yields the following result

$$R_{rad.} = 30\{2Cin(2\beta\ell) - (Cin\,4\beta\ell - 2Cin\,2\beta\ell)\cos 2\beta\ell + (Si\,4\beta\ell - 2Si\,2\beta\ell)\sin 2\beta\ell\} \qquad (3)$$

where $Cin(x) = \int_0^x \frac{1-\cos u}{u}\,du$

$$Si(x) = \int_0^x \frac{\sin u}{u}\,du$$

These integrals have been tabulated and for a half wave aerial the value of $R_{rad.}$ is

$$R_{rad.} = 73.2 \text{ ohms.}$$

A more convenient form of equation (3) is given below in terms of the tabulated cosine integral defined by

$$Ci(x) = -\int_x^\infty \frac{\cos v}{v}\,dv = \log \gamma x - Cin(x)$$

where $\log \gamma$ = C = Euler's Number = 0.5772

$$R_{rad} = 30\{2\log 2\beta\ell + 2C - 2Ci\,2\beta\ell + \cos 2\beta\ell(\log\beta\ell + C + Ci\,4\beta\ell - 2Ci\,2\beta\ell) + \sin 2\beta\ell(Si\,4\beta\ell - Si\,2\beta\ell)\} \qquad (4)$$

The following table of radiation resistance versus semi-length to wavelength ratio has been computed and plotted from equation (4) by the use of tabulated integrals.[21,22] It will be assumed that the radiation resistance does not alter appreciably with variation in $\frac{r}{\ell}$ ratio since radiation is a distant field phenomenon.

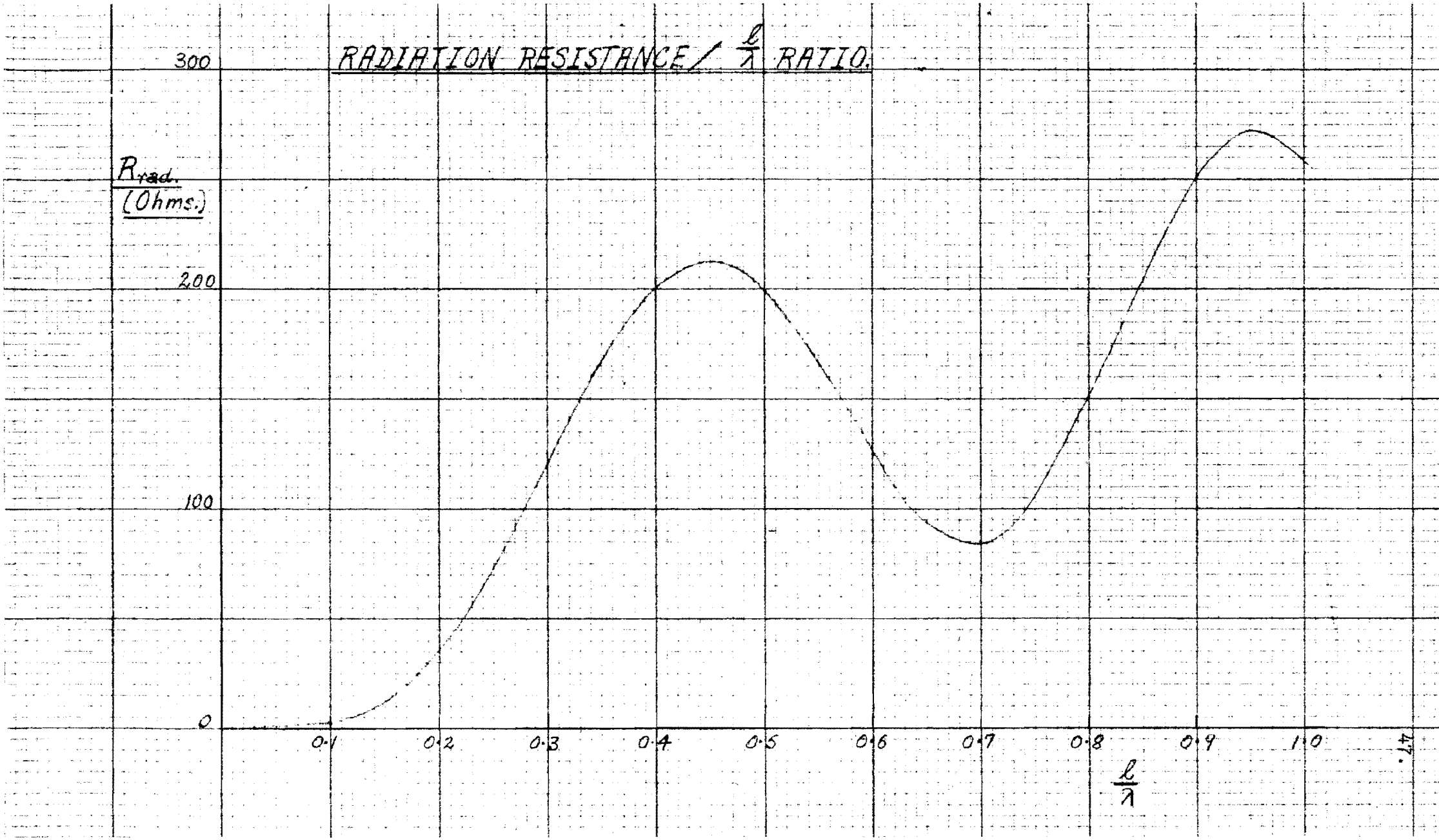
RADIATION RESISTANCE / $\frac{\ell}{\lambda}$ RATIO.
300
$R_{rad.}$ (Ohms.)
200
100
0
0·1
0·2
0·3
0·4
0·5
0·6
0·7
0·8
0·9
1·0
$\frac{\ell}{\lambda}$
47.

$\frac{\ell}{\lambda}$	$R_{rad.}$ (Ohms.)	$\frac{\ell}{\lambda}$	$R_{rad.}$ (Ohms.)
0.10	2.9	0.45	212.7
0.15	13.2	0.50	199.0
0.20	36.1	0.55	165.3
0.21	42.5	0.60	124.6
0.22	49.4	0.65	93.0
0.23	56.8	0.70	84.7
0.24	65.7	0.75	105.5
0.25	73.1	0.80	150.4
0.26	81.9	0.85	205.0
0.27	91.1	0.90	250.7
0.30	119.8	0.95	271.6
0.35	166.5	1.00	259.6
0.40	200.7		

The above analysis gives the radiation resistance or resistance referred to a current maximum only. If the reactance and resistance at the input terminals are required alternative methods must be used.

(3) <u>The Aerial Impedance by the Induced E.M.F. Method</u>.[23-28]

In deducing the impedance by the induced e.m.f. method a sinusoidal current distribution is assumed. Also, as mentioned earlier, the assumption of an effective radius of $\sqrt{2}\,r$ as given by O. Zinke is used. The electric field intensity E_z and current density J are constant around the circumference of the aerial at a given height. The linear current density J, integrated around the circumference is the total aerial current $I(z)$ at that height. The aerial Radiation Resistance and Reactance from Poynting's Vector will be

$$R = -\frac{1}{I_m^2}\int_0^{\ell} |E_z|\,|I(z)|\cos\psi\,dz$$

$$X = -\frac{1}{I_m^2}\int_0^{\ell} |E_z|\,|I(z)|\sin\psi\,dz$$

where ψ = The time phase angle

$I(z) = I_m \sin\beta(\ell - z)$ and E_z is given in sub-section (b)

$$\therefore Z = R+jX = -\frac{1}{I_m^2}\int_0^{\ell} |E_z|\,|I(z)|\; e^{j\psi}\, dz \qquad (5)$$

$$E_z = -j30 I_m \left\{ \frac{e^{-j\beta r_1}}{r_1} + \frac{e^{-j\beta r_2}}{r_2} - \frac{2\cos\beta\ell\, e^{-j\beta r_0}}{r_0} \right\}$$

$$r_0 = \sqrt{2r^2+z^2}$$

$$r_1 = \sqrt{2r^2+(\ell-z)^2}$$

$$r_2 = \sqrt{2r^2+(\ell+z)^2}$$

Substituting in equation (5) integrating and separating into real and imaginary parts gives

$$R = 30\left\{ \frac{\sin 2\beta\ell}{2}\left(Siu_2 - Siv_2 - 2Siv_1 + 2Siu_1\right) - \frac{\cos 2\beta\ell}{2}\left(2Ciu_1 - 2Ciu_0 + 2Civ_1 - Ciu_2 - Civ_2\right) - \left(Ciu_1 - 2Ciu_0 + Civ_1\right)\right\} \qquad (6)$$

$$X = -30\left\{ \frac{\sin 2\beta\ell}{2}\left(2Civ_1 - 2Ciu_1 + Civ_2 - Ciu_2\right) - \frac{\cos 2\beta\ell}{2}\left(2Siu_1 - 2Siu_0 + 2Siv_1 - Siu_2 - Siv_2\right) - \left(Siu_1 - 2Siu_0 + Siv_1\right)\right\} \qquad (7)$$

where $u_0 = 2\pi\sqrt{2}\,\frac{r}{\lambda}$

$$u_1 = \frac{2\pi}{\lambda}\left(\sqrt{\ell^2+2r^2} - \ell\right) \qquad v_1 = \frac{2\pi}{\lambda}\left(\sqrt{\ell^2+2r^2} + \ell\right)$$

$$u_2 = \frac{2\pi}{\lambda}\left(\sqrt{2r^2+(2\ell)^2} + 2\ell\right) \qquad v_2 = \frac{2\pi}{\lambda}\left(\sqrt{2r^2+(2\ell)^2} - 2\ell\right)$$

The equation for Resistance is not directly computable because of the lack of tabulated values. However equation (7) may be somewhat reduced and used for calculations as follows

For $\frac{r}{\ell}$ small $v_2 \doteqdot u_1 \doteqdot 0$

$$\therefore Siu_1 = Siv_2 = 0$$

Also $$-2Ciu_1 + Civ_2 \doteqdot -C + \log\frac{\ell}{2\beta r^2}$$

Substituting these approximations in equation (7) gives

$$X = -30\left\{ \frac{\sin 2\beta\ell}{2}\left(2Civ_1 - C + \log\left(\frac{1}{2\beta\ell}\,\frac{\ell^2}{r^2}\right) - Ciu_2\right) - \frac{\cos 2\beta\ell}{2}\left(-2Siu_0 + 2Siv_1 - Siu_2\right) - \left(Siv_1 - 2Siu_0\right)\right\} \qquad (8)$$

The following table has been calculated and plotted from equation (8) with the aid of tabulated integrals. All values of the loop reactance X are in ohms.

$\frac{\ell}{\lambda}$ \ $\frac{r}{\ell}$	0.001	0.005	0.010	0.020	0.030	0.040	0.050
0.10	-290	-198	-159	-119	-114	-108	-97
0.15	-299	-207	-167	-128	-117	-102	-90
0.20	-178	-121	- 97	- 72	- 56	- 47	-40
0.21	-140	- 93	- 73	- 53	- 39	- 32	-27
0.22	- 98	- 63	- 47	- 32	- 21	- 16	-12
0.23	- 53	- 29	- 19	- 9	- 2	1.3	3
0.24	-6.1	5.9	11.2	16.4	18.2	19.1	19.5
0.25	42.5	42.5	42.5	42.5	38.5	37.2	35.9
0.26	92	80	75	70	59	55	52
0.27	142	118	107	97	79	73	69
0.28	191	154	139	124	99	91	85
0.29	238	190	170	150	118	108	100
0.30	282	224	200	175	136	124	114
0.35	447	348	308	269	204	184	168
0.40	461	363	324	284	219	198	180
0.45	336	274	249	225	180	163	148
0.50	125	125	125	125	102	93	86
0.55	- 84	- 23	2	26	14	16	16
0.60	-218	-129	- 89	- 50	- 32	- 23	- 17
0.65	-243	-155	-115	- 75	- 68	- 57	- 50
0.70	-146	- 89	- 65	- 40	- 35	- 30	- 26
0.75	46	46	46	46	34	30	26
0.80	258	199	174	150	112	97	84
0.85	403	308	269	229	169	145	125
0.90	426	331	292	252	184	157	133
0.95	319	262	238	213	153	128	107
1.00	133	133	133	133	85	68	54

The variation of loop reactance and resistance are known with change in $\frac{r}{\ell}$ and $\frac{\ell}{\lambda}$ ratio so that the input resistance and reactance variations become the next important calculations.

Before considering the next section we discuss the limitations of the induced e.m.f. method.

The results of calculations based on the induced e.m.f. method have a limitation imposed on them due to the relationship between the scalar and vector potentials used in calculating field intensity.

$$div A + \mu\epsilon \frac{\partial V}{\partial t} = 0$$

The divergence is taken with respect to the field points but the integral for evaluating A is taken along

LOOP REACTANCE — ℓ/λ RATIO FOR A RANGE OF r/ℓ RATIOS.

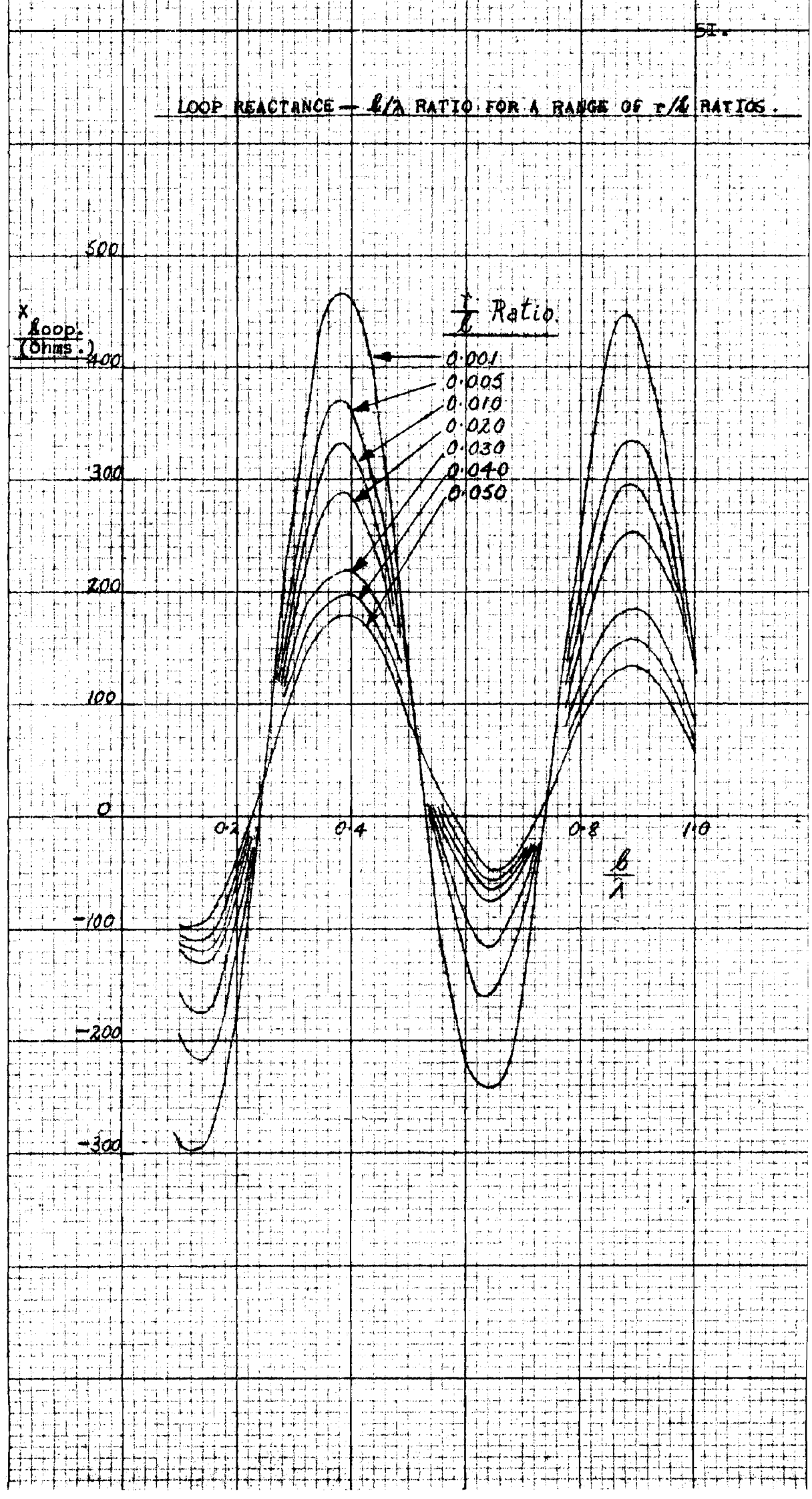

the radiator. The equation of continuity shows that this process is only strictly true if no energy is supplied from an external source. The inference of this criterion is that the induced e.m.f. method will hold for standing wave aerials but not for travelling wave types. Another disadvantage of the induced e.m.f. method is known as the Radiation Paradox.[29] The induced e.m.f. method violates the boundary conditions of Maxwell's equations since at the surface of an aerial the tangential component of E_z is zero. The reason for its calculated existence is that a sinusoidal distribution is not quite the true distribution of current. The following argument due to Burgess shows that impedances calculated in terms of this non-existent electric intensity are in fact true.

Let Z_o = The aerial input impedance
I_o = The current at the terminals
V_o = The voltage across the terminals
$I_t(z)$ = The transmitting current distribution
$E(z)$ = The electric field intensity distribution

$$V_o = I_o Z_o$$

The reciprocity theorem gives the induced terminal e.m.f. as

$$V_o^* = \frac{1}{I_o}\int E(z) I_t(z)\, dz$$

For a current I_o in the receiving condition

$$V_o^* = V_o$$

$$\int E(z) I_t(z)\, dz = I_o^2 Z_o$$

The current I_o produced by the incident field $E(z)$ is expressed in terms of the transmitting current distribution. A sinusoidal current $I_s(z)$ having a value I_o at the terminals would be accompanied by a field distribution $E_s(z)$ which is equal and opposite to the incident field $E(z)$ which would in turn produce a receiving distribution of $I_s(z)$

$$E(z) = -E_s(z)$$

$$Z_o = -\frac{1}{I_o^2}\int E_s(z)\, I_t(z)\, dz$$

Now $I_t(z)$ is approximately sinusoidal so that the value of Z_o would be changed very little by the substitution

$$I_s(z) = I_t(z)$$

$$Z_o = -\frac{1}{I_o^2}\int E_s(z)\, I_s(z)\, dz$$

and this is the value calculated by the induced e.m.f. method. The above argument shows that calculations based on a non-existent field intensity does yield approximately true results. The paradox was first pointed out by S.A. Schelkunoff.

(4) The Input Impedance by the Equivalent Transmission Line Method.[30,31]

Siegel and Labus have developed the following relationship for the average characteristic impedance of a dipole aerial of height ℓ and radius r by comparison of the scalar potential for an aerial with a sinusoidal current distribution and the scalar potential along a uniform transmission line.

$$Z_o(av.) = \frac{1}{\ell}\int_o^{\ell} Z_o(x)\, dx$$

$$Z_o(av.) = 120\left\{\log\left(\frac{\ell}{r}\right) - 1 - \frac{1}{2}\log\left(\frac{2\ell}{\lambda}\right)\right\}$$

The following relationships are derived from the open circuited transmission line theory.

$$V_x = V_R \cosh \gamma x$$

$$I_x = \frac{V_R}{Z_o(av.)} \sinh \gamma x$$

$$Z_x = \frac{V_x}{I_x} = Z_o(av.) \coth \gamma x$$

$$Z_{in.} = Z_\ell = Z_o(av.) \coth \gamma \ell \qquad (9)$$

For maximum current $x = \frac{\lambda}{4}$

$$\therefore I_m = I_{\frac{\lambda}{4}} = \frac{j V_R}{Z_o(av.)} \cosh \frac{\alpha\lambda}{4} \sin \frac{\beta\lambda}{4}$$

$$= \frac{j V_R}{Z_o(av.)} \quad \text{if } \alpha \text{ is small.}$$

$$\therefore I_x = I_m(\cosh \alpha x \sin \beta x - j \sinh \alpha x \cos \beta x)$$

where I_x, V_x = The current and voltage at a distance x from the open end of the line

V_R = The voltage at the open circuit

γ = The propagation constant

$= \alpha + j\beta \qquad \beta = \frac{2\pi}{\lambda}$

Siegel and Labus have assumed that in a transmission line representation of an aerial the radiated power is replaced by an equal resistance drop along the transmission line.

If it is assumed that

$$I_m^2 r = V_m^2 g$$

where V_m, I_m = The maximum loop voltage and current

r, g = The resistance and conductance per unit length of the equivalent transmission line

Then the total loss due to resistance and conductance is equal to the radiated power.

$$W = \int_0^{\ell} (I_x^2 r + V_x^2 g)\, dx$$

On reduction this becomes

$$W = I_m^2 r \ell \frac{\sinh 2\alpha\ell}{2\alpha\ell}$$

Now the power loss is equal to the radiated power

$$\therefore I_m^2 r \ell \frac{\sinh 2\alpha\ell}{2\alpha\ell} = I_m^2 R_{rad.}$$

$$r = \frac{R_{rad}}{\ell} \frac{2\alpha\ell}{\sinh 2\alpha\ell}$$

Also $$\frac{I_m^2}{V_m^2} = \frac{1}{Z_o(av.)^2}$$

$$g = \frac{I_m^2}{V_m^2} r = \frac{R_{rad}}{\ell Z_{o(av.)}^2} \frac{2\alpha\ell}{\sinh 2\alpha\ell}$$

For a low loss transmission line

$$r \ll \omega L \qquad g \ll \omega C$$

$$\alpha = \frac{1}{2}\left(\frac{r}{Z_o} + gZ_o\right)$$

$$= \frac{R_{rad.}}{\ell Z_{o(av)}} \frac{2\alpha\ell}{\sinh 2\alpha\ell}$$

$$\therefore \sinh 2\alpha\ell = \frac{2R_{rad}}{Z_{o(av.)}} \qquad (10)$$

Now expanding equation (9) gives

$$Z_{in} = R_{in} + jX_{in} = Z_{o(av.)} \coth \gamma\ell$$

$$R_{in} = Z_{o(av.)} \frac{\sinh 2\alpha\ell}{\cosh 2\alpha\ell - \cos 2\beta\ell} \qquad (11)$$

$$X_{in} = -Z_{o(av.)} \frac{\sin 2\beta\ell}{\cosh 2\alpha\ell - \cos 2\beta\ell} \qquad (12)$$

where R_{in}, X_{in} = The Input Resistance and Reactance of the Aerial.

The input resistance and reactance have been computed and plotted from equations (10), (11) and (12) and are shown tabulated below.

$\frac{\ell}{\lambda}$ \ $\frac{r}{\ell}$	R_{in} (ohms.)						
	0.001	0.005	0.010	0.020	0.030	0.040	0.050
0.10	8	8	8	8	8	8	8
0.15	20	20	20	20	20	20	20
0.20	40	40	40	40	40	39	39
0.21	45	45	45	45	45	44	44
0.22	51	51	51	51	50	50	50
0.23	58	57	57	57	56	56	56
0.24	66	65	65	65	64	63	63
0.25	73	72	72	71	70	69	69
0.26	82	81	80	79	78	77	76
0.27	91	90	89	88	87	85	84
0.30	129	126	124	121	117	115	112
0.35	236	224	215	202	191	181	173
0.40	481	419	388	339	305	279	256
0.45	1200	885	730	567	474	408	357
0.50	2710	1508	1112	772	605	500	424
0.55	1120	864	725	572	479	411	358
0.60	331	309	292	267	247	230	213
0.65	138	136	133	128	124	120	116
0.70	92	91	90	88	86	84	82
0.75	103	101	99	96	93	91	88
0.80	158	152	147	138	135	124	118
0.85	281	254	236	211	192	176	162
0.90	535	442	386	319	274	241	214
0.95	1140	770	609	451	365	306	262
1.00	1950	1076	785	540	419	342	287

$\frac{\ell}{\lambda}$ \ $\frac{r}{\ell}$	X_{in} (ohms.)						
	0.001	0.005	0.010	0.020	0.030	0.040	0.050
0.10	-1110	-844	-728	-614	-547	-500	-463
0.15	-568	-427	-366	-306	-271	-246	-226
0.20	-248	-185	-158	-131	-115	-103	-94
0.21	-195	-145	-124	-102	- 89	-81	-73
0.22	-144	-107	-91	-75	-66	-59	-54
0.23	-95	-70	-60	-49	-43	-38	-35
0.24	-47	-35	-29	-24	-21	-19	-17
0.25	0	0	0	0	0	0	0
0.26	47	34	29	24	20	18	16
0.27	93	68	57	46	40	35	32
0.30	234	169	141	112	95	84	74
0.35	493	344	279	214	176	149	129
0.40	823	514	410	292	228	185	154
0.45	1187	639	442	278	200	154	121
0.50	0	0	0	0	0	0	0
0.55	-1400	-785	-551	-350	-250	-190	-149
0.60	-882	-595	-471	-345	-274	-224	-186
0.65	-490	-346	-283	-219	-181	-154	-133
0.70	-220	-156	-129	-100	-83	-72	-62
0.75	0	0	0	0	0	0	0
0.80	211	145	116	87	72	58	49
0.85	436	284	219	156	120	96	78
0.90	684	402	291	190	138	106	83
0.95	826	398	260	152	104	75	57
1.00	0	0	0	0	0	0	0

The diagram (see later) of $\frac{r}{\ell} \Big/ \frac{\ell}{\lambda}$ for zero loop reactance has been determined from the graph for zero loop reactance and is given in tabular form below.

In addition the maximum input resistance and $\frac{\ell}{\lambda}$ ratio for a range of $\frac{r}{\ell}$ ratios were deduced from the curves of input resistance. The results are as follows:

$\frac{r}{\ell}$	$\frac{\ell}{\lambda}$	% Foreshortening	R_{in} (ohms)
0.001	0.241	3.6	66
0.005	0.238	4.8	64
0.010	0.236	5.6	61
0.020	0.233	6.8	59
0.030	0.231	7.6	58
0.040	0.230	8.0	57
0.050	0.228	8.8	56

$X_{loop} = 0.$

$\frac{r}{\ell}$	0.001	0.005	0.010	0.020	0.030	0.040	0.050
$\frac{\ell}{\lambda}$	0.50	0.50	0.50	0.50	0.50	0.50	0.50
R_{in} (ohms.)	2900	1515	1110	770	600	500	420

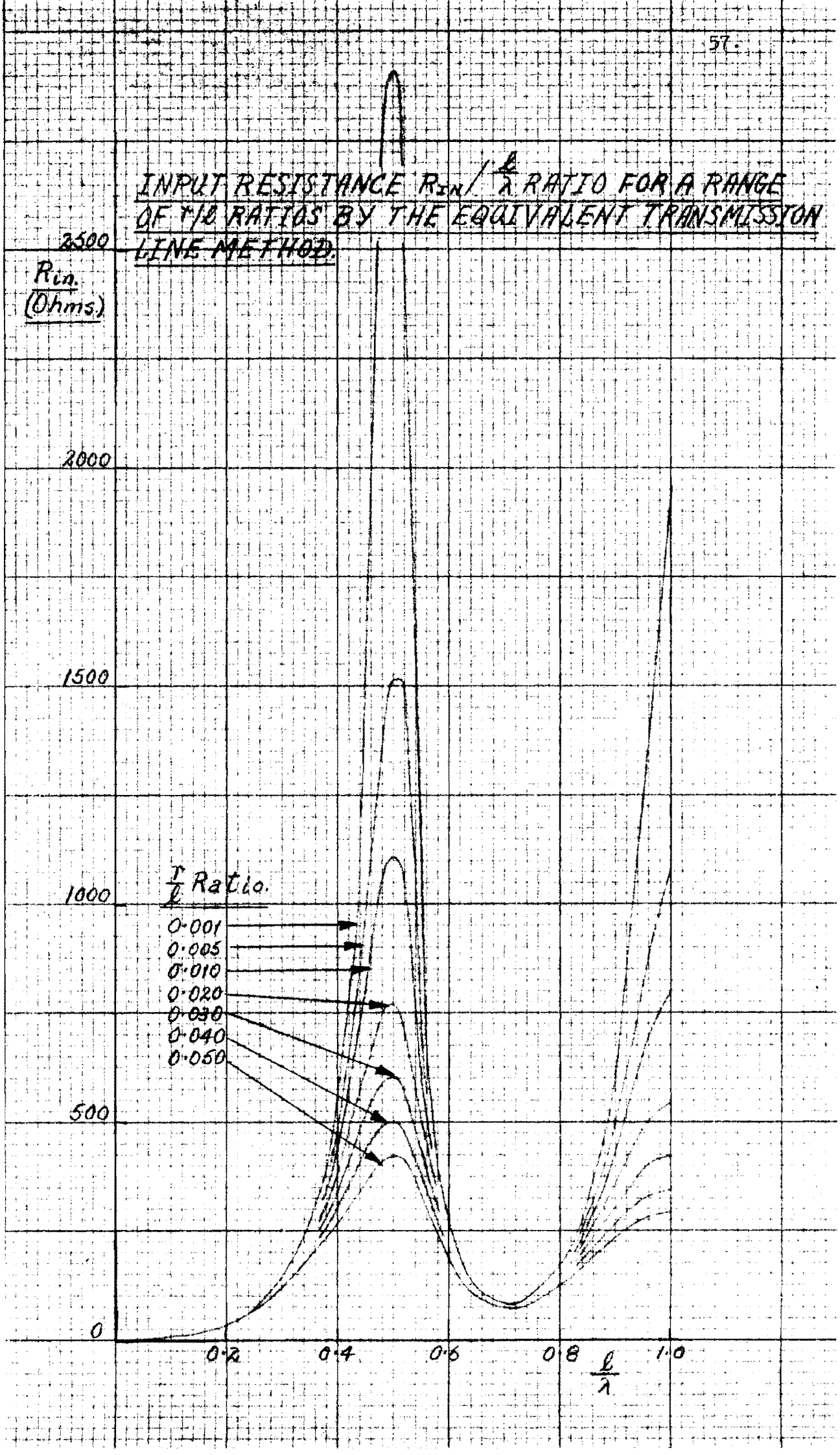
INPUT RESISTANCE R_{IN} / $\frac{\ell}{\lambda}$ RATIO FOR A RANGE OF r/ℓ RATIOS BY THE EQUIVALENT TRANSMISSION LINE METHOD.
$R_{in.}$ (Ohms.)
2500
2000
1500
1000
500
0
$\frac{r}{\ell}$ Ratio.
0·001
0·005
0·010
0·020
0·030
0·040
0·050
0·2
0·4
0·6
0·8
1·0
$\frac{\ell}{\lambda}$

INPUT REACTANCE X_{IN} / $\frac{\ell}{\lambda}$ RATIO FOR A RANGE OF $\frac{r}{\ell}$ RATIOS BY THE EQUIVALENT TRANSMISSION LINE METHOD.

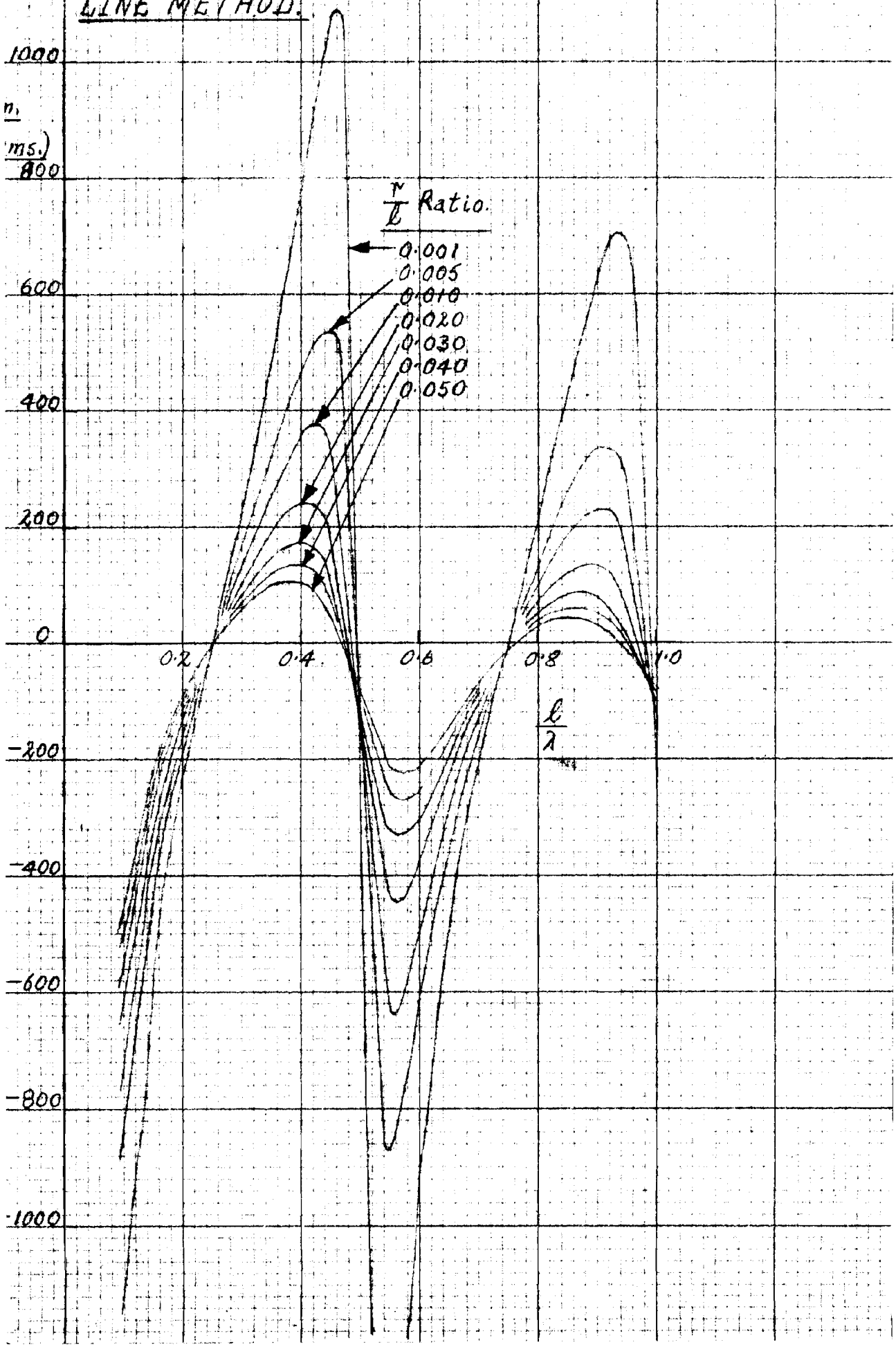

The above method shows that the first resonance occurs at $\frac{\ell}{\lambda} = 0.25$ which is known to be untrue since in practice the first resonance occurs at some $\frac{\ell}{\lambda}$ ratio less than 0.25 dependant on the r/l ratio. A further improvement on the above approximation was attempted.

$$Z_o = \sqrt{\frac{r+j\omega L}{g+j\omega C}}$$

$$\gamma = \alpha + j\beta = \sqrt{(r+j\omega L)(g+j\omega C)}$$

$$\doteq \omega\sqrt{LC}\left(j + \frac{r}{2\omega C} + \cdots\cdots\right)$$

$$\therefore \alpha = \frac{r}{2}\sqrt{\frac{C}{L}} = \frac{r}{2Z_o} = \frac{\beta}{2Q}$$

Since $\beta = \frac{2\pi}{\lambda} \doteq \omega\sqrt{LC}$

$$Q = \frac{\omega L}{r}$$

More exactly $\beta = \omega\sqrt{LC}\left(1 + \frac{r^2}{8\omega^2 L^2}\right)$

$$Z_o = \sqrt{\frac{r+j\omega L}{j\omega C}} \doteq \sqrt{\frac{L}{C}}\left(1 - j\frac{r}{2\omega L}\right)$$

$$= |Z_o|\left(1 - j\frac{\alpha}{\beta}\right) \qquad (13)$$

Substituting equation (13) in equations (11) and (12) gives

$$R_{in} = Z_o \frac{\sinh 2\alpha\ell - \frac{\alpha}{\beta}\sin 2\beta\ell}{\cosh 2\alpha\ell - \cos 2\beta\ell} \qquad (14)$$

$$X_{in} = -Z_o \frac{\sin 2\beta\ell + \frac{\alpha}{\beta}\sinh 2\alpha\ell}{\cosh 2\alpha\ell - \cos 2\beta\ell} \qquad (15)$$

The above equation shows that first resonance will occur at a $\frac{\ell}{\lambda}$ ratio greater than 0.25 which is untrue so that the above approximations break down.

Siegel has shown by considering the fundamental telegraph equations and using the scalar and vector potential method the non validity of linear relations between vector potential A and current and scalar potential V and voltage in the "terminal" zone of an aerial. The terminal zone is only a short distance from the open circuit but the results greatly affect the current and voltage relationships of the aerial. The results obtained by Siegel are not directly applicable here but calculations of aerial

foreshortening and current distribution by modifications of this method agree well with experimental values.

(5) The Input Impedance by the Biconical Aerial Method.[11,29]

The following subsection has been treated in detail since most of the important impedance phenomena follow from the results.

The biconical aerial is important because it has a uniform characteristic impedance and Schelkunoff has obtained characteristics for this aerial and other shapes by defining for shapes with variable characteristic impedance an average characteristic impedance with respect to length and using the biconical aerial as a basis for analysis. An aerial has an infinite number of oscillation modes of which the "principal mode" is dominant. Wherever a discontinuity occurs higher oscillation modes occur but these are rapidly attenuated so that aerials may be considered in terms of principal waves only with lumped reactances at discontinuities. The biconical aerial is a uniform transmission line with an abrupt discontinuity at the surface of the sphere surrounding the aerial. Consequently the current along the cones may be resolved into

(a) a wave travelling outwards from the apex,

(b) a wave of smaller amplitude travelling inwards,

(c) waves representing higher oscillation modes travelling inwards but suffering rapid attenuation.

The principal wave is given by (a) and (b). If the capacity of the end caps is negligible the total current at the end of the cones will be zero and the sum of (b) and (c) will be equal to (a). The higher modes (c) are small except at the extreme ends of the aerial, hence the input impedance depends only on the principal wave. The problem of the biconical aerial is one of finding the appropriate boundary conditions at the sphere of discontinuity and

expressing them in the form of a complex impedance. This impedance is therefore the apparent termination of the line, so that the input impedance may be calculated by normal transmission line methods on the assumption of a principal wave only. The physical significance of the aerial problem is best understood from the following remarks due to Schelkunoff.[29]

"It is permissible to think that a wave emerging from a generator in the center of an antenna is guided by an antenna until it reaches its "boundary sphere" passing through the ends of the antenna and separating the antenna region from the external space; at the boundary sphere some energy passes into the external space and some is reflected back - a situation existing at the juncture between two transmission lines with different characteristic impedances. We may also think of the antenna as the wall of an electric horn with an aperture so wide that one can hardly see the horn itself - just like a Chesire Cat: only the grin can be seen. In fact, the mathematics that we use is that appropriate to waveguides and electric horns."

The following analysis considers a biconical aerial and deduces the results for a cylindrical aerial.[10,32]

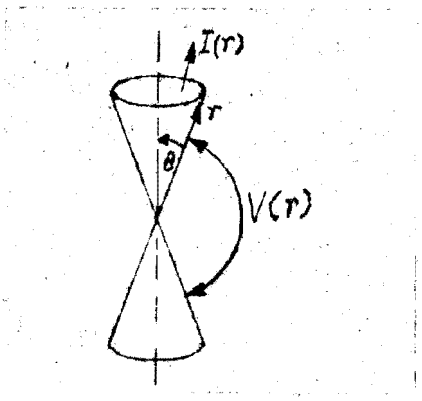

Consider the accompanying diagram; for a biconical transmission line the principal wave is such that the electric intensity $\underline{E}$ follows the lines of longitude and the magnetic intensity $\underline{H}$ the lines of latitude.

In Spherical Co-ordinates (r, θ, ϕ)

$$E_r = H_r = E_\phi = H_\theta = 0 \qquad E_\theta = \underline{E} \qquad H_\phi = \underline{H}$$

Let $I(r)$ = The total current along the cone

$V(r)$ = The voltage between cones along a line of longitude.

$$I(r) = 2\pi r \sin\theta \, H_\phi$$

$$V(r) = -\int r E_\theta \, d\theta$$

From Maxwell's Equations

$$\frac{\partial}{\partial r}(rH_\phi) = -j\omega\epsilon r E_\theta$$

$$\frac{\partial}{\partial r}(rE_\theta) = -j\omega\mu r H_\phi$$

where for free space $g = 0$

The equivalent transmission line equations are

$$\frac{\partial V}{\partial r} = -j\omega L I \quad ; \qquad \frac{\partial I}{\partial r} = -j\omega C V$$

Solving $C = \dfrac{\pi\epsilon}{\log(\cot\frac{\theta}{2})}$

$$L = \frac{\mu}{\pi}\log(\cot\frac{\theta}{2})$$

$$K = Z_0 = \sqrt{\frac{L}{C}} = 120\log(\cot\frac{\theta}{2})$$

$\eta = \sqrt{\dfrac{\mu}{\epsilon}}$ = The intrinsic impedance for free space

$= 120\pi$

For narrow cones

$$K = 120\log\frac{2}{\theta} = 120\log\frac{2\ell}{a}$$

where

ℓ = The length of a single cone

a = The radius at the end of a cone.

The principal voltage and current in terms of positive and negative waves are

$$V_o(r) = V_o^+ e^{-j\beta r} + V_o^- e^{j\beta r} \qquad V_o^+ = KI_o^+$$

$$I_o(r) = I_o^+ e^{-j\beta r} + I_o^- e^{j\beta r} \qquad V_o^- = -KI_o^-$$

At the sphere of discontinuity $r = \ell$ and the total current disappears giving

$$I_o(r) = I_o \sin\beta(\ell - r) \qquad V_o = -jKI_o$$

$$V_o(r) = V_o \cos\beta(\ell - r)$$

If the spherical sheet at $r = \ell$ has a finite impedance then

$$I_o(r) = I_o \sin\beta(\ell - r) + I^\circ \cos\beta(\ell - r)$$

$$V_o(r) = V_o \cos\beta(\ell - r) + V^\circ \sin\beta(\ell - r)$$

$$V_o = -jKI_o \qquad V^\circ = jKI^\circ$$

The Input Impedance

$$Z_{in} = \frac{V_o(o)}{I_o(o)} = K\,\frac{-jI_o\cos\beta\ell + jI^\circ\sin\beta\ell}{I_o\sin\beta\ell + I^\circ\cos\beta\ell}$$

The Terminal Impedance

$$Z_t = \frac{V_o(\ell)}{I_o(\ell)} = \frac{V_o}{I^\circ} = -\frac{jKI_o}{I^\circ}$$

The mathematical equations derived above would be valid if the space outside the boundary sphere did not exist. The space outside the boundary sphere acts as a transmission line in which several transmission modes are present. The imperfect conductivity of an aerial will manifest itself largely through the principal wave.

$$\gamma = \alpha + j\beta = \frac{R}{2K} + j\beta$$

where R = The resistance of both cones per unit length.

Then $I_o(r) = -jI_o \sinh\gamma(\ell - r) + I^\circ \cosh\gamma(\ell - r)$

$$V_o(r) = -jKI_o \cosh\gamma(\ell - r) + KI^\circ \sinh\gamma(\ell - r)$$

If K is large and the total current is zero at the end of the aerial it may be shown that

$$\frac{I^o}{I_o} = \frac{F(\beta\ell) - jG(\beta\ell)}{K}$$

where F and G are functions of $\beta\ell$

$$Z_t = -jK\frac{I_o}{I^o} = \frac{K^2}{G+jF}$$

Substitute for $\frac{I^o}{I_o}$ in the equation for the input impedance and on reduction

$$Z_{in} = \frac{G - j\left\{\frac{K}{2}\sin 2\beta\ell + F\cos 2\beta\ell - \frac{F^2+G^2}{2K}\sin 2\beta\ell\right\}}{\sin^2\beta\ell + \frac{F}{K}\sin 2\beta\ell + \frac{F^2+G^2}{K^2}\cos^2\beta\ell}$$

Formulae for F and G may be developed from the unrationalized form of Z_{in}

$$Z_{in} = K\frac{G\sin\beta\ell + j(F\sin\beta\ell - K\cos\beta\ell)}{(K\sin\beta\ell + F\cos\beta\ell) - jG\cos\beta\ell}$$

$$= K\left\{\frac{(G+jF)\sin\beta\ell - jK\cos\beta\ell}{K\sin\beta\ell - j(G+jF)\cos\beta\ell}\right\}$$

$$= \frac{(G+jF) - jK\cot\beta\ell}{1 - j\left(\frac{G+jF}{K}\right)\cot\beta\ell}$$

Let $K \to \infty$

$$= \left\{(G+jF) - jK\cot\beta\ell\right\}\left\{1 + j\frac{G+jF}{K}\cot\beta\ell\right\}$$

$$= \frac{G+jF}{\sin^2\beta\ell} - jK\cot\beta\ell$$

As $K \to \infty$ $I^o \to 0$ $\gamma \to j\beta$ $\therefore I_{in} \to I_o\sin\beta\ell$

The Complex Power Flow

$$= \frac{1}{2}Z_{in}I_{in}^2$$

$$= \frac{1}{2}\left\{G(\beta\ell) + jF(\beta\ell) - \frac{1}{2}jK\sin 2\beta\ell\right\}I_o^2$$

The complex input power may be obtained by the induced e.m.f. method. The real part of which gives $G(\beta\ell)$ which will be independent of the antenna shape and will consequently be the same as that calculated for the infinitely thin cylindrical antenna. However the reactive part which

determines $F(\beta\ell)$ will be a function of shape which must be taken into account. By comparing the above form for the complex power input with

$$-\frac{1}{2}\int_{-\ell}^{+\ell} E_r(r)\, I(r)\, dr$$

the following results for F and G are obtained.

$$G(L) = 60(C+\log 2L - Ci\,2L) + 30(C+\log L - 2Ci\,2L + Ci\,4L)\cos 2L + 30(Si\,4L - 2Si\,2L)\sin 2L$$

$$F(L) = 60\,Si\,2L + 30(Ci\,4L - \log L - C)\sin 2L - 30\,Si\,4L\cos 2L$$

where $L = \beta\ell$

Consider now the deviation from the resonant length

$$X_{in} = 0 \quad \text{when}$$

$$\frac{K}{2}\sin 2\beta\ell + F\cos 2\beta\ell - \frac{F^2+G^2}{2K}\sin 2\beta\ell = 0$$

$$\therefore \tan 2\beta\ell = \frac{-2KF}{K^2-(F^2+G^2)}$$

To first order in K. $\tan 2\beta\ell = -\frac{2F}{K}$

$$\therefore 2\beta\ell \doteq n\pi - \frac{2F(\frac{n\pi}{2})}{K}$$

where $n = 1, 2, 3,$

$$\frac{4\ell}{n\lambda} = 1 - \frac{120\,Si(n\pi) + 60(-1)^{n+1}Si(2n\pi)}{\pi n K}$$

The deviation from the resonant length is consequently

$$1 - \frac{4\ell}{n\lambda} = \frac{120\,Si(n\pi) + 60(-1)^{n+1}Si(2n\pi)}{\pi n K}$$

The above analysis is for a biconical aerial. The following remarks apply to a cylindrical aerial.

If the transverse dimensions of a cylindrical aerial are small it will support approximately spherical waves. The distributed shunt capacitance, series inductance and transmission equations for principal waves are defined as for the biconical aerial and a new quantity called the average characteristic impedance is defined.

$$C = \frac{\pi\epsilon}{\log\frac{2r}{\rho}} \qquad L = \frac{\mu}{\pi}\log\frac{2r}{\rho}$$

$$\frac{\partial V}{\partial r} = -j\omega LI \qquad \frac{\partial I}{\partial r} = -j\omega CV$$

$$K(r,\rho) = \frac{1}{\pi}\sqrt{\frac{\mu}{\epsilon}}\log\frac{2r}{\rho} = 120\log\frac{2r}{\rho}$$

ρ = The radius of the cylindrical aerial

r = The distance from the centre feed point along the aerial.

The average characteristic impedance

$$K_a = \frac{1}{\ell}\int_0^{\ell} K(r,\rho)\,dr$$

$$= 120\left(\log\frac{2\ell}{a} - 1\right)$$

As $K_a \longrightarrow \infty \quad \frac{K(r,\rho) - K_a}{K_a} \longrightarrow 0$

Hence a line with characteristic impedance K_a is a first approximation to the non-uniform line.

The foreshortening of a cylindrical aerial is determined as follows:

The transmission line equations are

$$\frac{dV}{dr} = -j\omega LI \qquad \frac{dI}{dr} = -j\omega CV$$

Let I^x and V^x = The conjugates of I and V.

Then $$V(\ell)\bar{I}(\ell) - V(0)I^x(0) = j\omega\int_0^{\ell}(CVV^x - LII^x)\,dr$$

If the termination of the transmission line is open circuited the left hand side is zero

$$\therefore \int_0^{\ell} CVV^x\,dr = \int_0^{\ell} LII^x\,dr$$

Now $LC = \frac{1}{V^2}$

$$I = \frac{j}{\omega L}\frac{dV}{dr} = j\frac{V^2C}{\omega}\frac{dV}{dr}$$

$$V = j\frac{V^2L}{\omega}\frac{dI}{dr}$$

$$\therefore \int_0^{\ell} C\left|j\frac{V^2L}{\omega}\frac{dI}{dr}\right|^2 dr = \int_0^{\ell} L|I|^2\,dr$$

$$\therefore \frac{\omega^2}{V^2} = \frac{4\pi^2}{\lambda^2} = \frac{\int_0^{\ell} L\left|\frac{dI}{dr}\right|^2 dr}{\int_0^{\ell} L|I|^2 dr} = \frac{\int_0^{\ell} C\left|\frac{dV}{dr}\right|^2 dr}{\int_0^{\ell} C|V|^2 dr}$$

Assuming a simusoidal theory and considering the first resonance only

$$I(r) = I_m \cos\frac{\pi r}{2\ell} \qquad V(r) = V_m \sin\frac{\pi r}{2\ell}$$

Also $$\frac{4\pi^2}{\lambda^2} = \frac{\int_0^\ell L\left|\frac{dI}{dr}\right|^2 dr}{\int_0^\ell L\,|I|^2 dr}$$

Substitution and reduction gives

$$\frac{16\ell^2}{\lambda^2} = \frac{1-\chi}{1+\chi}$$

where $$\chi = \frac{\int_0^\ell L\cos\frac{\pi r}{\ell}\,dr}{\int_0^\ell L\,dr}$$

For a cylindrical wire $L(r) = \frac{\mu}{\pi}\log\frac{2r}{\rho}$

Hence $$\chi = -\frac{120\,Si\,\pi}{\pi K_a}$$

From above $$\frac{4\ell}{\lambda} = 1-\chi+Const.$$

Also it was shown earlier that

$$\frac{4\ell}{n\lambda} = 1-\frac{2F\left(\frac{n\pi}{2}\right)}{\pi n K_a}$$

For the first resonance $n = 1$ and allowing for χ the coefficient of non-uniform distribution of L and C gives

$$\frac{4\ell}{\lambda} = 1-\frac{2F\left(\frac{\pi}{2}\right)}{\pi K_a} - \chi$$

$$\therefore 1-\frac{4\ell}{\lambda} = \frac{60\,Si\,2\pi}{\pi K_a} = \frac{27{\cdot}08}{K_a} \qquad (17)$$

By a similar process the foreshortening for the second resonance may be shown to be

$$1-\frac{2\ell}{\lambda} = \frac{39{\cdot}92}{K_a}$$

The average characteristic impedance K_a represents the effect of the aerial size on the resonant length. The variation in resonant length is small with change in r/l ratio. The following table has been computed from equation (17) and agrees well with known values.

$\frac{r}{\ell}$	$\frac{\ell}{\lambda}$	% Foreshortening
0.001	0.241	3.6
0.005	0.239	4.4
0.010	0.237	5.2
0.020	0.234	6.4
0.030	0.232	7.2
0.040	0.230	8.0
0.050	0.229	8.4

The input impedance of a cylindrical aerial may be found by treating the aerial as a transmission line with slightly varying characteristic impedance. The following solution is based on Picard's Method of solving differential equations with non-constant coefficients and is due to Carson.[33,34] The following analysis is given briefly and only serves as an indication of the method.

The line parameters (r, L, g, C) are assumed to be varying functions of distance.

The line equations are

$$\frac{dV}{dx} = -Z(x)I = -ZI$$

$$\frac{dI}{dx} = -Y(x)V = -YV$$

$$Z = r + j\omega L \qquad Y = g + j\omega C$$

Assume steady state conditions and integrate

$$V = V_0 - \int_0^x ZI\,dx \quad ; \quad I = I_0 - \int_0^x YV\,dx$$

By repeated approximations V and I are the limits of the infinite sequences defined below.

$$V_0 V_1 \ldots\ldots\ldots\ldots V_n$$

$$I_0 I_1 \ldots\ldots\ldots\ldots I_n$$

$$V_1 = V_0 - \int_0^x Z I_0\,dx \qquad I_1 = I_0 - \int_0^x Y V_0\,dx$$

$$V_n = V_0 - \int_0^x Z I_{n-1}\,dx \qquad I_n = I_0 - \int_0^x Y V_{n-1}\,dx$$

Let $r_0 = s_0 = 1$

$$r_n = \int_0^x Z\, s_{n-1}\, dx \qquad s_n = \int_0^x Y\, r_{n-1}\, dx$$

Then it may be proved by induction that

$$V_n = V_0 \sum_{n=0}^{\infty} r_{2n} - I_0 \sum_{n=0}^{\infty} r_{2n-1}$$

$$I_n = V_0 \sum s_{2n} - I_0 \sum s_{2n-1}$$

Consider now the case of a cylindrical aerial in which the variations of line parameters are small

$$Z = Z_0(1 + z(x))$$

$$Y = Y_0(1 + y(x))$$

where Z_0, Y_0 are the mean values of Z and Y and z and y are functions of x less than unity.

Let $$\gamma = \sqrt{Z_0 Y_0}$$

$$K_0 = \sqrt{\frac{Z_0}{Y_0}}$$

and z_{jK}, y_{jK} be given by

$$\frac{x^K}{K!}\begin{pmatrix} z_{jK} \\ y_{jK} \end{pmatrix} = \int_0^x \frac{x_1^{j-K}(x-x_1)^{K-j}}{(K-j)!(K-1)!}\begin{pmatrix} z(x_1) \\ y(x_1) \end{pmatrix} dx_1$$

To first order the following results for the voltage and current coefficients are obtained

$$r_n = \frac{(\gamma x)^n}{n!}\left(1 + z_{1n} + y_{2n} + z_{3n} + \cdots\cdots + y_{nn}\right)$$

$$s_n = \frac{(\gamma x)^n}{n!}\left(1 + y_{1n} + z_{2n} + y_{3n} + \cdots\cdots + z_{nn}\right)$$

when n is even.

$$r_n = K_0\frac{(\gamma x)^n}{n!}\left(1 + z_{1n} + y_{2n} + z_{3n} + \cdots\cdots + z_{nn}\right)$$

$$s_n = \frac{(\gamma x)^n}{K_0 n!}\left(1 + y_{1n} + z_{2n} + y_{3n} + \cdots\cdots + y_{nn}\right)$$

when n is odd.

Summing the above results gives

$$\sum s_{2n} = (1 - d_1)\cosh \gamma x + (d_2 + d_3)\sinh \gamma x$$

$$\sum r_{2n} = (1 + d_1)\cosh \gamma x - (d_2 - d_3)\sinh \gamma x$$

$$K_o \leq S_{2n-1} = (1+d_1)\sinh \gamma x - (d_2 - d_3)\cosh \gamma x$$

$$\frac{1}{K_o} \leq r_{2n-1} = (1-d_1)\sinh \gamma x + (d_2 + d_3)\cosh \gamma x$$

where
$$d_1 = \frac{\gamma}{2}\int_o^x \sinh 2\gamma x \,(z(x) - y(x))\,dx$$

$$d_2 = \frac{\gamma}{2}\int_o^x \cosh 2\gamma x \,(z(x) - y(x))\,dx$$

$$d_3 = \frac{\gamma}{2}\int_o^x (z(x) - y(x))\,dx$$

The line equations for current and voltage are now defined in terms of $\gamma, K_o, d_1, d_2, d_3$

$$Z_o = j\omega L \qquad Y_o = j\omega C$$

$$\gamma = \sqrt{Z_o Y_o} = j\omega\sqrt{LC} = j\beta$$

$$K_o = \sqrt{\frac{Z_o}{Y_o}} = \sqrt{\frac{L}{C}} \doteq K_a \;;\; \sqrt{\frac{Z}{Y}} = K(r,\rho)$$

$$\frac{Z}{Y} = \frac{Z_o}{Y_o}\frac{(1+z)}{(1+y)} \doteq \frac{Z_o}{Y_o}(1+z-y)$$

$$z(r) - y(r) = \frac{\frac{Z}{Y} - \frac{Z_o}{Y_o}}{\frac{Z_o}{Y_o}} = \frac{K(r,\rho)^2 - K_a^2}{K_a^2}$$

$$\doteq -\frac{2}{K_a}\left(K_a - K(r,\rho)\right) \quad \text{since} \quad K_a \doteq K(r,\rho)$$

$$d_1 = \frac{\gamma}{2}\int_o^r \sinh 2\gamma r \,\{z(r) - y(r)\}\,dr$$

$$= \frac{\beta}{K_a}\int_o^r \{K_a - K(r,\rho)\}\sin 2\beta r\,dr$$

$$= \frac{M(\beta r)}{K_a} \quad \text{where} \quad M(\beta r) = \beta\int_o^r \{K_a - K(r,\rho)\}\sin 2\beta r\,dr$$

$$d_2 = \frac{\gamma}{2}\int_o^r \cosh 2\gamma r \,\{z(r) - y(r)\}\,dr$$

$$= -\frac{j\beta}{K_a}\int_o^r \{K_a - K(r,\rho)\}\cos 2\beta r\,dr$$

$$= -\frac{jN(\beta r)}{K_a} \quad \text{where} \quad N(\beta r) = \beta\int_o^r \{K_a - K(r,\rho)\}\cos 2\beta r\,dr$$

$$d_3 = \frac{\gamma}{2}\int_o^r \{z(r) - y(r)\}\,dr \doteq 0$$

Substitute for $\gamma, K_o, d_1, d_2, d_3$ in terms of K_a, M, N and βr in the formulae for $\leq S_{2n}, \leq r_{2n}, \leq r_{2n-1}$ and $\leq S_{2n-1}$ Then substitute these results in the equations for V and I.

$$V = V_o \leq r_{2n} - I_o \leq r_{2n-1}$$

$$I = I_o \leq S_{2n} - V_o \leq S_{2n-1}$$

and noting that

$$\frac{V_o}{I_o} = \left(\frac{V_o}{I_o}\right)_{r=\ell} = Z_t = \frac{K_a^2}{G(L) + jF(L)}$$

gives $Z_{in} = \left(\frac{V}{I}\right)_{r=\ell}$. The value of Z_{in} obtained becomes as below on neglecting terms of order $\frac{1}{K_a}$ and higher

$$Z_{in} = K_a \frac{G\sin L + j\{(F-N)\sin L - (K_a - M)\cos L\}}{\{(K_a+M)\sin L + (F+N)\cos L\} - jG\cos L}$$

Rationalizing this function gives

$$R_{in} = \frac{GK_a(K_a + N\sin 2L - M\cos 2L)}{G^2\cos^2 L + \{(K_a+M)\sin L + (F+N)\cos L\}^2}$$

$$X_{in} = K_a \frac{\frac{1}{2}(G^2 - K_a^2 + M^2 + F^2 - N^2)\sin 2L + (MN - FK_a)\cos 2L + (MF - NK_a)}{G^2\cos^2 L + \{(K_a+M)\sin L + (F+N)\cos L\}^2}$$

The following formulae are obtained for M and N for cylindrical aerials.

$$K(r,\rho) = 120 \log \frac{2r}{\rho}$$

$$K_a = 120\left(\log \frac{2\ell}{a} - 1\right)$$

$$M(L) = \beta \int_0^{\ell} (K_a - K(r,\rho)) \sin 2\beta r \, dr$$

$$= 60(\cos 2L - 1 + \log 2L - Ci\,2L + C)$$

$$N(L) = \beta \int_0^{\ell} (K_a - K(r,\rho)) \cos 2\beta r \, dr$$

$$= 60\,(Si\,2L - \sin 2L) \qquad L = \beta\ell$$

The following table has been computed from the formulae for F, G, M and N and from these results the table of input impedance has been calculated and plotted. The symbol a is now replaced by r to fit in with the other theoretical results.

$\frac{\ell}{\lambda}$	F(L)	G(L)	M(L)	N(L)
0.10	57.4	2.9	-19.3	12.0
0.15	92.4	13.2	-32.5	36.0
0.20	126.9	36.1	-35.5	71.6
0.21	133.2	42.5	-34.3	79.6
0.22	139.1	49.4	-32.0	87.5
0.23	144.5	56.8	-29.2	95.7
0.24	149.3	65.7	-25.5	103.5
0.25	153.7	73.1	-21.1	111.1
0.26	157.2	81.9	-15.9	118.6
0.27	160.1	91.1	-10.1	125.5
0.30	164.0	119.8	11.6	143.4
0.35	152.8	166.5	56.2	157.8
0.40	121.5	200.7	101.3	150.0
0.45	79.4	212.7	134.2	122.0
0.50	40.3	199.0	146	85.0
0.55	18.4	165.3	135	51.5
0.60	22.8	124.6	107	33.8
0.65	53.2	93.0	75.1	38.6
0.70	109.6	84.7	52	63.9
0.75	146.0	105.5	48.6	100.5
0.80	174.9	150.4	67.6	134.8
0.85	174.9	205.0	103	153.5
0.90	144.8	250.7	144	150.2
0.95	96.1	271.6	176	125.8
1.00	43.6	259.6	186	89.5

$\frac{\ell}{\lambda}$ \ $\frac{r}{\ell}$	R_{in} (Ohms.)							X_{in} (Ohms.)						
	0.001	0.005	0.010	0.020	0.030	0.040	0.050	0.001	0.005	0.010	0.020	0.030	0.040	0.050
0.10	7.2	6.8	6.6	6.3	6.1	5.9	5.8	-980	-716	-600	-489	-424	-378	-344
0.15	18.0	17.3	16.9	16.4	16.0	15.6	15.3	-505	-366	-304	-246	-212	-187	-169
0.20	37.9	37.3	36.9	36.3	35.8	35.4	35.2	-207	-144	-117	-90	-74.3	-63.1	-54.7
0.21	43.5	42.9	42.7	42.3	41.8	41.4	41.0	-154	- 105	-83.5	-62.4	-50.2	-40.7	-34.7
0.22	50.1	49.7	49.5	48.8	48.5	48.4	48.1	-104	-67.2	-50.6	-34.8	-25.4	-18.7	-14.4
0.23	57.2	57.0	57.0	57.0	56.6	56.8	56.4	-54.3	-30.1	-18.9	-8.4	-2.1	2.6	5.3
0.24	66.8	67.1	67.0	67.5	67.6	67.7	67.9	-5.5	7.0	12.6	18.1	20.8	23.3	25.6
0.25	75.4	76.0	76.2	77.2	77.5	78.0	78.3	43.9	43.9	44.0	44.7	45.0	45.4	45.1
0.26	86.6	87.3	88.4	89.9	91.0	91.8	92.6	93.5	81.2	75.4	70.9	69.0	66.5	65.1
0.27	99.3	101.5	103	105	107	109	110	145	119	109	98.6	93	89.5	85.6
0.30	152	158.3	163.7	170.8	176	181.3	188	302	236	207	178	159	145	136
0.35	333	359	372	394	406	411	409	613	446	354	258	189	125	72.4
0.40	825	814	758	638	529	429	354	979	525	288	51.9	-69	-138	-171
0.45	2075	1260	898	560	396	289	224	720	256	-131	-188	-187	-174	-162
0.50	1850	977	689	446	330	254	206	-1170	-616	-434	-280	-207	-160	-130
0.55	629	466	386	303	254	217	192	-1156	-675	-488	-325	-242	-185	-149
0.60	230	200	185	164	150	139	130	-736	-484	-378	-275	-219	-179	-152
0.65	110	102	96.4	90.6	86.1	82.7	79.9	-424	-288	-228	-174	-142	-119	-103.5
0.70	79.7	75.8	74.0	70.8	68.5	66.5	65.0	-169.8	-109	-83	-58.4	-44.4	-34.1	-27.3
0.75	99.5	97.6	96.5	94.9	93.7	92.9	91.8	-42.8	-41.9	-41.7	-41.0	-40.5	-40.1	-39.3
0.80	175	177	180	182	183	183.5	185	277	210	181	149	131	116	106
0.85	372	383	391	390	387	379	367	548	370	278	182	114	60.7	18
0.90	867	767	669	517	409	319	257	760	317	114	-61.5	-136	-174	-191
0.95	1666	924	629	377	257	180	134	316	-91	-162	-175	-163	-147	-135
1.00	1470	752	519	323	231	171	134	-745	-386	-266	-165	-118.5	-88.2	-68.8

INPUT RESISTANCE / $\frac{\ell}{\lambda}$ RATIO FOR A RANGE OF $\frac{r}{\ell}$ RATIOS BY THE BICONICAL AERIAL METHOD.

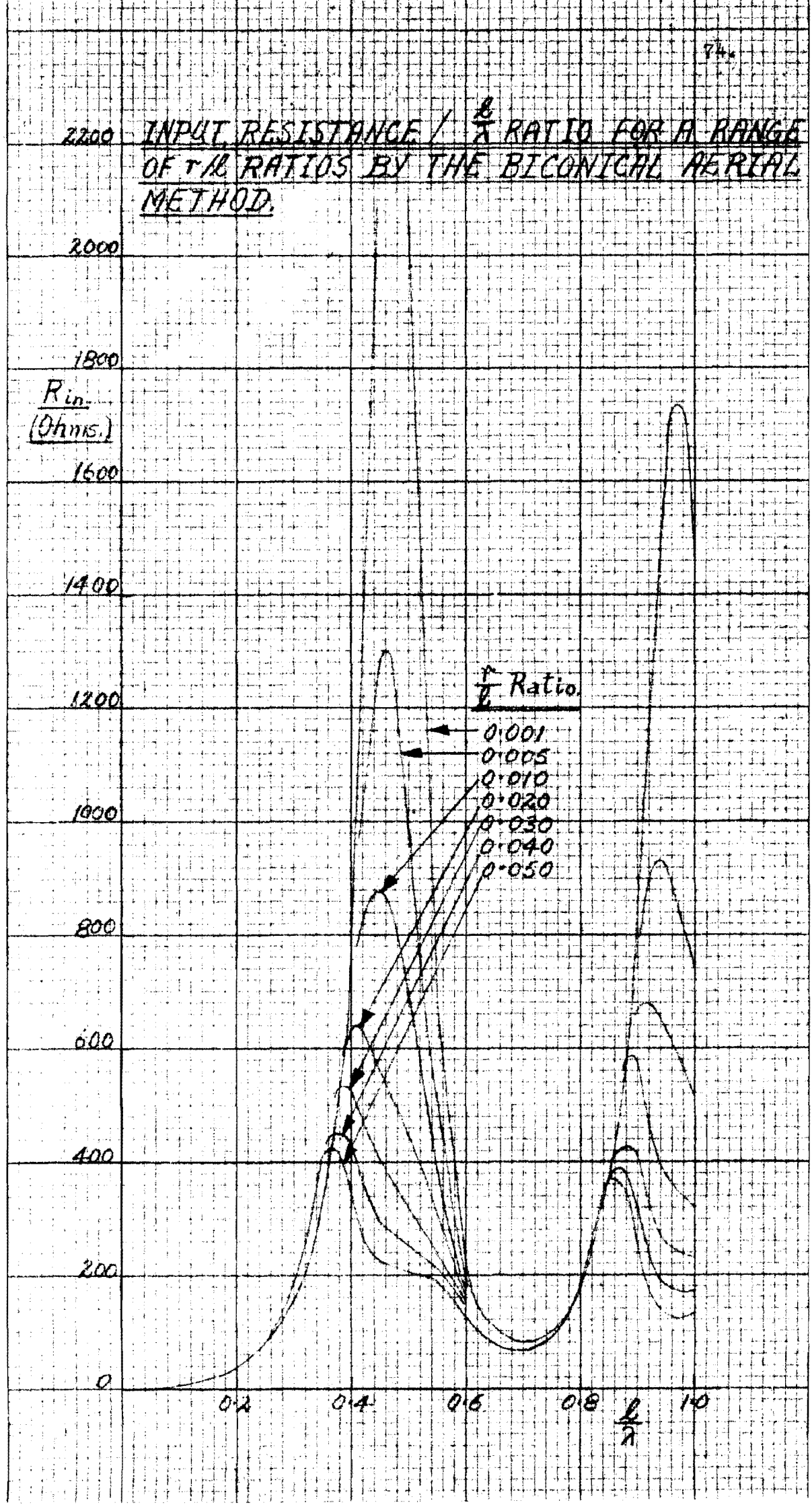

INPUT REACTANCE / $\frac{\ell}{\lambda}$ RATIO FOR A RANGE OF $\frac{r}{\ell}$ RATIOS BY THE BICONICAL AERIAL METHOD.

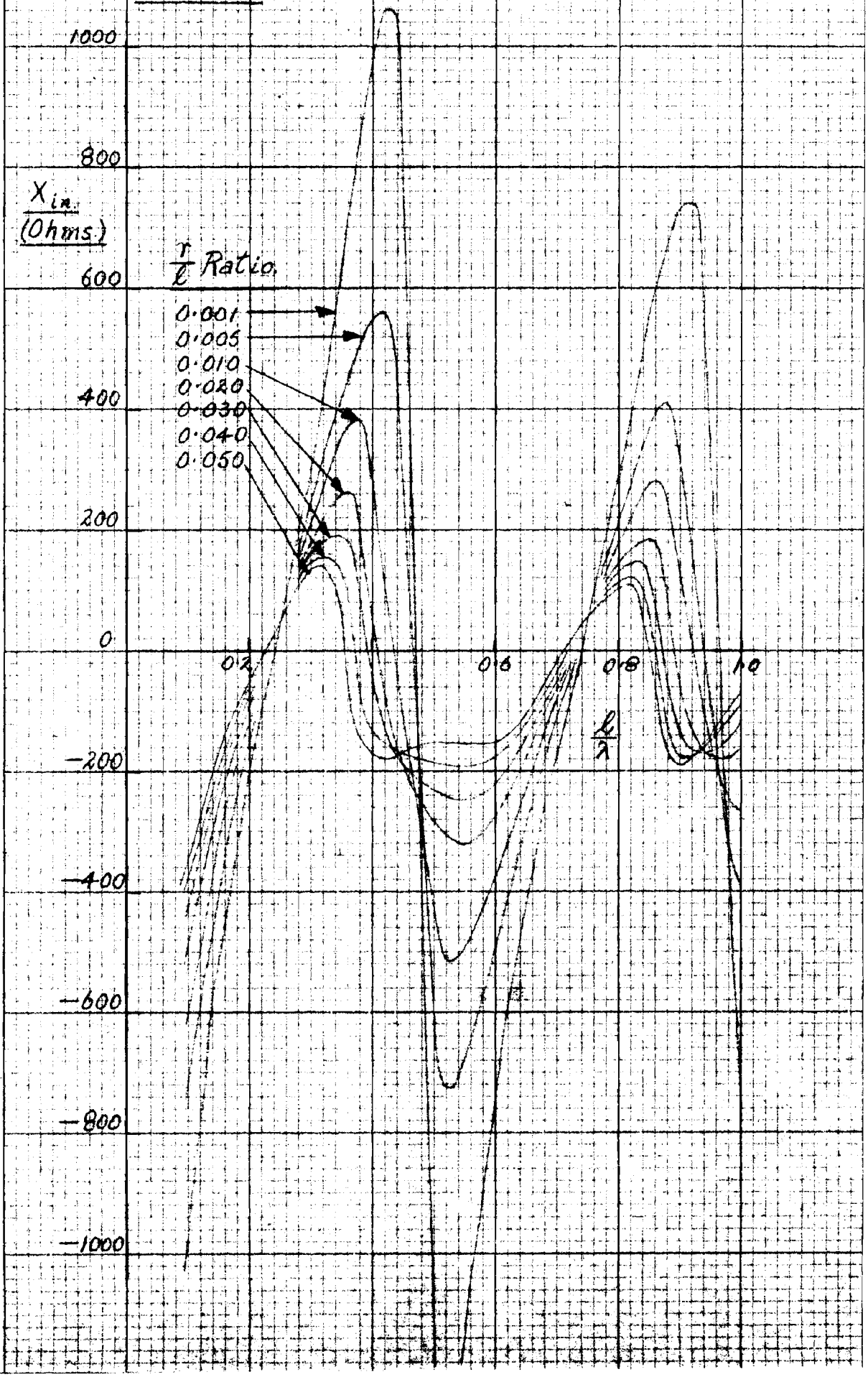

The values of R_{in} against r/l for zero input reactance and r/l against Foreshortening have been deduced from the above tables and are tabulated below.

$\frac{r}{\ell}$	$\frac{\ell}{\lambda}$	% Foreshortening	R_{in} (ohms.)
0.001	0.241	3.6	67.7
0.005	0.238	4.8	65.1
0.010	0.236	5.6	63.0
0.020	0.233	6.8	60.2
0.030	0.231	7.6	57.7
0.040	0.229	8.4	56.0
0.050	0.227	9.2	53.9

$X_{in} = 0$

The maximum input resistance and $\frac{\ell}{\lambda}$ ratio for a range of constant r/l ratios were deduced from the curves of input resistance. The results are as follows:

$\frac{r}{\ell}$	0.001	0.005	0.010	0.020	0.030	0.040	0.050
$\frac{\ell}{\lambda}$	0.470	0.460	0.450	0.410	0.390	0.375	0.367
R (ohms)	2700	1300	880	640	530	450	425

(6) <u>The Input Impedance by the Cylindrical Aerial Method.</u>[35-43]

The method involves setting up an integral equation for current. Approximate solutions of this integral equation give the current distribution. If the potential across the input terminals is known the input impedance is obtained as the ratio of the voltage to the current at the terminals. The method has the advantage that the degree of approximation is known at any stage in the iteration.

The following paragraphs give the derivation of the current distribution and input impedance by this method.

Consider a cylindrical centre fed dipole aerial of radius r and length 2ℓ as in the diagram.

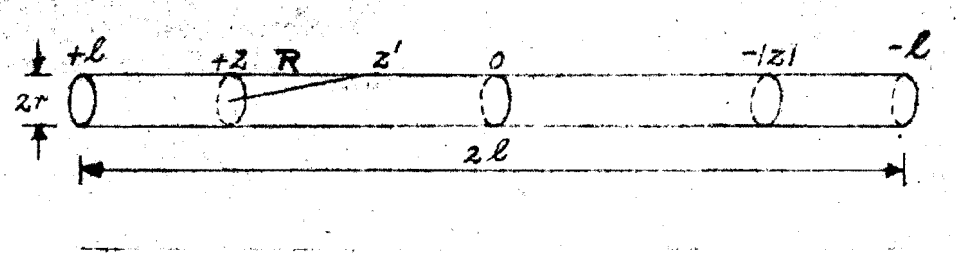

The components of the electric field are equal at the boundary of the cylindrical surface

$$(E_z)_1 = (E_z)_2$$

where $(E_z)_1$ is the field intensity at $\rho = r - \delta r$

$(E_z)_2$ is the field intensity at $\rho = r + \delta r$

and $\delta r \to 0$

Also the radial components of field intensity are equal at the boundary of the end face

$$(E_\rho)_1 = (E_\rho)_2$$

where $(E_\rho)_1$ is the field intensity at $\rho = \ell - \delta\ell$ or $-\ell + \delta\ell$

$(E_\rho)_2$ is the field intensity at $\rho = \ell + \delta\ell$ or $-\ell - \delta\ell$

and $\delta\ell \to 0$

We assume that the aerial is centre driven by a slice generator at $z = 0$. The scalar potential difference $V_2 = \lim_{z\to 0}\left(\phi_2(+z) - \phi_2(-z)\right) = \phi_2(+0) - \phi_2(-0)$ is maintained between the faces. Also all other conductors and dielectrics are assumed to be at a minimum distance R where

$$\beta R \gg 1 \quad \text{and} \quad R \gg \ell$$

Let the radius be small compared to the length of the aerial and the wavelength

$$\ell \gg r$$
$$\beta r \ll 1$$

The effect of the end faces is then small and the current I_z may be taken equal to zero at $z = \pm\ell$

$$(E_z)_1 = Z I_z \qquad (1)$$

where Z = The skin effect impedance (Ohms/metre)

I_z = The total current at height z

The assumption of no radial flow of current on the end faces is a valid one provided the aerial is small in radius compared with the wavelength. The problem of radial flow of current in the case of a thick aerial is complicated. The axial and cross-sectional distributions of current are mutually independent provided the aerial is a good conductor. The above is generally assumed in deriving the skin effect impedance and also in deriving the transmission line equations.

$$Z = \frac{1}{2\pi r}\sqrt{\frac{\omega \mu \overline{\Pi}}{2g}}\,(1+j) \qquad (2)$$

where $\overline{\Pi}$ = $4\pi \times 10^{-7}$ henries/metre

g = The conductivity (mhos/metre)

μ = The relative permeability of the aerial.

From Maxwell's Equations and using cylindrical co-ordinates (ρ, θ, z)

$$\nabla_A A = B$$

$$\nabla . A = -\frac{j\omega}{c^2}\phi$$

$$-\nabla\phi = E + j\omega A$$

$$E = -j\omega A - \nabla\nabla . A \frac{jc^2}{\omega}$$

$$= -\frac{jc^2}{\omega}\left(\nabla\nabla . A + \frac{\omega^2}{c^2}A\right)$$

where A = The vector potential

ϕ = The scalar potential.

$A_\rho \ll A_z$ except near the end faces

$A_\theta = 0$ for all points

$$\therefore E_z = -\frac{j\omega}{\beta^2}\left(\frac{d^2 A_z}{dz^2} + \beta^2 A_z\right)$$ except near the end faces

where $\beta = \frac{\omega}{c}$

Substituting in the above equation for E_z gives

$$\frac{d^2 A_{z_2}}{dz^2} + \beta^2 A_{z_1} = j\frac{\beta^2}{\omega} Z I_z$$

The vector potential is a one dimensionsal wave equation which is homogeneous for a perfect conductor.

Since a centre fed aerial is symmetrical

$$I(z) = I(-z) \qquad A(z)_z = A(-z)_z$$

The general solution is

$$A_{z_2} = -\frac{j}{c}\left\{D_1 \cos\beta z + D_2 \sin\beta z - Z\int_0^z I(s)\sin\beta(z-s)\,ds\right\} \qquad (3)$$

where D_1 and D_2 are arbitrary constants of integration for the complementary function.

Let V_2 be the driving point potential.

Then for conductors infinitely closely spaced

$$V_2 = \lim_{z\to 0}\left\{\phi_2(z) - \phi_2(-z)\right\}$$

where ϕ is the scalar potential.

Now $A_\rho << A_z \;;\; A_\theta = 0$

$$\therefore \frac{\partial A_{z_2}}{\partial z} = -\frac{j\omega}{c^2}\phi_2$$

$$\frac{\partial A_{z_2}(z)}{\partial z} = -\frac{j\omega}{c^2}\phi_2(z)$$

$$\frac{\partial A_{z_2}(-z)}{-\partial z} = -\frac{j\omega}{c^2}\phi_2(-z)$$

$$\therefore \phi_2(-z) = -\phi_2(z) = \frac{jc^2}{\omega}\frac{\partial A_{z_2}(z)}{\partial z}$$

$$V_2 = 2\lim_{z\to 0}\phi_2(z) = \frac{2jc^2}{\omega}\lim_{z\to 0}\frac{\partial A_{z_2}(z)}{\partial z} = -\frac{j}{c}D_2\beta\frac{2jc^2}{\omega}$$

Now $\omega = \beta c$

$$\therefore D_2 = \frac{V_2}{2} \qquad (4)$$

The vector potential at all points on the surface of the cylindrical conductor except near the end faces and at all points outside the conductor is given by the Helmholtz Integral

$$A_{z_2} = \frac{\mu}{4\pi}\int_{-\ell}^{+\ell} I'_{z_1}\frac{e^{-j\beta R}}{R}\,dz'$$

where R is the distance (ρ,θ,z) to dz' at z' on the axis of the aerial

$$R^2 = (z-z')^2 + \rho^2$$

Substituting in the equation for vector potential (3) gives

$$\frac{jc\overline{\Pi}}{4\pi}\int_{-\ell}^{+\ell} I_z' \frac{e^{-j\beta R}}{R} dz' = D_1\cos\beta z + \frac{V_2}{2}\sin\beta|z| - Z\int_0^z I(s)\sin\beta(z-s)\,ds \qquad (5)$$

The solution of this integral equation is carried out as follows

$$\int_{-\ell}^{+\ell} I_z' \frac{e^{-j\beta R}}{R} dz' = I_z\int_{-\ell}^{+\ell} \frac{dz'}{R} + \int_{-\ell}^{+\ell} \frac{I_z' e^{-j\beta R} - I_z}{R}\, dz' \qquad (6)$$

It may be shown that

$$\int_{-\ell}^{+\ell} \frac{dz'}{R} = \log\left\{\frac{\sqrt{(\ell-z)^2+\rho^2}+(\ell-z)}{\sqrt{(\ell+z)^2+\rho^2}-(\ell+z)}\right\}$$

$$= \Omega + \log\left(1-\frac{z^2}{\ell^2}\right) + \delta \qquad (7)$$

where $\Omega = 2\log\frac{2\ell}{r}$

$$\delta = \log\frac{1}{4}\left\{1+\sqrt{1+\left(\frac{\rho}{\ell-z}\right)^2}\right\}\left\{1+\sqrt{1+\left(\frac{\rho}{\ell+z}\right)^2}\right\}$$

The parameter δ is small except near the ends where it is still finite.

It may be shown that

$$\left[\int_{-\ell}^{+\ell}\frac{dz'}{R}\right]_{z=\pm\ell} = \frac{1}{2}\Omega + \log 2 \qquad (8)$$

Substitute (7) in (6)

$$\int_{-\ell}^{+\ell} I_z' \frac{e^{-j\beta R}}{R} dz' = I_z\Omega + I_z\log\left(1-\frac{z^2}{\ell^2}\right) + I_z\delta + \int_{-\ell}^{+\ell}\frac{I_z' e^{-j\beta R} - I_z}{R}\, dz' \qquad (9)$$

Substitute (9) in (5)

$$jc\frac{\overline{\Pi}}{4\pi}\left\{I_z\Omega + I_z\log\left(1-\frac{z^2}{\ell^2}\right) + I_z\delta + \int_{-\ell}^{+\ell}\frac{I_z' e^{-j\beta R} - I_z}{R}\, dz'\right\}$$

$$= D_1\cos\beta z + \frac{V_2}{2}\sin\beta|z| - Z\int_0^z I(s)\sin\beta(z-s)\,ds$$

Now $\eta = c\overline{\Pi}$

$$I_z = -\frac{j4\pi}{\eta\Omega}\left\{D_1\cos\beta z + \frac{V_2}{2}\sin\beta|z| - Z\int_0^z I(s)\sin\beta(z-s)\,ds\right\}$$

$$-\frac{1}{\Omega}\left\{I_z\log\left(1-\frac{z^2}{\ell^2}\right) + I_z\delta + \int_{-\ell}^{+\ell}\frac{I_z' e^{-j\beta R} - I_z}{R}\, dz'\right\} \qquad (10)$$

Now $\left\{\log\left(1-\frac{z^2}{\ell^2}\right)+\delta\right\}_{z=\pm\ell} = \log 2-\frac{1}{2}\Omega$ is finite

Let $(I_z)_{z=+\ell} = 0$ in (10) giving

$$0 = -\frac{j4\pi}{\eta\Omega}\left\{D_1\cos\beta\ell+\frac{V_2}{2}\sin\beta\ell\right\} - \frac{1}{\Omega}\left\{-\frac{j4\pi Z}{\eta}\int_0^{\ell} I(s)\sin\beta(\ell-s)\,ds + \int_{-\ell}^{+\ell} I_z'\frac{e^{-j\beta R_\ell}}{R_\ell}\,dz'\right\} \qquad (11)$$

where $R_\ell^2 = (\ell-z')^2+\rho^2$

Subtract (11) from (10)

$$I_z = -\frac{j4\pi}{\Omega\eta}\left\{D_1(\cos\beta z-\cos\beta\ell)+\frac{V_2}{2}(\sin\beta|z|-\sin\beta\ell)\right\} - \frac{1}{\Omega}\left\{I_z\log\left(1-\frac{z^2}{\ell^2}\right)+I_z\delta+\int_{-\ell}^{+\ell}\frac{I_z'e^{-j\beta R}-I_z}{R}\,dz'-j\frac{4\pi Z}{\eta}\int_0^{z} I(s)\sin\beta(z-s)\,ds\right\} + \frac{1}{\Omega}\left\{\int_{-\ell}^{+\ell}\frac{I_z'e^{-j\beta R_\ell}}{R_\ell}\,dz' - j\frac{4\pi Z}{\eta}\int_0^{\ell} I(s)\sin\beta(\ell-s)\,ds\right\} \qquad (12)$$

This equation is similar to Hallen's Integro-Differential Equation.

The process of iteration from this equation is indicated below.

Let $F_0(z) = \cos\beta z$

$G_0(z) = \sin\beta|z|$

$F_{0z} = F_0(z)-F_0(\ell)$

$G_{0z} = G_0(z)-G_0(\ell)$

The zeroth order approximation for I_z is

$$(I_z)_0 = -\frac{j4\pi}{\Omega\eta}\left\{D_1F_{0z}+\frac{V_2}{2}G_{0z}\right\} \qquad (13)$$

Substitute (13) in the R.H.S. of (12), group and let

$$F_1(z) = -F_{0z}\log\left(1-\frac{z^2}{\ell^2}\right)-F_{0z}\delta-\int_{-\ell}^{+\ell}\frac{F_{0z}'e^{-j\beta R}-F_{0z}}{R}\,dz' + \frac{j4\pi Z}{\eta}\int_0^{z} F_{0s}\sin\beta(z-s)\,ds$$

$$F_1(\ell) = -\int_{-\ell}^{+\ell} F_{0z}'\frac{e^{-j\beta R_\ell}}{R_\ell}\,dz'+\frac{j4\pi Z}{\eta}\int_0^{\ell} F_{0s}\sin\beta(\ell-s)\,ds$$

$$F_{1z} = F_1(z)-F_1(\ell)$$

$G_1(z), G_1(\ell), G_{1z}$ are obtained by putting G for F in the above expressions.

The following equation for the first order solution

for I_z becomes on reduction

$$(I_z)_1 = -\frac{j4\pi}{\Omega\eta}\left\{D_1\left(F_{oz}+\frac{F_{1z}}{\Omega}\right)+\frac{V_2}{2}\left(G_{oz}+\frac{G_{1z}}{\Omega}\right)\right\}$$

This approximation is again substituted in equation (12) and a second approximation for I_z obtained. This process may be repeated until the solution for the current distribution given below is obtained.

$$I_z = -\frac{j4\pi}{\Omega\eta}\left\{D_1\left(F_{oz}+\frac{F_{1z}}{\Omega}+\frac{F_{2z}}{\Omega^2}+\cdots\right)+\frac{V_2}{2}\left(G_{oz}+\frac{G_{1z}}{\Omega}+\frac{G_{2z}}{\Omega^2}+\cdots\right)\right\} \quad (14)$$

The constant of integration D_1 is obtained by substituting (14) in (11) and reducing

$$D_1 = -\frac{V_2}{2}\left\{\frac{G_o(\ell)+\frac{G_1(\ell)}{\Omega}+\frac{G_2(\ell)}{\Omega^2}+}{F_o(\ell)+\frac{F_1(\ell)}{\Omega}+\frac{F_2(\ell)}{\Omega^2}+}\right\} \quad (15)$$

Substitute (15) in (14) and reduce

$$I_z = \frac{j2\pi V_2}{\Omega\eta}\,\frac{\sin\beta(\ell-|z|)+\frac{1}{\pi}\left[F_1(z)\sin\beta\ell-F_1(\ell)\sin\beta|z|+G_1(\ell)\cos\beta z-G_1(z)\cos\beta\ell\right]}{\cos\beta\ell+\frac{F_1(\ell)}{\Omega}} \quad (16)$$

In order to evaluate $F_1(z), F_1(\ell), G_1(z), G_1(\ell)$ certain approximations are made which are consistent for thin aerials.

$$\rho^2 \ll (\ell-z)^2$$

$$\rho^2 \ll (\ell+z)^2$$

The approximation is obviously in error when $z=\pm\ell$ but it is known that the current is then zero. The approximation will give good results provided it is remembered that the results will not hold near the ends of the aerial.

With these approximations it is possible to neglect δ and to write

$$R = \pm(z'-z)$$

The results obtained will be true at the input section of the aerial and hence the value of input impedance obtained by this method will be a true one.

The F and G functions are evaluated by normal methods. The integration is heavy and is not included. The results are

$$Ei(x) = Ci(x) + jSi(x)$$

$$F_1(z) = -(\cos\beta z - \cos\beta\ell)\log\left(1-\frac{z^2}{\ell^2}\right) - \cos\beta\ell\left\{Ei\,\beta(\ell-z) - Ei^{x}\beta(\ell+z)\right\}$$
$$+\frac{\cos\beta z}{2}\left\{Ei\,2\beta(\ell-z) - Ei^{x}2\beta(\ell+z)\right\} - \frac{j\sin\beta z}{2}\left\{Ei\,2\beta(\ell-z) - Ei^{x}2\beta(\ell+z)\right\}$$
$$+\frac{j4\pi Z\ell}{\eta}\left\{\frac{z}{2\ell}\sin\beta z - \frac{\cos\beta\ell}{\beta\ell}(1-\cos\beta z)\right\}$$

$$F_1(\ell) = \frac{\cos\beta\ell}{2}\left\{Ei\,4\beta\ell - 2Ei\,2\beta\ell\right\} + \frac{j\sin\beta\ell}{2}Ei\,4\beta\ell$$
$$+\frac{j4\pi Z\ell}{\eta}\left\{\frac{\sin\beta\ell}{2} - \frac{\cos\beta\ell}{\beta\ell}(1-\cos\beta\ell)\right\}$$

$$G_1(z) = -(\sin\beta|z| - \sin\beta\ell)\log\left(1-\frac{z^2}{\ell^2}\right) + 2\sin\beta z\log\left(\frac{|z|}{\ell+|z|}\right)$$
$$+\frac{\sin\beta z + j\cos\beta z}{2}\left\{Ei^{x}2\beta(\ell+z) + Ei\,2\beta(\ell-z) - 2Ei^{x}2\beta z\right\}$$
$$+\sin\beta\ell\left\{Ei\,\beta(\ell-z) - Ei^{x}\beta(\ell+z)\right\}$$
$$+j\frac{4\pi Z\ell}{\eta}\left\{\frac{\sin\beta|z|}{2\beta\ell} - \frac{|z|\cos\beta z}{2\ell} - \frac{\sin\beta\ell}{\beta\ell}(1-\cos\beta z)\right\}$$

$$G_1(\ell) = \frac{\sin\beta\ell - j\cos\beta\ell}{2}\left\{2Ei\,2\beta\ell - Ei\,4\beta\ell\right\} + 2\sin\beta\ell\log 2$$
$$-\sin\beta\ell\,Ei\,2\beta\ell - \frac{j4\pi Z\ell}{\eta}\left\{\frac{\sin\beta\ell}{2\beta\ell} + \frac{\cos\beta\ell}{2} - \frac{\sin\beta\ell\cos\beta\ell}{\beta\ell}\right\}$$

Let $A' + jA'' = F_1(\ell)$

$$B' + jB'' = F_1(0)\sin\beta\ell + G_1(\ell) - G_1(0)\cos\beta\ell$$

Then the first order solution for the input impedance is obtained by putting z = o in equation (16).

$$Z(0)_1 = \frac{V_2}{I_o} = -\frac{j\Omega\eta}{2\pi}\left\{\frac{\cos\beta\ell + \frac{1}{\pi}(A'+jA'')}{\sin\beta\ell + \frac{1}{\pi}(B'+jB'')}\right\} \qquad (17)$$

Let $\alpha_1 = A'+jA'' = \alpha_1' + j\alpha_1'' + \frac{j\ell r_\alpha}{30}(r_i + jx_i)$

$$\beta_1 = B'+jB'' = \beta_1' + j\beta_1'' + \frac{j\ell r_\beta}{30}(r_i + jx_i)$$

$$L = \beta\ell\,;\ Z = r_i + jx_i\,;\ \frac{\eta}{2\pi} = 60\ ;\ \Omega = 2\log\frac{2\ell}{r}$$

Substitution and reduction gives

$$\alpha_1' = \frac{1}{2}\left\{\cos L\,(Ci\,4L - 2Ci\,2L) - \sin L\,Si\,4L\right\}$$

$$\alpha_1'' = \frac{1}{2}\left\{\cos L(Si\,4L - 2Si\,2L) + \sin L\, Ci\,4L\right\}$$

$$\beta_1' = \frac{1}{2}\left\{\cos L(4Si\,2L - Si\,4L) + \sin L(4\log 2 + 2\,Ci\,2L - Ci\,4L)\right\}$$

$$\beta_1'' = \frac{1}{2}\left\{\cos L(Ci\,4L - 4Ci\,2L) + \sin L(2Si\,2L - Si\,4L)\right\}$$

$$\gamma_\alpha = \frac{\sin L}{2} - \frac{\cos L}{L}(1 - \cos L)$$

$$\gamma_\beta = \frac{\sin 2L - \sin L}{2L} - \frac{1}{2}\cos L$$

γ_i and x_i may be obtained in the form of modified Bessel Functions.

Substitution of the above quantities in equation (17) gives the first order approximation for the input impedance.

$$Z(0)_1 = -j60\Omega\left\{\frac{\cos\beta\ell + \frac{\alpha_1}{\Omega}}{\sin\beta\ell + \frac{\beta_1}{\Omega}}\right\} \qquad (18)$$

The impedance given by equation (18) is the input impedance for a symmetrical centre driven aerial. The ends of the aerial at the driving point are assumed to be close together. If the ends are not close together a certain amount of mutual coupling between the ends of the aerial will occur.

The process of iteration may be carried out again giving the second order approximation for the input impedance.

$$Z(0)_2 = -j60\Omega\left\{\frac{\cos\beta\ell + \frac{\alpha_1}{\Omega} + \frac{\alpha_2}{\Omega^2}}{\sin\beta\ell + \frac{\beta_1}{\Omega} + \frac{\beta_2}{\Omega^2}}\right\} \qquad (19)$$

After considerable mathematical analysis similar to that used in determining α_1 and β_1 the coefficients α_2 and β_2 are obtained

$$\alpha_2 = \left(\frac{3}{2}e^{j\beta\ell} - \frac{1}{2}e^{-j\beta\ell}\right)Ei_{11}4L - 2\cos L\, Ei_{11}2L - \frac{1}{2}e^{jL}Ei\,4L\,Ei\,2L + \frac{1}{2}\cos L\, Ei^2 2L - (e^{jL}Ei\,4L - 2\cos L\, Ei\,2L)\log 2$$

$$\beta_2 = -\sin L\, Ei_{11}4L - j6\cos L\, Ei_{11}2L + j2e^{-jL}Ei_{21}2L - \frac{j}{2}e^{jL}Ei\,4L\,Ei\,2L + \frac{1}{2}\sin L\, Ei^2 2L + j\left(e^{-jL}Ei^{x}2L - e^{-jL}Ei\,2L\right)\log 4$$

where $$Ei(x) = \int_0^x \frac{1 - e^{-j\eta}}{\eta}\,d\eta$$

$$Ei_{11}(x) = \int_0^x \frac{Ei(\xi)}{\xi}\, d\xi$$

$$Ei_{21}(x) = \int_0^x \frac{e^{j\xi}}{\xi} \left\{ Ei\, 2\xi - Ei\, \xi \right\} d\xi$$

The last two equations define the iterative sine and cosine integrals.[37]

Substitution of α_2 and β_2 in equation (19) gives the second order approximation for the input impedance.

The input impedance has been calculated as a function of $\frac{\ell}{\lambda}$ using equations (18) and (19) for a range of r/l ratio. The skin effect impedance Z contributes a negligible amount to the input impedance and has been neglected.[44,45] The results of the calculations and the curves of input impedance plotted from them are shown below. A discussion of the results is given later.

Input Resistance by the Cylindrical Aerial Method.

First Approximation.

L	$\frac{r}{\ell}$ 0.001	0.005	0.010	0.020	0.030	0.040	0.050
0.0	0	0	0	0	0	0	0
0.1	0	0.3	0.3	0.3	0.3	0.3	0.2
0.2	0.7	0.7	0.7	0.7	0.7	0.7	1.1
0.3	1.7	1.7	1.7	1.6	1.6	1.6	1.6
0.4	3.2	3.0	3.0	3.0	3.0	3.0	3.0
0.5	4.9	4.9	4.8	4.8	6.3	4.7	4.5
0.6	7.4	7.5	8.2	7.0	6.9	6.9	6.9
0.7	10.0	10.0	9.8	9.7	9.6	9.5	9.2
0.8	13.3	13.1	13.1	12.9	12.7	12.6	12.5
0.9	17.2	17.0	16.8	16.6	16.3	16.3	16.2
1.0	21.9	21.4	21.4	20.9	20.7	20.5	20.3
1.1	27.2	26.7	26.5	26.0	25.7	25.5	25.3
1.2	33.6	32.8	32.4	31.8	31.7	31.3	31.1
1.3	40.9	39.9	39.7	38.9	38.5	38.1	37.7
1.4	49.4	48.4	47.4	46.9	44.5	45.8	45.4
1.5	59.4	58.0	57.1	56.4	55.9	55.4	54.8
1.6	71.4	69.9	69.0	67.5	66.9	61.5	65.8
1.7	85.8	84.0	83.3	81.5	80.0	79.3	78.5
1.8	104.0	101.2	99.7	98.0	96.4	95.1	94.3
1.9	125.8	121.4	121.0	118.1	119	114.3	113
2.0	153.2	150	146.5	143	141	138.1	137
2.1	197.5	183.5	180	175	171	152.1	167
2.2	236	229	203	218	213	208	204
2.3	300	291	284	274	267	260	254
2.4	394	379	368	353	340	328	320
2.5	534	510	489	462	443	422	408
2.6	750	706	669	618	580	547	522
2.7	1122	1019	937	838	765	705	658
2.8	1770	1500	1320	1105	974	872	795
2.9	2840	2096	1735	1331	1120	960	860
3.0	3800	2380	1810	1328	1075	907	795

Input Resistance by the Cylindrical Aerial Method.

First Approximation.

L	$\frac{r}{\ell}$ 0.001	0.005	0.010	0.020	0.030	0.040	0.050
3.1	3265	1940	1518	1069	865	738	650
3.2	2000	1297	1020	774	644	551	489
3.3	1169	822	675	532	451	397	356
3.4	707	534	454	370	322	286	262
3.5	456	364	312	263	233	210	195
3.6	313	247	225	194	174	160	149
3.7	224	189	169	148	130	125	117
3.8	168	144	132	117	108.3	93.7	90.6
3.9	132	115	106.8	96.7	89.8	84.8	80.7
4.0	108	96.2	90.3	82	77.8	74.0	71.0
4.1	92	84.0	79.9	73.8	70.6	67.4	65.0
4.2	82.2	76.4	73	68.9	66.0	63.8	62.2
4.3	77.4	72.9	70.1	67.1	64.7	63.0	61.9
4.4	76.0	71.8	70.5	67.9	66.0	64.5	63.5
4.5	78.4	75.4	73.5	71.0	69.4	68.2	67.2
4.6	83.4	80.5	79.1	76.8	75.2	74.1	73.1
4.7	91.7	88.7	87.0	85.1	83.0	82.2	81.1
4.8	103.1	100	98.1	93.4	94.4	92.5	91.5
4.9	119.0	114.6	106.3	109.4	107.5	106	104.5
5.0	139.7	134.4	131.2	127.8	125.7	123	121
5.1	166.5	160.0	156	151	147	144	141
5.2	202	192.8	186.7	180	166.5	170.5	167
5.3	248	235	227	218	211	204	200
5.4	310	294	282	268	257	248	243
5.5	399	373	355	333	318	304	291
5.6	526	482	456	421	394	373	355
5.7	715	645	594	535	493	459	432
5.8	1013	876	787	681	614	560	516
5.9	1470	1181	1026	829	735	650	589
6.0	2135	1541	1261	975	817	705	621
6.1	2800	1772	1377	1011	826	700	615
6.2	2820	1677	1261	920	745	625	549
6.3	2380	1311	1007	740	605	515	452
6.4	1420	1191	756	567	472	406	362
6.5	933	654	537	424	361	298	284
6.6	621	462	395	318	277	245	223
6.7	433	327	292	240	215	193	177
6.8	311	251	221	188	170	155	143
6.9	234	195	175	153	137	127	119
7.0	182	156	142	125	115	107	101

Input Reactance by the Cylindrical Aerial Method

First Approximation.

L	$\frac{r}{\ell}$ 0.001	0.005	0.010	0.020	0.030	0.040	0.050
0							
0.1		-5600	-4790	-4050	-3590	-3265	-3020
0.2	-3680	-2780	-2380	-1995	-1770	-1687	-1490
0.3	-2407	-1820	-1554	-1304	-1155	-1055	-976
0.4	-1800	-1330	-1133	-949	-871	-771	-711
0.5	-1363	-1022	-879	-734	-653	-592	-549
0.6	-1087	-811	-695	-580	-517	-468	-440
0.7	-871	-654	-561	-468	-414	-376	-348
0.8	-712	-535	-455	-378	-334	-303	-280
0.9	-576	-431	-368	-305	-269	-244	-225
1.0	-460	-350	-292	-240	-222	-191	-176
1.1	-359	-265	-225	-185	-163	-146	-134
1.2	-268	-196	-165	-135	-118	-106	-97

Input Reactance by the Cylindrical Aerial Method.

First Approximation

L	$\frac{r}{\ell}$ 0.001	0.005	0.010	0.020	0.030	0.040	0.050
1.3	-182	-130	-110	-88.4	-76.2	-66.9	-60.9
1.4	-100	-69.9	-56.5	-43.9	-36.8	-31.5	-27.6
1.5	-21.7	-10.3	-5.5	-1.1	+1.5	+3.2	+4.3
1.6	+56.2	+48.9	+45.6	+41.3	+38.8	+37.1	+35.6
1.7	+135	+109	+96.5	+83.7	+76.2	+70.7	+67.0
1.8	+216	+170	+148	+127	+114	+105	+98
1.9	+301	+232	+203	+172	+158	+140	+131
2.0	+396	+303	+261	+219	+195	+177	+164
2.1	+492	+376	+317	+269	+236	+214	+197
2.2	+609	+457	+392	+321	+284	+254	+231
2.3	+736	+550	+465	+381	+332	+293	+265
2.4	+895	+656	+549	+443	+380	+330	+297
2.5	+1075	+776	+636	+502	+422	+359	+315
2.6	+1288	+900	+721	+544	+442	+366	+314
2.7	+1532	+1000	+767	+535	+414	+325	+263
2.8	+1720	+990	+684	+413	+281	+195	+137
2.9	+1511	+625	+305	+104	+12.1	-39	-71.5
3.0	+220	-234	-306	-323	-313	-299	-284
3.1	-308	-1028	-822	-635	-536	-471	-423
3.2	-2067	-1288	-1002	-748	-617	-535	-475
3.3	-1897	-1220	-957	-724	-603	-520	-461
3.4	-1592	-1061	-849	-652	-549	-475	-424
3.5	-1320	-907	-726	-566	-478	-415	-373
3.6	-1104	-767	-624	-490	-420	-368	-331
3.7	-921	-646	-529	-418	-356	-313	-284
3.8	-765	-537	-448	-356	-306	-268	-243
3.9	-643	-456	-377	-301	-257	-227	-205
4.0	-530	-379	-315	-249	-209	-189	-170
4.1	-436	-310	-257	-204	-171	-153	-138
4.2	-347	-246	-202	-161	-138	-121	-108
4.3	-267	-188	-154	-121	-103	-90	-81
4.4	-189	-122	-107	-84	-70	-62	-53
4.5	-116	-79.3	-63.1	-47	-38	-27	-27
4.6	-40.6	-26.4	-18.4	-10.6	-6.7	-3.7	-1.7
4.7	+25.6	+25.6	+25.5	+24.8	+24.3	+24.0	+23.6
4.8	+98	+78	+70	+59	+56	+52	+49
4.9	+171	+132	+109	+97	+87	+80	+74
5.0	+247	+188	+160	+134	+118	+107	+99
5.1	+329	+247	+211	+173	+152	+136	+124
5.2	+414	+310	+261	+213	+177	+165	+149
5.3	+514	+376	+315	+253	+218	+192	+174
5.4	+622	+451	+372	+296	+252	+218	+194
5.5	+745	+528	+434	+337	+282	+240	+210
5.6	+882	+610	+489	+371	+302	+252	+216
5.7	+1040	+689	+535	+387	+305	+246	+205
5.8	+1187	+738	+543	+366	+271	+207	+162
5.9	+1279	+701	+475	+292	+185	+124	+83
6.0	+1122	+476	+264	+101	+31.4	-9.6	-34.6
6.1	+451	+20.2	-86.4	-141	-157	-161	-159
6.2	-657	-528	-453	-371	-323	-288	-267
6.3	-1250	-865	-669	-504	-419	-360	-322
6.4	-1548	-908	-752	-546	-451	-385	-342
6.5	-1442	-910	-709	-531	-439	-357	-334
6.6	-1249	-815	-649	-487	-409	-350	-312
6.7	-1062	-712	-562	-436	-366	-315	-281
6.8	- 896	-613	-495	-382	-323	-280	-248
6.9	-761	-526	-428	-333	-281	-243	-217
7.0	-646	-449	-364	-284	-241	-210	-186

Input Resistance by the Cylindrical Aerial Method.

Second Approximation.

L	$\frac{r}{\ell}$ 0.001	0.005	0.010	0.020	0.030	0.040	0.050
0.0	0	0	0	0	0	0	0
0.1	0.1	0.4	0.3	0.3	0.3	0.3	0.3
0.2	1.4	1.4	0.7	0.8	0.7	0.8	0.8
0.3	1.7	1.7	1.8	1.8	1.8	1.8	1.8
0.4	3.7	3.2	3.3	3.3	3.3	3.3	3.3
0.5	5.2	5.1	5.2	5.3	5.3	5.3	5.3
0.6	7.6	11.6	7.7	7.7	7.7	7.8	7.8
0.7	10.6	12.6	10.7	10.6	10.7	10.7	10.7
0.8	14.1	14.2	14.3	14.3	14.3	14.3	14.4
0.9	18.4	18.4	18.3	18.7	18.8	18.7	18.8
1.0	23.4	23.4	23.7	23.8	23.8	24.0	24.0
1.1	29.4	29.6	29.8	30.0	29.9	30.4	30.3
1.2	36.8	36.9	37.2	37.4	37.6	37.6	37.8
1.3	45.2	45.5	46.0	46.2	46.5	47.0	47.2
1.4	55.4	56.1	56.5	57.2	57.5	57.9	58.2
1.5	62.7	68.6	69.4	70.5	71.0	71.5	71.9
1.6	83.7	84.7	86.1	86.7	87.6	88.4	89.0
1.7	92.6	104.8	106	107.5	108.5	109.7	110
1.8	126	129	131	134	135	136	137
1.9	156	161	164	167	169	170	171
2.0	196	204	206	210	212	212	204
2.1	247	259	262	267	267	267	266
2.2	318	343	338	341	339	333	328
2.3	420	436	442	436	427	411	392
2.4	565	485	580	555	525	489	460
2.5	790	788	755	686	615	554	499
2.6	1122	1050	955	794	675	577	503
2.7	1625	1360	1128	851	676	556	470
2.8	2280	1570	1188	812	623	495	411
2.9	2760	1555	1075	706	530	415	347
3.0	2545	1290	889	575	432	342	283
3.1	1850	978	689	454	342	276	230
3.2	1250	707	515	352	275	224	188
3.3	832	514	389	277	220	181	155
3.4	569	380	296	219	178	148	129
3.5	401	287	230	175	144	123	109
3.6	294	220	182	143	121	104	92.5
3.7	224	173	146	119	102	90	80.5
3.8	173	140	121	101	88.7	79.4	72.5
3.9	139	116	103	88	79.2	72.2	66.5
4.0	115	99.7	90.7	80	72.8	67.3	63.1
4.1	100	89	84	74.5	69.4	65.4	62.0
4.2	93.1	82.3	78	72.6	69.0	65.7	63.4
4.3	85.5	80.5	77.7	73.6	70.7	68.6	66.6
4.4	85.2	80.2	80.2	77.4	75.6	74.3	72.9
4.5	88.9	87.5	88.0	84.2	83.4	82.3	81.4
4.6	96.7	95.6	95.4	95.3	94.4	93.7	93.0
4.7	109	109	109.1	109.4	109	109	109
4.8	127	128	128	128	129	128	128
4.9	154	151	153	153	153	153	152
5.0	180	184	185	186	185	183	183
5.1	221	226	226	225	223	219	216
5.2	277	279	279	273	267	259	252
5.3	351	352	347	332	316	301	288
5.4	445	441	427	396	369	340	317
5.5	589	560	525	464	415	369	339
5.6	775	700	628	521	445	383	336
5.7	1035	859	726	557	452	375	322
5.8	1368	999	787	561	439	353	300
5.9	1700	1070	825	537	405	321	268

Input Resistance by the Cylindrical Aerial Method.

Second Approximation.

L	$\frac{r}{\ell}$ 0.001	0.005	0.010	0.020	0.030	0.040	0.050
6.0	1915	1050	744	482	362	284	232
6.1	1850	948	654	423	316	246	206
6.2	1550	796	554	360	270	214	178
6.3	1304	646	455	304	230	183	154
6.4	894	589	373	254	197	158	133
6.5	662	407	304	214	168	137	117
6.6	498	323	250	181	151	119	103
6.7	378	260	207	154	126	106	92
6.8	293	212	173	133	88	95.1	83
6.9	232	176	148	117	58.5	86.7	77.1
7.0	189	148	128	104	27.7	80.3	72.2

Input Reactance by the Cylindrical Aerial Method.

Second Approximation.

L	$\frac{r}{\ell}$ 0.001	0.005	0.010	0.020	0.030	0.040	0.050
0.0							
0.1	-23,900	-5240	-4400	-3607	-3160	-2820	-2595
0.2	-3520	-2620	-2193	-1782	-1560	-1503	-1329
0.3	-2320	-1690	-1430	-1171	-1019	-910	-836
0.4	-1687	-1244	-1040	-854	-760	-661	-606
0.5	-1304	-954	-805	-655	-572	-512	-466
0.6	-1029	-758	-639	-520	-451	-402	-371
0.7	-834	-607	-514	-417	-363	-322	-294
0.8	-686	-496	-417	-338	-292	-259	-236
0.9	-551	-400	-336	-271	-234	-207	-188
1.0	-438	-324	-264	-212	-184	-160	-146
1.1	-341	-244	-213	-161	-137	-120	-109
1.2	-254	-178	-147	-116	-97	-84	-75
1.3	-170	-116	-95	-71.5	-59	-49.2	-43.1
1.4	-90	-57.6	-44.0	-30.3	-22.6	-17.0	-13.1
1.5	-12.6	-0.2	+5.0	+10.3	+13.0	+14.9	+30.2
1.6	+64.9	+57.9	+54.4	+50.4	+48	+46	+44
1.7	+142	+117	+104	+91	+83	+77	+72
1.8	+224	+177	+154	+132	+118	+106	+98
1.9	+312	+240	+207	+173	+151	+134	+122
2.0	+406	+309	+262	+213	+184	+159	+141
2.1	+504	+378	+319	+251	+210	+177	+152
2.2	+619	+467	+373	+284	+227	+182	+148
2.3	+746	+530	+418	+302	+227	+167	+123
2.4	+888	+600	+455	+292	+193	+119	+70.1
2.5	+1044	+642	+444	+233	+116	+38.1	-11.9
2.6	+1170	+612	+353	+111	-3.0	-68.3	-104
2.7	+1188	+437	+149	-66.9	-142	-176	-188
2.8	+892	+70.3	-147	-250	-265	-260	-249
2.9	+76.2	-390	-432	-386	-345	-308	-282
3.0	-912	-728	-594	-457	-380	-327	-289
3.1	-1428	-868	-656	-475	-383	-325	-283
3.2	-1497	-868	-645	-460	-371	-311	-269
3.3	-1369	-805	-605	-430	-345	-288	-250
3.4	-1192	-726	-548	-394	-316	-263	-229
3.5	-1035	-647	-488	-355	-284	-237	-206
3.6	-888	-563	-432	-314	-255	-212	-184
3.7	-761	-489	-379	-277	-229	-187	-162
3.8	-654	-423	-328	-238	-195	-162	-141
3.9	-556	-360	-275	-207	-168	-139	-119

Input Reactance by the Cylindrical Aerial Method.

Second Approximation.

L	$\frac{r}{\ell}$ 0.001	0.005	0.010	0.020	0.030	0.040	0.050
4.0	-459	-304	-237	-174	-140	-115	-98
4.1	-381	-250	-194	-142	-113	-93	-79
4.2	-313	-202	-154	-111	-88	-71	-64
4.3	-224	-151	-115	-81	-62	-49	-39
4.4	-162	-103	-76	-51	-37	-27	-20
4.5	-94	-56	-34	-21.4	-12.1	-2.5	-0.7
4.6	-29.8	-9.1	0	+8.5	+13.1	+15.8	+17.8
4.7	+37.4	+38.2	+38.2	+37.6	+37.0	+36.4	+35.5
4.8	+106	+86	+77	+68	+60	+55	+51
4.9	+172	+135	+116	+95	+82	+72	+65
5.0	+249	+186	+153	+121	+101	+85	+73
5.1	+326	+236	+191	+144	+115	+92	+75
5.2	+410	+284	+225	+159	+120	+89	+66
5.3	+499	+333	+252	+165	+112	+74	+46
5.4	+585	+370	+264	+154	+90	+45	+13.0
5.5	+677	+390	+256	+121	+48.9	+0.5	-27.2
5.6	+750	+379	+212	+62	-8.8	-50.6	-75
5.7	+780	+311	+127	-18.2	-76	-104	-118
5.8	+714	+169	+0.2	-108	-139	-150	-152
5.9	+470	-33.1	-146	-124	-193	-184	-175
6.0	+23.2	-254	-275	-254	-228	-205	-186
6.1	-486	-435	-369	-292	-247	-214	-192
6.2	-857	-546	-421	-310	-253	-215	-190
6.3	-990	-589	-439	-312	-250	-209	-182
6.4	-1035	-585	-431	-303	-241	-199	-171
6.5	-972	-558	-404	-287	-226	-186	-160
6.6	-885	-515	-382	-266	-209	-171	-147
6.7	-780	-468	-348	-243	-192	-156	-133
6.8	-691	-418	-312	-219	-172	-140	-118
6.9	-604	-372	-279	-195	-155	-123	-104
7.0	-523	-322	-244	-170	-132	-106	-88

The following table of maximum input resistance has been deduced from the above input resistance values.

First Approximation

$\frac{r}{\ell}$	0.001	0.005	0.010	0.020	0.030	0.040	0.050
$\frac{\ell}{\lambda}$	0.484	0.478	0.473	0.470	0.468	0.466	0.462
R (Ohms)	3830	2370	1800	1350	1120	950	850

Second Approximation

$\frac{r}{\ell}$	0.001	0.005	0.010	0.020	0.030	0.040	0.050
$\frac{\ell}{\lambda}$	0.477	0.451	0.444	0.430	0.422	0.414	0.411
R (Ohms)	3800	1580	1180	850	680	575	500

INPUT RESISTANCE / $\beta\ell$ FOR A RANGE OF $\frac{r}{\ell}$ RATIOS BY THE CYLINDRICAL AERIAL METHOD. FIRST APPROXIMATION.

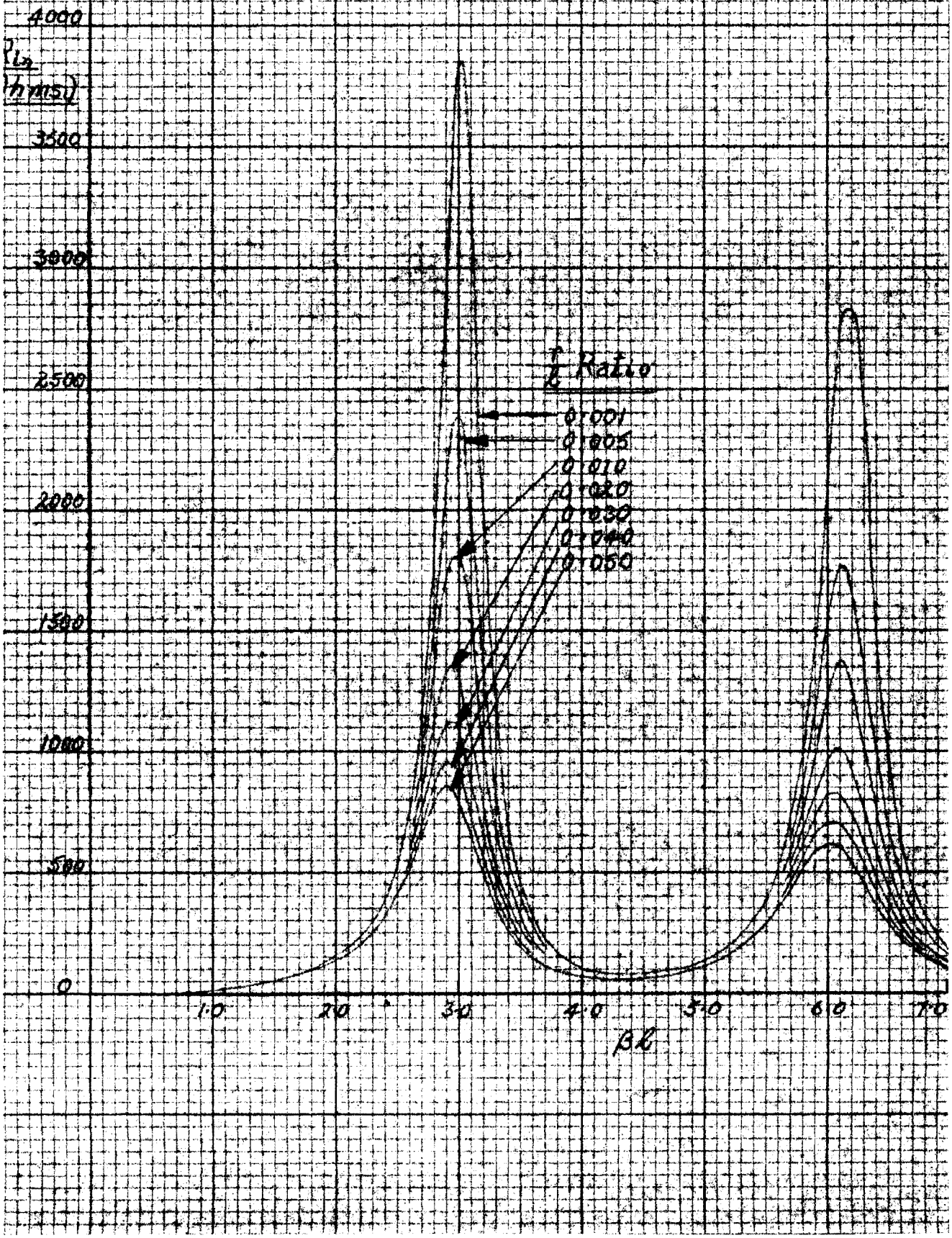

INPUT REACTANCE / $\beta\ell$ FOR A RANGE OF $\frac{r}{\ell}$ RATIOS BY THE CYLINDRICAL AERIAL METHOD. FIRST APPROXIMATION.

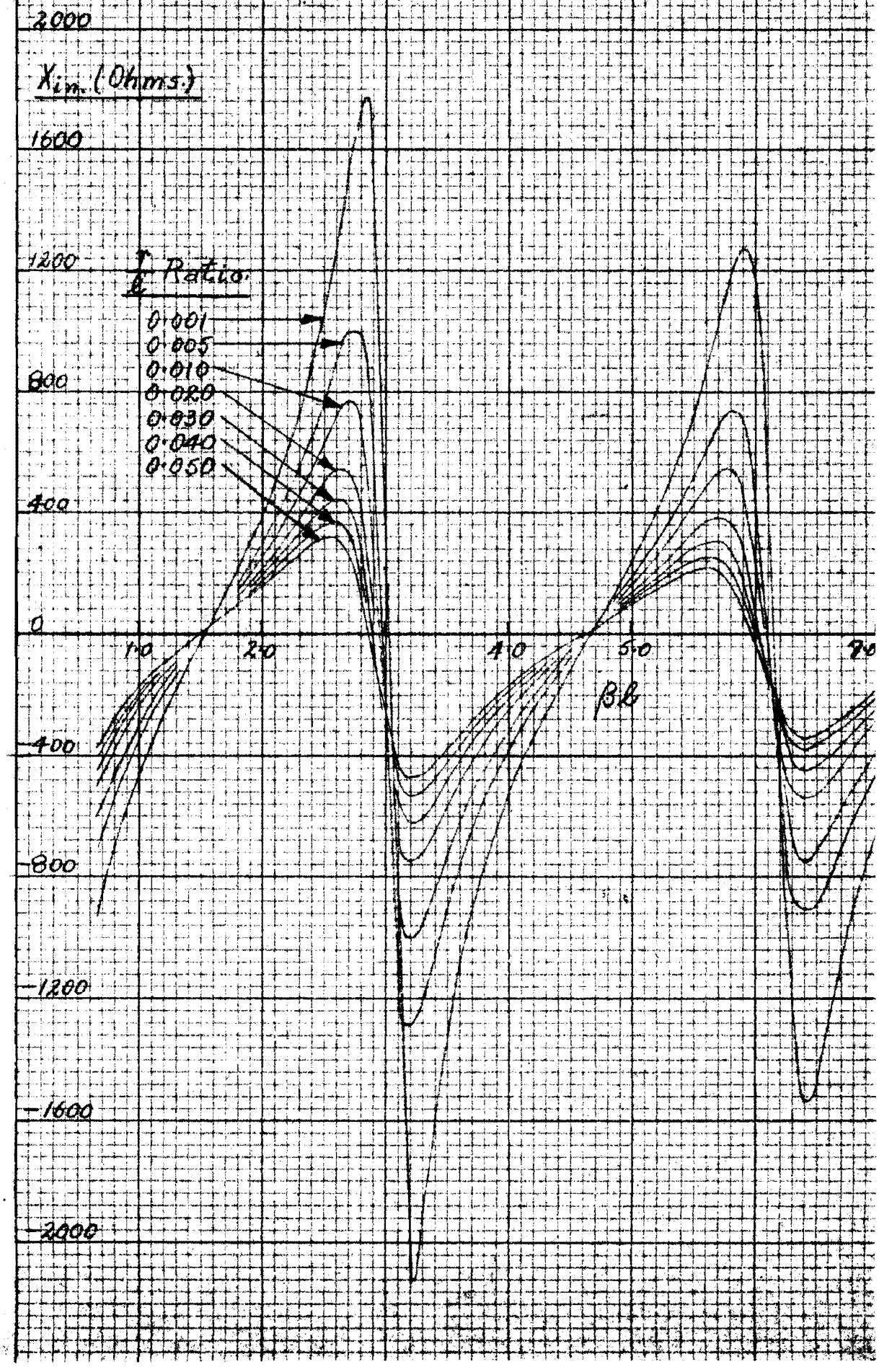

INPUT RESISTANCE / $\beta\ell$ FOR A RANGE OF r/ℓ RATIOS BY THE CYLINDRICAL AERIAL METHOD. SECOND APPROXIMATION.

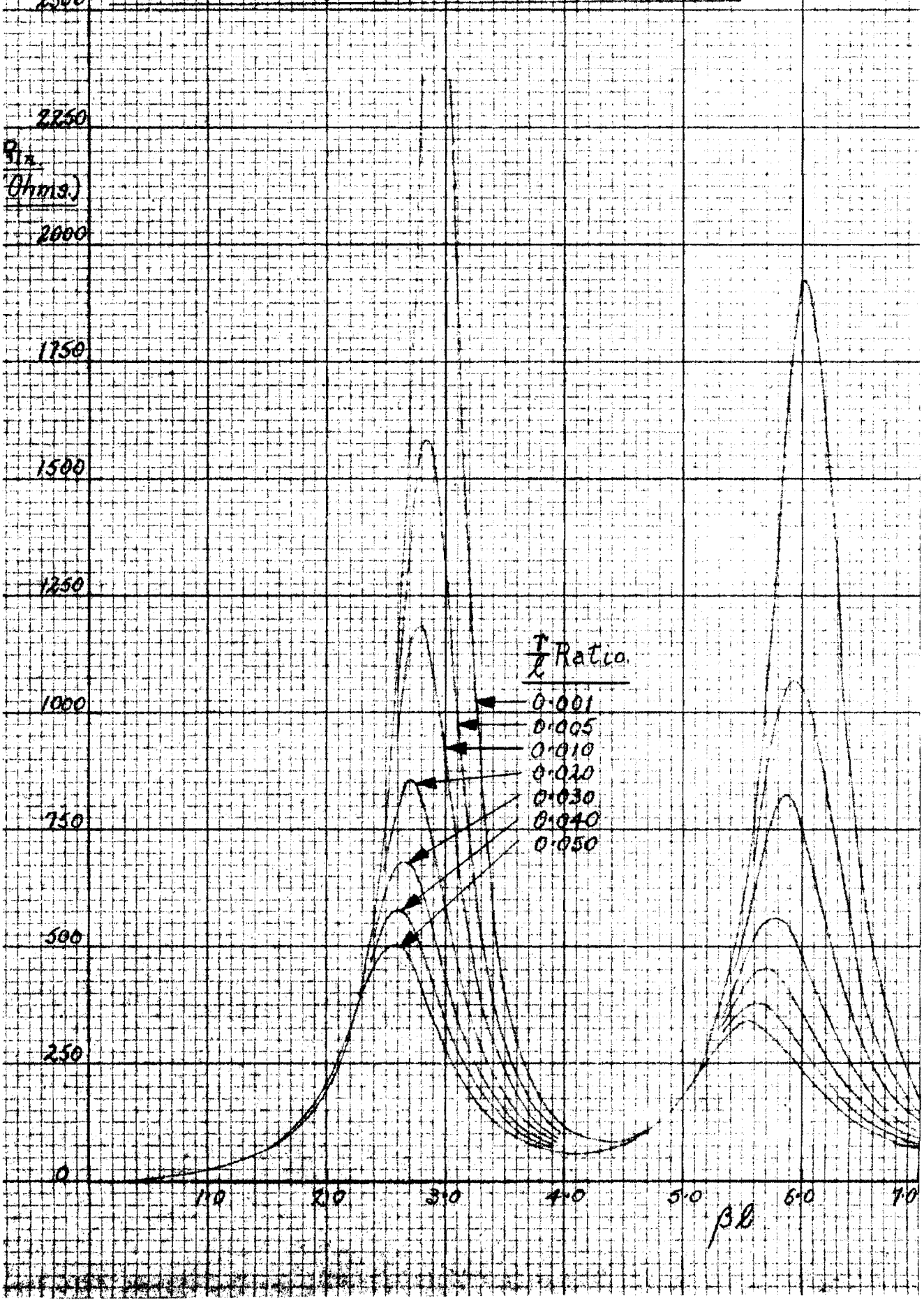

INPUT REACTANCE/$\beta\ell$ FOR A RANGE OF r/ℓ RATIOS BY THE CYLINDRICAL AERIAL METHOD. SECOND APPROXIMATION.

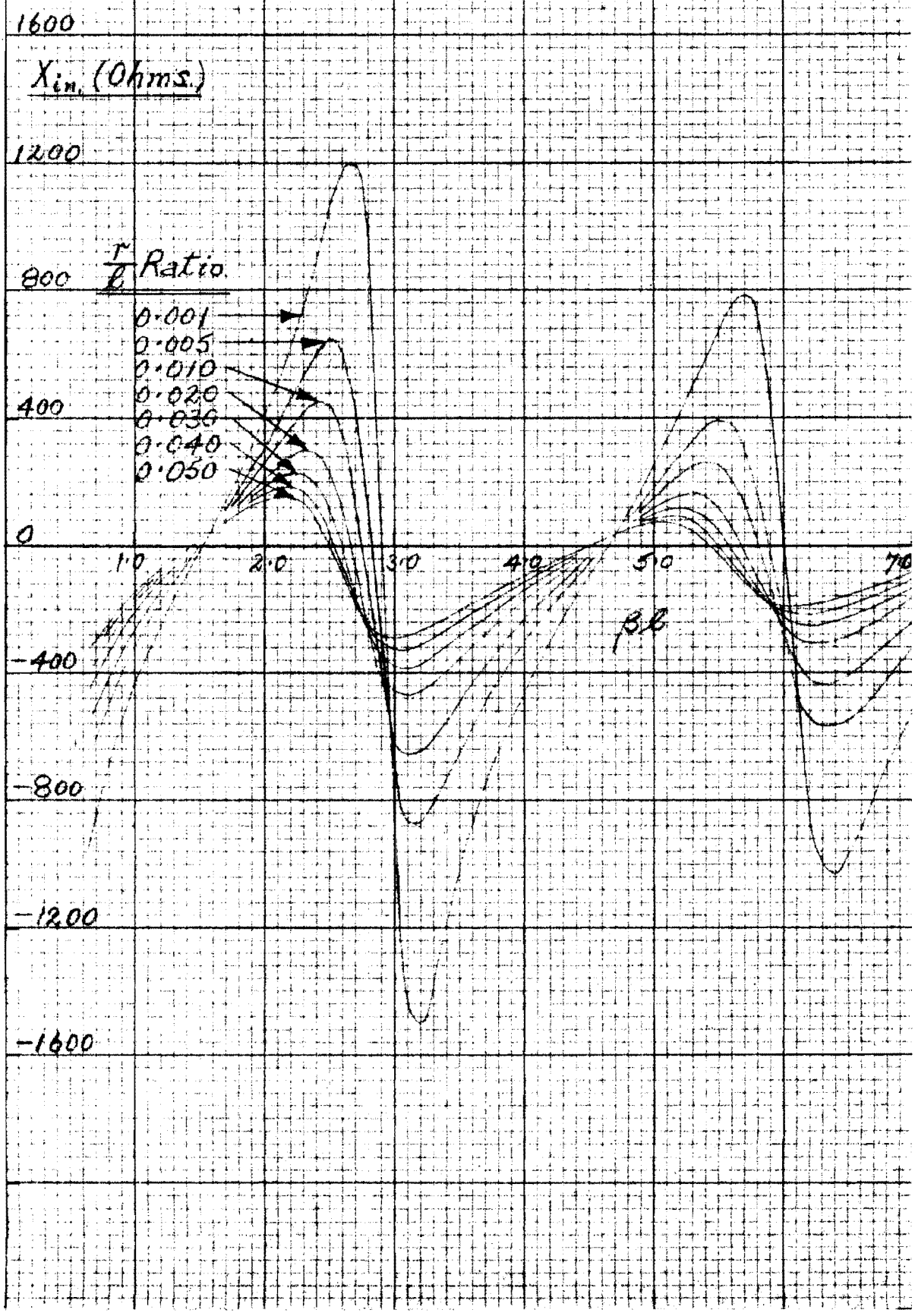

We consider now the theoretical expressions for the first resonant length.

We assume that $\left|\cos L+\frac{\alpha_1}{\Omega}\right| \ll \left|\frac{\alpha_2}{\Omega^2}\right|$

$\left|\sin L+\frac{\beta_1}{\Omega}\right| \ll \left|\frac{\beta_2}{\Omega^2}\right|$

The resonant lengths satisfy the equation $X(0)=0$

From equation (17)

$$X(0) = -j60\Omega\left\{\frac{(\Omega\cos L+A')(\Omega\sin L+B') + A''B''}{(\Omega\sin L+B')^2+(B'')^2}\right\}$$

If we neglect contributions due to the internal impedance of the aerial then

$$A' = \alpha_1' \; ; \; B' = \beta_1' \; ; \; A'' = \alpha_1'' \; ; \; B'' = \beta_1''$$

The condition for resonance becomes

$$(\Omega\cos L+\alpha_1')(\Omega\sin L+\beta_1') + \alpha_1''\beta_1'' = 0$$

If all but the leading terms are neglected in the first instance then it is seen that the resonant length is defined by

$$\cos L \sin L = 0$$

$L = \frac{n\pi}{2} - \delta$ where n = 1, 2, 3 -----

and δ is a small number.

Consider the odd resonances,

$$\cos L = \pm\delta \; ; \quad \sin L = \pm 1$$

Substituting these values in the condition for resonance we obtain on reduction

$$(\Omega \pm \beta_1')(\delta\Omega \pm \alpha_1') + \alpha_1''\beta_1'' = 0$$

Retaining terms in Ω only

$$\delta\Omega = \mp\alpha_1' \quad \text{or} \quad \Omega \pm \beta_1' = 0$$

It is required to find a solution for δ . For lengths near $L = \frac{n\pi}{2}$ the integral functions and Ω

are slowly varying functions. Hence we write $L = \frac{n\pi}{2}$ in the integral functions and in Ω .

We use the following conditions and approximations

$$\cos L = \pm\delta \; ; \quad \sin L = \pm 1 \; ; \quad L = \frac{n\pi}{2}$$

$$Si(x) \doteqdot \frac{\pi}{2} - \frac{\cos x}{x} \qquad Ci(x) \doteqdot \frac{\sin x}{x}$$

$$Cin(x) = \log \gamma x - Ci(x)$$

Substitute in $\delta\Omega = \mp\alpha_1'$ and reduce

$$\delta = \frac{Si\, 2n\pi}{4 \log\left(\frac{n\lambda}{r}\right)}$$

where $\frac{\gamma n\pi}{32}$ is neglected compared with $\left(\frac{n\lambda}{r}\right)^4$

The resonant lengths are for n odd

$$L = \frac{n\pi}{2} - \frac{Si\, 2n\pi}{4 \log\left(\frac{n\lambda}{r}\right)} \qquad (20)$$

By a similar method the antiresonant lengths are

$$L = \frac{n\pi}{2} - \frac{(4\, Si\, n\pi) - Si\, 2n\pi)}{4 \log\left(\frac{n\lambda}{r}\right)} \qquad (n \text{ even})$$

The following table of values of first resonant length has been calculated from equation (20).

$\frac{r}{\ell}$	0.001	0.005	0.010	0.020	0.030	0.040	0.050
$\frac{\ell}{\lambda}$	0.2474	0.2427	0.2405	0.2392	0.2385	0.2379	0.2370
% Fore-shortening	1.0	3.8	3.8	4.3	4.6	4.8	5.2

The following table of results for the first resonance has been deduced from the curves of input impedance given above. These values together with those obtained by other methods are shown in the accompanying graphs.

$\frac{r}{\ell}$	1st Approx. $\frac{\ell}{\lambda}$	1st Approx. R_{in} (Ohms.)	2nd Approx. $\frac{\ell}{\lambda}$	2nd Approx. R_{in} (Ohms.)
0.001	0.2435	62.8	0.2415	
0.005	0.2420	60.1	0.2390	68.7
0.010	0.2410	58.4	0.2375	68.1
0.020	0.2400	56.7	0.2350	67.1
0.030	0.2385	55.4	0.2335	66.3
0.040	0.2380	54.5	0.2320	65.1
0.050	0.2367	53.5	0.2280	62.3

A discussion of the above results will be given in a later section.

$\frac{l}{\lambda}$ RATIO / $\frac{r}{l}$ RATIO FOR THE FIRST RESONANT LENGTH.

(a) The Cylindrical Aerial Method. First Approximation.
(b) The Cylindrical Aerial Method. Theory.

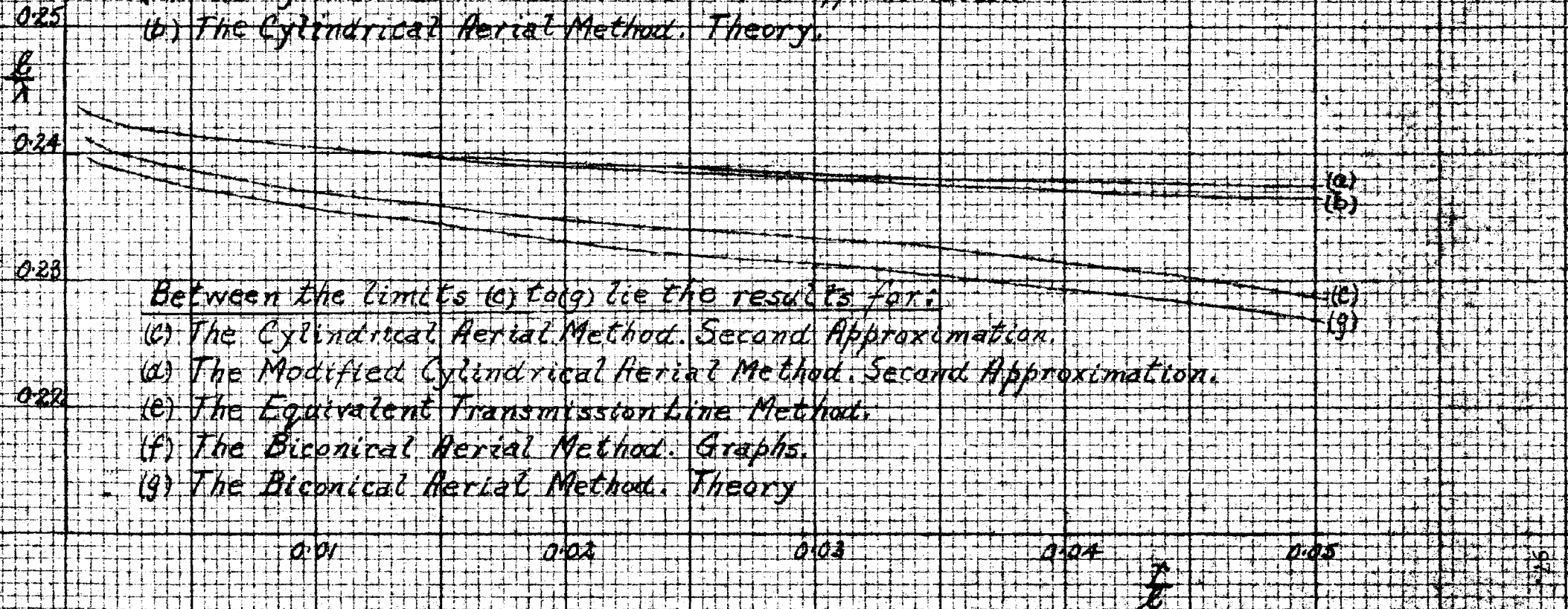

Between the limits (a) to (g) lie the results for:
(c) The Cylindrical Aerial Method. Second Approximation.
(d) The Modified Cylindrical Aerial Method. Second Approximation.
(e) The Equivalent Transmission Line Method.
(f) The Biconical Aerial Method. Graphs.
(g) The Biconical Aerial Method. Theory

INPUT RESISTANCE / $\frac{r}{\ell}$ RATIO FOR THE FIRST RESONANT LENGTH.

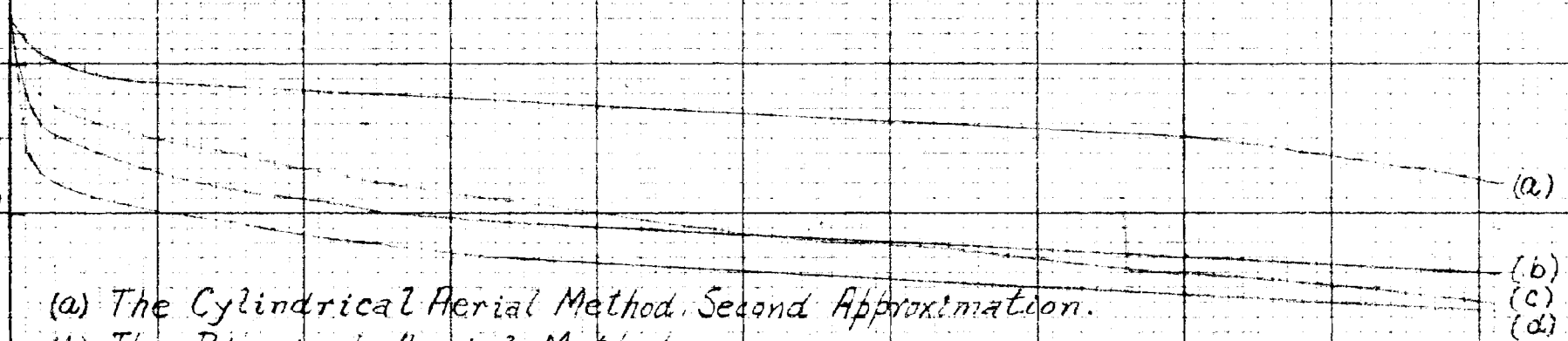

(a) The Cylindrical Aerial Method. Second Approximation.
(b) The Biconical Aerial Method.
(c) The Equivalent Transmission Line Method.
(a) The Cylindrical Aerial Method. First Approximation.

0 0·01 0·02 0·03 $\frac{r}{\ell}$ 0·04 0·05

The value of the maximum input resistance is determined as follows:

From Equation (17) the input resistance is

$$R(0) = 60\Omega \left\{ \frac{A''(\Omega \sin L + B') - B''(\Omega \cos L + A')}{(\Omega \sin L + B')^2 + (B'')^2} \right\} \qquad (20)_1$$

The input resistance to first order is from this equation

$$R(0) = 60 \frac{(A'' - B'' \cot L)}{\sin L}$$

A maximum value of $R(0)$ will occur from this equation when

$$L = 2m\frac{\pi}{2} \qquad m = 1, 2, 3 \text{ -----}$$

Now this value of $R(0)$ is the leading term in the total expression for $R(0)$ so that the true maximum will occur at

$$L = 2m\frac{\pi}{2} - \epsilon \quad \text{where} \quad |\epsilon| < 1$$

Consider now the general Equation $(20)_1$ for input resistance. The leading term in the numerator is $B''\Omega \cos L$ with the possible exception of $A'B''$. The shape factor Ω is usually large enough to make $B''\Omega \cos L$ the leading term. The three functions in the numerator are slowly varying functions for L near $m\pi$ so that maximization of $R(0)$ will occur when the denominator is a minimum. Since B'' is slowly varying this condition will occur when

$$\Omega \sin L + B' = 0 \qquad (21)$$

Now $B' = \beta_1' - \frac{\ell r_0 x_i}{30}$. Hence for good conductors we may write $B' = \beta_1'$

$$\beta_1' = \frac{1}{2}\left\{\cos L(4Si2L - Si4L) + \sin L(4\log 2 + 2Ci2L - Ci4L)\right\}$$

$$\Omega = 2\log\frac{2\ell}{r}$$

Substitute in equation (21) and the following expression is obtained on reduction.

$$\tan L = \frac{Si4L - 4Si2L}{4\log\frac{4\ell}{r} + 2Ci2L - Ci4L} \qquad (22)$$

The integral functions are slowly varying functions near $L = m\pi$; we therefore substitute $L = m\pi$ in the integral functions. The following reductions apply for large arguments

$$Si(x) \doteq \frac{\pi}{2} - \frac{\cos x}{x} \quad ; \quad Ci(x) \doteq \frac{\sin x}{x}$$

$$Cin(x) = \int_0^x \frac{1-\cos u}{u}\, du = \log \gamma x - Ci(x)$$

where $\log \gamma = C = 0{\cdot}577 \cdots$ Euler's Constant

Also $\tan(m\pi - \epsilon) \doteq -\epsilon$

$$\frac{4\ell}{r} = \frac{2m\lambda}{r}$$

Making the appropriate substitutions in equation (22) we have on reduction

$$\epsilon = \frac{\frac{3\pi}{2} - \frac{7}{4m\pi}}{4\log\frac{2m\lambda}{r} + \log \gamma m\pi}$$

The following reductions are obtained for the functions in equation (20) when $L = 2m\frac{\pi}{2}$

$$B' = \frac{1}{2}(-1)^m \left\{\frac{3\pi}{2} - \frac{7}{4m\pi}\right\}$$

$$A'' = \frac{1}{2}(-1)^m \left\{\frac{3}{4m\pi} - \frac{\pi}{2}\right\}$$

$$B'' = \frac{1}{2}(-1)^{m+1} \log 4(\gamma m\pi)^3$$

$$A' = \frac{1}{2}(-1)^{m+1} \log \gamma m\pi$$

$$\sin L = (-1)^{m+1}\epsilon \quad ; \quad \cos L = (-1)^m$$

Substitution of the above expressions in the terms of equation (20) yields on reduction

$$A''(\Omega \sin L + B') = \frac{1}{4}\left(\frac{3}{4m\pi} - \frac{\pi}{2}\right)\epsilon \log 16\,\gamma m\pi$$

$$-B'(\Omega \cos L + A') = \frac{1}{4}\log 4(\gamma m\pi)^3 \left\{2\Omega - \log \gamma m\pi\right\}$$

$$(\Omega \sin L + B')^2 = \left\{\frac{1}{2}\epsilon \log 16\,\gamma m\pi\right\}^2$$

$$(B'')^2 = \frac{1}{4}\left\{\log 4(\gamma m\pi)^3\right\}^2$$

Neglecting terms of order ϵ which will be small compared to the other terms and substituting the above quantities in equation (20) yields on reduction

$$R(o)_{max.} = \frac{60\{2\Omega - \log \gamma m\pi\}}{3\log \gamma m\pi + 2\log 2}$$

The following table of maximum input resistance has been calculated from the above equation.

$\frac{r}{\ell}$	0.001	0.005	0.010	0.020	0.030	0.040	0.050
$\frac{\ell}{\lambda}$	0.4815	0.4767	0.4743	0.4713	0.4688	0.4673	0.4662
R (Ohms)	3670	2520	1920	1430	1140	1000	940

The above values of maximum input resistance will be discussed in a later section.

A modified form of the above method for determining the input impedance gives a clear understanding of the principles involved. Also the iterative process converges more rapidly than for the above method. The method is treated below together with the results of calculations for the input impedance as a function of $\frac{\ell}{\lambda}$ ratio for a range of constant r/l ratios.[46,47,48]

This method is essentially the same as the one given above until the integral equation; that is equation (5) is obtained.

Since there is no exact solution of the integral equation in closed form an approximate solution is found by expanding the integral in a converging power series in terms of an appropriately chosen current distribution function. It is important to choose the distribution function in such a way that convergence is rapid so that the sum of two or three terms gives a satisfactory approximation.

Let I_o be the input current

$f(z)$ the current distribution function

$$I_z = I_o f(z) \quad I_z' = I_o f(z') = I_z \frac{f(z')}{f(z)} = I_z\, g(z,z')$$

where $g(z,z')$ is the relative distribution function.

Let $\psi(z) = \int_{-\ell}^{+\ell} g(z,z') \frac{e^{-j\beta R}}{R} dz'$

Then $\frac{4\pi}{\eta} A_z = \int_{-\ell}^{+\ell} I'_z \frac{e^{-j\beta R}}{R} dz' = I_z \psi(z) + \int_{-\ell}^{+\ell} \left\{ \frac{I'_z - I_z g(z,z')}{R} \right\} e^{-j\beta R} dz'$

The nearer $g(z,z')$ is to the true distribution the smaller will the correction term or integral on the right hand side be. If the distribution function is exact then

$$\psi(z) = \frac{4\pi}{\eta} \frac{A_z}{I_z}$$

Now A_z is largely dependent on the current at and near Z It is consistent therefore that $\psi(z)$ be reasonably constant and predominantly real at all points along the aerial except at and near very small or zero values of the current.

Let $\psi(z) = \psi + \gamma(z)$

The function $\gamma(z)$ is a small complex correction function except at values of Z where I_z is small or zero.

The process between equations (6) and (16) of the above method is carried out and the current distribution obtained.

$$I_z = \frac{j2\pi V_z}{\eta\psi} \left\{ \frac{\sin\beta(\ell-|z|) + \sum_{n=1}^{m} \frac{M_n(z)}{\psi^n}}{\cos\beta\ell + \sum_{n=1}^{m} \frac{F_n(\ell)}{\psi^n}} \right\} \qquad (23)$$

where

$$F_n(z) - F_n(\ell) = F_{nz} \; ; \; F_0(z) = \cos\beta z \; ; \; F_0(\ell) = \cos\beta\ell$$

$$G_0(z) = \sin\beta|z| \; ; \; G_0(\ell) = \sin\beta\ell$$

$$F_n(z) = F_{n-1,z}\psi - \int_{-\ell}^{+\ell} F_{n-1,z'} \frac{e^{-j\beta R}}{R} dz'$$

$$F_n(\ell) = -\int_{-\ell}^{+\ell} F_{n-1,z'} \frac{e^{-j\beta R_\ell}}{R_\ell} dz'$$

The G functions are obtained by putting G for F in the above expressions.

$$M_1(z) = M'_1(z) + jM''_1(z)$$

$$= F_1(z)\sin\beta\ell - F_1(\ell)\sin\beta|z| + G_1(\ell)\cos\beta z - G_1(z)\cos\beta\ell$$

$$M_2(z) = M'_2(z) + jM''_2(z)$$

$$= F_2(z)\sin\beta\ell - F_2(\ell)\sin\beta|z| + G_1(\ell)F_1(z) - G_1(z)F_1(\ell) + G_2(\ell)\cos\beta z - G_2(z)\cos\beta\ell$$

$$\alpha_{n_1} = \alpha'_{n_1} + j\alpha''_{n_1} = F_n(\ell)$$

$$\beta_{n_1} = \beta'_{n_1} + j\beta''_{n_1} = M_n(0) = M'_n(0) + jM''_n(0)$$

Put $z = 0$ in equation (23) then the input impedance is

$$Z(0) = \frac{-j\eta\psi}{2\pi}\left\{\frac{\cos\beta\ell + \sum_1^m \frac{\alpha_{n_1}}{\psi^n}}{\sin\beta\ell + \sum_1^m \frac{\beta_{n_1}}{\psi^n}}\right\} \qquad (24)$$

The expressions for the current distribution and for the input impedance depend upon the constant ψ and this in turn depends upon the relative distribution function $g(z,z')$ These quantities are now considered. The relative distribution function $g(z,z')$ must be chosen so that it is a sufficiently good approximation of the actual distribution to make the difference integral small. Furthermore, it must be sufficiently simple in form so that the integral for $\psi(z)$ may be evaluated and separated into a principal, constant real part ψ and a small correction term $\gamma(z)$.

The distribution function chosen in the previous analysis depended on the reasonable assumption that the vector potential A_z at z depends primarily upon the current at and near z . If contributions from all more distant elements of current are small, A_z may be evaluated approximately by assuming the current at all points to be I_z and by neglecting retardation. This is equivalent to putting

$$g(z,z') = e^{j\beta R}$$

The above relative distribution function is the simplest and most obvious one if an attempt is made to solve the integral equation. If the formal solution of equation (23) is attempted it is clear that the predominant term of the current distribution must be of the form

$$I_z = Kf_1(z) \quad \text{where } f_1(z) = \sin\beta(\ell - |z|)$$

where K is an amplitude factor independent of z

Let $$g(z,z') = \frac{\sin\beta(\ell - |z'|)}{\sin\beta(\ell - |z|)} = \frac{f_1(z')}{f_1(z)}$$

This function is a better approximation for the actual current than the previous relative distribution function since the function $f_1(z) = \sin\beta(\ell-|z|)$ is proportional to the principal part of the current and the function $e^{j\beta R}$ is not.

$$\psi(z) = \int_{-\ell}^{+\ell} g(z,z') \frac{e^{-j\beta R}}{R} dz'$$

$$\psi_1(z) = \int_{-\ell}^{+\ell} f_1(z') \frac{e^{-j\beta R}}{R} dz' = C(z)\sin\beta\ell - S(z)\cos\beta\ell$$

where $\psi(z) = \frac{\psi_1(z)}{f_1(z)}$; $f_1(z) = \sin\beta(\ell-|z|)$

$$C(z) = \int_{-\ell}^{+\ell} \cos\beta z' \frac{e^{-j\beta R}}{R} dz'$$

$$S(z) = \int_{-\ell}^{+\ell} \sin\beta z' \frac{e^{-j\beta R}}{R} dz'$$

Evaluation of $\psi(z)$ for $\beta\ell = \frac{\pi}{2}$ and π show that $\psi(z)$ has a small imaginary part in confirmation of the above assumptions regarding $\psi(z)$.

Further analyses show that

(i) The relative distribution function $g(z,z') = \frac{\sin\beta(\ell-|z'|)}{\sin\beta(\ell-|z|)}$ is a good approximation for all values of ℓ.

(ii) Suitable parameters for expansion are

$$\psi = \begin{cases} |\psi(0)| = |\psi_1(0)| & \beta\ell \leq \frac{\pi}{2} \\ |\psi(\ell-\frac{\lambda}{4})| = |\psi_1(\ell-\frac{\lambda}{4})| & \beta\ell \geq \frac{\pi}{2} \end{cases}$$

Since $\psi(z)$ has such a small imaginary part and is well represented by the above equations except at the ends of the aerial, the correction function $\gamma(z)$ is sufficiently small to be neglected.

We return now to an evaluation of the input impedance from equation (24).

The functions $F, G, M, \alpha_n, \beta_n$ may be expressed in terms of known functions. The analysis is long and is not presented here. When the results of this analysis are substituted in equation (24) the following equation is obtained.

$$Z(0) = \frac{-j\eta\psi}{2\pi} \left\{ \frac{\cos\beta\ell + \sum_{n=1}^{m} (D_n)_{m-1} \frac{\alpha_n}{\psi^n}}{(D_1)_m \sin\beta\ell + \sum_{n=1}^{m} (D_{n+1})_m \frac{\beta_n}{\psi^n}} \right\} \qquad (25)$$

Equation (25) may be reduced to the following

$$Z(o) = 60\psi \left|\frac{A_1 + jA_2}{B_1 + jB_2}\right| e^{j\left(\tan^{-1}\frac{A_2}{A_1} - \tan^{-1}\frac{B_2}{B_1}\right)} \qquad (26)$$

where for the first order solution

$$A_1 = (D_1)_o \alpha_1''$$

$$A_2 = -\{\psi \cos\beta\ell - (D_1)_o \alpha_1'\}$$

$$B_1 = \psi (D_1)_1 \sin\beta\ell + \beta_1'$$

$$B_2 = \beta_1''$$

For the second order solution

$$A_1 = (D_1)_1 \frac{\alpha_1''}{\psi} + (D_2)_1 \frac{\alpha_2''}{\psi^2}$$

$$A_2 = -\left\{\cos\beta\ell + (D_1)_1 \frac{\alpha_1'}{\psi} + (D_2)_1 \frac{\alpha_2'}{\psi^2}\right\}$$

$$B_1 = (D_1)_2 \sin\beta\ell + (D_2)_2 \frac{\beta_1'}{\psi} + \frac{\beta_2'}{\psi^2}$$

$$B_2 = (D_2)_2 \frac{\beta_1''}{\psi} + \frac{\beta_2''}{\psi^2}$$

$$x = 1 - \frac{\Omega}{\psi} \qquad (D)_o = 1;\ (D_1)_1 = 1;\ (D_2)_1 = 1;\ (D_1)_2 = 1 + x + x^2$$

$$(D_2)_2 = 1 + 2x$$

The following formulae have been evaluated for $C(z)$ and $S(z)$

$$C(z) \doteqdot -\tfrac{1}{2}\cos\beta z \{Ei\,2\beta(\ell+z) + Ei\,2\beta(\ell-z)\}$$
$$+ \tfrac{j}{2}\sin\beta z \{Ei\,2\beta(\ell-z) - Ei\,2\beta(\ell+z)\}$$
$$+ \cos\beta z \left\{sh^{-1}\frac{\ell+z}{r} + sh^{-1}\frac{\ell-z}{r}\right\}$$

$$S(z) \doteqdot -\tfrac{j}{2}\cos\beta z \{Ei\,2\beta(\ell+z) + Ei\,2\beta(\ell-z) - Ei\,2\beta|z|\}$$
$$+ \tfrac{1}{2}\sin\beta z \{Ei\,2\beta(\ell+z) - Ei\,2\beta(\ell-z) - 2jSi\,2\beta z\}$$
$$- \sin\beta|z|\, Ci\,2\beta z + \sin\beta|z| \left\{sh^{-1}\frac{\ell+z}{r} + sh^{-1}\frac{\ell-z}{r}\right\}$$
$$+ 2\sin\beta|z| \log\left\{\frac{|z|}{\ell+|z|}\right\}$$

These functions give ψ the cylindrical aerial shape factor after substitution and suitable reduction.

The input impedance was calculated using equation (26) as a function of $\frac{\ell}{\lambda}$ ratio for a range of r/l ratios. The results are tabulated and plotted below. The above analysis has been treated very sketchily for the sake of brevity.

The results will be discussed in a later section. The quantitative results were obtained by graphical interpolation. It follows that the accuracy of the values obtained for R and X will not be very high.

Input Resistance by Modified Cylindrical Aerial Method

First Approximation

L \ $\frac{r}{\ell}$	0.001	0.005	0.010	0.020	0.030	0.040	0.050
0.9	13.4	18.6	16.3	14.4	17.9	16.1	15.6
1.0	22.3	22.4	21.7	20.8	20.6	19.6	20.0
1.1	33.0	29.2	29.3	26.5	28.2	25.7	24.2
1.2	43.1	39.0	36.3	33.0	33.6	31.1	29.8
1.3	52.6	48.6	45.4	41.5	40.9	38.6	36.2
1.4	61.0	57.1	51.5	49.1	52.1	48.4	43.0
1.5	59.2	61.6	61.7	54.9	53.9	52.9	46.7
1.6	73.6	74.4	70.9	67.4	63.0	63.9	63.5
1.7	107	98.4	89.9	85.0	63.0	71.0	78.0
1.8	135	122	110.5	101.9	76.6	85.6	98.9
1.9	163	145.7	128.6	121.2	100.5	114.8	121.9
2.0	172	156	166.8	163.5	160	158	153.9
2.1	208	206	228	220	211	206	197
2.2	285	266	304	302	279	263	251
2.3	391	362	397	390	358	338	312
2.4	566	514	519	486	440	410	371
2.5	776	706	663	589	528	472	423
2.6	1087	922	822	684	591	519	444
2.7	1422	1180	978	750	614	522	439
2.8	1745	1390	1087	761	603	500	412
2.9	1995	1470	1100	729	565	462	376
3.0	2060	1409	1009	660	502	412	345
3.1	1913	1257	869	577	439	366	311
3.2	1578	1020	720	494	387	321	274
3.3	1145	775	577	417	341	291	247
3.4	819	590	472	359	298	256	224
3.5	597	451	383	308	261	227	203
3.6	454	375	325	260	231	204	185
3.7	345	300	264	219	200	183	170
3.8	267	238	212	182	172	160	149
3.9	210	192	173	149	146	139	130
4.0	163	148	140	125	123	118	114

Input Reactance by the Modified Cylindrical Aerial Method.

First Approximation

L \ r/ℓ	0.001	0.005	0.010	0.020	0.030	0.040	0.050
0.5	-9150	-3330	-2407	-1590	-1237	-966	-913
0.6	-6750	-2500	-1735	-1220	-715	-560	-520
0.7	-4600	-1650	-1210	-690	-482	-420	-397
0.8	-2450	-940	-650	-475	-380	-335	-306
0.9	-850	-560	-465	-375	-309	-279	-267
1.0	-544	-414	-355	-300	-268	-238	-221
1.1	-429	-334	-289	-251	-226	-206	-194
1.2	-327	-267	-229	-203	-187	-173	-164
1.3	-237	-204	-184	-164	-153	-144	-134
1.4	-169	-149	-134	-122	-117	-109	-103
1.5	-104	-97	-93	-79	-76	-74	-76
1.6	-68	-54.1	-47	-43	-33	-33	-42
1.7	-25.6	-10.4	-5.0	-3.0	-1.7	0	-11.9
1.8	+36.7	+42.1	+44.6	+35.9	+26.4	+27.8	+24.8
1.9	+163	+122	+95	+88	+66	+59	+49
2.0	+333	+244	+191	+144	+116	+93	+78
2.1	+515	+355	+279	+204	+154	+123	+102
2.2	+705	+459	+352	+262	+194	+144	+115
2.3	+839	+558	+409	+305	+217	+151	+110
2.4	+942	+614	+441	+316	+215	+132	+86
2.5	+972	+619	+437	+266	+167	+89	+35
2.6	+960	+599	+366	+171	+72	+7.2	-38
2.7	+795	+429	+226	+26.2	-42	-82.9	-105
2.8	+516	+159	+9.5	-114	-141	-157	-161
2.9	+69.6	-193.5	-224	-251	-230	-216	-198
3.0	-480	-520	-442	-346	-291	-254	-224
3.1	-932	-725	-554	-404	-331	-276	-239
3.2	-1325	-869	-620	-437	-346	-287	-241
3.3	-1415	-890	-641	-447	-353	-287	-243
3.4	-1363	-842	-627	-443	-350	-284	-242
3.5	-1189	-764	-590	-430	-340	-280	-241
3.6	-1069	-706	-563	-415	-331	-278	-239
3.7	-938	-644	-519	-394	-321	-275	-239
3.8	-822	-584	-475	-373	-305	-266	-237
3.9	-730	-526	-436	-349	-287	-258	-229
4.0	-628	-460	-386	-326	-272	-243	-220

Input Resistance by the Modified Cylindrical Aerial Method

Second Approximation

L \ r/ℓ	0.001	0.005	0.010	0.020	0.030	0.040	0.050
0.5	4.3	4.5	4.1	-	3.0	2.4	4.3
0.6	10.3	8.3	6.9	5.4	4.8	5.5	8.8
0.7	19.1	14.2	11.7	9.0	7.9	7.1	8.0
0.8	34.0	24.1	18.9	15.2	13.1	11.2	11.7
0.9	-	-	-	-	17.1	16.1	17.0
1.0	30.1	23.4	22.3	22.8	22.7	23.2	22.4
1.1	45.3	36.0	33.0	32.8	33.8	34.5	31.0
1.2	70.2	52.5	50.2	49.6	47.6	48.0	41.3
1.3	89.4	63.9	64.3	63.3	61.0	54.4	50.3
1.4	78.9	53.5	61.5	67.1	65.3	59.4	62.9
1.5	-	47.6	-	70.4	67.6	71.0	79.2
1.6	-	54.6	62.1	72.7	82.5	88.8	99.9
1.7	89.1	76.1	74.5	98.0	103.8	111.1	129
1.8	141	123.3	107.8	133.1	136.8	143.5	170
1.9	196	180	160	165.8	178.2	185	209

Input Resistance by the Modified Cylindrical Aerial Method

Second Approximation (Contd.)

L \ r/ℓ	0.001	0.005	0.010	0.020	0.030	0.040	0.050
2.0	229	238	246	229	237	246	265
2.1	335	339	336	315	314	301	327
2.2	529	454	411	411	400	361	377
2.3	577	577	532	517	476	412	392
2.4	688	742	751	601	519	422	361
2.5	946	976	909	644	512	385	305
2.6	1359	1178	930	625	464	329	237
2.7	1845	1310	965	559	382	264	185
2.8	2210	1289	870	470	299	206	143
2.9	2210	1136	702	362	226	156	111.7
3.0	1920	825	501	277	175	123	91.4
3.1	1375	642	381	213	142	104	74.6
3.2	973	487	294	173	118	87	61.0
3.3	684	366	227	147	102	74	52.4
3.4	484	276	186	127	91.8	66	46.1
3.5	305	199	147	111	78.3	58.3	41.9
3.6	223	161	121	95.3	70.9	56.1	39.9
3.7	155	124	108	88.8	70.0	55.5	39.8
3.8	113	103	100	86.8	70.9	59.1	41.2
3.9	92	91	179	87.5	75.9	63.5	43.4
4.0	79.5	90	86.9	91.8	82.8	71.0	47.2

Input Reactance by the Modified Cylindrical Aerial Method

Second Approximation

L \ r/ℓ	0.001	0.005	0.010	0.020	0.030	0.040	0.050
0.6	-740	-590	-490	-385	-345	-317	-314
0.7	-730	-540	-445	-342	-300	-270	-220
0.8	-649	-459	-360	-290	-250	-212	-191
0.9	-545	-370	-305	-240	-203	-167	-156
1.0	-430	-297	-249	-197	-166	-142	-124.1
1.1	-322	-227	-187	-155	-131	-113	-93.5
1.2	-230	-162	-131	-112	-93.8	-83.2	-64.0
1.3	-133	-89.6	-76.6	-66.7	-59.0	-44	-34.7
1.4	-49.3	-27.2	-23.3	-23.2	-22.5	-13.7	-8.1
1.5	-1.1	+1.7	+5.8	+12.7	+14.2	+16.7	+18.9
1.6	+19.4	+24.9	+27.7	+30.9	+35.9	+39.9	+45.1
1.7	+87.6	+72.3	+63.6	+60.1	+62.3	+65.5	+69.4
1.8	+191	+144.5	+116	+104.1	+95.8	+87	+88.5
1.9	+326	+237	+186	+144.7	+125.8	+103.3	+100.8
2.0	+444	+326	+272	+184.5	+150.6	+109.8	+96.5
2.1	+569	+433	+314	+204	+153.5	+94.7	+67.9
2.2	+744	+517	+543	+196	+125.3	+44.1	+3.3
2.3	+879	+568	+446	+153.5	+58.5	-35.3	-84.6
2.4	+983	+586	+304	+63.3	-45.3	-121	-161.2
2.5	+1040	+519	+216	-54.1	-151	-196	-214
2.6	+1007	+294	0	-178.2	-236	-239	-238
2.7	+746	0	-223	-290	-293	-260	-237
2.8	+193.8	-333	-406	-355	-315	-264	-224
2.9	-509	-591	-530	-375	-305	-250	-208
3.0	-1159	-756	-557	-374	-289	-229	-191.5
3.1	-1239	-752	-544	-362	-267	-213	-173
3.2	-1181	-696	-500	-339	-248	-196	-155.5
3.3	-1093	-625	-445	-317	-228	-176	-140.6
3.4	-972	-566	-393	-291	-216	-162	-125.9
3.5	-816	-483	-347	-264	-194	-150	-113.2
3.6	-685	-432	-313	-242	-176	-139	-101.0
3.7	-549	-370	-282	-220	-166	-131	-91.1
3.8	-436	-334	-261	-204	-156	-121	-79.9
3.9	-369	-297	-242	-196	-149	-112	-69.2
4.0	-325	-279	-224	-188	-139	-102	-59.2

INPUT RESISTANCE/βℓ FOR A RANGE OF r/ℓ RATIOS BY THE MODIFIED CYLINDRICAL AERIAL METHOD. FIRST APPROXIMATION.

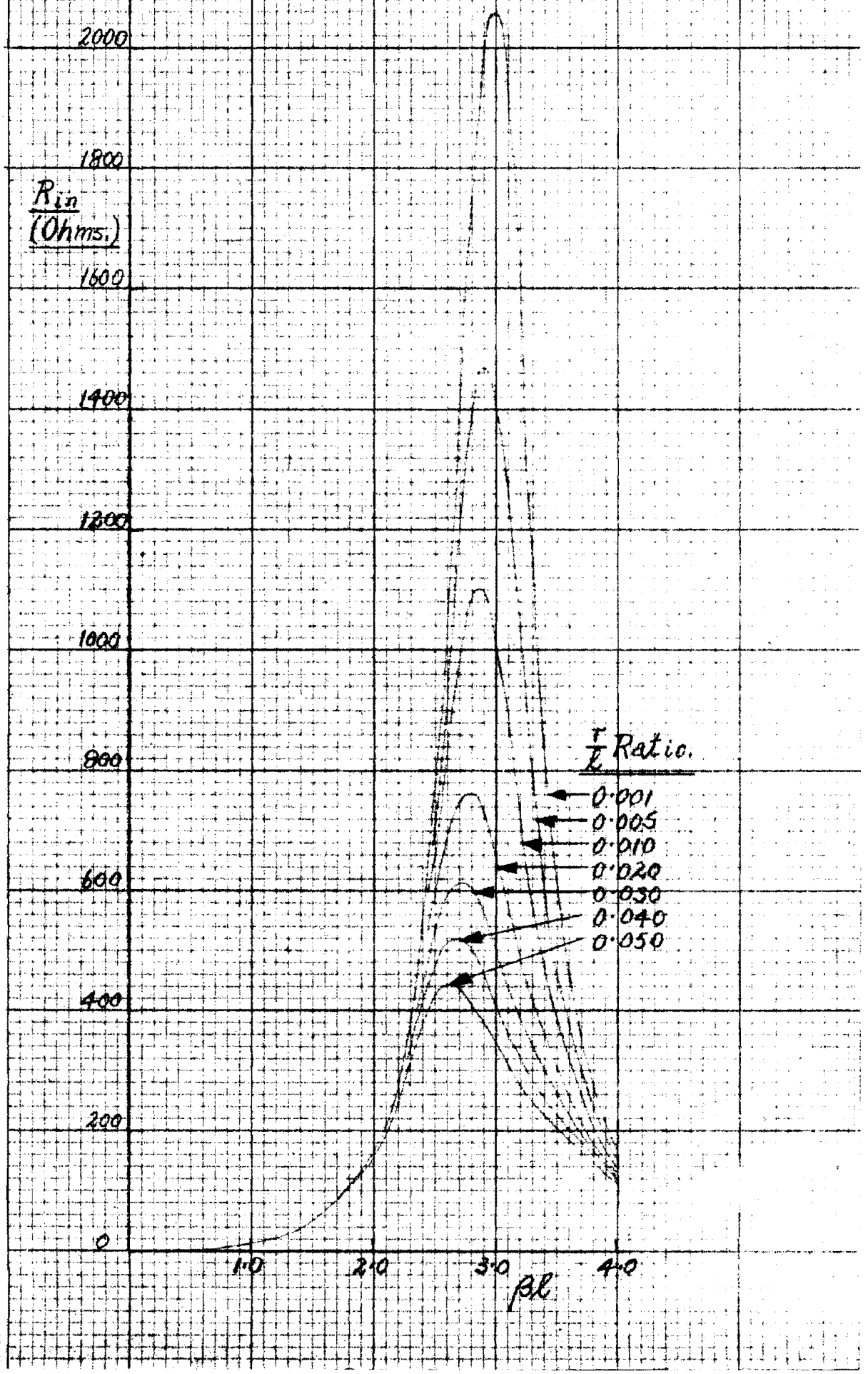

INPUT REACTANCE / βℓ FOR A RANGE OF r/ℓ RATIOS BY THE MODIFIED CYLINDRICAL AERIAL METHOD. FIRST APPROXIMATION.

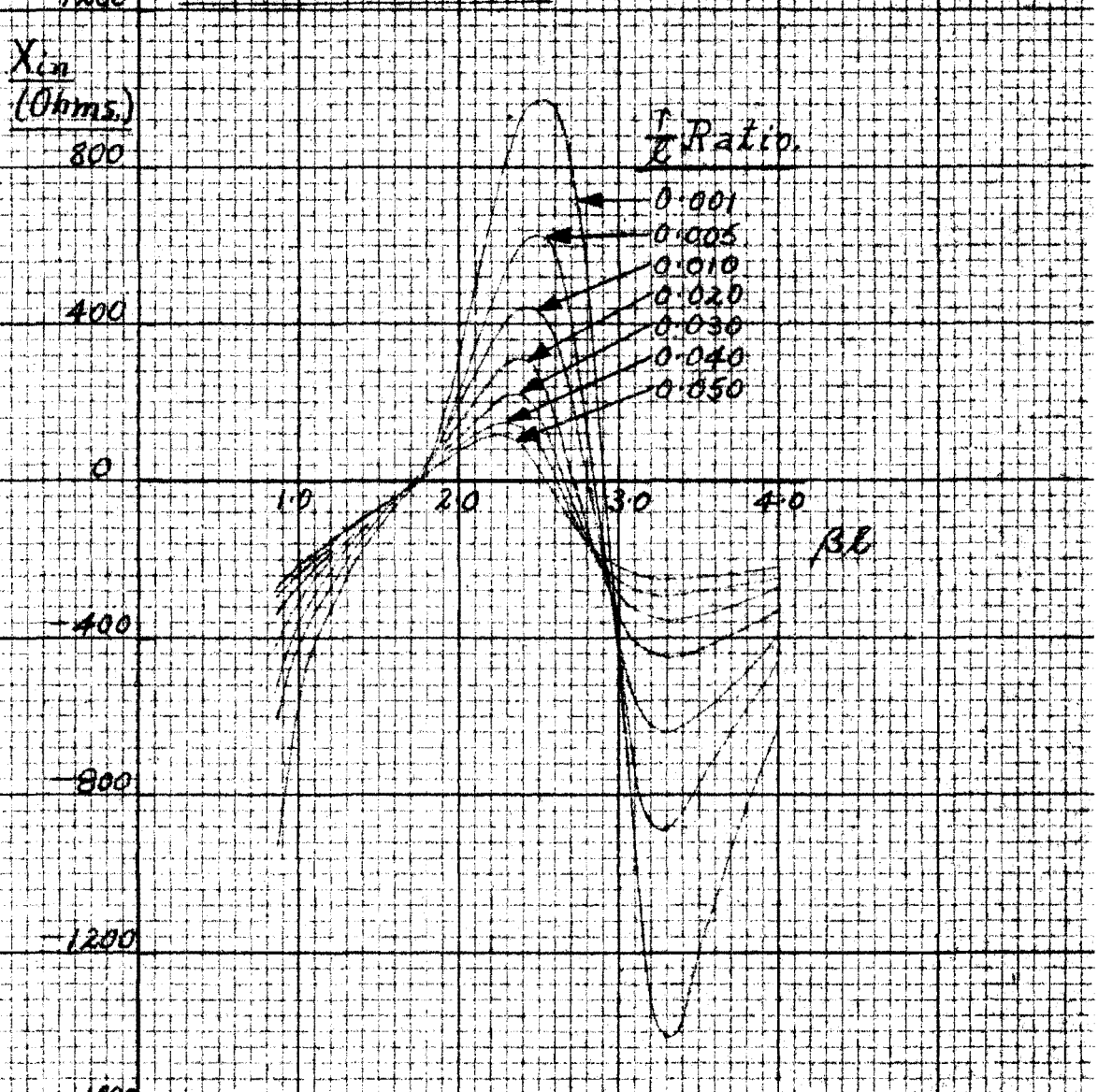

INPUT RESISTANCE / βℓ FOR A RANGE OF r/ℓ RATIOS BY THE MODIFIED CYLINDRICAL AERIAL METHOD. SECOND APPROXIMATION.

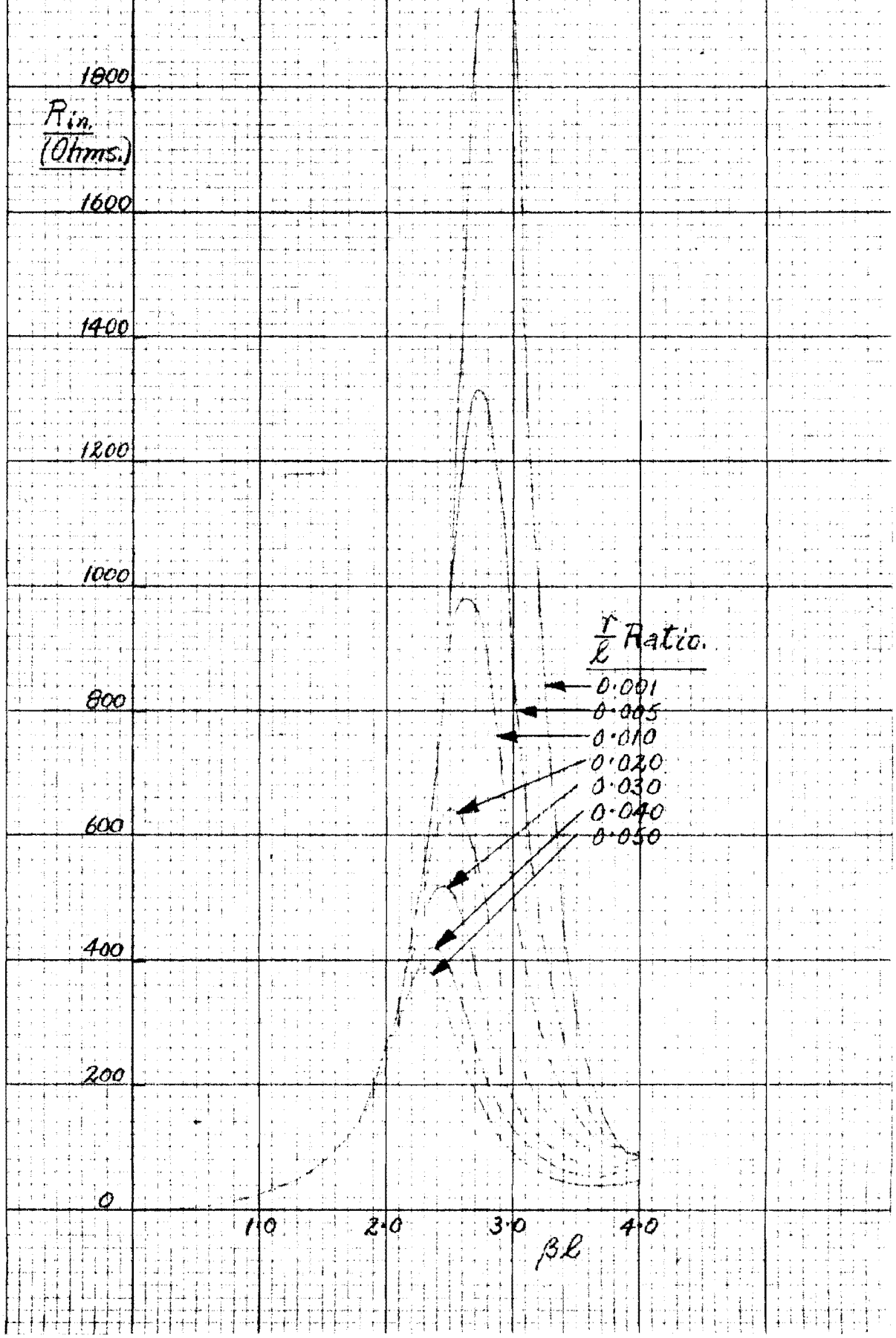

INPUT REACTANCE / βℓ FOR A RANGE OF r/ℓ RATIOS BY THE MODIFIED CYLINDRICAL AERIAL METHOD. SECOND APPROXIMATION.

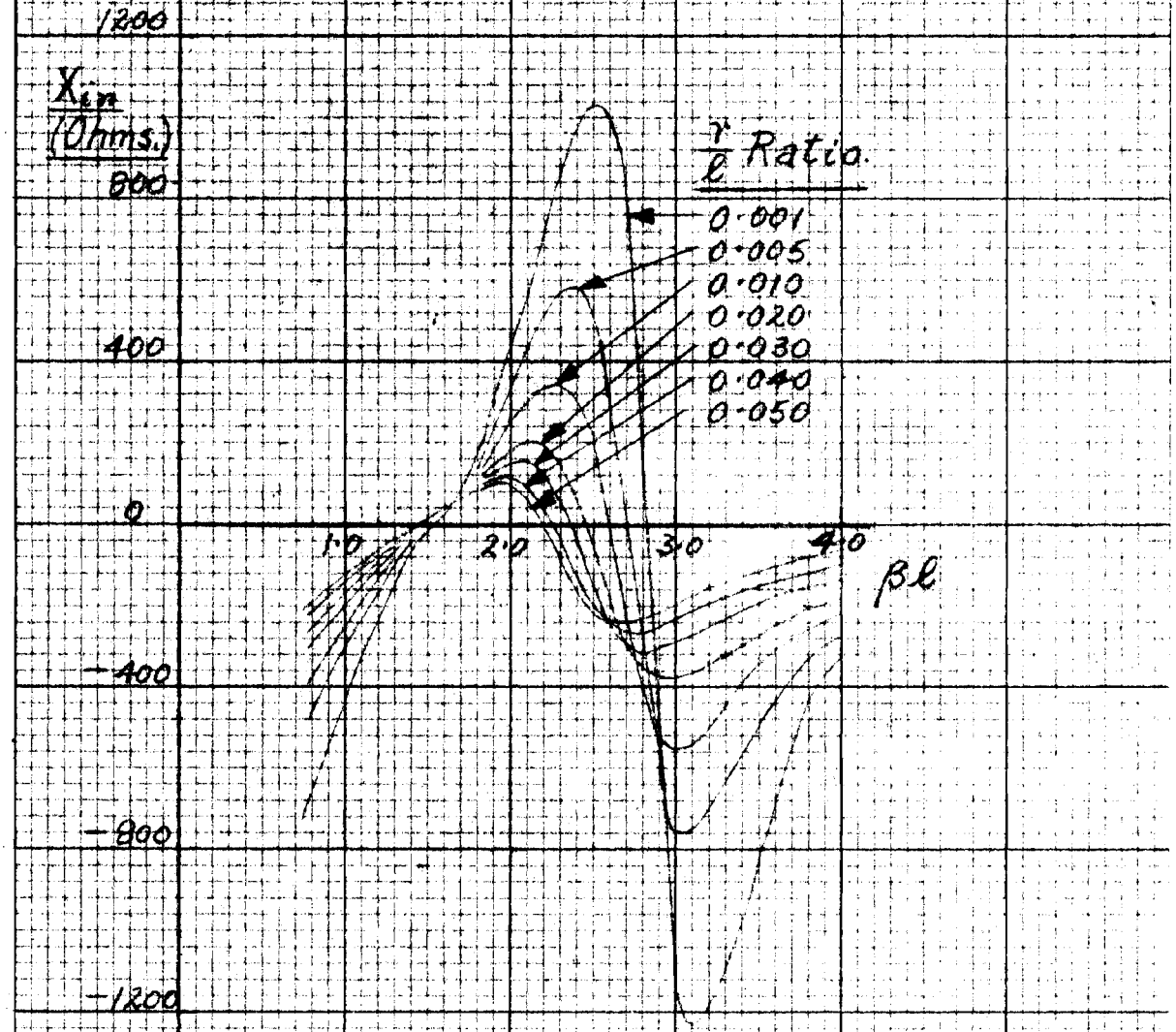

The maximum input resistance and $\frac{\ell}{\lambda}$ ratio for a range of r/l ratios were deduced from the curves of input resistance. The results are as follows:

First Approximation

$\frac{r}{\ell}$	0.001	0.005	0.010	0.020	0.030	0.040	0.050
$\frac{\ell}{\lambda}$	0.478	0.462	0.454	0.444	0.431	0.426	0.416
R (Ohms)	2060	1468	1100	760	610	520	440

Second Approximation

$\frac{r}{\ell}$	0.001	0.005	0.010	0.020	0.030	0.040	0.050
$\frac{\ell}{\lambda}$	0.454	0.436	0.417	0.398	0.390	0.379	0.366
R (Ohms)	2840	1315	980	640	520	420	387

(7) The Effect of the Earth on Aerial Impedance.[23]

The induced e.m.f. method enables calculations on the effect of a perfectly conducting earth and also a finitely conducting earth on the input impedance to be carried out. The method consists of replacing the earth by a mirror image aerial fed with equal current and 180° of phase difference. By the use of the linear equations between current and voltage in the two elements and allowing for the mutual impedance between the aerial and its image the impedance of the aerial in the presence of the earth may be calculated by the induced e.m.f. method. For a dipole aerial at height h above a perfectly conducting earth

$$e_1 = Z_{11} i_1 + Z_{12} i_2$$

where e_1 = The driving point e.m.f.

i_1 = The aerial current

i_2 = The image aerial current

Z_{11} = The self impedance of the aerial

Z_{12} = The mutual impedance of the aerial and the image aerial

Let $i_1 = -i_2 = i$

The input impedance

$$Z = \frac{e_1}{I} = Z_{11} - Z_{12}(h,o)$$

The input resistance will be

$$R = R_{11} - R_{12}(h,o)$$

and will pass through a series of maxima and minima as h is varied.

A perfect ground affects only the radiation properties of an aerial; but an imperfect ground absorbs power as well. Power absorbed at fairly large distances from an aerial has already been radiated from the aerial and has no effect on the aerial input impedance. On the other hand, power absorbed in the region of the near field of the aerial must appear as an increase in the input resistance.

The calculation of $R_{12}(h,o)$ by the induced e.m.f. method is simple but laborious for a perfectly conducting earth. The imperfectly conducting earth is a little more difficult to calculate and the non-uniform earth more complicated.

The effect of the finite conductivity of the earth on the impedance of half wavelength dipole aerials, either vertical or horizontal, is negligible provided the height above the ground of the aerial is of the order of a wavelength. The wavelength at 500 Mcps. is 60 cms. so that the presence of the earth will not alter the values of the aerial impedance from the free space values assumed in the experiments carried out.

(d) STUB COMPENSATION.

Any compensation supplied by a transmission line stub depends for its operation on an understanding of elementary transmission line theory. The elementary theory for transmission lines is given below. The exact methods by which stubs are designed is not given because it was found

impracticable to carry out adequate tests with these stubs. A qualitative discussion of the requirements of wide band aerials and the means of achieving these requirements by using compensating stubs is then presented.

(1) Elementary Transmission Line Theory.[49]

The following treatment of a transmission line gives the formulae used in determining a suitable stub to compensate any given impedance.

Consider the following diagram:

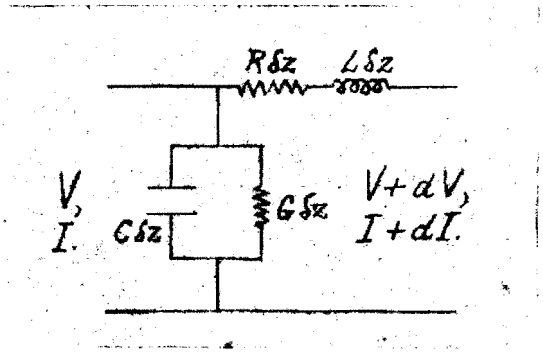

Let V, I be the voltage and current at z

δz = The element of line considered

R, L, C, G the resistance, inductance, capacitance and conductance per unit length.

Then $$-(I+dI)+I = V(G+j\omega C)\,\delta z$$

$$\therefore \frac{dI}{dz} = -V(G+j\omega C)$$

$$-(V+dV)+V = I(R+j\omega L)\,\delta z$$

$$\therefore \frac{dV}{dz} = -I(R+j\omega L)$$

$$\therefore \frac{d^2V}{dz^2} = \gamma^2 V \qquad \frac{d^2I}{dz^2} = \gamma^2 I$$

where $$\gamma^2 = (R+j\omega L)(G+j\omega C)$$

The solution is

$$V = V_1 e^{-\gamma z} + V_2 e^{+\gamma z}$$

$$I = I_1 e^{-\gamma z} + I_2 e^{+\gamma z}$$

Now for the wave travelling in the positive direction $Z_o = \frac{V_1}{I_1}$

For the wave travelling in the negative direction $-Z_o = \frac{V_2}{I_2}$

where Z_o = The characteristic impedance = $\sqrt{\frac{R+j\omega L}{G+j\omega C}}$

For a termination Z_R at $z=0$

$$Z_R = \frac{V}{I} = \frac{V_1+V_2}{I_1+I_2} = \frac{Z_o(I_1-I_2)}{I_1+I_2}$$

whence $\frac{V_2}{V_1} = \frac{Z_R-Z_o}{Z_R+Z_o}$ $\frac{I_2}{I_1} = \frac{Z_o-Z_R}{Z_o+Z_R}$

These quantities are the reflection coefficients.

The alternative solution in hyperbolic form is

$$V = A_1 \cosh \gamma z + B_1 \sinh \gamma z$$

$$I = A_2 \cosh \gamma z + B_2 \sinh \gamma z$$

We have the conditions

$$V = V_R \quad I = I_R \quad \text{at} \quad z=0$$

$$V = V_S \quad I = I_S \quad \text{at} \quad z=-\ell$$

Hence from the equations for $V, I, \frac{dV}{dz}$ and $\frac{dI}{dz}$ the four constants are evaluated yielding

$$V_S = V_R \cosh \gamma\ell + Z_o I_R \sinh \gamma\ell$$

$$I_S = I_R \cosh \gamma\ell + \frac{V_R}{Z_o} \sinh \gamma\ell$$

$$Z_{in} = \frac{V_\ell}{I_\ell} = Z_o \frac{Z_R \cosh \gamma\ell + Z_o \sinh \gamma\ell}{Z_o \cosh \gamma\ell + Z_R \sinh \gamma\ell}$$

For a short circuit $Z_R = 0$ $Z_{in} = Z_{sc} = Z_o \tanh \gamma\ell$

For an open circuit $Z_R = \infty$ $Z_{in} = Z_{oc} = Z_o \coth \gamma\ell$

For a low loss line we approximate as follows

$$R \ll \omega L \qquad G \ll \omega C$$

then $Z = R+j\omega L \doteq j\omega L$ $\therefore Z_o = \sqrt{\frac{L}{C}}$ $\gamma = j\omega\sqrt{LC}$

$$Y = G+j\omega C \doteq j\omega C$$

and hence $\alpha = 0$ and $\beta = \omega\sqrt{LC}$

In some cases the lines have small losses.

$$\gamma = \sqrt{(R+j\omega L)(G+j\omega C)} = j\omega\sqrt{LC}\sqrt{\left(1+\frac{R}{j\omega L}\right)\left(1+\frac{G}{j\omega C}\right)}$$

$$= j\omega\sqrt{LC}+\frac{R}{2\sqrt{\frac{L}{C}}}+\frac{G}{2}\sqrt{\frac{L}{C}}$$

Now $\gamma = \alpha+j\beta \quad \therefore \alpha = \frac{1}{2}\left(\frac{R}{Z_o}+GZ_o\right)\ ;\ \beta = \omega\sqrt{LC}$

For a low loss line $\alpha = 0$

$$\therefore V_\ell = V_R\cos\beta\ell + jI_R Z_o \sin\beta\ell \qquad Z_o = \sqrt{\frac{L}{C}}$$

$$I_\ell = I_R\cos\beta\ell + j\frac{V_R}{Z_o}\sin\beta\ell$$

$$Z_{in} = \frac{V_\ell}{I_\ell} = Z_o\frac{Z_R\cos\beta\ell + jZ_o\sin\beta\ell}{Z_o\cos\beta\ell + jZ_R\sin\beta\ell}$$

(2) <u>Wideband Aerials</u>.[8,50,51]

The following paragraphs investigate the requirements for a wideband aerial. By comparison with normal engineering practice it is possible to represent the circuit of an aerial for a small range of frequencies by a lumped circuit arrangement. In the proximity of the first resonance the reactive component of the equivalent impedance passes from capacitive to inductive reactance as the frequency is increased through the resonant frequency. Now as a first approximation it is possible to consider an aerial as being made up of series resistance R, inductance L and capacitance C, all of which are constants. For a closer approximation these three elements should be made variable and also other elements would need to be added. However the band of frequencies considered is only 8 megacycles or 8.4% of the carrier frequency so that in the first instance we assume constant values for R, L and C.

The Input Impedance

$$Z = R+j\left(\omega L-\frac{1}{\omega C}\right)$$

where $\omega_r = \frac{1}{\sqrt{LC}}$ and $Z_r = R$

$$\frac{\partial Z}{\partial\omega} = j\left(L+\frac{1}{\omega^2 C}\right)$$

$$\therefore \frac{\partial Z}{Z_r} = j\left(\frac{L\delta\omega}{R}+\frac{\delta\omega}{\omega^2 CR}\right)$$

Now $Q = \frac{\omega_r L}{R} = \frac{1}{\omega_r C R}$

If $\omega = \omega_r$ then

$$\frac{\delta Z}{Z_r} = j 2Q \frac{\delta\omega}{\omega_r}$$

$$\frac{\delta\omega}{\omega_r} = \frac{1}{2Q} \frac{\delta Z}{R}$$

Let $\delta Z = R$ i.e. the half power points.

The frequency difference between half power points is the bandwidth $\Delta\omega$

$$\Delta\omega = 2\delta\omega = \frac{\omega_r}{Q}$$

This solution does not agree with experimental results. Now consider C and L fixed and R a function of frequency.

$$R(\omega) = R_r\left(1+K\frac{\delta\omega}{\omega_r}\right)$$

where R_r = The resonant resistance

K = A positive constant

Let $\omega = \omega_r + \delta\omega$

$$Z = R + j\left(\omega L - \frac{1}{\omega C}\right)$$

$$= R_r\left(1+K\frac{\delta\omega}{\omega_r}\right) + j\left(\omega_r L + L\delta\omega - \frac{1}{\omega_r C\left(1+\frac{\delta\omega}{\omega_r}\right)}\right)$$

$$= R_r\left(1+K\frac{\delta\omega}{\omega_r}\right) + j\left(\omega_r L + L\delta\omega - \frac{1}{\omega_r C} + \frac{\delta\omega}{\omega_r^2 C}\right)$$

Now $\omega_r^2 = \frac{1}{LC}$

$$= R_r\left(1+K\frac{\delta\omega}{\omega_r}\right) + 2jL\delta\omega$$

$$\therefore \frac{Z}{R_r} = 1 + \frac{\delta\omega}{\omega_r}\left(K + j\frac{2\omega_r L}{R_r}\right)$$

$$= 1 + \frac{\delta\omega}{\omega_r}(K + j2Q)$$

The impedance minimum is given by

$$\frac{\partial}{\partial(\delta\omega)}\left\{\left|\frac{Z}{R_r}\right|^2\right\} = 2\left(1+K\frac{\delta\omega}{\omega_r}\right)\frac{K}{\omega_r} + 4\frac{Q^2\,2\delta\omega}{\omega_r^2} = 0$$

$$\therefore \frac{\delta\omega}{\omega_r} = \frac{-K}{K^2+4Q^2}$$

Since K is positive the impedance minimum occurs at some frequency less than the frequency corresponding

to ω_r as found in practice.

$$Z_{min.} = R_r\left\{1 - \frac{K}{K^2+4Q^2}(K+j2Q)\right\}$$
$$= R_r\left\{\frac{4Q^2}{K^2+4Q^2} - j\frac{2KQ}{K^2+4Q^2}\right\}$$

In order to make use of the above theory it is necessary to determine R, L and C in terms of the dimensions of the aerial. These may be found from curves of R and X versus $\frac{\ell}{\lambda}$ for various r/l.

Alternatively $R = R_{rad.}$

$$Q = \frac{\omega L_1}{R_1} = \frac{2\pi}{\lambda}\frac{Z_o}{R_1}$$

A half wavelength dipole aerial approximates to a quarter wavelength open circuited line.

$$R = \frac{R_1\ell}{2} = \frac{R_1\lambda}{8}$$

$$\omega_r L = QR = \frac{R_1\lambda}{8}\frac{2\pi Z_o}{\lambda R_1} = \frac{\pi Z_o}{4}$$

$$\therefore \omega_r C = \frac{4}{\pi Z_o}$$

Hence L $= \frac{Z_o}{8f_r}$; $C = \frac{2}{\pi^2 f_r Z_o}$; $Q = \frac{\pi Z_o}{4R}$; $R = R_{rad.}$

These equations define the parameters of the equivalent circuit in terms of the characteristic impedance Z_o, the radiation resistance $R_{rad.}$ and the carrier frequency f_r. The characteristic impedance $Z_o(\ell, r)$ is a function of length and radius.

The following table has been calculated:

$\frac{r}{\ell}$	$\frac{\ell}{\lambda}$	Z_o (ohms)	L μH	C $\mu\mu f$	R ohms.	Q	Q loaded $=\frac{1}{2}Q$	Band-width %
0.001	0.241	752	0.99	2.8	66	9.0	4.5	11.1
0.005	0.238	560	0.73	3.8	63	7.0	3.5	14.3
0.010	0.236	477	0.63	4.5	61	6.2	3.1	16.1
0.020	0.233	395	0.52	5.4	60	5.2	2.6	19.2
0.030	0.231	347	0.46	6.2	58	4.7	2.4	21.3
0.040	0.229	313	0.41	6.8	57	4.3	2.2	23.2
0.050	0.228	287	0.38	7.4	56.5	4.0	2.0	25.0

The above derivations apply only strictly when $Q > 10$.

The results do give an indication of the aerial's behaviour for $Q < 10$. From the results it is apparent that increase in $\frac{r}{\ell}$ ratio or decrease in quality factor Q will improve the bandwidth properties of an aerial since $\Delta\omega = \frac{\omega r}{Q}$.

It follows that the thicker the aerial the better its transmission characteristics for broadband communication services such as television.

(3) Wide Band Impedance Matching.[52,53]

The matching of an aerial to the transmission line or radio frequency output which feeds it is accomplished in the following manner. If the impedance of the aerial remains relatively constant over the frequency range the matching is readily accomplished using band pass filters. However in most cases the aerial impedance varies over wide limits through the frequency range and a combination of graphical and analytical methods is best used since the analysis is complicated.

The method is to plot the $\frac{R}{Z_o}, \frac{X}{Z_o}$ versus $\frac{f}{f_o}$ or $\frac{G}{Y_o}$, $\frac{B}{Y_o}$ versus relative frequency diagram also the complex impedance diagram of $\frac{R}{Z_o}$ versus $\frac{X}{Z_o}$ with relative frequency points marked on them and similarly for the admittance diagrams. Now the locus of impedances that produce constant S.W.R. is a circle. The problem of wideband matching is usually to keep the S.W.R. below some stated value e.g. $\rho = \rho_K$. The problem then is to introduce some circuit element which will bring the impedance curve inside the $\rho = \rho_K$ circle over the frequency range desired. The bandwidth is given by $\frac{f_2 - f_1}{f_1}$ where f_1 and f_2 are the lower and upper frequencies at which the impedance curve intersects the $\rho = \rho_K$ circle.

From a $G-B$ diagram for a dipole aerial it is apparent that near the first resonance the susceptance has a negative slope and at the second resonance the reactance

has a negative slope. Hence in the region of the first resonance it is possible to cancel the aerial susceptance by a suitable parallel positive susceptance, and in the region of the second resonance it is possible to cancel the reactance by insertion of suitable positive series reactance. The above remarks form the basis of techniques used in increasing the bandwidth of an aerial.

By adding series capacitance, i.e. negative reactance the impedance diagram is moved downwards whereas a series inductance, i.e. positive reactance, moves the impedance diagram upwards. The addition of series reactance on admittance diagrams alters the conductance and susceptance. The addition of series capacitance rotates the curve counter-clockwise and series inductance clockwise. By these means the bandwidth may be appreciably increased, maximum bandwidth being achieved when the curve is slightly above the centre of the definition circle, i.e. f_1 is decreased at the same time as Δf is increased for maximum bandwidth. The circuit elements used are usually sections of transmission lines.

An important case is the shorted $\frac{\lambda}{4}$ parallel stub which is best treated from an admittance diagram. The aerial at the first resonance has a negative susceptance slope and a shorted $\frac{\lambda}{4}$ parallel stub a positive susceptance variation. By combining the stub and aerial in parallel a small variation in susceptance may be achieved.

The parallel broad banding stub is used in the folded dipole type of aerial due to Carter, who has shown that the main purpose of folding is to increase the input impedance of the aerial but in addition there are two stubs in series which increase the antenna bandwidth.[51] Sometimes it is required to match an unbalanced co-axial cable to a balanced antenna and this is done by "baluns", balance to unbalance transformers. These elements are formed from resonant line

sections so that it is often possible to incorporate balun and widebanding stub in one element.

It is seen from this discussion that by the use of one or two elements a great increase in aerial bandwidth may be achieved.

(e) THE AERIAL CURRENT DISTRIBUTION.[54,55,56]

The current distribution is normally assumed to be sinusoidal for ease in calculations. Calculations of the variation from a sinusoidal current distribution are extremely laborious, involving Hankel and Bessel Functions. The following qualitative results apply for cylindrical dipole aerials.

For small radius to length ratio the current distribution is approximately sinusoidal. As the r/l ratio increases the divergence from sinusoidal becomes greater. The divergence is greatest near the input to the aerial and to a lesser extent near the free ends of the aerial.

Some equations for aerial current distribution are given in the sub-section on Input Impedance.

The current distribution of an aerial is not an easily measurable property and consequently has not been treated in any detail.

(f) PROPAGATION.[8,57-72]

(1) Introduction.

The possible means by which propagation from a transmitter T reach a receiver R are shown in the diagram below. The ground wave is concerned with all waves other than sky and tropospheric waves. The ground wave is divided into two types, (i) space, (ii) surface. The space wave is further subdivided into direct, reflected and diffracted waves. The surface wave is a wave that is guided along the earth's

surface in the same way as electromagnetic waves are guided down a transmission line.

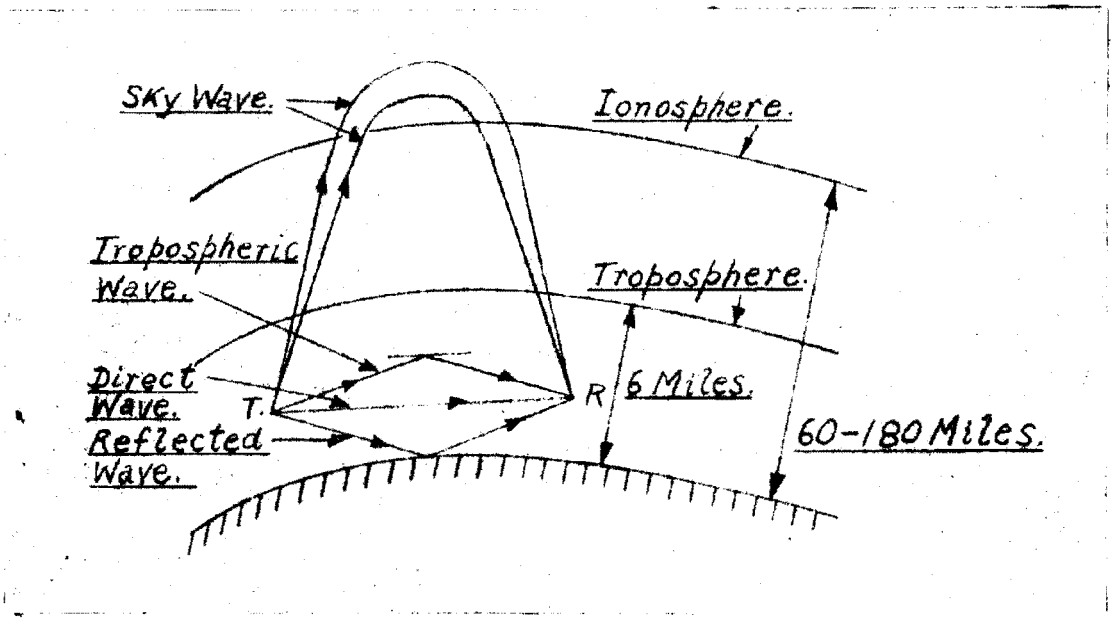

The factors which affect propagation over each of these paths are

(1) The frequency

(2) The effect of the ground

(3) The curvature of the earth

(4) The homogeneity of the troposphere

(5) The time of day, year and solar cycle

(6) The characteristics of the ionosphere

(7) The earth's magnetic field

(8) Local disturbances such as thunderstorms which result in the introduction of noise

(9) Distant disturbances such as magnetic storms on the sun.

The vital factor is frequency and it will be shown that in the case of U.H.F. propagation the effect of several of the above factors and of some of the possible propagation paths contribute little to the propagation. The calculations for determining the radiation pattern of an aerial operating above the surface of the earth are complicated and laborious. Approximate results may be obtained by first considering the earth to be a perfectly non-conducting plane surface. The results of the simplified calculations may then be modified

to include the effects of the finite conductivity and curvature of the earth as well as atmospheric refraction. The above procedure is adopted below.

(2) Reflection from a Perfect Dielectric Plane Earth.

If a plane wave is incident upon a boundary surface which is not parallel to the plane containing $\underline{E}$ and $\underline{H}$ the boundary conditions are complex. Part of the wave will be refracted and part will be reflected. Consider the diagram below:

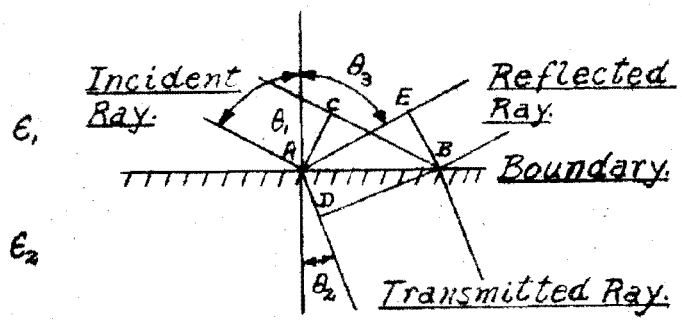

Let $\epsilon_{1,2}, \mu_{1,2}, V_{1,2}$ = The dielectric constant, permeability and velocity of propagation in medium $\frac{1}{2}$

The Incident Ray travels a distance CB in the same time as the Transmitted Ray travels a distance AD and the Reflected Ray a distance AE.

$$\frac{V_1}{V_2} = \frac{CB}{AD} = \frac{AB\sin\theta_1}{AB\sin\theta_2} = \frac{\sin\theta_1}{\sin\theta_2}$$

Also $$V_r = \frac{1}{\sqrt{\mu_r \epsilon_r}} \qquad \mu_1 = \mu_2$$

$$\therefore \frac{\sin\theta_1}{\sin\theta_2} = \sqrt{\frac{\epsilon_2}{\epsilon_1}}$$

Also $AE = CB$ since the velocity is constant

$$\therefore \sin\theta_1 = \sin\theta_3$$

$$\theta_1 = \theta_3$$

Hence we have the well-known optical laws:

1. The angle of incidence equals the angle of reflection.

2. $\frac{\text{Sine of angle of incidence}}{\text{Sine of angle of refraction}}$ = a constant

The second law is known as Snell's Law.

Now from Poynting's Theorem:

The power flow per square metre = $\underline{E} \wedge \underline{H}$

Also $\underline{E}$ is perpendicular to $\underline{H}$

$\underline{E} = \eta \underline{H}$ where η = The Intrinsic Impedance

$$\therefore P = \frac{E^2}{\eta}$$

$\therefore$ The Power Incident on AB $\propto \frac{1}{\eta_1} E_i^2 \cos\theta_1$

The Power Reflected from AB $\propto \frac{1}{\eta_1} E_r^2 \cos\theta_1$

The Power Transmitted through AB $\propto \frac{1}{\eta_2} E_t^2 \cos\theta_2$

From Conservation of Energy

$$\frac{1}{\eta_1} E_i^2 \cos\theta_1 = \frac{1}{\eta_1} E_r^2 \cos\theta_1 + \frac{1}{\eta_2} E_t^2 \cos\theta_2$$

$$\frac{E_r^2}{E_i^2} = 1 - \frac{\eta_1 E_t^2 \cos\theta_2}{\eta_2 E_i^2 \cos\theta_1}$$

$$= 1 - \frac{\sqrt{\epsilon_2}\, E_t^2 \cos\theta_2}{\sqrt{\epsilon_1}\, E_i^2 \cos\theta_1}$$

Since $\eta = \sqrt{\frac{\mu}{\epsilon}}$

It is now necessary to consider two cases.

(i) Horizontal Polarization in which $\underline{E}$ is parallel to the boundary surface and perpendicular to the plane of incidence.

(ii) Vertical Polarization in which $\underline{H}$ is parallel to the boundary surface and perpendicular to the plane of incidence.

(i) Horizontal Polarization.

Consider the accompanying diagram. The tangential component of $\underline{E}$ is to be continuous across the boundary.

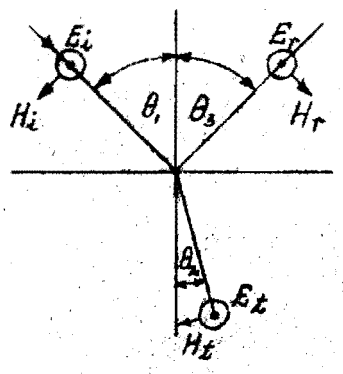

$$E_i + E_r = E_t \qquad (1)$$

$$\left(\frac{E_r}{E_i}\right)^2 = 1 - \frac{\sqrt{\epsilon_2}\, E_t^2 \cos\theta_2}{\sqrt{\epsilon_1}\, E_i^2 \cos\theta_1} \qquad (2)$$

Substitute (1) in (2) and reduce giving

$$\frac{E_r}{E_i} = \frac{\sqrt{\epsilon_1}\cos\theta_1 - \sqrt{\epsilon_2}\cos\theta_2}{\sqrt{\epsilon_1}\cos\theta_1 + \sqrt{\epsilon_2}\cos\theta_2}$$

Now $\sqrt{\epsilon_2}\cos\theta_2 = \sqrt{\epsilon_2 - \epsilon_2 \sin^2\theta_2}$

$$= \sqrt{\epsilon_2 - \epsilon_1 \sin^2\theta_1} \qquad \text{(Snell's Law)}$$

$$\frac{E_r}{E_i} = \frac{\sqrt{\epsilon_1}\cos\theta_1 - \sqrt{\epsilon_2 - \epsilon_1 \sin^2\theta_1}}{\sqrt{\epsilon_1}\cos\theta_1 + \sqrt{\epsilon_2 - \epsilon_1 \sin^2\theta_1}}$$

$\therefore$ The Reflection Factor

$$R_h = \frac{E_r}{E_i} = \frac{\cos\theta_1 - \sqrt{\frac{\epsilon_2}{\epsilon_1} - \sin^2\theta_1}}{\cos\theta_1 + \sqrt{\frac{\epsilon_2}{\epsilon_1} - \sin^2\theta_1}}$$

(11) Vertical Polarization.

Again the tangential component of $\underline{E}$ must be continuous across the boundary

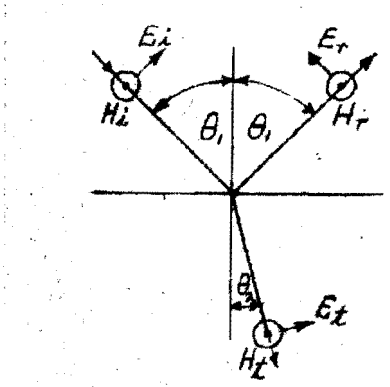

$$\therefore (E_i - E_r)\cos\theta_1 = E_t \cos\theta_2 \qquad (3)$$

Substitute (3) in (2) and reduce giving

$$\frac{E_r}{E_i} = \frac{\sqrt{\epsilon_2}\cos\theta_1 - \sqrt{\epsilon_1(1-\sin^2\theta_2)}}{\sqrt{\epsilon_2}\cos\theta_1 + \sqrt{\epsilon_1(1-\sin^2\theta_2)}}$$

$$\sin^2\theta_2 = \frac{\epsilon_1}{\epsilon_2}\sin^2\theta_1 \qquad \text{(Snell's Law)}$$

$\therefore$ The Reflection Factor

$$R_v = \frac{E_r}{E_i} = \frac{\frac{\epsilon_2}{\epsilon_1}\cos\theta_1 - \sqrt{\frac{\epsilon_2}{\epsilon_1} - \sin^2\theta_1}}{\frac{\epsilon_2}{\epsilon_1}\cos\theta_1 + \sqrt{\frac{\epsilon_2}{\epsilon_1} - \sin^2\theta_1}}$$

If there is no reflection $R_v = 0$

$$\therefore \sqrt{\frac{\epsilon_2}{\epsilon_1} - \sin^2\theta_1} = \frac{\epsilon_2}{\epsilon_1}\cos\theta_1$$

$$\therefore \frac{\epsilon_2}{\epsilon_1} - \sin^2\theta_1 = \frac{\epsilon_2^2}{\epsilon_1^2} - \frac{\epsilon_2^2}{\epsilon_1^2}\cos^2\theta_1$$

$$\sin^2\theta_1 \left(1-\frac{\epsilon_2}{\epsilon_1}\right)\left(1+\frac{\epsilon_2}{\epsilon_1}\right) = \frac{\epsilon_2}{\epsilon_1}\left(1-\frac{\epsilon_2}{\epsilon_1}\right)$$

$$\sin\theta_1 = \sqrt{\frac{\epsilon_2}{\epsilon_1+\epsilon_2}}$$

$$\tan(\theta_1)_b = \sqrt{\frac{\epsilon_2}{\epsilon_1}}$$

This angle is known as the pseudo-Brewster Angle. There is no similar angle for horizontally polarized radiation.

(3) Reflection at the Surface of a Finitely Conducting Plane Earth.

From Maxwell's Equation

$$curl\ \underline{H} = \epsilon \frac{\partial \underline{E}}{\partial t} + g\underline{E}$$

where g = The conductivity of the earth

ϵ = The dielectric constant of the earth.

If $\underline{E}$ varies simusoidally with time

$$\underline{E} = E_0 e^{j\omega t}$$

$$curl\ H = \left(\epsilon + \frac{g}{j\omega}\right)\frac{\partial E}{\partial t} = \epsilon' \frac{\partial E}{\partial t}$$

Hence a partially conducting dielectric such as the earth may be considered as a perfect dielectric of complex dielectric constant ϵ'

$$\epsilon' = \epsilon\left(1+\frac{g}{j\omega\epsilon}\right)$$

The reflection factors obtained for perfect dielectrics will be directly applicable provided

$$\epsilon_1 = \epsilon_{vacuo} = \epsilon_v$$

$$\epsilon_2 = \epsilon'$$

$$R_h = \frac{E_r}{E_i} = \frac{\sqrt{\epsilon_v}\cos\theta - \sqrt{\left(\epsilon+\frac{g}{j\omega}\right) - \epsilon_v \sin^2\theta}}{\sqrt{\epsilon_v}\cos\theta + \sqrt{\left(\epsilon+\frac{g}{j\omega}\right) - \epsilon_v \sin^2\theta}}$$

θ = The angle between the ray and the normal

ψ = The angle between the ray and the plane earth.

$$\therefore \psi = 90 - \theta$$

Let $\epsilon_r = \frac{\epsilon}{\epsilon_v}$ i.e. The relative dielectric constant

$$x = \frac{g}{\omega \epsilon_v} = \frac{18 \times 10^3 g}{f_{mcps.}}$$

Then $$R_h = \frac{\sin\psi - \sqrt{(\epsilon_r - jx) - \cos^2\psi}}{\sin\psi + \sqrt{(\epsilon_r - jx) - \cos^2\psi}}$$

The vertical polarization reflection coefficient using this nomenclature becomes

$$R_v = \frac{(\epsilon_r - jx)\sin\psi - \sqrt{(\epsilon_r - jx) - \cos^2\psi}}{(\epsilon_r - jx)\sin\psi + \sqrt{(\epsilon_r - jx) - \cos^2\psi}}$$

The dielectric constant varies from 7 for poor low conductivity earth to 30 for a good high conductivity earth. The conductivity varies between 0 and 30×10^{-3} mhos/metre.

The following remarks may be deduced from the above equations. The phase of the reflected waves differs from that of the incident waves by nearly 180° for all angles of incidence for horizontally polarized waves. If the incidence is near grazing, i.e. $\psi = 0$ the reflected wave is equal in magnitude but 180° out of phase with the incident wave for all frequencies and ground conductivities for a horizontally polarized wave. As the angle ψ increases the magnitude and phase of the reflection factor changes, the change being greater for high frequencies than for low.

In the case of vertically polarized waves the results are in general different from those obtained for horizontally polarized waves. At grazing incidence the reflected wave is equal to the incident wave in magnitude and 180° out of phase for all frequencies. As the angle ψ increases $|R_v|$ passes through a minimum at which $\angle R_v = -90^\circ$. This angle is known as the pseudo-Brewster Angle. As ψ further increases the magnitude of the reflection coefficient increases and its phase decreases to zero. If the incidence is near normal, i.e. $\psi = 90^\circ$ the results are the same for both horizontal and vertical polarization.

(4) <u>The Space and Surface Waves</u>.

Although the sky wave is important in many communication systems it need not be considered here because for wavelengths

shorter than 7 metres the radiation is not returned to the earth from the ionosphere. The components of the ground wave therefore make up the total signal reaching a receiver for a television transmitter. The direct ray of the space wave travels a nearly straight line path from the transmitter to the receiver. The reflected ray of the space wave is reflected from the earth in such a way as to reach the receiver. Energy radiated from a non-directional aerial strikes the earth at all points between the base of the aerial and the horizon, but only one ray after reflection reaches the receiver because of the geometrical relationships which must obtain.

The surface wave which is the third component of the ground wave, is a wave diffracted around the surface of the earth or guided by the ground-air interface. This component is important at broadcast frequencies but at 100 megacycles per second, the surface wave is rapidly attenuated, and at a distance of one mile from the aerial it has a small amplitude in comparison with the space wave. However the surface wave must be considered when the distance from the transmitting aerial is small.

It is with the above general remarks in view that the general theory of space and surface waves is considered below.

The general solution of radiation from a vertical aerial over a plane earth of finite conductivity was originally solved in 1909 by Sommerfeld. The solution is such that it is too cumbersome for normal engineering use. K.A. Norton has reduced the complex expressions of Sommerfeld's Theory to expressions which have engineering application. In Sommerfeld's Theory it is shown that the ground wave field intensity may be divided into two parts: the space and surface waves: the former predominating at large distances from the earth's surface and the latter close to the earth's surface. In the form due to Norton

the expressions for the electric field of an electric dipole above the surface of a finitely conducting plane earth are in a form that clearly shows this separation into space and surface waves.

Norton has obtained exact expressions for the axial and radial components of field intensity of a vertical dipole by development from an equation for vector potential due to Van der Pol. The equations given below are derived from equations (55) and (70) of Norton's paper,[58] for large distances from a vertical dipole so that terms of order higher than the first in $\frac{1}{R_1}$ and $\frac{1}{R_2}$ may be neglected. The result of this approximation gives

$$E_z = j30\beta I dl\left\{\cos^2\psi\left(\frac{e^{-j\beta R_1}}{R_1}+R_v\frac{e^{-j\beta R_2}}{R_2}\right)-(1-R_v)(1-u^2+u^4\cos^2\psi)F\frac{e^{-j\beta R_2}}{R_2}\right\}$$

$$E_\rho = -j30\beta I dl\left\{\sin\psi\cos\psi\left(\frac{e^{-j\beta R_1}}{R_1}+R_v\frac{e^{-j\beta R_2}}{R_2}\right)-\cos\psi(1-R_v)\sqrt{1-u^2\cos^2\psi}\;F\frac{e^{-j\beta R_2}}{R_2}\left(1+\sin^2\frac{\psi}{2}\right)\right\}$$

where

E_z = The z component of electric field intensity

E_ρ = The radial component of electric field intensity

R_1 = The distance from the dipole to the field point P

R_2 = The distance from the dipole's image to the field point P

R_v = The plane wave reflection coefficient

F = The attenuation factor

$u^2 = \dfrac{1}{\epsilon_r + jx}$

$x = \dfrac{18\times10^3\, g}{f_{mcps.}}$

g = The earth's conductivity in mhos/metre

$\epsilon_r = \dfrac{\epsilon}{\epsilon_v}$ = The earth's relative dielectric constant

$\beta = \dfrac{2\pi}{\lambda}$ = The wave's propagation rotation

It is apparent from the above equations that the field intensity equations consist of inverse distance terms due to space waves and attenuation terms due to surface waves.

Hence

$$E_{space} = \sqrt{E_{z\,space}^2 + E_{\rho\,space}^2}$$

$$= j30\beta I d\ell \left(\frac{e^{-j\beta R_1}}{R_1} + R_v \frac{e^{-j\beta R_2}}{R_2} \right) \sqrt{\cos^4\psi + \sin^2\psi\cos^2\psi}$$

$$= j30\beta I d\ell \cos\psi \left(\frac{e^{-j\beta R_1}}{R_1} + R_v \frac{e^{-j\beta R_2}}{R_2} \right)$$

$$E_{surface} = \sqrt{E_{z\,surface}^2 + E_{\rho\,surface}^2}$$

$$= j30\beta I d\ell (1-R_v) F \frac{e^{-j\beta R_2}}{R_2} \sqrt{(1-u^2+u^4\cos^2\psi)^2 + \cos^2\psi u^2 (1-u^2\cos^2\psi)(1+\sin^2\tfrac{\psi}{2})}$$

Neglecting terms in u^4 which will be small

$$E_{surface} = j30\beta I d\ell (1-R_v) F \frac{e^{-j\beta R_2}}{R_2} \sqrt{1-2u^2+\cos^2\psi\, u^2 (1+\sin^2\tfrac{\psi}{2})}$$

Consider the equation given above for the space wave. The first term represents a spherical wave from the dipole. The second term represents a spherical wave from the dipole's image modified by the plane wave reflection factor R_v. When the dipole is situated far from the earth the incident wave is approximately a plane wave and the space wave is made up of a direct wave and a reflected wave modified in phase and magnitude by the plane wave reflection coefficient. Again when the dipole is close to the earth the incident wave is not plane and additional terms must be included in the reflection field, i.e. the surface wave terms.

The following conclusions may be made about the field intensities by inspection of the various parameters. The main effect of the earth's finite conductivity occurs at low angles of incidence where the space wave will be considerably reduced from its value over a perfectly conducting earth. The reason for this phenomenon is the rapid change of phase of R_v. The phase of R_v for grazing incidence is -180° decreasing to -90° at the pseudo-Brewster angle and thereafter tending rapidly to zero. The rapid change in phase of the reflection coefficient near the pseudo-Brewster angle will consequently cause the sharp decrease in space wave field intensity for low angles of incidence.

In a similar manner to that described for a vertical dipole Norton's results may be adapted using equations (72) and (73) of his paper to give the following approximate result for a horisontal dipole:

$$E_{space} = j30\beta I dl\left(\frac{e^{-j\beta R_1}}{R_1} + R_h\frac{e^{-j\beta R_2}}{R_2}\right)$$

The radiation patterns will not differ appreciably from those obtained for a perfect conducting earth since $R_h \doteq -1$ for all angles of incidence and this is the value of the term's coefficient in the perfectly conducting case.

The total field intensity of the surface wave for a vertical dipole above a finitely conducting earth is found by compounding the Z and ρ components giving

$$E_{surface} = j30\beta\ell I(1-R_v)F\frac{e^{-j\beta R}}{R}\left\{\underline{K}(1-u^2)+\underline{r}\cos\psi(1+\sin^2\tfrac{\psi}{2})u\sqrt{1-u^2\cos^2\psi}\right\}$$

where R is the distance from the dipole to the field point $R \gg \lambda$ and $\underline{K}$ and $\underline{r}$ are unit vectors in the Z and ρ directions and all other quantities are as previously defined.

The attenuation constant F has been developed as a function of the earth's constants and distance by K.A. Norton[59] using approximate methods on an exact expression for the ground wave potential function of a vertical doublet $\Pi(r,0)$ due to B. van der Pol and K.F. Neissen.[60]

The results obtained by K.A. Norton for the Attenuation constant are developed below. The ground wave potential function and defining equations of van der Pol are

$$\Pi(r,0) = \frac{e^{-j\beta R}}{R}\frac{1}{1-u^2}\left\{1-u^2e^{p_2-p_1}-u\theta e^{-p_1}\int_{\sqrt{p_2}}^{\sqrt{p_1}}\frac{e^{\omega^2}d\omega}{(\omega^2+\theta)^{\frac{1}{2}}}\right\}$$

$$u^2 = \frac{1}{\epsilon_r + jx}$$

$$p_1 = \frac{2\pi jR}{\lambda}\left\{1-(1+u^2)^{-\frac{1}{2}}\right\} = pe^{jb}$$

$$p_2 = \frac{2\pi jR}{\lambda}\left\{u^{-1}-(1+u^2)^{-\frac{1}{2}}\right\}$$

$$\theta = \frac{4\pi jR}{\lambda}\left\{1+u^2\right\}^{-\frac{1}{2}}$$

Now $p_1 = \frac{2\pi jR}{\lambda}\left\{1-(1+u^2)^{-\frac{1}{2}}\right\} = pe^{jb}$

$$\therefore\ p_1 = j\beta R\ \frac{u^2(1-u^2)}{2} = pe^{jb}$$

$$\therefore \frac{p}{u^2}\,\frac{1}{1-u^2} = \frac{j\beta R}{2}e^{-jb} \doteq \frac{p}{u^2}(1+u^2)$$

$$\therefore p(1+\epsilon_r+jx) = \frac{j\beta R}{2}(\cos b - j\sin b)$$

$$= \frac{\beta R}{2}(\cos b\, j + \sin b)$$

Equating Real and Imaginary Parts yields

$$p = \frac{\pi}{\lambda}\frac{R}{\epsilon_r+1}\sin b = \frac{\pi}{\lambda}\frac{R}{x}\cos b$$

$$\tan b = \frac{\epsilon_r+1}{x}$$

For low frequencies or good conductivities when $x \gg \epsilon_r+1$ $b = 0$. Then, the propagation is independent of the earth's dielectric constant and Norton's equation (40) for attenuation constant F reduces to

$$F = \left|1 - 2\sqrt{p}\,e^{-p}\int_0^{\sqrt{p}} e^{\omega^2}d\omega + j\sqrt{\pi p}\,e^{-p}\right|$$

where $x \gg \epsilon_r+1$ $\quad p = \frac{\pi}{x}\frac{R}{\lambda}$

Tables for evaluating F in this range may be computed from tables of the integral due to H.G. Dawson.[61]

For high frequencies or poor conductivities when $x \ll \epsilon_r+1$ $b = 90^\circ$

$$p = \frac{\pi}{\lambda}\frac{R}{\epsilon_r+1} \qquad x \ll \epsilon_r+1$$

The expression for the attenuation factor F may be reduced to

$$F = \left|1 - \sqrt{\pi p}\,e^{-j\frac{\pi}{4}}e^{-jp}\left\{1 - C(p) - S(p) - j\left(S(p) - C(p)\right)\right\}\right|$$

where $C(p)$ and $S(p)$ are Fresnel's Integrals which have been tabulated by G.N. Watson.

$$C(p) = \int_0^p \cos\left(\frac{\pi x}{2}\right)^2 dx$$

$$S(p) = \int_0^p \sin\left(\frac{\pi x}{2}\right)^2 dx$$

For intermediate frequencies the attenuation factor becomes in terms of an error function

$$F = \left|1 - j\sqrt{\pi p_1}\,e^{-p_1}\,\mathrm{erfc}\left(-j\sqrt{p_1}\right)\right|$$

where $\qquad \mathrm{erfc}\left(-j\sqrt{p}\right) = \frac{2}{\sqrt{\pi}}\int_{-j\sqrt{p}}^{\infty} e^{-\omega^2}d\omega$

$$\omega = \frac{j\beta R u^2(1-u^2\cos^2\psi)}{2}\left\{1 - \frac{\sin\psi}{u\sqrt{1-u^2\cos^2\psi}}\right\}$$

It is evident that the attenuation factor F is dependent on distance, frequency and ground constants. Also as R tends to zero F will tend to unity. For low frequencies and good ground conductivity the unattenuated surface wave is small except near grazing angles. At $\psi = 0$ it has the value 2 whilst the space wave is zero since the direct and ground reflected waves cancel. For higher frequencies and poorer conductivity the unattenuated surface wave still has a value of 2 at $\psi = 0$, but it also has appreciable value at higher angles though this wave attenuates rapidly with distance because of the factor F.

At $\psi = 0$ F has been calculated and is termed the "ground wave attenuation factor A" and the above expressions for F are really expressions for A. The general expression for F is given later.

When $\psi = 0$

$$F = A \qquad \omega = p_1$$

$$F = \left|1 + j\sqrt{\pi\omega}\, e^{-\omega}\, \mathrm{erfc}(-j\sqrt{\omega})\right|$$

$$A = \left|1 + j\sqrt{\pi p_1}\, e^{-p_1}\, \mathrm{erfc}(-j\sqrt{p_1})\right|$$

$$p_1 = p e^{jb}$$

where p is defined as the numerical distance and b is the phase constant

$$\omega = p_1 = \frac{j\beta R u^2(1-u^2)}{2} = p e^{jb}$$

whence $p = \frac{\pi}{\lambda}\frac{R}{\epsilon_r+1}\sin b = \frac{\pi}{\lambda}\frac{R}{x}\cos b$

$$\tan b = \frac{\epsilon_r+1}{x}$$

Let b'' be the phase angle of u^2

$$\tan b'' = \frac{\epsilon_r}{u^2}$$

We define another angle b' such that

$$\tan b = 2\tan b'' - \tan b'$$

$$\therefore \quad b' = \tan^{-1}\frac{\epsilon_r - 1}{x}$$

The ground wave attenuation factor A is usually expressed as a function of the numerical distance p . The numerical distance is a function of distance, frequency and ground constants and is directly proportional to distance and frequency squared and inversely proportional to ground conductivity. When $x >> \epsilon_r$ the angle $b = o$ i.e. the power factor angle of the earth b'' will be approximately zero and and the earth's impedance will be approximately resistive. This condition obtains for good average earth at broadcast frequencies. Again when $x << \epsilon_r$ the earth's impedance will be reactive. This condition applies at V.H.F. over poor earths. Hence it is apparent that the earth may act as a conductor at low frequencies and at the same time act as a leaky dielectric at V.H.F.

Several empirical formulae have been deduced for the ground wave attenuation factor A.

All b $\quad A \doteq \frac{0{\cdot}3p+2}{0{\cdot}6p^2+p+2} - \sin b\sqrt{\frac{p}{2}}\, e^{-\frac{5}{8}p}$

$b < 5^\circ \quad A \doteq \frac{0{\cdot}3p+2}{0{\cdot}6p^2+p+2}$

$p < 4{\cdot}5 \quad b < 5^\circ \quad A \doteq e^{-0{\cdot}43p+0{\cdot}01p^2}$

$p \geqslant 4{\cdot}5 \quad b < 5^\circ \quad A \doteq \frac{1}{2p-3{\cdot}7}$

These relations show that for b small and for short numerical distances the variation of A is almost exponential with p whilst for large numerical distances A is inversely proportional to p . This means that at large numerical distances the field strength of the surface wave will vary inversely as the square of the distance from the transmitter.

The following expressions for space and surface waves from a horizontal dipole are obtained from Equations (72),

(73) and (74) of Norton's paper[58] by letting $R_1=R_2=R$ and taking only first order terms of $\frac{1}{R}$

$$E_{space} = \frac{j30\beta I d\ell\, e^{-j\beta R}}{R}\left\{\cos\phi\sin\psi(1-R_v)(\underline{K}\cos\psi-\underline{\rho}\sin\psi)+\sin\phi(1+R_h)\underline{\phi}\right\}$$

where $\underline{K},\underline{\rho},\underline{\phi}$ are unit vectors in cylindrical polar co-ordinates.

Letting $\underline{\Psi} = \underline{K}\cos\psi - \underline{\rho}\sin\psi$

$$E_{space} = \frac{j30\beta I d\ell\, e^{-j\beta R}}{R}\left\{\cos\phi\sin\psi(1-R_v)\underline{\Psi}+\sin\phi(1+R_h)\underline{\phi}\right\}$$

$$E_{surface} = 30I d\ell\Big\{j\beta\cos\phi\cos\psi(1-R_v)u\sqrt{1-u^2\cos^2\psi}\,F\frac{e^{-j\beta R}}{R}\left(1+\frac{\sin^2\psi}{2}\right)\underline{K}$$

$$-j\beta\cos\phi\left[(1+R_h)G\frac{e^{-j\beta R}}{R}-\cos^2\psi\,u^2(1-R_v)F\frac{e^{-j\beta R}}{R}+u^2\cos^2\psi(1-R_v)F(-\sin^2\psi)\frac{e^{-j\beta R}}{R}\right]\underline{\rho}$$

$$+j\beta\sin\phi(1+R_h)G\frac{e^{-j\beta R}}{R}\,\underline{\phi}\Big\}$$

$$= \frac{j30\beta I d\ell\, e^{-j\beta R}}{R}\Big\{\cos\phi\,u\sqrt{1-u^2\cos^2\psi}\,(1-R_v)F\Big[\cos^2\psi\left(1+\frac{\sin^2\psi}{2}\right)\underline{K}$$

$$+u\sqrt{1-u^2\cos^2\psi}\left(\frac{1-\sin^4\psi-\frac{(1+R_h)G}{(1-R_v)u^2F}}{1-u^2\cos^2\psi}\right)\underline{\rho}+\sin^2\phi(1+R_h)G\,\underline{\phi}\Big]\Big\}$$

where $G = \left[1+j\sqrt{\pi V}\,e^{-V}\,\mathrm{erfc}(-j\sqrt{V})\right]$

$$V = \frac{j\beta R(1-u^2\cos^2\psi)}{2u^2}\left(1+\frac{u\sin\psi}{\sqrt{1-u^2\cos^2\psi}}\right)^2$$

The function G is the attenuation function for horizontal polarization. For large ρ $G\doteq u^4F$ and since $u^2<1$ it is immediately apparent that the horizontally polarized surface wave will be attenuated more rapidly than a vertically polarized wave of the same frequency.

Norton has carried out similar analyses for horizontal elementary dipoles as for vertical dipoles. The numerical distance is defined from equation (62) of his paper as follows.[58]

$$q_1 = \frac{j\beta R(1-u^2\cos^2\psi)}{2u^2} = -\rho e^{-jb'}$$

whence $\rho = \frac{\pi R}{\lambda}\frac{x}{\cos b'} = \frac{\pi R}{\lambda}\frac{\epsilon_r-\cos^2\psi}{\sin b'}$

$$\tan b' = \frac{\epsilon_r-\cos^2\psi}{x} \doteq \frac{\epsilon_r-1}{x}$$

Now $-\rho e^{-jb'} = \rho e^{jb}$

whence $b = \pi - b'$

Also $\alpha = \frac{18 \times 10^3 g}{f_{meps.}}$

The attenuation of a horizontally polarized wave along the surface of the earth may be found using the same ground wave attenuation factor A as is used for vertical polarization and the above definitions of p and b.

The ratio of the numerical distance p to the actual distance R will be greater for horizontal polarization than for vertical polarization. Consequently horizontally polarized surface waves suffer greater attenuation than vertically polarized waves. At low and medium frequencies, where α is large this difference in attenuation is very great and only vertically polarized surface waves need be considered. In this frequency range the aerials used will be vertical types. At H.F. and V.H.F. the attenuation of the surface wave is very large for both polarizations with the result that surface wave propagation is limited to very short distances. In the V.H.F. range elevated aerials are used and propagation is mainly by space wave. Both vertical and horizontal polarization may be used for space wave propagation.

(5) Elevated Dipole Aerials.

In a system in which the transmitting and receiving aerials are placed on the earth's surface the reflection coefficient is approximately -1 since the angle $\psi \div o$ and the direct and ground reflected waves cancel so that propagation is by means of the surface wave only. This state of affairs exists with normal broadcast frequencies during daytime transmission. However, for V.H.F. transmission the aerial may be placed at some distance from the earth's surface so that the space wave is no longer zero and the signal at the receiving aerial is the resultant of space and surface waves.

Consider two aerials one transmitting, one receiving, at heights h_1 h_2 above the earth's surface. Then the vertical component of field intensity at 2 due to the

vertical dipole at 1 is as given above. Neglecting u^2 and higher powers this becomes

$$E_z = j30\beta I d\ell \cos^2\psi \left\{ \frac{e^{-j\beta R_1}}{R_1} + R_v \frac{e^{-j\beta R_2}}{R_2} - \frac{(1-R_v)F}{\cos^2\psi} \frac{e^{-j\beta R_2}}{R_2} \right\}$$

Consider the case where $r \gg h_1 + h_2$

where r = The distance between the two aerials.

Then $\cos\psi \doteq 1$ $R_1 \doteq R_2 \doteq d$ in the denominator.

Also for p large

$$F = 1 + j\sqrt{\pi\omega}\, e^{-\omega}\, \mathrm{erfc}(-j\sqrt{\omega})$$
$$= 1 - \frac{1 + \frac{1}{2\omega} + \frac{1.3}{(2\omega)^2} + \cdots}{1 + \frac{h_1+h_2}{uR_2}}$$
$$\doteq -\frac{1}{2\omega} \qquad \text{If } uR_2 \gg h_1+h_2 \text{ and } |\omega| > 20$$

$$E_z = \frac{j30\beta I d\ell}{d} \left\{ e^{-j\beta R_1} + e^{-j\beta R_2} \left[R_v + \frac{(1-R_v)}{2\omega} \right] \right\}$$

Norton's equation (51) yields for ω .[58]

$$\omega = p_1 \left(1 + \frac{h_1+h_2}{R_2 u\sqrt{1-u^2}} \right)^2 \doteq p_1 \quad \text{since } uR_2 \gg h_1+h_2$$

Also under the same conditions $F \doteq -\frac{1}{2\omega}$ will not change appreciably with height of either transmitting or receiving aerial and will be equal to the ground wave attenuation factor A. Hence

$$E_z \doteq \frac{j30\beta I d\ell}{d} \left\{ e^{-j\beta R_1} + e^{-j\beta R_2} \left[R_v + \frac{1-R_v}{2p} \right] \right\}$$
$$\doteq \frac{j30\beta I d\ell}{d} \left\{ e^{-j\beta R_1} + e^{-j\beta R_2} [R_v + (1-R_v)A] \right\}$$

The above expression is true for short vertical dipoles but Norton has shown that it also holds for elevated half wave dipoles provided $d\ell$ is replaced by the effective length of a half wave dipole i.e. $\frac{\lambda}{\pi}$ [58]

The expression for horizontal dipoles may be deduced from Norton's equation (74), which on reduction becomes:[58]

$$E_\phi = \frac{j60 I \sin\phi}{d} \left\{ e^{-j\beta R_1} + R_h e^{-j\beta R_2} + (1-R_h) G e^{-j\beta R_2} \right\}$$

where the sign of R_h is changed to keep the convention

correct. When $|\omega| > 20$ $G \to u^4 F$ and hence G is very small. The surface wave attenuation for horizontal polarization is so large that the surface wave becomes negligible at very short distances, and ordinarily only space wave propagation need be considered. At large numerical distances the factor G may be replaced by $A = \frac{1}{2p}$ where p has already been defined for horizontal polarization.

The following example illustrates the more important features of space and surface wave propagation.

A half wavelength dipole aerial is elevated 100' above the ground. A receiving dipole is elevated 30'. Determine the space and surface wave field strengths at the receiving aerial when the transmitting aerial carries a current of one ampere at 100 megacycles per second for distances between transmitter and receiver equal to 1, 2 and 3 miles. Let $\epsilon_r = 10$ and $g = 5 \times 10^{-3}$ mhos/metre

(a) Vertical Half Wavelength Dipole Aerial.

(b) Horizontal Half Wavelength Dipole Aerial.

Vertical Dipole Aerial.

Formulae $E_{space} = \frac{j30\beta I \ell_{eff}}{d}\left(e^{-j\beta R_1} + R_v e^{-j\beta R_2}\right)$

$= \frac{j60}{d} e^{-j\beta R_1}\left(1 + R_v e^{-j\beta(R_2 - R_1)}\right)$

$\psi = \tan^{-1}\left(\frac{h_1+h_2}{r}\right)$ $\quad x = \frac{18 \times 10^3 g}{f_{mcps.}}$ hence from curves

$R_v = |R_v| \angle R_v$

$R_1 = \sqrt{d^2 + (h_1 - h_2)^2} = d\sqrt{1 + \left(\frac{h_1 - h_2}{d}\right)^2}$

$R_2 = \sqrt{d^2 + (h_1 + h_2)^2} = d\sqrt{1 + \left(\frac{h_1 + h_2}{d}\right)^2}$

Hence $\frac{2\pi}{\lambda}(R_2 - R_1)$ and hence E_{space}

$E_{surface} = \frac{60}{d}\left|\frac{1 - R_v}{2p}\right|$

$b = \tan^{-1}\frac{\epsilon_r + 1}{x}$ hence $p = \frac{\pi R}{\lambda x}\cos b$ and hence $E_{surface}$

Horizontal Dipole Aerial.

Formulae $\psi = \tan^{-1}\left(\frac{h_1+h_2}{r}\right)$ $\quad x = \frac{18 \times 10^3 g}{f_{mcps.}}$ hence from curves $R_h = |R_h| \angle R_h$; again $\frac{2\pi}{\lambda}(R_2 - R_1)$ is found

and $E_{space} = \frac{60}{d} e^{-j\beta R_1}\left(1+R_h e^{-j\beta(R_2-R_1)}\right)$

$b' = \tan^{-1}\frac{\epsilon_r - 1}{x}$ hence $p = \frac{\pi R}{\lambda}\frac{x}{\cos b'}$ and hence

$E_{surface} = \frac{60}{d}\left|\frac{1-R_h}{2p}\right|$ is found

The calculated results are shown in tabular form:

Distance	Horizontal Dipole		Vertical Dipole		Approximate Formula.
	E_{space}	$E_{surface}$	E_{space}	$E_{surface}$	
1 mile	25.9	0.00156	24.6	0.325	27.0
2 miles	6.8	0.00039	6.7	0.085	6.8
3 miles	3.0	0.00017	3.0	0.038	3.0

All field strengths are expressed in millivolts per metre.

From the above calculation the following approximations may be made for V.H.F. propagation between elevated aerials.

(1) The surface wave may be neglected in comparison with the space wave.

(2) The angle ψ approaches zero so that R_h and R_v are approximately -1.

Then the field intensity at the receiver due to I amperes flowing in the transmitting dipole becomes

$$|E| = \frac{60I}{d}\left|1+R_h^v \angle -\alpha\right| = \frac{60I}{d}\left|1-1\angle -\alpha\right|$$

where α is the difference in path length between the direct and reflected waves.

$R_1 = \sqrt{d^2+(h_1-h_2)^2}$ $R_2 = \sqrt{d^2+(h_1+h_2)^2}$ then provided $d \gg h_1+h_2$

$$\alpha = \frac{2\pi}{\lambda}(R_2-R_1) = \frac{4\pi h_1 h_2}{\lambda d}$$

$$|E| = \frac{60I}{d}\left|1-\cos\alpha+j\sin\alpha\right| = \frac{60I\alpha}{d} \quad \text{If } \alpha \to 0$$

$$\therefore \quad |E| = \frac{240\pi I h_1 h_2}{\lambda d^2}$$

The received field strength is proportional to the

height of the transmitter and receiver and inversely proportional to the square of the distance between them. In most of the propagation problems in T.V. applications the necessary approximations obtain so that the above expression may be used in determining the field intensity.

A comparison of experimental and theoretical results shows that the approximate formula is reasonable in view of the fact that no allowance is made for buildings and irregularities of the earth's terrain.[62]

(6) Spherical Wave Propagation.

The theory briefly described above is based on the tacit assumption of a plane earth. This assumption gives results which are true for small distances but it will not yield results which are correct at large distances. The maximum distance at which the plane wave attenuation formula holds is given by $d = \frac{50}{(f_{mcps})^{\frac{1}{3}}}$ = 10.8 miles for a 100 megacycle per second wave and beyond this distance the field strength deviates from that determined by plane earth considerations due to the curvature of the earth. The effects of earth curvature on the ground wave signals are

(1) The surface wave will not reach the receiving point by a straight line path. The path of the surface wave is provided by diffraction around the earth and refraction in the lower atmosphere above the earth.

(2) The space wave is effected since the ground-reflected wave is now reflected from a curved surface and its energy is diverged by a greater amount than for the plane earth case; this means that the ground-reflected wave reaching the receiver will be weaker than for a plane earth by a factor less than unity.

(3) The heights of the transmitting and receiving aerials above the tangent plane to the surface of the earth, at the point of reflection of the ground-reflected waves, will be less than the heights of the respective aerials above the surface of the earth.

The exact solution of propagation over a finitely conducting spherical earth may be obtained by solving Maxwell's Equations subject to the boundary conditions. Although formal solutions to this problem have been set up, these solutions are much more involved than even the rigorous plane earth solution. For example, one such solution is in the form of an infinite series of spherical harmonics with coefficients containing twelve Bessel functions. The convergence of the series is very slow, the main contributions being given by those terms for which the order n is of the order of $\frac{2\pi R}{\lambda}$ where $\frac{R}{\lambda}$ is the radius of the earth in wavelengths i.e. a very large number for the frequencies being considered. In order to obtain a solution suitable for engineering use, consideration of various particular cases has yielded results. The detailed analysis and results have been given by K.A. Norton in graphical form for several particular cases.[63]

The effect of refraction in the lower atmosphere and method of taking it into account will now be considered.

A wave travelling horizontally in the earth's atmosphere follows a path which has a slightly downward curvature due to refraction of the wave in the atmosphere. This curvature of the path tends to overcome partially the loss of signal due to curvature of the earth and permits the direct ray to reach points slightly beyond the horizon as determined by the straight line path. In calculations the effect of refraction is accounted for by using an effective radius of curvature for the earth that is somewhat larger than the actual radius, and thereafter assuming straight line paths of propagation in the atmosphere.

The refraction of waves in the atmosphere occurs because the dielectric constant and hence the refractive index of the atmosphere varies with height above the earth. The dielectric constant of dry air is slightly greater than the value unity

that applies for a vacuum, and the presence of water vapour increases the dielectric constant still further. For this reason, the dielectric constant of the atmosphere is greater than unity near the earth's surface, but decreases to unity at very great heights where the air density approaches zero. Although the dielectric constant and its variation with height are quantities that vary with the weather, the assumption is usually made that the variation of dielectric constant with height above the earth is uniform, and an atmosphere that has the assumed conditions is called a standard atmosphere. The justification for the use of a standard atmosphere in calculations is that the results determined agree fairly well with those obtained in practice.[71] The relationship between radius of curvature of the path and the change in dielectric constant with height is obtained from the following diagram.

Let V = The velocity of the wave.
The other quantities are given on the diagram.

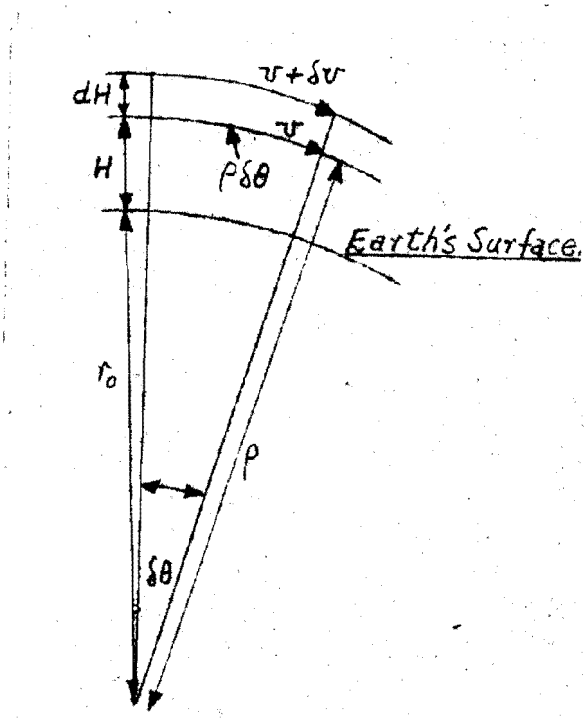

$$\rho\delta\theta = v\delta t$$

$$V = \frac{1}{\sqrt{\mu_v \epsilon_r \epsilon_v}} = K_1 \epsilon_r^{-\frac{1}{2}}$$

$$dH = d\rho$$

$$V+\delta V = (\rho+\delta\rho)\frac{\delta\theta}{\delta t} = (\rho+\delta H)\frac{\delta\theta}{\delta t}$$

$$\therefore \frac{dV}{dH} = \frac{d\theta}{dt} = \frac{V}{\rho}$$

$$\rho = \frac{V}{\frac{dV}{dH}} = \frac{K_1\epsilon_r^{-\frac{1}{2}}}{-\frac{1}{2}K_1\epsilon_r^{-\frac{3}{2}}\frac{d\epsilon_r}{dH}} = \frac{-2\epsilon_r}{\frac{d\epsilon_r}{dH}}$$

Now $\epsilon_r \doteqdot 1$ $\rho = \frac{-2}{\frac{d\epsilon_r}{dH}}$

Since the radius of curvature ρ is dependent on the rate of change of dielectric constant, it will vary with the weather. However, in practice an average value of 4 times the radius of the earth is used in calculations.

It is often convenient to consider the ray paths as straight lines instead of being curved as they actually are, and to compensate for the curvature by using a larger value for the effective radius of the earth. In order to carry out this transfer it is necessary that dH the increment of height should be equal for both curved and straight line paths. From the diagrams we have

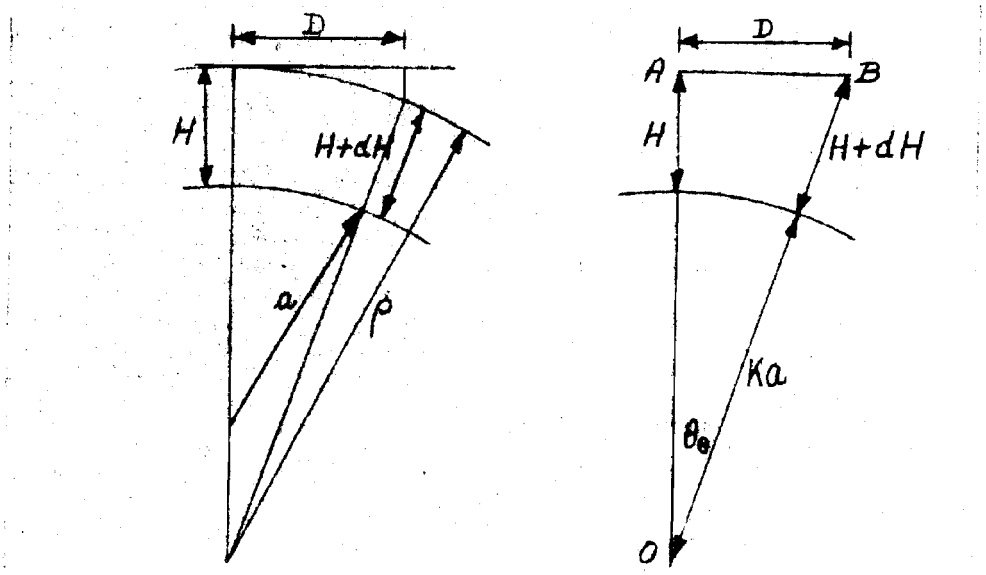

$$dH = \frac{D^2}{2a} - \frac{D^2}{2\rho}$$

Let Ka = The effective radius of the earth

$$dH = BQ - AO$$

$$= (Ka+H)(\sec\theta_e - 1)$$

If $H \ll Ka$ $\theta_e \to 0$ $dH = Ka\frac{\theta_e^2}{2}$

$$\theta_e \doteqdot \sin\theta_e = \frac{D}{Ka+H} \doteqdot \frac{D}{Ka}$$

$$\therefore dH = \frac{D^2}{2Ka}$$

$$\therefore dH = \frac{D^2}{2a} - \frac{D^2}{2\rho} = \frac{D^2}{2Ka} \qquad \therefore K = \frac{1}{1 - \frac{a}{\rho}}$$

Now $\rho = 4a$ $\qquad \therefore K = 1.33$

The use of this factor in ground wave path calculations replaces the bending of waves in the atmosphere and straight line paths may be assumed. The above transfer assumptions for wave refraction have been used by Schelleng, Burrows and Ferrell.[64]

The above approximation allows for refraction of ground reflected waves. The diagram for spherical earth transmission of the space wave is shown below. By finding the position of the tangent plane and using this as the new "earth", the method of calculation is reduced to that used for a plane earth. The only difference is that the reflected ray is reduced in magnitude by a divergence factor which allows for the fact that reflection is taking place from a curved surface. The equation for space wave field intensity becomes

$$E = \frac{j60\, e^{-j\beta R_1}}{d}\left\{1 + DR_h^v\, e^{-j\beta(R_2 - R_1)}\right\}$$

where D = The spherical surface divergence factor

$$D^2 = 1 + \frac{4 h_1'' r_2}{h_1' r}$$

$$= 1 + \frac{2 r_1 r_2}{Ka \tan\delta}$$

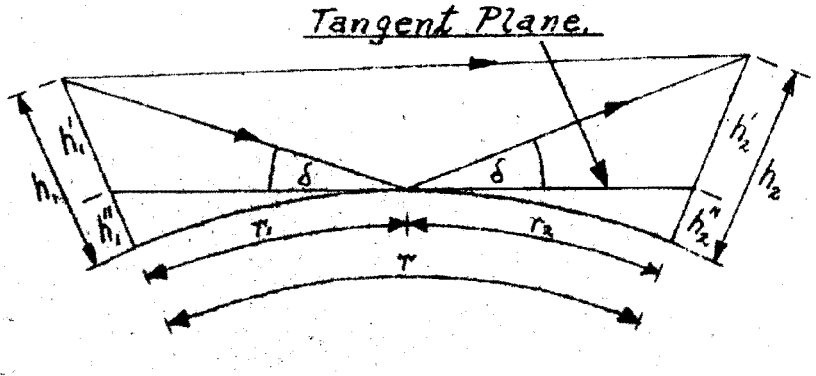

The height of the tangent plane above the earth is as shown earlier

$$h = \frac{r^2}{2Ka}$$

The values of h_1'', h_2'' are given by the above equation for h

on inserting r_1 and r_2 for the distance r.

$$\tan\delta = \frac{h_1' + h_2'}{r} = \frac{h_1'}{r_1} = \frac{h_2'}{r_2}$$

Also $$h_1' = h_1 - \frac{r_1^2}{2Ka} \qquad h_2' = h_2 - \frac{r_2^2}{2Ka}$$

In most cases h_1, h_2 and r are known and r_1 and r_2 are unknown. The simplest method is to plot a curve of $\tan\delta$ versus distance r for various fixed aerial heights h. For any two given height values h_1, h_2 add the corresponding distances for equal values of $\tan\delta$, thereby obtaining a combined curve from which the appropriate distance values may be read off giving the spherical surface divergence factor and hence the field intensity.

The maximum distance at which propagation is received may be determined from the accompanying diagram.

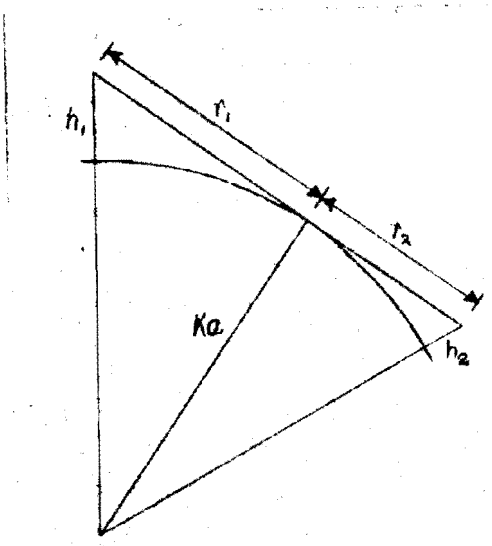

$$(h_1 + Ka)^2 = r_1^2 + (Ka)^2$$

$$\therefore r_1^2 \doteq 2h_1Ka$$

if $h_1 \ll Ka$

$$\therefore r_2^2 = 2h_2Ka$$

$\therefore$ Maximum Distance of Transmission

$$= r_1 + r_2$$

$$= \sqrt{2h_1} + \sqrt{2h_2}$$ miles where h_1 and h_2 are in feet

If $h_1 = 100'$ $h_2 = 30'$ then $r_1 + r_2 = 22$ miles.

(7) Tropospheric Refraction and Reflection.

If the frequency is above 50 megacycles ionospheric reflection does not occur and propagation paths are limited to ground wave transmission. At H.F. and V.H.F. for these ground wave propagation paths the field intensity attenuates rapidly for distances beyond the line of sight. Consequently at these frequencies useful transmission beyond the horizon would not be expected. However it is found that under certain conditions of weather useful transmission considerably beyond the horizon does occur. This increase in range is due to the refraction and reflection of radio waves in the troposphere. The troposphere is that region of the earth's atmosphere immediately above the earth and extending upwards for approximately 6 miles. Tropospheric effects on radio waves may be divided into refraction and reflection. Tropospheric refraction is a gradual bending of the rays that occurs because of the changing effective dielectric constant of the atmosphere through which the wave is passing. As shown above normal refraction effects may be accounted for by using an effective value for the radius of the earth that differs from the actual value. Hence tropospheric refraction effects are automatically included in ground wave calculations. Tropospheric reflection occurs at a place where there is an abrupt change in the atmosphere's dielectric constant. Such tropospheric reflected waves often result in useful signals at distances beyond the normal horizon, a fact of considerable importance in television reception. The allowances to be made for tropospheric refraction have been noted previously so that it now remains to consider tropospheric reflection.

Reflection of waves in the troposphere may extend the range of reception by a hundred miles or more. Let us assume abrupt changes in the value of the dielectric constant do exist in the troposphere. For a wave travelling in a dielectric medium having a dielectric constant ϵ_1 and incident upon a second medium of dielectric constant ϵ_2 the reflection factors have already been deduced.

Let $\epsilon_2 = \epsilon_1 + \Delta\epsilon$ where $\Delta\epsilon$ is the change in dielectric constant at the layer in the troposphere

Then $$R_v = \frac{\left(1+\frac{\Delta\epsilon}{\epsilon_1}\right)\cos\theta_1 - \sqrt{\cos^2\theta_1 + \frac{\Delta\epsilon}{\epsilon_1}}}{\left(1+\frac{\Delta\epsilon}{\epsilon_1}\right)\cos\theta_1 + \sqrt{\cos^2\theta_1 + \frac{\Delta\epsilon}{\epsilon_1}}}$$

For $\Delta\epsilon \rightarrow 0$

$$R_v = \frac{\Delta\epsilon}{2} - \frac{\Delta\epsilon}{4\cos^2\theta_1}$$

Similarly $$R_h = \frac{-\Delta\epsilon}{4\cos^2\theta_1}$$

Using these reflection coefficients and various assumed $\Delta\epsilon$ and layer height K.A. Norton has calculated the field intensities of tropospheric waves. From the curves given by Norton of Field Intensity versus distance it is apparent that there may be times when reflections from the troposphere may be expected to produce usable signals at distances considerably beyond those that result when only ground wave propagation paths are considered. Experience with T.V. reception seems to bear this out. Another mode of transmission known as duct transmission is important because it accounts for reception at distances greater than those possible for reception by tropospheric reflection processes. The process briefly consists of a duct of air acting as a wave guide and guiding energy around the earth's surface. Duct transmission is mainly limited to U.H.F. rather than V.H.F. transmission.

Finally it should be mentioned that sky wave transmission is not possible with V.H.F. waves since the waves penetrate the ionosphere and are not reflected back towards the earth as is the case for longer wavelength transmissions. Also in the main, plane earth space wave transmission is the main consideration in field intensity determinations. Surface wave transmission is only considered when the distance between the transmitting aerial and the field point is small.

SECTION 3.

EQUIPMENT

(a) Introduction.

In order to verify by measurement some of the theoretical results of aerial impedance and polar diagram obtained in the previous sections, certain pieces of equipment were required. A brief outline of the basic equipment required and the use to which this equipment was put will be given in this introduction, together with a list of the individual items of equipment. This introduction will be followed by a description of the individual items of equipment under separate headings.

The basic features of the equipment required for aerial impedance measurements are shown on the accompanying block diagram.

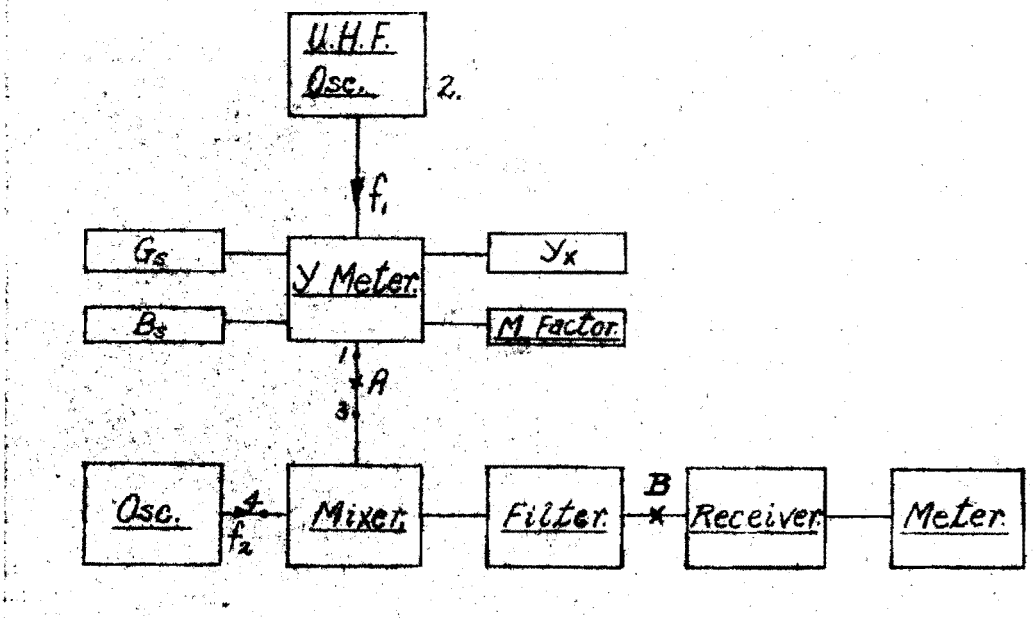

The equipment required for impedance measurements will be described with the aid of this diagram.

The unknown admittance to be measured is connected by coaxial line to an admittance meter fed with a small amount of power from an U.H.F. Oscillator at frequency f_1. The admittance meter has basically three movable coils or more properly loops, which are fed inductively from the U.H.F. source. These three loops feed into a common point which is the output from the admittance meter. When this bridge

circuit is balanced the output from the admittance meter is zero and the unknown admittance may be determined from the readings of calibrated scales on the admittance meter's face. In the case of unbalance a voltage at frequency f_1 will appear at the output plug of the admittance meter. This voltage at frequency f_1 is fed into a coaxial mixer together with a signal from a second oscillator of known frequency f_2. The resulting products are fed through a low pass filter which allows only the product $f_1 \sim f_2$ to pass to a receiver where the signal is sufficiently amplified to be presented to the observer either as a tone or as a reading on a voltmeter included in the output stage of the receiver. Alternatively both forms of detection may be used. The method of measurement consists of making the intensity of the tone and the voltmeter reading a minimum by adjustment of the admittance meter scales. When this condition is obtained the bridge is said to be balanced and the measurement is completed. The above remarks give the bare essentials of the process required for the aerial impedance measurements. There are several small pieces of apparatus required for these measurements which are described below.

The equipment required for aerial polar diagram measurements is quite simple. The aerial whose polar diagram is to be measured is placed on top of a tower and fed with U.H.F. power. The aerial transmits power and must be capable of rotation in the horizontal plane. Several wavelengths away another aerial is placed on top of a tower and the signal received by this aerial in volts is measured by means of an U.H.F. Receiver. The field strength at the receiver aerial is measured on a meter, the transmitting aerial rotated by a known amount and a further reading taken. The resulting voltage readings after suitable correction give the aerial's polar diagram. It is necessary to carry out the measurements in an open space to prevent interference from objects in close proximity, and to place the aerials

at a sufficient height to prevent interference from the ground. The author was able to use a field in Ilam Road for these tests. A hut was erected in the middle of the field and power laid on to the hut and an enclosure further down the field by underground cable.

The apparatus required for these tests together with ancillary equipment associated with the measurements are listed below:

(1) Oscillator: Frequency Range 450-500 Mcps., 1 volt output and adequately shielded
(2) Admittance Meter
(3) Local Oscillator: Frequency 500 Mcps. with adequate shielding
(4) Mixer Unit
(5) Receiver with sensitivity better than 10 μ volts
(6) R.F. Amplifier, Local Oscillator and I.F. Chain to act as a Receiver at 500 Mcps.
(7) Aerials
(8) Aerial Supports
(9) Transmission Lines and Baluns
(10) Compensating Stub
(11) Ilam Road Equipment

The following paragraphs give an account of the pieces of equipment, their design and operation.

(b) U.H.F. Oscillator.[73-81]

The main requirements of the oscillator required to feed the bridge are

(i) The Prevention of Oscillator Radiation. This phenomenon caused considerable difficulty as will be shown later but was overcome by double shielding the oscillator and providing adequate bypasses in all supply leads.

(ii) Stability and Correct Mode of Oscillation. Very early in the development of this oscillator it was found that frequency drift and discontinuity were unavoidable except with the Colpitts circuit. The oscillator finally developed is completely stable, having a frequency drift less than

the audio pass band of a Hallicrafters Receiver. Also the phenomenon known as pulling has been avoided by loosely coupling the output circuit.

(iii) Output. In order to operate the bridge satisfactorily it is necessary that an output between 1 and 10 volts into 50 ohms be achieved. This presented a large difficulty since the efficiency of tubes at these frequencies is about 30% and hence a tube of 6 watt capacity was required. The EC81 just meets this requirement.

(iv) Bandwidth. At least 40 Mcps. of bandwidth were required in order that measurements could be carried out at all the frequencies in a normal composite video signal. It will be realized that 40 Mcps. represents 8 Mcps. of bandwidth for the parent aerial.

Considerable difficulty had to be overcome before the oscillator finally built met the above stringent requirements. The final design consisted of a parallel $\frac{\lambda}{4}$ line oscillator using an EC81 tube. The circuit is shown below. The stages carried out before this final design was achieved involved the building of five experimental oscillators all of which did not meet the above requirements.

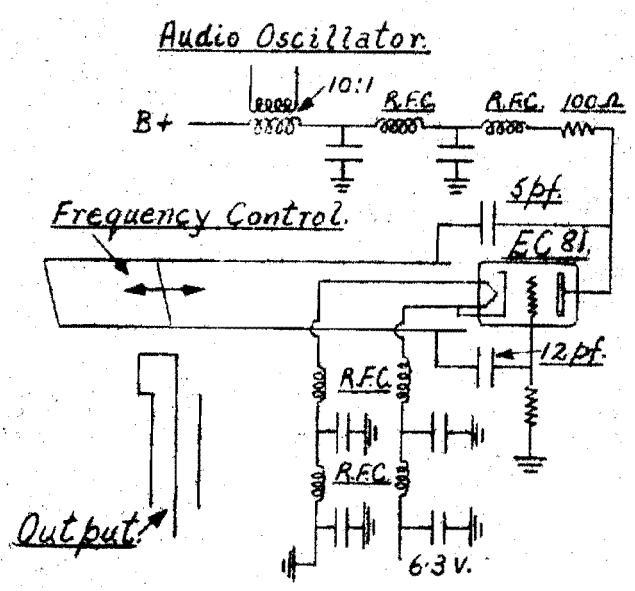

The oscillator design is based on tuning the tube capacitance and strays with a short circuited line less than one quarter wavelength for which

$$Z = jZ_0 \tan\beta\ell = j\omega L$$

The oscillation conditions for a Colpitts circuit are given below.[73] Self oscillation will be sustained if the gain is such that

$$G \geq \frac{C_{gK}}{C_{pK}}$$

The gain is fixed for a given tube and loading. Maximum efficiency is achieved in Class C operation and this is obtained by suitable adjustment of grid leak bias. The frequency of oscillation is given by

$$f_0 = \frac{1}{2\pi\sqrt{L\left\{\frac{C_{gK}C_{pK}}{C_{gK}+C_{pK}} + C_{gp}\right\}}}$$

Modulation of the oscillator was achieved in the plate circuit using a 10:1 transformer and a 20 v. audio oscillator.

Power was measured in two ways. The first method consisted of using a 50 ohm slotted line and a non-inductive lamp placed at a current maximum. This proved unsatisfactory as the lamp brightness was compared with a similar lamp fed with D.C. power, the second lamp's brightness being brought into equality by changing its power input. The difficulty with this method was the lack of facility of the human eye to detect small changes in power input. The set-up did however give a measure of the power output obtained from the oscillator. A second method consisted of feeding the output of the oscillator into a standard 50 ohm termination and measuring the voltage across it with a Crystal Galvanometer. The advantage of this method was that the Galvanometer could be calibrated on 50 c.p.s. and the instrument has no appreciable error up to 1000 Mcps. The power output obtained from the oscillator was measured using this technique.

The oscillator finally built satisfied all the requirements listed above.

(c) Admittance Meter.[82-92]

An admittance meter with an accuracy of 5% was purchased from the General Radio Co., together with conductance and susceptance standards, line stretcher, short circuit and open circuit terminations, coaxial fittings and low loss coaxial cable. The bridge requirements are:

(i) Adequate input : 1-10 volts into 50 ohms

(ii) Adequate receiver sensitivity, better than 10 μv

(iii) No current in the shields.

The methods of achieving these criteria are discussed under each item of the complete experimental layout.

A brief description of the G.R. Admittance Meter's operation is given below.

The Meter is a null device. Through adjustable loops, it samples the currents flowing in three coaxial lines fed from a common source at a common junction point. The outputs of the three loops are combined and when the loops are properly oriented, the combined output becomes zero. The device therefore balances in the same manner as a bridge. It indicates conductance and susceptance on direct reading dials, the calibrations of which are independent of frequency, and the null settings for both components are completely independant.

The meter has a standard conductance G_s , which is a resistor having a value equal to the characteristic impedance Z_o of the line; the standard susceptance jB_s is an adjustable stub which is set to one-eighth wavelength at the operating frequency.

Since the voltage from the oscillator is common to all three lines, the sending end current in each line is proportional to the sending-end admittance. This admittance is Y_x for the line terminated in the unknown, $G_s = Y_o$ for the line terminated in the standard conductance, and $jB_s = -jY_o$ for the line terminated in the eighth-wave stub.

The induced voltage in each loop is proportional to the mutual inductance (M_x, M_G or M_B), and to the current in the corresponding line. Thus, the induced voltage in the loop associated with the unknown admittance is proportional to the product,

$$M_x Y_x = M_x G_x + j M_x B_x$$

the induced voltage in the loop associated with the standard conductance is proportional to the product, $M_G G_S$; and the induced voltage in the loop associated with the standard susceptance is proportional to the product, $j M_B B_S$. It follows that these three induced voltages add up to zero and produce a null when the couplings of the three loops have been adjusted to have the following relations:

$$G_x = -\frac{M_G}{M_x} G_S \qquad\qquad B_x = -\frac{M_B}{M_x} B_S$$

G_S and B_S are constants, so the M_G scale may be calibrated in terms of G_x , the M_B scale in terms of B_x , and the M_x scale in terms of a multiplying factor to be applied to the other two scale readings. Since each coupling can be varied through zero, the two balance equations show that the theoretically measurable ranges of conductance and susceptance extend from zero to infinity. However, the percentage accuracy of reading the scales naturally decreases as the position of zero coupling is approached, and the 1 millimho to 400 millimho range is found practical for reading and setting.

The loops associated with the unknown admittance and the standard conductance can each be rotated through an angle of 90°, but the loop associated with the standard susceptance is arranged to be rotatable through an angle of 180°, thus allowing the measurement of positive as well as negative values of unknown susceptance with a single susceptance standard.

(d) Local Oscillator.[93]

Initially it was decided to build a local oscillator

and mixer unit in one assembly close to the detector plug of the admittance meter. However, an existing piece of equipment was finally chosen because of its perfect shielding and adequate frequency coverage. The instrument used was a Marconi U.H.F. Signal Generator. The power output from the Marconi Oscillator is low, 0.5 milliwatts into 50 ohms, but with the good conversion gain obtained, and high receiver sensitivity the desired accuracy of measurement with the admittance meter was achieved.

(e) Mixer Unit.[94,95]

The requirements of the mixer unit are

(1) High conversion,

(2) Extremely good shielding, in order to ensure that the beat signal as measured by the receiver was only produced by the local oscillator beating with the output signal from the admittance meter and not from any spurious signal radiated from the instruments or from the element being tested.

The development showed that conventional mixer circuits with low pass filters in the form of lumped circuits were inadequate because the filters did not follow conventional low pass filter characteristics. The first filter designed for a 40 Mcps. cut-off did in fact cut off at the required frequency but became a high pass filter for frequencies in excess of 250 Mcps. because the inductance of the condenser leads had a greater effect than the condensers themselves at the higher frequencies.

The reasen for using a low pass filter becomes apparent if the block diagram in the introduction to this section is examined. In the diagram if point A is disconnected and a plug placed across the input to the mixer from the admittance meter then signal radiated from points 1 or 2 is picked up by B and passes to the mixer; then the mixed signal passes back to the receiver where its presence is noted in the form of a beat. By placing a low pass filter between B and the mixer the 500 Mcps. signal picked up by B will not reach the mixer and hence the beat note of the

receiver will be entirely that produced by signal entering the mixer box at 3. This assumes that 4. is adequately shielded, as it is in this case.

One form of low pass filter used consisted of a section of coaxial line placed across the output from the mixer box. The line was $\frac{\lambda}{2}$ long at 500 Mcps. The coaxial line consisted of a brass plug fitting the inner surface of the outer coaxial element with a polystyrene cylinder fitting inside the brass plug and over the inner coaxial element. The function of this arrangement is that the condenser so formed acts as a short circuit to 500 Mcps. signal but does not attenuate signals at the I.F. 30 Mcps. The $\frac{\lambda}{2}$ line was tested for filter action using a signal generator input and the crystal galvanometer in the output lead. The line gave excellent attenuation to 500 Mcps. signal and the frequency of high attenuation could be altered by changing the length of the line. When connected in the experimental circuit this element while correcting for some of the stray signal did not give an acceptable level and was eventually discarded. Its failure to perform the function required of it, namely to act as a low pass filter, is due to the leaky connections required for its use.

The final assembly developed for the mixer filter box consisted of a completely coaxial arrangement, each filter was enclosed in its own cell and the by pass condensers were parallel plate mica type. Schematically the circuit diagram is as below.

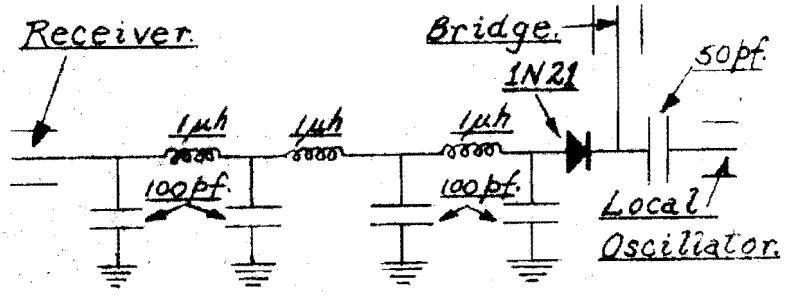

The circuit has good conversion, passes the low frequency components and attenuates all the high frequency components

present.

(f) Receiver.

The availability of a standard piece of laboratory equipment made the receiver problem simple. Tests on the receiver showed that its sensitivity at 30 Mcps., the I.F. for the Bridge Measurements was better than 1 μv. The shielding of the receiver is poor but the presence of the low pass filter in this line eliminates transmission of unwanted signal along this line.

(g) U.H.F. Receiver.[96,97,98]

In order to carry out field strength measurements a 500 Mcps. Receiver was required. Numerous examples of instruments which have been used are available in the technical literature but each suffers from some disadvantage so that a conventional superheterodyne was developed. The functions of the receiver are:

(i) To detect weak signals

(ii) To amplify. The usual procedure is to effect sufficient gain at the R.F. to raise the signal above the noise of the succeeding mixer and I.F. amplifier stages. Then the main amplification is carried out at the I.F. after which detection and display either on meter or loudspeaker is effected.

(iii) To possess adequate tuning adjustment

(iv) To be completely stable.

The design of the receiver will be treated in detail below from aerial to meter.

(1) Receiver Aerial.

The gain required by the receiver was determined from the equation already derived in Section 2

$$P_{rec.} = \frac{9}{64\pi^2}\left(\frac{\lambda}{r}\right)^2 P_{tr.}$$

$$r \doteq 70\lambda$$

The attenuation in the aerial cables was found to be 6 db. and this figure was used in determining the gain required by the U.H.F. Receiver.

The aerial used consisted of a simple dipole 0.475 λ long with a director 0.456 λ long, placed 0.1 λ in front of the dipole.

The dipole aerial with parasite was found to give the best results for the simple types of aerial tested. The aerial was mounted on top of a mast at a distance of 10 λ above the earth.

(2) <u>The R.F. Amplifier, Mixer and Local Oscillator.</u>[99,100]

At these frequencies conventional receivers employ a stage of R.F. Amplification using negative grid U.H.F. pentodes such as the acorn type with variable inductance tuning. It was hoped to be able to obtain a gain approaching unity between the R.F. Input Signal and the I.F. Input Signal, but using this conventional circuitry the gain was very much reduced and so the first experimental amplifier was discarded. The use of direct mixing of R.F. and Local Oscillator Signal while being theoretically possible at these frequencies gave trouble due to harmonics giving spurious beat signals. The use of at least one stage of R.F. amplification is consequently necessary. Another method described in detail for U.H.F. amplification is the grounded-grid amplifier. This circuit is described here in detail as it furnished the means of providing the necessary R.F. amplification. Consider the accompanying diagram:

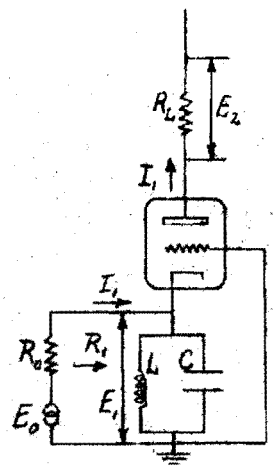

The impedance of the tuned circuit is high compared to the input resistance of the tube

$$\therefore I_1 \text{ cathode} = I_1 \text{ plate}$$

$$E_2 = I_1 R_L$$

The Fundamental Frequency Component of Current in a triode is

$$I_1 = g_m\left(E_g + \frac{E_p}{\mu}\right)$$

$$= g_m\left(-E_1 + \frac{(-I_1 R_L - E_1)}{\mu}\right) \qquad R_p g_m = \mu$$

$$\therefore G = \frac{E_2}{E_1} = \frac{R_L(1+\mu)}{R_L + R_p} = \frac{1+\mu}{1+\frac{R_p}{R_L}}$$

Now consider the transfer of maximum power at the cathode. Looking forward the power = $\frac{E_1^2}{R_1}$. Now since the line is matched we see looking back a generator E_o and a load $2R_o$. If the maximum power condition obtains then $\frac{1}{2}$ of this power is taken up in this load.

$$\text{Looking backward the power} = \frac{1}{2}\frac{E_o^2}{2R_o}$$

$$\therefore \text{Gain } G_a = \frac{E_1}{E_o} = \frac{1}{2}\sqrt{\frac{R_1}{R_o}}$$

To determine R_1 we note that

$$G = \frac{E_2}{E_1} = \frac{I_1 R_L}{I_1 R_1} = \frac{R_L(1+\mu)}{R_L + R_p}$$

$$\therefore R_1 = \frac{R_L + R_p}{1+\mu}$$

The gain from aerial to mixer input is therefore

$$G = \frac{1}{2}\sqrt{\frac{R_L + R_p}{R_o(1+\mu)}}\ \frac{R_L(1+\mu)}{R_L + R_p}$$

$$= \frac{1}{2} R_L \sqrt{\frac{1+\mu}{R_o(R_L + R_p)}}$$

$$= \frac{1}{2}\sqrt{\frac{R_L}{R_o}\ \frac{1+\mu}{1+\frac{R_p}{R_L}}}$$

A grounded grid amplifier was designed and built using the above design formula and an EC80 triode valve. This R.F. Amplifier employed a high Q coaxial resonant circuit for its plate load. Unfortunately, the Q could not be made high enough due to constructional difficulties. In the final arrangement of the amplifier capacitance tuning

was used with matching to the mixer.

The final form of the R.F. Amplifier and Mixer is shown below:

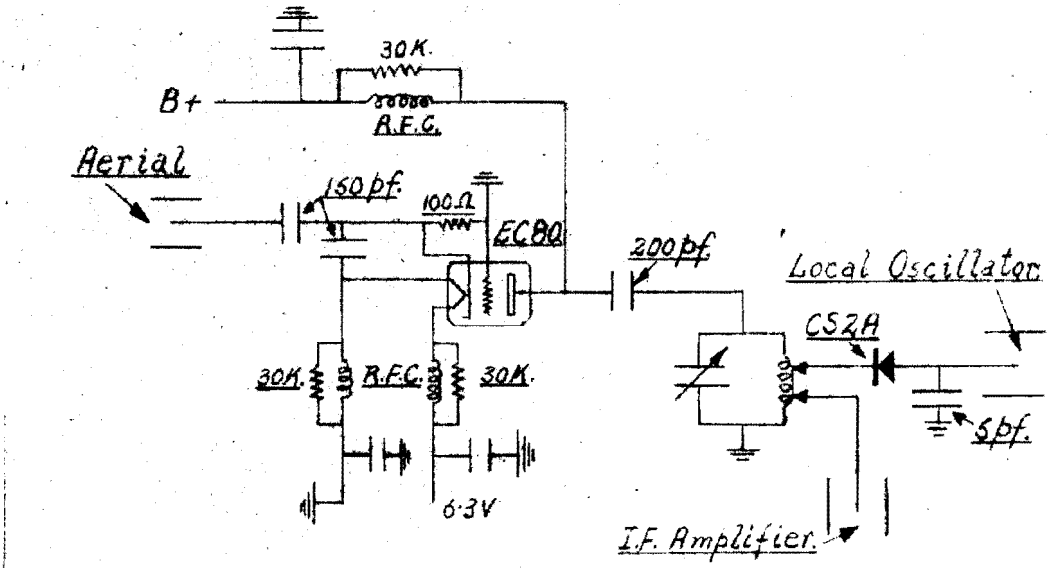

The mixer, a CS2a was incorporated in the same cell as the R.F. Amplifier. The Local Oscillator similar to the type described previously was placed in such a position as to give maximum conversion gain. The gain of the total arrangement as measured with a crystal galvanometer is 0.4. The arrangement gives a very sharp resonance and the Local Oscillator Signal is 20 Mcps. above the R.F. Signal.

(3) <u>The I.F. Amplifier.</u>[101]

Initially an I.F. amplifier with a gain of 1000 was considered to be adequate. As development proceeded it was found that a higher gain would be required. The I.F. of 20 Mcps. was chosen to give sufficient deviation between the R.F. and the L.O. signals and at the same time sufficient gain. A three stage I.F. amplifier, audio amplifier, meter and attenuator were built employing 6AG5 valves. It was hoped that this unit incorporated in one cell with the other parts of the receiver would form a light weight unit. The I.F. amplifier consisted of cathode biased, inductance tuned stages with sharp resonance and gain greater than 1000.

On the assumption of unity gain from the preceding parts of the receiver, this unit would have been capable of detecting signals down to 50 μv /metre. The overall gain of the R.F. Section and Mixer as previously mentioned is only 0.4 so that the gain of the I.F. chain would have to be increased in order to measure small signals. As considerable time at this stage had been spent without producing any useful results a conventional all wave receiver was used instead of the above arrangement as an I.F. Amplifier. The gain of this arrangement, stability and flexibility make its use preferable to the I.F. amplifier chain developed by the author.

(h) Aerials.

The aerials for the measurements were made of copper tubing of 1/8", 3/16", 1/4", 5/16", 3/8" and 1/2" diameter. The copper tubes were approximately 7" long and had conical brass pieces with slope length s = o, $\frac{1}{4}$", $\frac{1}{2}$", $\frac{3}{4}$", 1" fitted into one end. The brass sections were tapped axially with a 10 B.A. thread so that the aerials could be attached to the transmission lines feeding them.

(i) Aerial Supports.

The aerials were supported for the unipole admittance tests by screwing them onto the centre core of the coaxial air line from the admittance meter. The unipole was fed against a ground plane in these tests. The ground plane was made of sheet aluminium approximately 9' x 9'. The field tests required special aerial supports. The receiving aerial was supported on a mast 3" x 2" and 30' long. The transmitting aerial was supported on a 3" x 2" mast 30' long and was capable of rotation from the ground by known amounts.

(j) Transmission Lines and Baluns.[102,103]

Several small lengths of air cored 50 ohm coaxial transmission line were made to fit the G.R. Admittance Meter.

Because of the balanced nature with respect to earth of a dipole aerial and the unbalanced nature of a coaxial line it was necessary to provide a balance to unbalance transformer between the dipole aerial and coaxial transmission line. A balun employs half wavelength phase inversion properties. A sleeve short circuited and one quarter wavelength long was fitted over the outer of the transmission line feeding the dipoles used in both the admittance and field strength measurements. The efficiency of such a balun for the frequency range used is greater than 96%.[39]

(k) Compensating Stub.[104]

A short circuited quarter wavelength transmission line has a susceptance-frequency variation which is approximately equal and opposite to the susceptance-frequency variation of a dipole aerial. If the two are combined in parallel the susceptance-frequency variation will be small. It is particularly desirable that the susceptance variation of wideband aerials should be small since the presence of susceptance represents a certain loss in the energy which may be transmitted by the aerial. A short circuited compensating stub was designed and built in order to determine the degree of compensation such a stub provides. The physical dimensions of the stub are dependent on the particular aerial it is required to match. The stub which was designed was a compromise. It provides a degree of compensation for all the dipole aerials with which it is used. The physical dimensions were representative of the dimensions required for the range of aerials tested and do not match any particular aerial.

A short circuit stub is designed as follows. Consider a lossless line short circuited at the far end and of length equal to one quarter of a wavelength at a frequency f_o. Then the admittance looking into the lossless line is

$$Y_{in} = -jY_o \cot \beta \ell$$

Consider a small change in frequency to $f_o+\delta f$

$$\lambda f_o = c = (\lambda+\delta\lambda)(f_o+\delta f)$$

$$\therefore \frac{\delta\lambda}{\lambda} = -\frac{\delta f}{f_o}$$

Now $$\beta\ell = \frac{2\pi}{\lambda+\delta\lambda}\frac{\lambda}{4} \doteq \frac{\pi}{2}\left(1-\frac{\delta\lambda}{\lambda}\right) = \frac{\pi}{2}\left(1+\frac{\delta f}{f_o}\right)$$

Now $\tan x \doteq x$ when x is small

$$\cot\left(\frac{\pi}{2}+x\right) = -\tan x = -x$$

$$\therefore Y_{in} = -jY_o\cot\beta\ell = -jY_o\cot\left(\frac{\pi}{2}+\frac{\pi}{2}\frac{\delta f}{f_o}\right) \doteq j\frac{Y_o\pi\delta f}{2f_o}$$

Near the first resonance the dipole admittance is

$$A = G - jK\frac{\delta f}{f_o}$$

If the stub is placed across the aerial then the total admittance is

$$A = G + j\left(\frac{\pi}{2}Y_o - K\right)\frac{\delta f}{f_o}$$

Hence if $Y_o = \frac{2K}{\pi}$ then the first order variation in susceptance is removed.

The characteristic admittance Y_o of the compensating stub was chosen by finding the representative slope of the susceptance-frequency curves of the dipole aerials tested.

The length of the stub was made approximately equal to a quarter of a wavelength at 477.5 Mcps. The length of the stub could be altered. The provision of a variable length stub made it possible to compensate for the capacitances introduced by the discontinuities in the coaxial air line.

(1) <u>Ilam Road Equipment</u>.

A hut 6' x 9' and 7' high was prefabricated and erected in a field at Ilam Road. Two enclosures were built and power cable laid to them from the M.E.D. supply.

The accompanying site plan and photographs show the items of equipment described above.

(m): Ilam Road Site Plan.

Scale : 1" = 65'

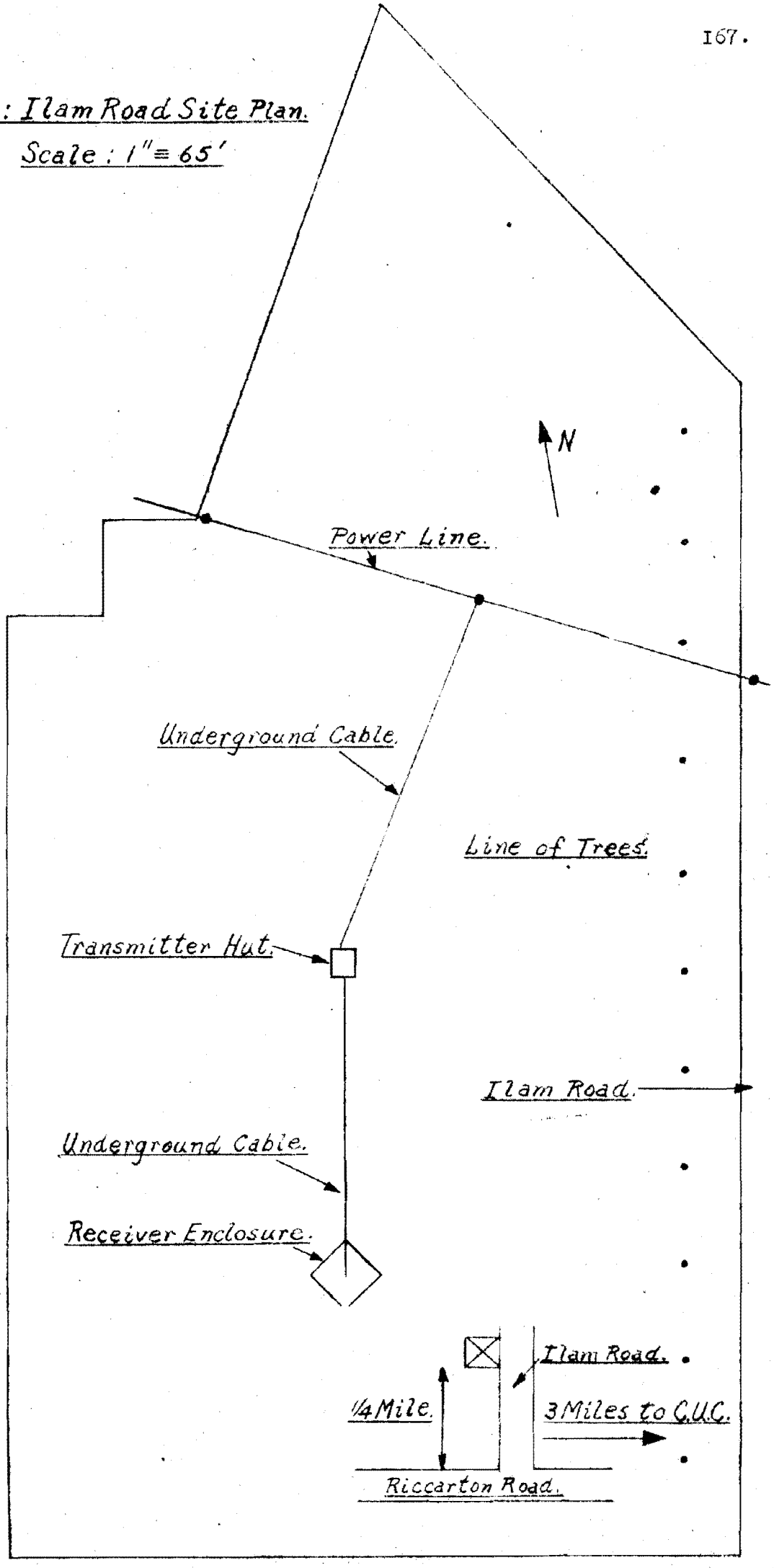

(n) Photographs of Equipment.

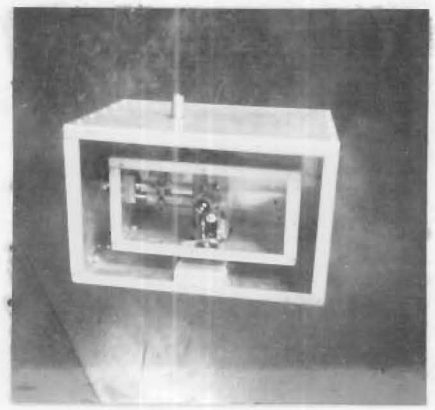

(1) U.H.F. Oscillator showing Shielding, Coaxial Line Structure and Output Plug.

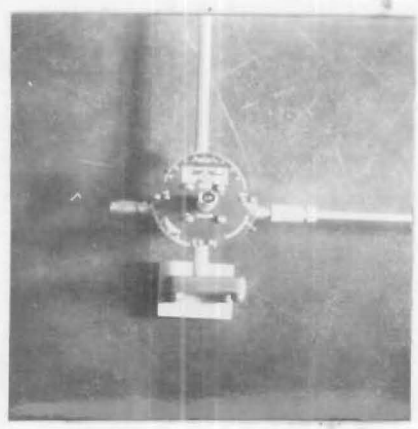

(2) U.H.F. Admittance Meter showing Conductance Standard at the left, Susceptance Standard at the top and Coaxial Line feeding the Unknown Admittance at the right.

(3) Typical Dipole Aerial arrangement showing Balun and section of Transmission Line.

(4) Typical Compensated Dipole Aerial arrangement showing Balun and adjustment for Short Circuited Stub.

(5) Layout for the Admittance Measurements.

Left foreground Modulating Oscillator, behind this Oscillator is the Mixer Unit and Admittance Meter with the Coaxial Transmission Line to the Unknown Admittance in a vertical position. Behind the Admittance Meter to the left is the Marconi Oscillator, the Receiver and the Receiver Voltmeter. To the right of the Admittance Meter is the U.H.F. Oscillator with the Modulation Transformer in front of this Oscillator. The remainder of the equipment provides the power required.

(6) View of Receiver Enclosure and Transmitter Hut looking North.

(7) View of Transmitter Hut and Receiver Enclosure looking South.

(8) Transmitter Hut and Aerial Mast looking West.

(9) View in door of Transmitter Hut showing Transmitting Equipment on the left, Frequency Meter in the centre and Marconi Oscillator on the right.

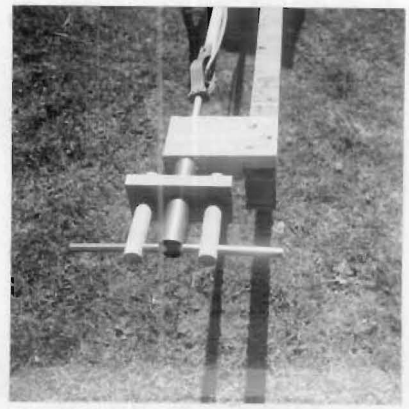

(10) Typical Dipole arrangement for Field Strength Test mounted on Transmitting Aerial Mast.

(11) View of Receiver Enclosure and Mast looking South-West.

(12) Receiver Aerial, Enclosure and Mast in the lowered position looking North.

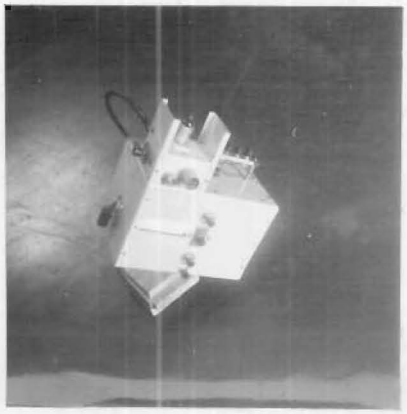

(13) The U.H.F. Receiver's Local Oscillator, R.F.Amplifier and Mixer.

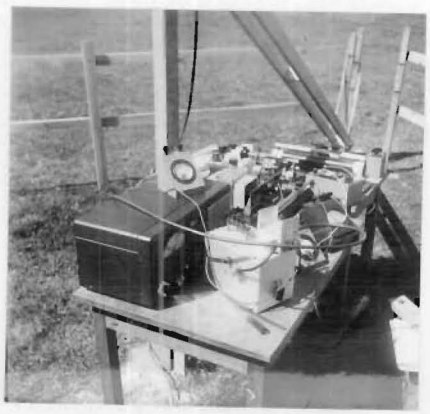

(14) The U.H.F. Receiver Equipment in the Receiver Enclosure.

SECTION 4

EXPERIMENTS.

(a) Introduction.

The purpose of this section is to give an outline of the methods of measurement adopted together with a comparison of alternative methods. Also the preliminary experiments and the admittance and field strength measurements made in order to determine the admittance and polar diagrams of cylindrical aerials are described.

The methods of deriving the aerial admittance and polar diagrams from these measurements will then be treated and the final calculations presented both in tabular and graphical forms. Comments on the results obtained will be given in the subsection dealing with the comparison of theoretical and experimental results.

(b) Methods of Measurement.[105,106]

The physical properties of an aerial are specified by the following quantities:

(1) Radiation Pattern

(2) Directivity

(3) Gain

(4) Input Admittance

(5) Current Distribution

(6) Polarization

We treat the method of measurement of each of the above properties below.

(1) Radiation Pattern.

The polar diagram of an aerial is determined by radiating a fixed amount of power from the aerial under test and receiving this power by means of an aerial on a receiver calibrated to read field strength. By rotating either one or other of these two aerials and noting the angular displacement with respect to the fixed aerial and the field strength as indicated by the meter, the polar diagram is obtained.

Methods based on transmitting a narrow beam of energy to the test aerial have been used and are quite satisfactory.

Where it is impossible to obtain an open field this method would be used.

There are certain precautions which must be observed to ensure that the field strength observed is in fact that due to the dipole alone and not due to an interference pattern set up from several waves picked up by the receiving aerial. Briefly the requirements are:

(i) The distance between the aerials must be sufficient so that the effects of the ends are negligible. This means that the field strength received is due to the radiation field alone. For distances greater than a wavelength the effect of the near or induction field is small. Hence if the distance between the aerials is large compared with a wavelength the field strength will be entirely due to the radiation field.

(ii) The height of the aerials above the ground must be sufficient so that the interference pattern set up between the aerial and its ground image is small. This effect is never overcome in practice but may be masked as shown below. If the dipole aerial is at a height greater than two wavelengths above the earth the pattern obtained does not differ appreciably from the true free space diagram.

(iii) The transmitting aerial should produce as nearly as possible a uniform field intensity over the region of the receiving aerial. In the tests carried out the angle subtended by the receiving aerial at the transmitter was 0.3 degrees so that the field intensity change over the length of the aerial is very small.

(iv) The combined effects of the direct and ground reflected waves between the transmitter and receiver should be a measure of the field intensity to some linear scale. Alteration of the angle between the transmitter and receiver aerials should not effect the magnitude of this scale value. A geometrical study of both vertical and horizontal cases shows that an additional factor due to the variation of

this scale factor must be included in the field strength results for the vertical arrangement, whereas for the horizontal arrangement the magnitude of the scale factor does not alter with angle between the transmitter and receiver. If horizontal aerials are used at a sufficient height above the ground this variation need not be considered.
(v) The exact distance between the transmitting and receiving aerial must be adjusted so that the difference between the direct wave path length and the ground reflected wave path length is equal to an odd number of half wavelengths. The two waves then reinforce each other for horizontal aerials. If the path difference is equal to a number of wavelengths partial cancellation occurs and the sensitivity of the measurement is impaired.
(vi) The experiments must be carried out in an open space to prevent interference due to reflections from objects.

All the above criteria were completely satisfied in the field strength experiments.

The method of polar diagram measurement will now be described. The measurements were made in a field at Ilam Road. The aerials to be tested were of length equal to the resonant length of the given aerial as determined from the admittance tests at the centre frequency of 477.5 Mcps. The aerial to be tested was fitted to the balun coaxial transmission line assembly as shown in photographs (3) and (10) of the last section. The aerial mast was pivoted at ground level and raised into a vertical position manually. It was then fixed to a wooden bracket cantilevered from the transmitter hut wall. The coaxial transmission line feeding this aerial passed through the hut wall to the output plug of the U.H.F. Oscillator suitably modulated with 1000 c.p.s. Audio Signal. The frequency of the transmitted signal was determined by a G.R. Superheterodyne Frequency Meter. The transmitter aerial was rotated from ground

level by known amounts. At a distance of 50 yards a receiving set was located. A dipole aerial with parasite and balun fed a coaxial cable whose output went to a U.H.F. Receiver. The Receiver was calibrated by a Marconi Signal Generator at the frequency of the measurements.

Tests were carried out at three frequencies, 457.5, 477.5 and 497.5 Mcps., corresponding to a coverage of a composite video signal of 8 Mcps. in the prototype aerial. The aerials were tested over a 90° mechanical displacement in the horizontal plane between receiver aerial and transmitter aerial in 5° intervals. Two observers made the measurements, one observer rotated the transmitting aerial and the other observer noted the readings of field strength. The U.H.F. Receiver's calibration was checked throughout the measurements.

(2) and (3) Gain and Directivity.

Once a polar diagram has been obtained for an aerial the directivity and gain may be obtained by mechanical processes such as graphical integration of the polar diagram. The gain is always referred to a half wave dipole.

(4) Input Admittance.

The methods of measurement of input admittance are limited at ultra high frequencies because the wavelength is small and lumped circuits such as conventional bridge circuits do not behave well.

All methods at ultra high frequencies are based on transmission line techniques. The literature gives copious refinements of these methods.[107-111] The method consists of measuring the S.W.R. of voltage or current along a line and the distance between either a voltage minimum or a current minimum and the aerial terminations. Operations on these quantities using the transmission line calculator yield the required input admittance .

Experiments based on these methods have been used by several authors for cylindrical dipole aerials.[112-115] The accuracy of the measurements has not been as high as one would wish.

The method employed by the author is a refinement of the above transmission line method. A detailed account of the method of measurement is given in the following paragraphs.

The admittance meter and its ancillary apparatus are set up as described in the section on equipment. Before any measurements may be made certain leakage checks must be made. At high frequencies, the reactance of even very short leads is high and hence, in order to minimize difficulties resulting from leakage, all connections between the admittance meter and the detector and generator must be completely coaxial. It is preferable to use a well shielded generator and detector. Leakage from the generator to the detector, from the generator to the circuit under test, or from the circuits under test to the detector can cause errors. Leakage may also be caused by loose joints in the coaxial system. For instance, if the outer nuts of the coaxial panel connectors are loose, leakage voltages can be developed across these junctions. Leakage from A.C. power cables may have effects similar to those described above. These may be eliminated by low-inductance mica condensers connected from either side of the A.C. line to ground.

Leakage effects were checked as follows:

(i) Hand-capacity effects, that is, a shift in the null caused by moving one's hand near or touching various parts of the equipment. This shift indicates the presence of leakage.

(ii) Detector Leakage. The method is to obtain a balance with a conventional setup then a short section of air transmission line with its centre core removed is connected in the detector line. If the detector still indicates zero signal, the detector leakage is negligible. It may be necessary to retune the detector slightly when the tube

is inserted as the difference in source impedance may affect the detector tuning.

(iii) Generator Leakage: The procedure is identical with that described for the detector. In this case the generator frequency may be slightly shifted due to the change in load impedance and the generator may have to be retuned.

(iv) Measure the admittance of an unknown with the generator and detector connected in their normal positions. Then reverse the generator and detector connections and remeasure the admittance. If no significant leakage is present in either measurement, the measured admittance will be the same in both cases.

The above checks for leakage were made for all admittance measurements.

After the above leakage checks had been made the following procedure was adopted for measuring an unknown admittance.

(i) A constant admittance adjustable line together with the length of coaxial air line which was to feed the aerial was connected to the admittance meter.

(ii) A G.R. Open Circuit Termination which produces an open circuit at the point at which the open circuit is desired, was placed over the end of the coaxial air line.

(iii) The Conductance and Susceptance scales are set to zero and the Scale Factor to unity. The adjustable line's length is now altered until a null is obtained. It is necessary to adjust the conductance arm slightly to obtain a complete null as small losses and errors produce small conductance readings. The adjustable line is clamped when the null has been obtained.

The admittance meter measures an admittance as seen at the centre of the meter. By adjusting the length of line so that an open circuit at the far end of the transmission line feeding the unknown appears as an open circuit at the centre of the bridge the line length is made equal to an even number of half wavelengths and the admittance readings

of the admittance meter will be the same as the unknown admittance at the far end of the transmission line.
(iv) Disconnect the open circuit, connect the unknown and balance the admittance meter by means of the conductance, susceptance and multiplying factor arms. The conductance of the unknown is the reading of the conductance scale multiplied by the multiplying factor. The susceptance of the unknown is the reading of the susceptance scale multiplied by the multiplying factor.

When the necessary corrections have been applied to these results the aerial admittance is obtained.

(5) Current Distribution.

The magnitude of the current along an aerial is obtained by inductively coupling a small loop to the aerial. The loop has some form of indicating device such as a crystal galvanometer. The loop is moved parallel to the axis of the aerial and the readings of the galvanometer noted for given distances from the centre of the aerial. The results give the current distribution. Careful shielding is required to ensure that the readings of the galvanometer are only due to that part of the coil close to the aerial. The presence of the coil affects the current distribution to such an extent that for aerials of small physical size the distribution obtained is considerably different from the actual distribution. Because of the small physical size of the aerials tested the current distribution experiments did not show any significant results.

(6) Polarisation.

In all the measurements carried out it has been assumed that plane wave propagation obtains.

(c) Preliminary Experiments

(1) Admittance.

(i) U.H.F. Oscillator and Mixer.

The U.H.F. Oscillator's power output was measured by measuring the R.F. voltage across a standard 50 ohm termination using a G.R. crystal galvanometer. The power output determined by this method was sufficient to operate the admittance meter. The conversion gain of the mixer unit was determined using the G.R. crystal galvanometer to measure the input voltage to the mixer unit and the output voltage from the mixer unit. The conversion gain of the mixer fell to a very low value during the admittance measurements due to breakdown of the crystal material. After replacement of the crystal the conversion gain returned to the original value.

(ii) U.H.F. Oscillator Frequency.

The frequency of the U.H.F. Oscillator was measured by four methods:

(i) The signal from a Superheterodyne Frequency Meter; an instrument which produces signals rich in harmonics was mixed with the signal from the U.H.F. Oscillator. The resultant beat notes were heard on earphones and the frequency of the beats noted from the frequency meter's calibrated dial. By noting several of these beat notes the frequency of the U.H.F. Oscillator may be determined.

(ii) The signal from the U.H.F. Oscillator is fed into a slotted line and the wavelength of oscillation measured by noting the physical difference between two positions on the slotted line where the standing wave indicator gives the same readings.

(iii) The beat note from the U.H.F. Oscillator and the Marconi Signal Generator was fed into a mixer unit. The resulting signal is fed from the mixer unit to a Hallicrafters Receiver for detection. The frequencies of the Hallicrafter Receiver and Marconi Signal Generator are known and hence the frequency of the U.H.F. Oscillator

may be determined.

(iv) A short circuit was placed on the end of the adjustable line which was connected to the unknown plug of the admittance meter. The procedure for measuring an unknown admittance is then carried out and the meter balanced. If the adjustable line is now altered by one half of a wavelength a null should be obtained again. By measuring the physical change in length between two successive nulls the frequency of oscillation of the U.H.F. Oscillator may be determined.

(iii) Admittance Meter Tests:

Tests were carried out on the admittance meter to determine the accuracy and sensitivity of the measurements. The tests consisted of connecting the adjustable line to the unknown arm of the admittance meter with open and short circuits placed on the end of the adjustable line. The tests are based on the following well known transmission line properties for lossless air lines.

(i) If the admittance looking into a short circuited line is a short circuit then a reduction or increase in length of the line by one half a wavelength is again a short circuit.

(ii) If the admittance looking into a short circuited line is a short circuit then a reduction or increase in length by one quarter of a wavelength is an open circuit.

(iii) If the admittance looking into a short circuited line is a short circuit then a reduction or increase in length by one eighth of a wavelength changes the admittance to $\pm j Y_o$, where Y_o is the characteristic admittance.

(iv) Inversion properties hold in the case of an open circuit terminating the adjustable line.

Tests based on the above properties were carried out. The admittance meter is sensitive to a change in length of the adjustable line less than 0.5 mm. The accuracy of the measurements by the admittance meter may be seen from the

following figures obtained for a piece of 50 Ω air cored transmission line.

Let Y_{sc} = The admittance measured looking into the air line with a short circuit on the far end.

Y_{oc} = The admittance measured looking into the air line with an open circuit on the far end.

$$Y_{sc} = 0.502 - j13.56 = 13.56 \angle -87^\circ 52'$$

$$Y_{oc} = 1.34 + j29.7 = 29.75 \angle +87^\circ 24'$$

$$Y_o = \sqrt{Y_{oc} Y_{sc}} = 20.08 \angle -0^\circ 14' = 20.08 - j0.08$$

$$\tanh \gamma \ell = \sqrt{\frac{Y_{oc}}{Y_{sc}}} = 1.48 \angle 87^\circ 38' = 0.061 + j1.48$$

$$\alpha = 0.22 \text{ decibels.}$$

The admittance meter is at least as sensitive as required for these measurements.

(iv) Unipole Tests.

A length of coaxial air line open circuited at the far end without an open circuit termination was required for the unipole tests. The effect of removing the open circuit termination from a length of 50 ohm coaxial air line was determined by placing the adjustable line connected to the coaxial air line in the unknown arm of the admittance meter. An open circuit termination was connected to the other end of the coaxial air line and the bridge balanced. The open circuit termination and coaxial plug on the end of the coaxial air line were removed and the length of the adjustable line changed until a balance was again obtained. The change in length of the adjustable line was equal to the combined length of the open circuit termination and coaxial plug removed, so that the position of the open circuit for a coaxial air line is known.

In carrying out the unipole tests, the coaxial air line used fits tightly into a brass sleeve fitted on the underside of a 9' x 9' sheet of aluminium, and then passes

through a hole in the aluminium sheet to finish in a position flush with the top surface of the aluminium sheet. The unipole aerial to be tested screws onto the centre core of the coaxial air line. Tests for leakage from the coaxial air line, the brass sleeve and the underside of the aluminium sheet were made by connecting the coaxial air line to the unknown arm of the admittance meter. The other end of the coaxial air line with a unipole attached was fitted into the brass sleeve and the admittance meter balanced. The leakage was noted by hand capacity effects changing the balance conditions. The change in balance conditions and consequently the leakage was negligible.

(v) Dipole Mouth Opening and Baluns.

In carrying out tests on balanced systems such as dipoles it is necessary to cut away part of the outer of the coaxial air line to connect one half of the dipole to the centre core of the coaxial air line and to place a quarter wavelength short section over the coaxial air line to act as a balance to unbalance transformer.

The effect of cutting away the outer of the coaxial air line on the position of the open circuit was observed by connecting the adjustable line connected to an open circuited coaxial air line to the unknown arm of the admittance meter. The admittance meter was then balanced and the coaxial air line removed. The outer of the coaxial air line was cut away and connected in the circuit again. The adjustable line's length was altered to produce a null again. It was necessary to alter the conductance by an immeasurable amount showing that the radiation from this slot is small. The change in length of the adjustable line was noted and the new position of the open circuit determined. This position was used for all the dipole aerial measurements. A quarter wavelength short circuited sleeve was fitted over the outer of the coaxial air line.

There was no shift in the null of the admittance meter showing that this balun has negligible effect on the open circuit conditions. A dipole was now fitted to the coaxial air line. The coaxial air line was connected to the adjustable line and the composite line connected to the unknown arm of the admittance meter. The total length between the centre of the admittance meter and the dipole was made equal to three wavelengths. The admittance meter was balanced and the tests for leakage were carried out and showed that the leakage was negligible. A change in the null was observed if a hand approached the dipole. Since the dipole is a radiator this action is quite normal.

(vi) Dipole Open Circuit Tests.

The dipole tests were carried out by altering the frequency of the U.H.F. oscillator. For each measurement it is necessary to know the length of line between the centre of the admittance meter and the unknown admittance to be measured so that the admittance as measured by the admittance meter may be referred to the point at which the unknown is connected. The length of coaxial air line to be used in the dipole tests was connected to the adjustable line and the adjustable line connected to the admittance meter. The conductance and susceptance scales of the admittance meter were set to zero and the scale factor to unity. The length of the adjustable line was altered until a null was obtained and the length of the adjustable line was noted. The conductance and susceptance scales were slightly adjusted to give a perfect balance and their readings noted. The open circuit admittance is now known after making allowance for the shift in the open circuit due to the cut away portion of the outer of the coaxial air line. The above procedure was carried out at eight different frequencies. The significance of this test will be appreciated after the section dealing with the calculation of aerial admittance has been treated.

(vii) Short Circuited Stub.

The purpose of the short circuit stub was to compensate for the dipole aerial's change in susceptance with frequency. The compensation was provided by making the slope of the susceptance-frequency curve for the short circuit stub equal and opposite to that for a typical dipole. A test was carried out to determine the susceptance-frequency curve of the short circuit stub as follows. The stub and associated coaxial air line was attached to the adjustable line and connected to the unknown arm of the admittance meter. The adjustable line's length was adjusted for the frequency of the measurement so that the admittance measured is that looking into the stub from the dipole connections, i.e. the amount of compensating susceptance placed across the dipole. Tests were carried out for two values of stub length at eight different frequencies. The results in millimhos after the necessary corrections had been applied to the measured values are given below.

f (Mcps.)		500.2	494	485.1	478.6	473	465.2	456.7	449.9
ℓ=13·9cm.	G	0.21	0.20	0.19	0.18	0.17	0.17	0.15	0.15
	B	+0.99	-0.47	-2.68	-3.90	-5.23	-7.21	-9.13	-10.31
ℓ=13·7cm	G	0.22	0.20	0.19	0.19	0.18	0.18	0.16	0.15
	B	+2.27	+0.72	-1.38	-2.78	-4.20	-5.97	-7.76	-8.89

These results give curves of susceptance-frequency which are approximately equal and opposite to those for an uncompensated dipole. The small amount of conductance is due to radiation from slots inherent in the construction of the stub. The above figures agree reasonably with the calculated admittance of the compensating stub.

(2) Polar Diagrams.

(i) Coaxial Cable Measurements.

The line loss of a G.R. 50 ohm Coaxial cable and the velocity of propagation in the cable were measured. The line loss is required so that the amount of power which

must be fed to the U.H.F. Oscillator for propagation in the Field Strength Tests may be determined.

The line loss was determined by connecting a length of coaxial cable to the unknown arm of the admittance meter and placing a short circuit termination on the other end of the coaxial cable. The admittance meter was balanced and the admittance looking into the short circuited coaxial cable was noted. The length of the coaxial cable was measured and the line loss determined as follows:

$$Y_{sc} = 5.7 + j0 \quad \text{millimhos}$$

$$\ell = 9.12 \quad \text{metres}$$

$$f = 477.5 \quad \text{mcps.}$$

$$Y_{sc} = Y_o \coth \gamma \ell$$

Since $B_{sc} = 0 \qquad \beta\ell = (2n+1)\frac{\pi}{2}$

$$\therefore \tanh \alpha \ell = \frac{Y_{sc}}{Y_o}$$

$$Y_o = 20 \quad \text{millimhos}$$

Whence $\alpha = 0.28$ decibels/metre.

This means that a piece of coaxial cable 30' long would have a loss of 3 decibels. This is a reasonable figure for the loss in a coaxial cable of this type at these frequencies.

The velocity of propagation in the cable was measured in the following manner. A short length of the coaxial cable was connected to the adjustable line and then the adjustable line was connected to the unknown arm of the admittance meter. The admittance meter was balanced, the length of the adjustable line noted and the frequency measured by the G.R. frequency meter. A known short length of coaxial cable was removed and the adjustable line's length altered until a balance was again obtained.

The change in length of the adjustable line was noted. The ratio of the change in length in the coaxial cable to the change in length of the adjustable air line gives the velocity of propagation in the cable. The velocity of propagation in the cable determined by this method was 0.69C. This figure is quite reasonable.

The lengths of cable suitable for feeding the transmitting and receiving aerials were calculated using the above figure for the velocity of propagation in the cable. The field strength theoretically obtainable was estimated using the above figure for the coaxial cable line loss.

(ii) U.H.F. Receiver.

The frequency of the U.H.F. Receiver's Local Oscillator output was calibrated using the method described above for the U.H.F. Oscillator. The sharpness of resonance of the R.F. Amplifier and the conversion gain of the mixer unit were tested using the Marconi Signal Generator to supply input signal and the G.R. Crystal Galvanometer to measure the output voltage. The results of these tests were satisfactory.

The complete U.H.F. Receiver was calibrated by feeding signals of known voltage and frequency from the Marconi Signal Generator into the receiver coaxial cable and noting the deflection of the voltmeter in the output circuit of the Hallicrafters Receiver. It will be remembered that the Hallicrafters Receiver was used as an I.F. amplifier in the U.H.F. Receiver. The intermediate frequency was 20 Mcps. and the sensitivity of the Hallicrafters Receiver was better than 0.5 microvolts.

Calibration curves of Input volts to receiver aerial versus Hallicrafter Receiver voltmeter reading were plotted for a ratio of 10,000 to 1 of the input signal voltage. These curves which are approximately linear were used in determining the field strength from the U.H.F. Receiver's voltmeter readings in the field strength experiments.

The test described above was repeated several times during the field tests in order to check the calibration curves.

(iii) Polar Diagram Test.

The experiments to be conducted at Ilam were simulated by tests in the North Quadrangle at Canterbury College. The purpose of these tests was to make sure that the equipment was operating satisfactorily before carrying out the experiments at Ilam. A dipole was fed from a U.H.F. Oscillator and placed on one side of the quadrangle. The receiving dipole and U.H.F. Receiver were placed on the opposite side of the quadrangle 50 yards away, and signal detected. Tests were carried out over the range of frequencies 450 - 500 Mcps. by rotating the transmitting aerial and observing the change in the voltmeter reading of the U.H.F. Receiver. The signal detected was more than adequate and the sensitivity as expected better than 1%.

The field strength equipment was completely satisfactory for the experiments to be carried out at Ilam Road.

(iv) Survey at Ilam Road.

A chain survey of the field at Ilam Road was made so that the positions of the transmitting hut, receiver enclosure and power cables could be fixed. The site plan of the last section resulted from this chain survey.

The difference in levels between the transmitting mast base and receiving mast base was measured using a surveyor's level and a Sopwith staff. This measurement was made so that the receiving and transmitting aerials could be placed at the same level.

A T12 Theodolite was used to determine the position where the transmitting and receiving aerials are parallel. This measurement was made so that the angular displacement between the receiving and transmitting aerials could be referred to a reference value.

(v) Maximum Signal at the U.H.F. Receiver.

The equipment was set up at Ilam Road to measure a polar diagram. The transmitting and receiving aerials were placed in a parallel position and the receiving aerial mast was moved in a line passing through the centre of both aerials until the signal received by the U.H.F. Receiver was a maximum. The receiving aerial was fixed in this position. Maximum signal received by the U.H.F. Receiver implies that the direct and ground reflected waves are reinforcing each other. The accuracy of the measurements when the aerials are nearly perpendicular to one another is considerably improved by making this adjustment.

(vi) Dipole Aerial Supports.

Measurements were made to determine the effect of the wooden pieces supporting the aerials being tested. These pieces are clearly seen in photograph (10). A negligible change was observed in the polar diagrams on removal of the wooden support pieces. Consequently the wooden support pieces were used throughout the field tests to give mechanical strength.

(d) Aerial Admittance Experiments and Results.

Tests were carried out on unipole aerials, dipole aerials and dipole aerials with stub compensation. The method of measurement has been described in subsection (b) of this section. The results given are those obtained after the corrections discussed in the next section had been applied to the measured values of conductance and susceptance. The admittance experiments and results are given under three separate sub-headings:

(i) Unipole Aerial Admittance Experiments and Results

(ii) Dipole Aerial Admittance Experiments and Results

(iii) Dipole Aerial with Stub Compensation Admittance Experiments and Results.

(i) Unipole Aerial Admittance Experiments and Results.

Experiments were carried out on unipole aerials for two reasons:

(a) The accuracy of the measurement is greater than for the equivalent dipole since the admittance of a unipole is twice the admittance of the equivalent dipole.

(b) The preliminary tests on dipole aerials showed that the leakage was very small but not zero. The preliminary tests on unipole aerials showed that leakage was entirely absent. The presence of a small amount of leakage in the dipole aerial tests raises the question of the accuracy of the experiments. For this reason coupled with that given in (a) the unipole experiments were carried out.

The measurements were made with the admittance meter for aerials of diameter 1/8", 3/16", 1/4", 5/16", 3/8" and ½", and conical input section slope length S = 0, ¼", ½", ¾" and 1".

The frequency of the measurements was 478.15 Mcps. and the aerial's length was altered from 7" to 3" in ¼" and sometimes 1/8" steps. The admittance as measured by the admittance meter was subjected to the corrections given in subsection (f) of this section. The results of these calculations are shown below in tabular and graphical forms. The results will be discussed later. All susceptance and conductance measurements are given in millimhos and resistances in ohms.

Unipole Admittance Results.

1/8" diameter.

s	0		1/4"		1/2"		3/4"		1"	
$\frac{\ell}{\lambda}$	G	B	G	B	G	B	G	B	G	B
0.283	6.6	-7.9	6.6	-7.4	6.5	-7.7	6.3	-7.6	6.2	-8.1
0.278	7.2	-8.3	7.2	-8.2	7.3	-8.1	7.1	-8.2	7.1	-8.8
0.273	8.2	-9.0	8.2	-8.8	8.0	-8.5	7.9	-8.6	8.1	-9.4
0.268	9.4	-9.4	9.4	-9.4	9.3	-9.2	9.0	-9.2	9.2	-10.2
0.263	11.0	-9.9	11.0	-9.9	10.9	-9.9	10.7	-10.0	10.4	-10.6
0.258	13.2	-10.5	12.7	-10.3	12.5	-10.2	12.4	-10.4	12.4	-11.1
0.253	15.4	-9.9	15.3	-10.5	15.1	-10.5	14.8	-10.6	14.6	-11.4
0.248	18.9	-9.9	18.6	-10.1	18.3	-10.1	17.8	-10.3	17.8	-11.2
0.243	21.9	-8.4	21.9	-8.6	21.5	-8.7	20.6	-9.2	20.8	-10.4
0.238	25.3	-5.01	25.3	-5.4	24.9	-5.7	24.5	-6.1	24.8	-7.4
0.233	27.8	+0.63	27.7	+0.6	27.7	+0.04	27.7	-1.5	28.2	-1.35
0.228	27.5	+7.7	28.1	+6.6	28.1	+ 6.4	28.1	+5.5	28.8	+4.65
0.223	25.3	+12.8	25.8	+12.8	25.5	+12.8	25.9	+11.8	26.8	+11.2
0.218	20.7	+16.8	21.1	+16.8	21.0	+16.8	21.9	+16.5	22.5	+16.3
0.213	15.9	+18.2	16.4	+18.2	16.7	+18.4	17.3	+17.8	17.8	+18.4
0.207	12.05	+18.1	12.4	+18.0	12.4	+18.0	12.9	+18.3	13.3	+18.7
0.203	8.8	+17.1	9.5	+17.3	9.6	+17.3	9.9	+17.6	9.8	+17.7
0.197	6.8	+16.0	6.9	+15.9	7.2	+16.1	7.3	+16.1	7.6	+16.6
0.192	5.3	+15.0	5.4	+14.8	5.6	+14.8	5.6	+15.1	5.9	+15.4
0.187	4.2	+13.9	4.1	+13.4	4.3	+13.7	4.3	+13.7	4.4	+13.9
0.182	3.3	+12.5	3.2	+12.3	3.4	+12.5	3.3	+12.7	3.5	+12.9
0.177	2.6	+11.6	2.6	+11.3	2.7	+11.5	2.7	+11.5	2.8	+11.7
0.172	2.1	+10.7	2.1	+10.4	2.2	+10.6	2.2	+10.7	2.2	+10.9
0.167	1.8	+9.9	1.8	+9.8	1.9	+9.9	1.8	+9.9	1.9	+10.0
0.162	1.5	+9.0	1.5	+9.2	1.6	+9.1	1.5	+9.2	1.5	+9.3
0.152	1.2	+7.8	1.0	+8.0	1.1	+7.9	1.0	+7.8	1.0	+8.0
0.142	0.8	+7.0	0.7	+6.8	0.8	+6.9	0.7	+6.9	0.8	+6.9
0.132	0.5	+6.0	0.5	+5.8	0.6	+6.1	0.5	+6.1	0.6	+6.1
0.122	0.5	+5.4	0.4	+5.2	0.5	+5.4	0.4	+5.3	0.5	+5.2

3/16" diameter.

S	0		¼"		½"		¾"		1"	
$\frac{\ell}{\lambda}$	G	B	G	B	G	B	G	B	G	B
0.283	6.8	-7.0	6.8	-7.1	6.7	-7.2	6.7	-7.5	6.6	-7.5
0.278	7.7	-7.6	7.8	-7.8	7.7	-7.9	7.3	-8.0	7.1	-7.9
0.273	8.7	-8.2	8.6	-8.4	8.4	-8.5	8.4	-8.8	8.1	-8.8
0.268	10.1	-8.9	9.7	-8.9	9.6	-9.1	9.1	-9.2	9.1	-9.2
0.263	11.5	-9.5	11.2	-9.7	10.8	-9.7	10.3	-9.7	10.2	-9.7
0.258	13.0	-9.7	12.9	-10.0	12.8	-10.0	12.5	-10.3	11.6	-10.2
0.253	15.7	-9.6	14.9	-10.0	14.8	-10.3	14.2	-10.6	14.1	-10.7
0.248	17.8	-9.4	17.8	-9.9	17.5	-10.2	17.0	-10.6	16.5	-10.7
0.243	20.7	-8.0	21.1	-8.6	20.4	-9.2	19.6	-10.3	19.8	-10.1
0.238	24.5	-5.8	24.3	-6.2	23.2	-7.5	23.4	-8.1	23.4	-8.1
0.233	26.9	-1.9	26.6	-3.3	25.1	-3.6	25.9	-4.7	25.7	-5.8
0.228	28.2	+3.2	28.3	+2.9	28.2	+0.8	28.5	-0.8	28.2	-1.2
0.223	27.0	+9.5	28.0	+8.9	27.7	+8.6	28.6	+6.6	28.6	+5.4
0.218	24.3	+15.0	25.2	+14.3	24.7	+14.4	26.4	+11.9	27.3	+11.9
0.213	19.7	+17.7	20.6	+17.5	21.4	+17.2	22.3	+16.8	22.6	+16.3
0.207	15.5	+17.8	16.5	+18.5	16.6	+18.6	17.9	+18.7	18.1	+18.7
0.203	12.4	+18.4	13.1	+19.1	13.5	+19.0	14.8	+19.4	14.7	+19.2
0.197	9.4	+17.6	9.9	+18.2	10.4	+18.4	10.8	+18.6	11.5	+18.7
0.192	7.3	+16.8	7.5	+16.8	7.9	+17.1	8.4	+17.6	8.4	+17.9
0.187	5.7	+15.7	5.9	+15.7	6.1	+16.2	6.4	+16.4	6.6	+16.7
0.182	4.6	+14.9	4.7	+15.1	4.8	+15.0	5.1	+15.3	5.0	+15.2
0.177	3.9	+13.7	3.7	+13.8	3.9	+13.8	3.8	+14.0	3.9	+14.0
0.172	2.8	+12.4	2.9	+12.7	2.8	+12.4	2.9	+12.5	3.1	+12.8
0.167	2.3	+11.8	2.3	+11.6	2.4	+11.5	2.5	+11.8	2.5	+11.7
0.162	1.9	+10.8	1.9	+10.7	1.9	+10.8	2.0	+10.9	1.9	+10.6
0.152	1.5	+ 9.5	1.3	+9.4	1.2	+9.2	1.4	+9.3	1.4	+9.3
0.142	0.9	+8.2	0.9	+8.1	0.9	+8.1	1.0	+8.1	1.0	+8.1
0.132	0.7	+7.1	0.7	+7.0	0.7	+7.2	0.7	+7.1	0.7	+7.1
0.122	0.5	+6.5	0.5	+6.4	0.5	+6.3	0.5	+6.3	0.5	+6.2

$\frac{1}{4}$" diameter.

S	0		$\frac{1}{4}$"		$\frac{1}{2}$"		$\frac{3}{4}$"		1"	
$\frac{\ell}{\lambda}$	G	B	G	B	G	B	G	B	G	B
0.283	7.4	-6.9	7.4	-7.1	7.1	-7.0	7.1	-7.2	6.9	-7.4
0.273	9.2	-7.8	8.6	-7.7	8.7	-8.3	8.7	-8.6	8.4	-8.4
0.263	12.0	-8.9	11.8	-9.0	11.5	-9.4	11.3	-9.6	11.0	-9.8
0.253	15.8	-9.2	15.1	-9.4	14.7	-10.2	14.4	-10.3	13.9	-10.5
0.243	21.1	-8.3	20.5	-9.0	19.8	-9.7	19.5	-10.2	18.6	-10.5
0.233	26.0	-2.5	25.8	-4.0	25.8	-5.3	25.8	-6.4	25.3	-7.3
0.228	28.0	+2.5	28.1	+1.0	28.4	-1.1	27.9	-2.8	27.6	-3.9
0.223	28.3	+7.4	28.7	+7.3	29.0	+4.5	29.4	+3.2	29.5	+1.7
0.213	22.4	+16.9	23.2	+16.3	25.1	+15.7	26.3	+14.7	29.2	+15.1
0.203	14.7	+19.3	15.9	+19.6	16.8	+19.6	17.4	+19.8	18.5	+19.7
0.192	8.8	+18.2	9.0	+18.0	9.9	+18.5	10.4	+18.7	11.1	+19.1
0.182	5.4	+15.8	5.7	+16.1	5.9	+16.3	6.3	+16.5	6.5	+16.9
0.172	3.5	+13.9	3.8	+14.4	3.8	+14.4	3.9	+14.5	4.1	+14.5
0.162	2.3	+12.1	2.4	+12.3	2.6	+12.4	2.5	+12.5	2.5	+12.4
0.152	1.6	+10.6	1.7	+10.6	1.7	+10.7	1.7	+10.6	1.7	+10.8
0.142	1.1	+9.5	1.1	+9.4	1.2	+9.5	1.2	+9.4	1.2	+9.4
0.132	0.8	+8.3	1.7	+8.2	1.7	+8.1	1.7	+8.1	1.7	+8.0
0.122	0.5	+7.5	0.6	+7.4	0.6	+7.2	0.6	+7.2	0.6	+7.1

5/16" diameter.

s	0		¼"		½"		¾"		1"	
$\frac{\ell}{\lambda}$	G	B	G	B	G	B	G	B	G	B
0.283	7.8	-6.2	7.6	-6.5	7.5	-6.9	7.2	-6.8	7.0	-7.2
0.273	9.6	-7.2	9.3	-7.6	9.0	-7.9	8.9	-8.0	8.4	-8.1
0.263	11.9	-8.1	11.7	-8.6	11.4	-8.6	11.1	-9.1	10.6	-9.0
0.253	15.5	-8.7	15.0	-8.9	14.6	-9.6	13.9	-9.9	13.4	-10.2
0.243	20.0	-7.3	19.4	-8.0	18.7	-9.1	18.1	-9.5	17.5	-9.1
0.233	25.5	-3.4	25.2	-4.4	25.1	-5.6	24.2	-7.5	23.6	-8.3
0.228	27.4	+1.3	27.6	-0.06	27.8	-1.9	27.3	-3.8	26.4	-5.2
0.223	28.0	+6.3	28.8	+4.7	29.0	+2.6	28.8	+1.2	29.2	-0.8
0.218									30.3	+4.7
0.213	24.9	+16.2	25.4	+15.0	27.0	+13.8	28.1	+11.9	29.6	+10.9
0.203	17.0	+20.2	17.9	+19.7	18.8	+19.6	20.8	+19.3	21.9	+18.7
0.192	10.6	+19.0	11.1	+19.3	12.0	+19.6	13.0	+19.7	13.5	+20.0
0.182	6.5	+18.1	6.7	+17.2	7.0	+18.1	7.5	+17.7	8.4	+18.1
0.172	4.3	+15.5	4.5	+15.0	4.6	+15.6	4.8	+15.7	5.0	+15.9
0.162	2.8	+13.4	2.9	+13.4	3.0	+13.4	3.1	+13.4	3.2	+13.5
0.152	2.0	+11.9	2.0	+11.6	2.0	+11.5	2.1	+11.6	2.2	+11.6
0.142	1.5	+10.5	1.4	+10.2	1.4	+10.2	1.5	+10.2	1.5	+10.2
0.132	1.0	+9.3	1.0	+9.1	1.0	+9.0	1.0	+8.9	1.0	+8.8
0.122	0.7	+8.3	0.7	+8.0	0.7	+8.0	0.7	+7.8	0.7	+7.8

3/8" diameter.

s	0		¼"		½"		¾"		1"	
$\frac{\ell}{\lambda}$	G	B	G	B	G	B	G	B	G	B
0.283	8.2	-5.5	8.1	-6.6	7.8	-6.8	7.8	-7.1	7.3	-7.0
0.273	10.1	-6.6	9.8	-7.5	9.5	-7.7	9.4	-8.0	8.8	-8.1
0.263	12.3	-7.4	12.1	-8.4	11.8	-8.7	11.4	-9.0	10.6	-9.0
0.253	16.0	-7.6	15.3	-8.8	15.0	-9.1	14.5	-9.7	13.1	-9.7
0.243	20.5	-6.9	19.6	-7.9	19.3	-9.1	18.3	-9.8	17.1	-10.1
0.233	25.3	-2.9	25.0	-4.8	24.8	-5.9	24.2	-7.6	22.2	-8.5
0.228	28.1	+0.7	27.7	-1.3	27.5	-3.0	27.2	-4.5	25.6	-6.2
0.223	28.3	+5.2	29.1	+2.7	29.0	+1.4	29.3	-0.4	28.8	-2.9
0.218							29.9	+4.6	31.0	+2.2
0.213	26.0	+15.2	26.8	+14.0	28.2	+12.1	29.9	+10.2	31.9	+9.0
0.203	18.9	+20.4	20.6	+20.0	21.7	+19.4	23.2	+18.8	26.4	+19.0
0.192	12.0	+20.6	13.3	+20.6	13.8	+20.5	14.8	+20.7	17.2	+22.4
0.182	7.6	+18.5	8.1	+18.6	8.6	+18.9	8.8	+18.9	10.2	+20.5
0.172	5.0	+16.8	5.2	+16.7	5.3	+16.7	5.8	+17.3	6.3	+18.3
0.162	3.2	+15.1	3.5	+14.9	3.6	+14.7	3.8	+15.0	4.2	+15.8
0.152	2.2	+13.2	2.3	+12.9	2.4	+12.9	2.4	+13.0	2.7	+13.7
0.142	1.5	+11.8	1.6	+11.5	1.6	+11.2	1.7	+11.2	1.9	+11.8
0.132	1.1	+10.4	1.1	+10.0	1.1	+9.8	1.2	+9.8	1.2	+10.1
0.122	0.8	+9.4	0.8	+9.0	0.8	+8.8	0.6	+8.7	1.0	+8. 8

$\frac{1}{2}$" diameter.

S	0		$\frac{1}{4}$"		$\frac{1}{2}$"		$\frac{3}{4}$"		1"	
$\frac{\ell}{\lambda}$	G	B	G	B	G	B	G	B	G	B
0.283	8.8	-3.3	8.8	-5.2	8.6	-6.1	8.2	-6.2	7.4	-6.4
0.273	10.4	-3.8	10.4	-6.2	10.0	-7.0	9.7	-7.1	9.1	-7.4
0.263	12.6	-4.8	12.6	-6.8	12.3	-7.9	11.6	-7.9	11.2	-8.4
0.253	15.5	-4.7	15.6	-7.2	15.0	-8.4	14.4	-8.7	13.3	-9.3
0.243	19.3	-4.0	19.2	-6.8	18.7	-8.3	17.6	-8.9	16.5	-9.8
0.233	24.0	-1.4	24.3	-4.0	23.4	-6.2	22.5	-7.6	22.0	-9.5
0.228	26.1	+1.1	26.8	-1.1					25.0	-7.8
0.223	29.7	+5.6	28.4	+2.0	28.3	-0.4	27.9	-3.1	28.0	-5.0
0.218					29.9	+3.9	30.1	+1.0	30.0	-1.6
0.213	27.2	+14.2	28.4	+11.5	29.8	+8.9	30.9	+5.6	31.1	+3.0
0.203	22.2	+20.9	23.3	+18.8	25.1	+17.4	28.1	+16.5	29.3	+14.4
0.192	15.1	+23.2	16.4	+21.8	18.3	+21.4	20.7	+22.8	22.4	+20.7
0.182	9.9	+22.6	10.3	+20.5	11.7	+21.1	13.9	+22.8	14.0	+21.8
0.172	6.6	+20.5	6.9	+19.0	7.6	+19.1	8.7	+20.7	9.0	+19.7
0.162	4.7	+18.5	4.7	+17.1	5.2	+17.2	5.9	+18.5	5.6	+17.4
0.152	3.1	+16.7	3.2	+15.2	3.4	+14.8	3.7	+16.1	3.7	+15.3
0.142	2.2	+15.2	2.1	+12.7	2.2	+13.2	2.5	+14.0	2.6	+13.4
0.132	1.5	+14.1	1.5	+12.1	1.5	+11.7	1.9	+12.3	1.8	+11.7
0.122	1.1	+12.5	1.0	+10.8	1.1	+10.5	1.2	+10.8	1.3	+10.2

UNIPOLE INPUT CONDUCTANCE / $\frac{\ell}{\lambda}$ RATIO FOR A RANGE OF $\frac{r}{\lambda}$ RATIOS. INPUT CONE LENGTH = 0λ.

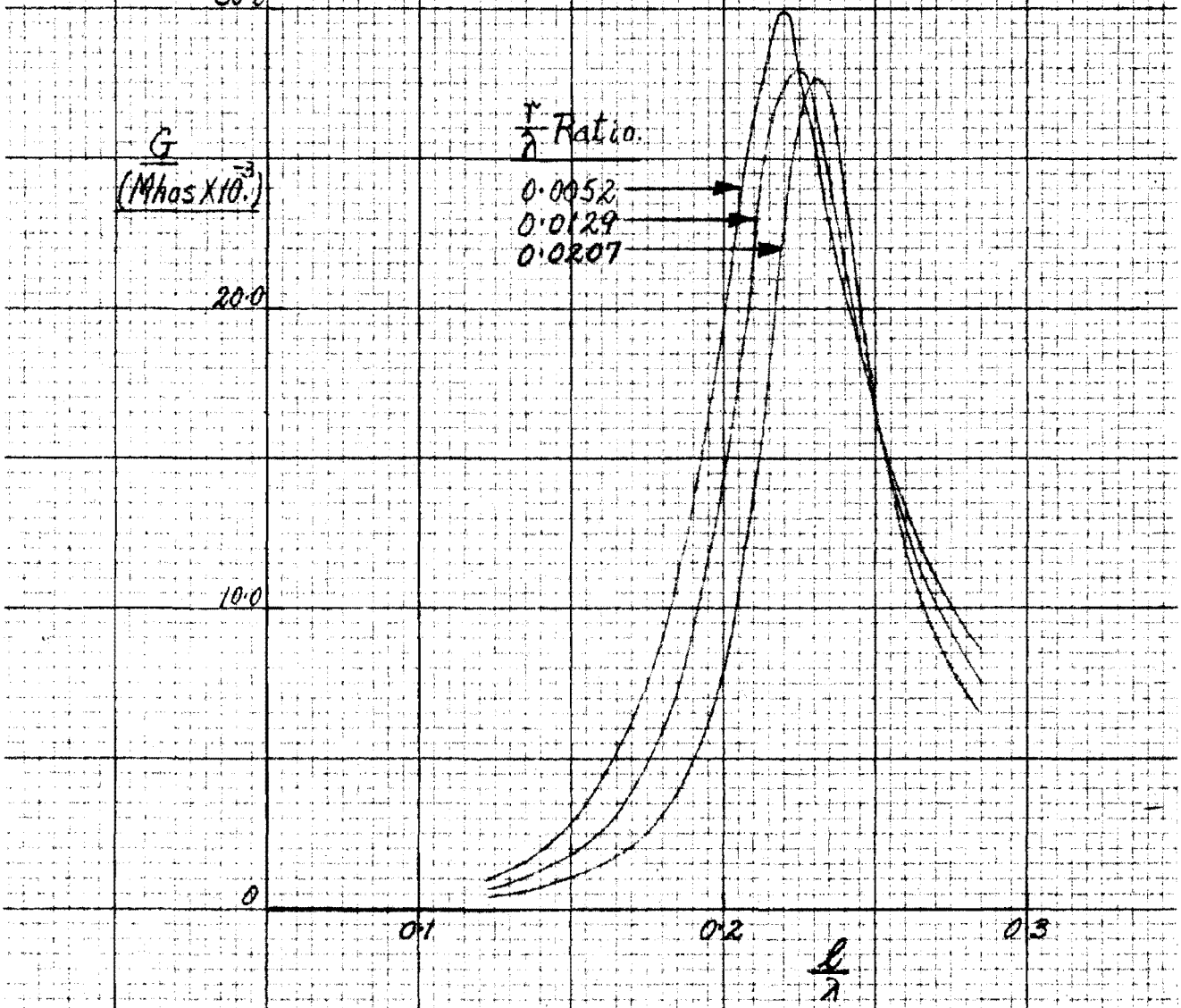

UNIPOLE INPUT SUSCEPTANCE / $\frac{\ell}{\lambda}$ RATIO FOR A RANGE OF r/λ RATIOS. INPUT CONE LENGTH $s = 0\lambda$.

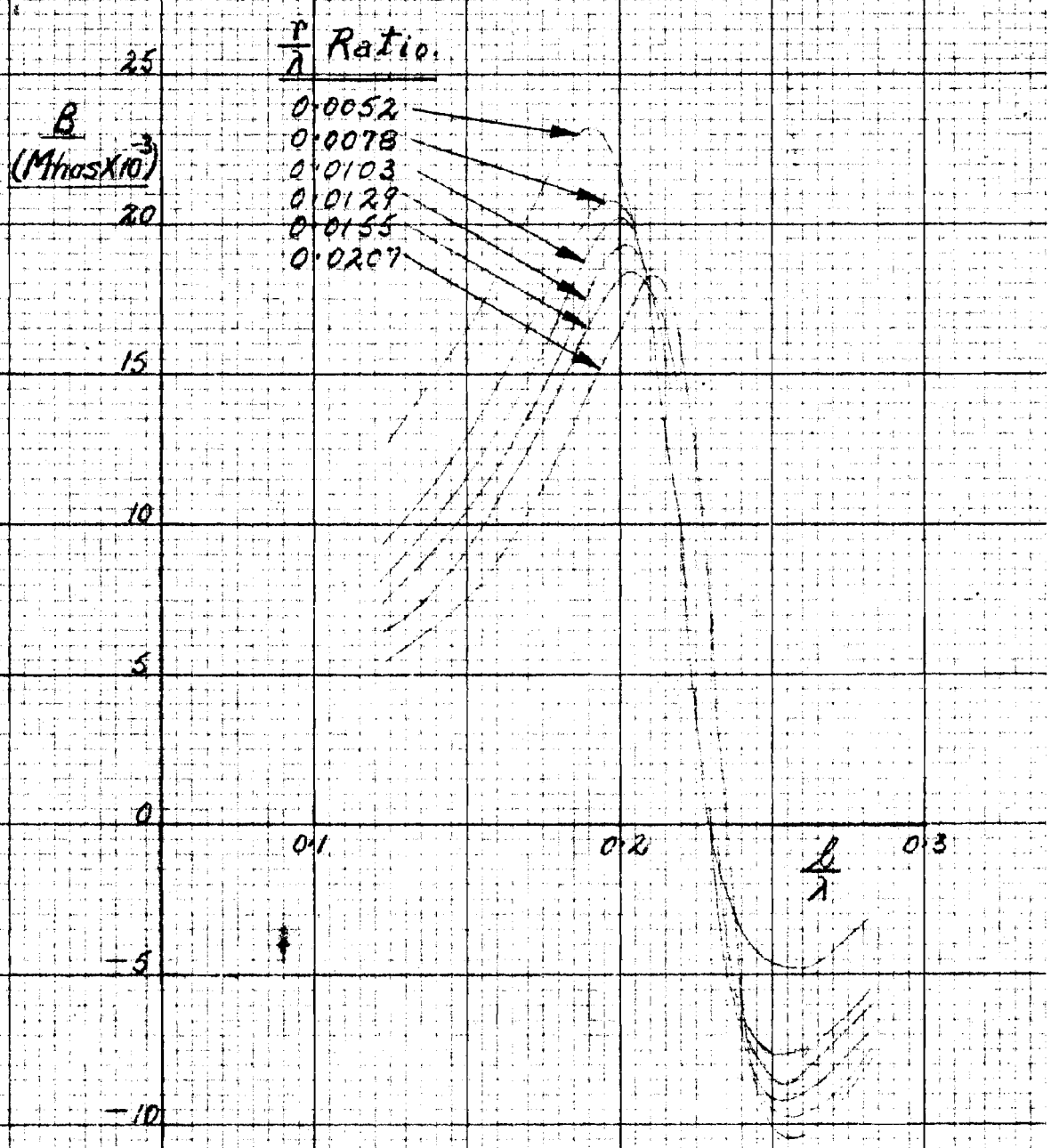

UNIPOLE INPUT CONDUCTANCE / $\frac{\ell}{\lambda}$ RATIO FOR A RANGE OF r/λ RATIOS. INPUT CONE LENGTH $S = 0{\cdot}0103\lambda$.

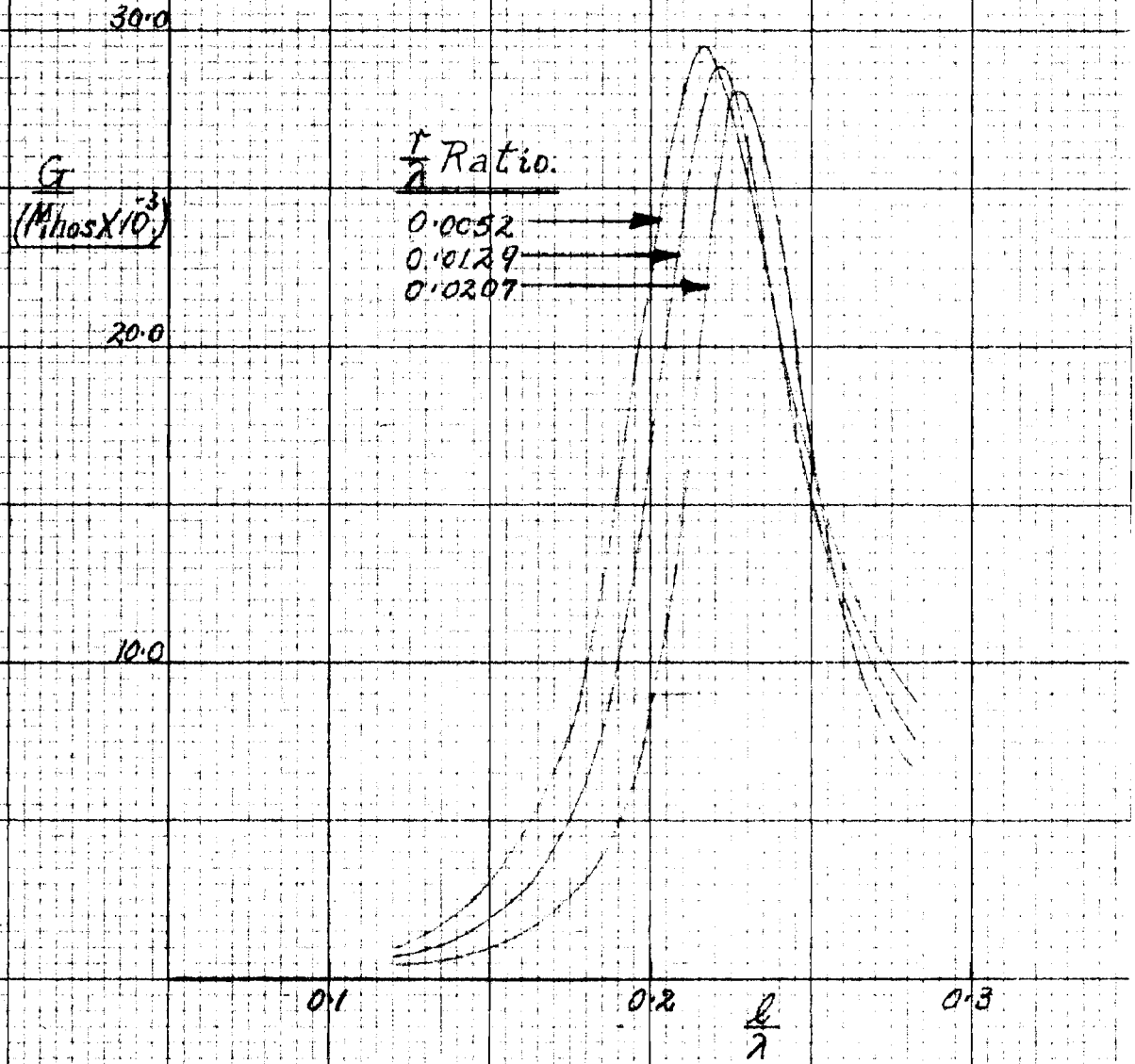

UNIPOLE INPUT SUSCEPTANCE/$\frac{\ell}{\lambda}$ RATIO FOR A RANGE OF r/λ RATIOS. INPUT CONE LENGTH $s = 0.0103\lambda$.

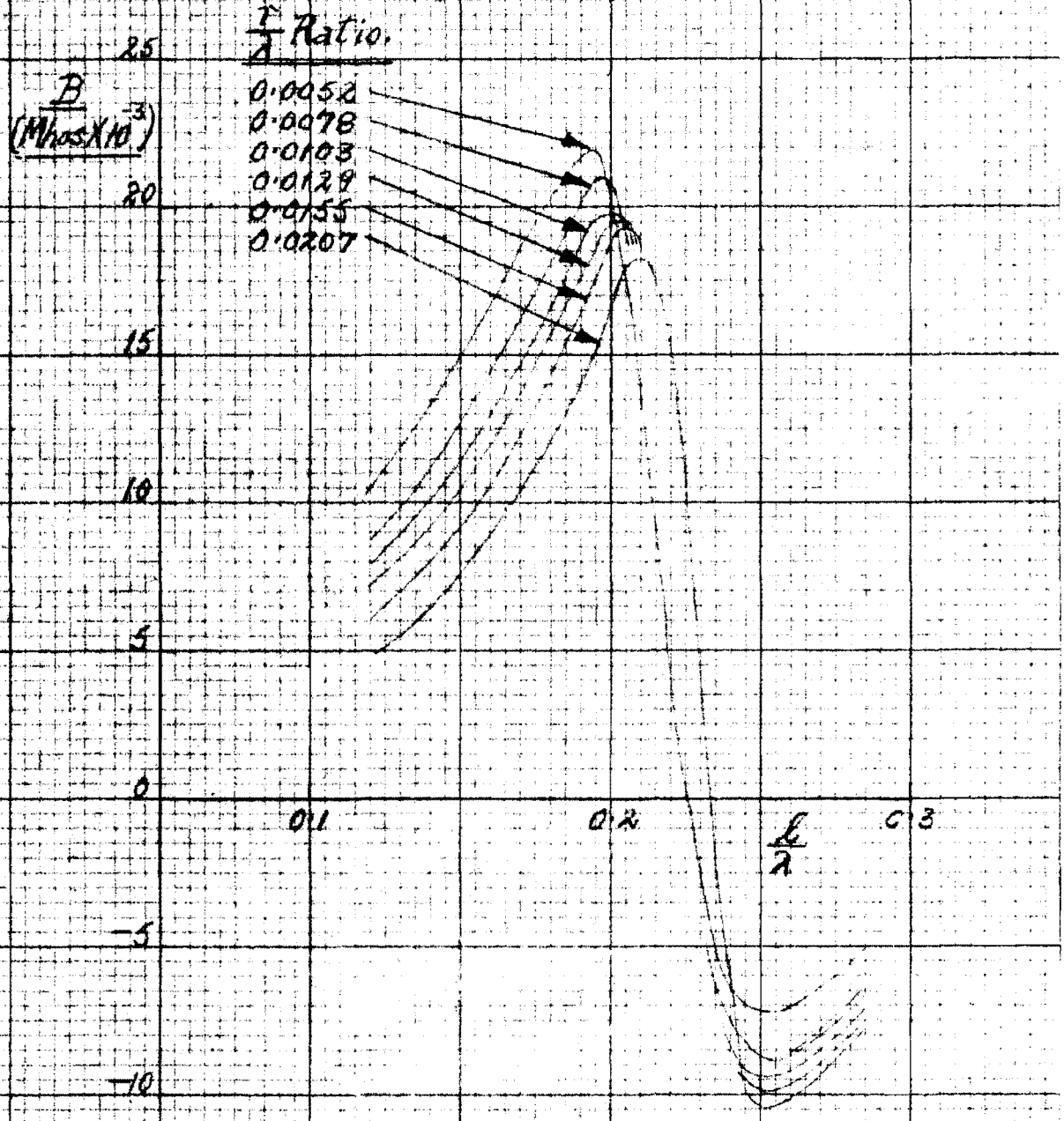

UNIPOLE INPUT CONDUCTANCE / $\frac{l}{\lambda}$ RATIO FOR A RANGE OF $\frac{r}{\lambda}$ RATIOS. INPUT CONE LENGTH $S = 0.2207\,\lambda$.

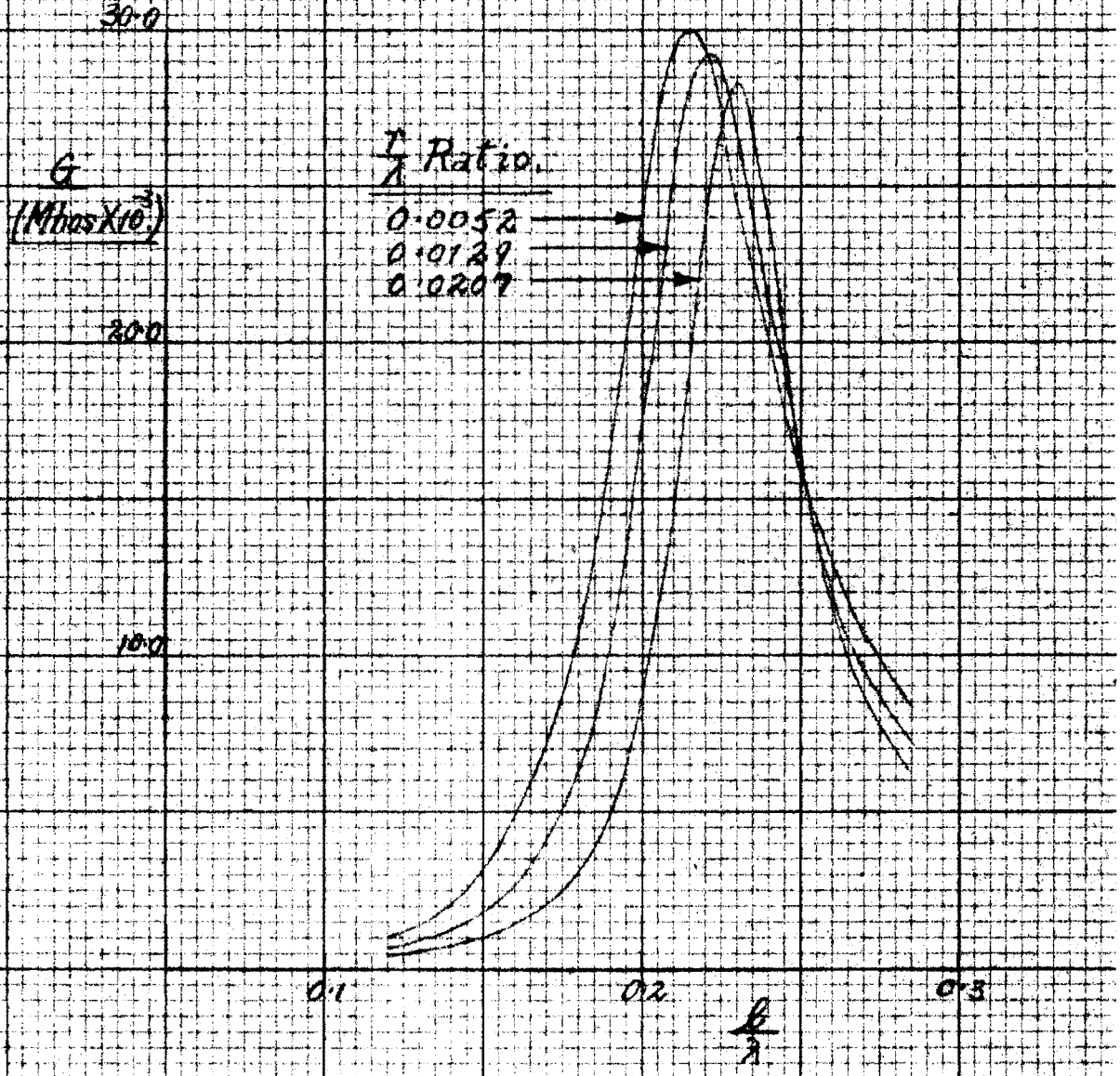

UNIPOLE INPUT SUSCEPTANCE / $\frac{\ell}{\lambda}$ RATIO FOR A RANGE OF $\frac{r}{\lambda}$ RATIOS. INPUT CONE LENGTH $s = 0.0207\lambda$.

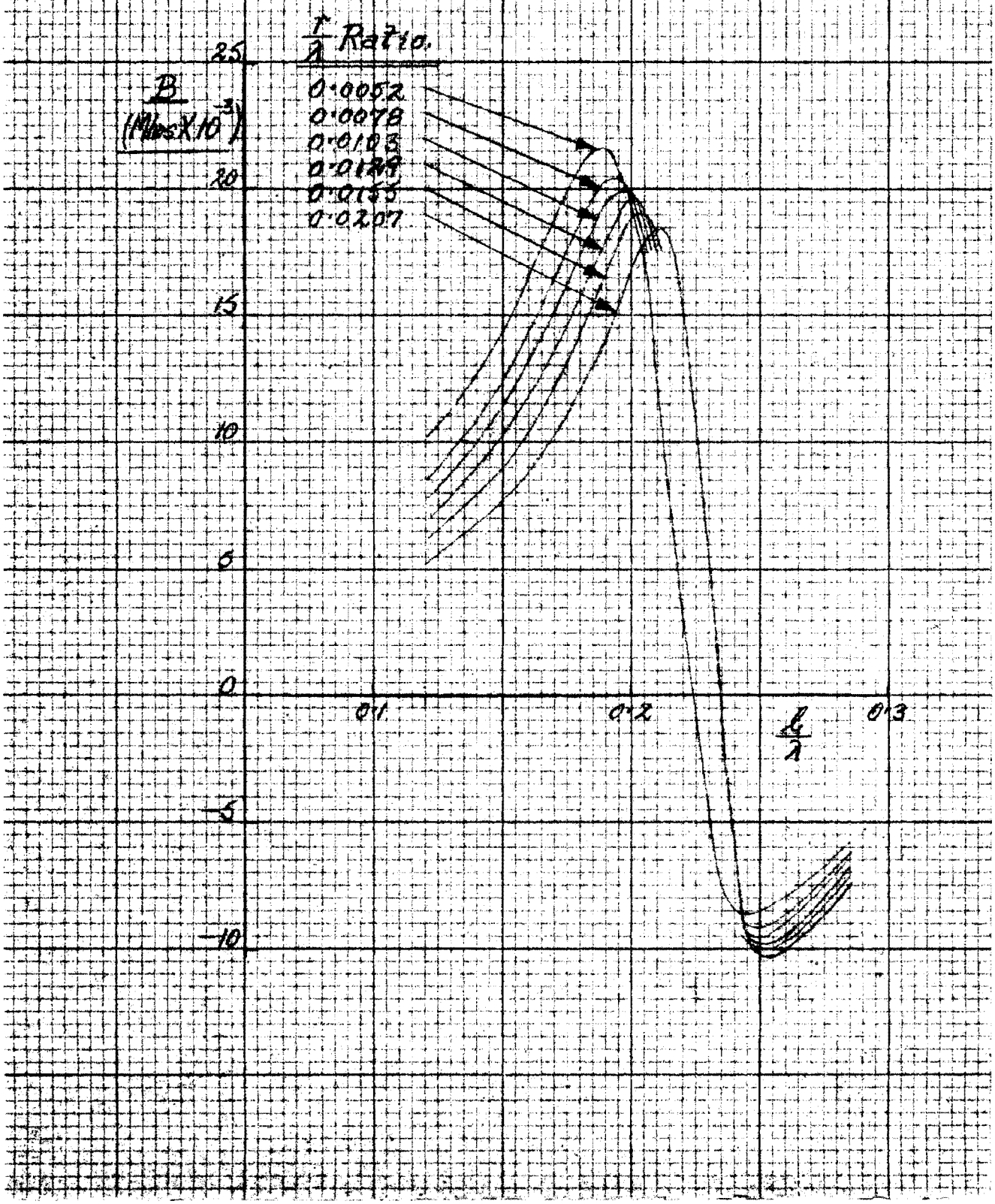

UNIPOLE INPUT CONDUCTANCE / $\frac{\ell}{\lambda}$ RATIO FOR A RANGE OF $\frac{r}{\lambda}$ RATIOS. INPUT CONE LENGTH $s = 0.0310\lambda$.

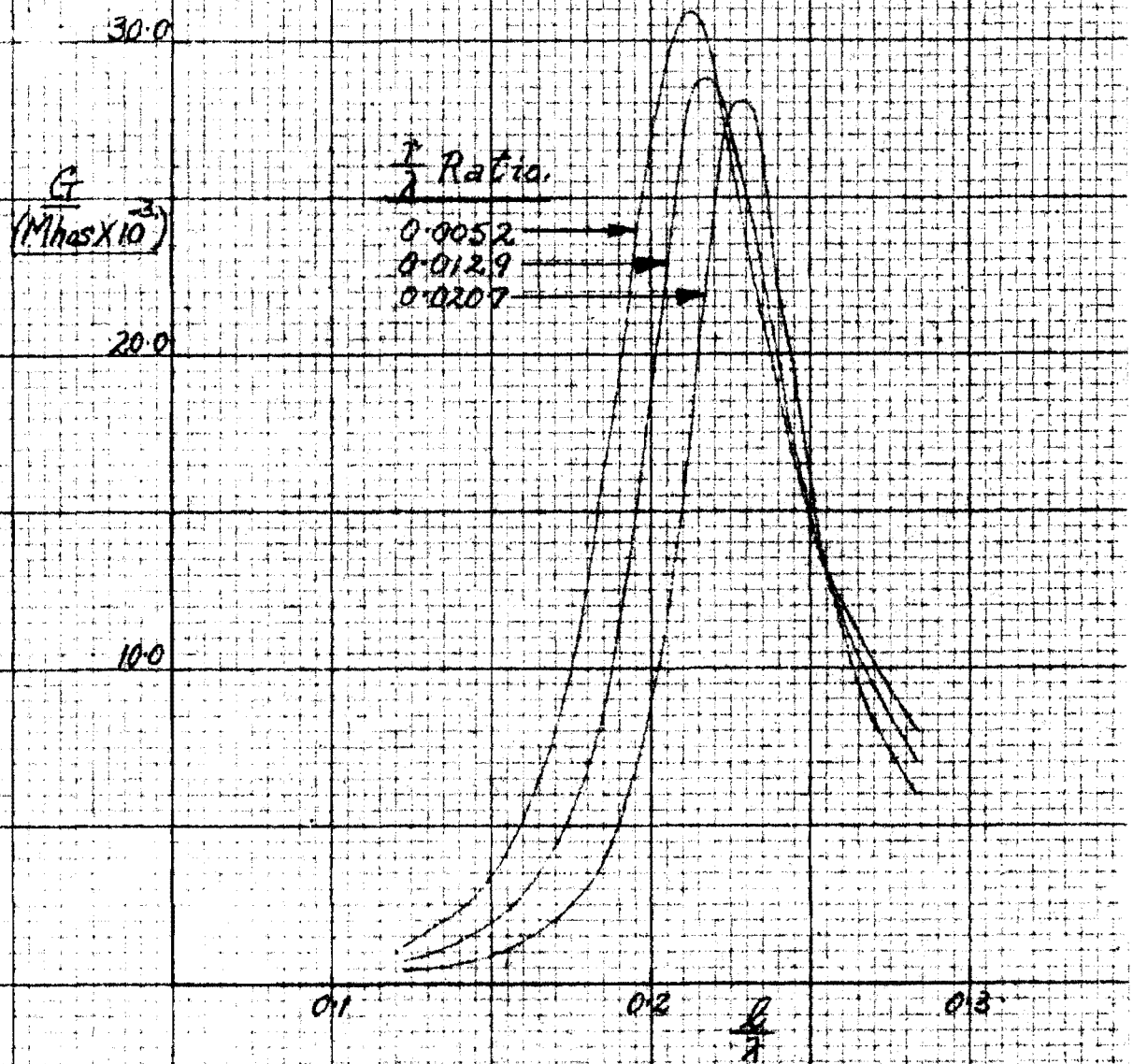

UNIPOLE INPUT SUSCEPTANCE/$\frac{b}{\lambda}$ RATIO FOR A RANGE OF r/λ RATIOS. INPUT CONE LENGTH $s = 0.03125\lambda$.

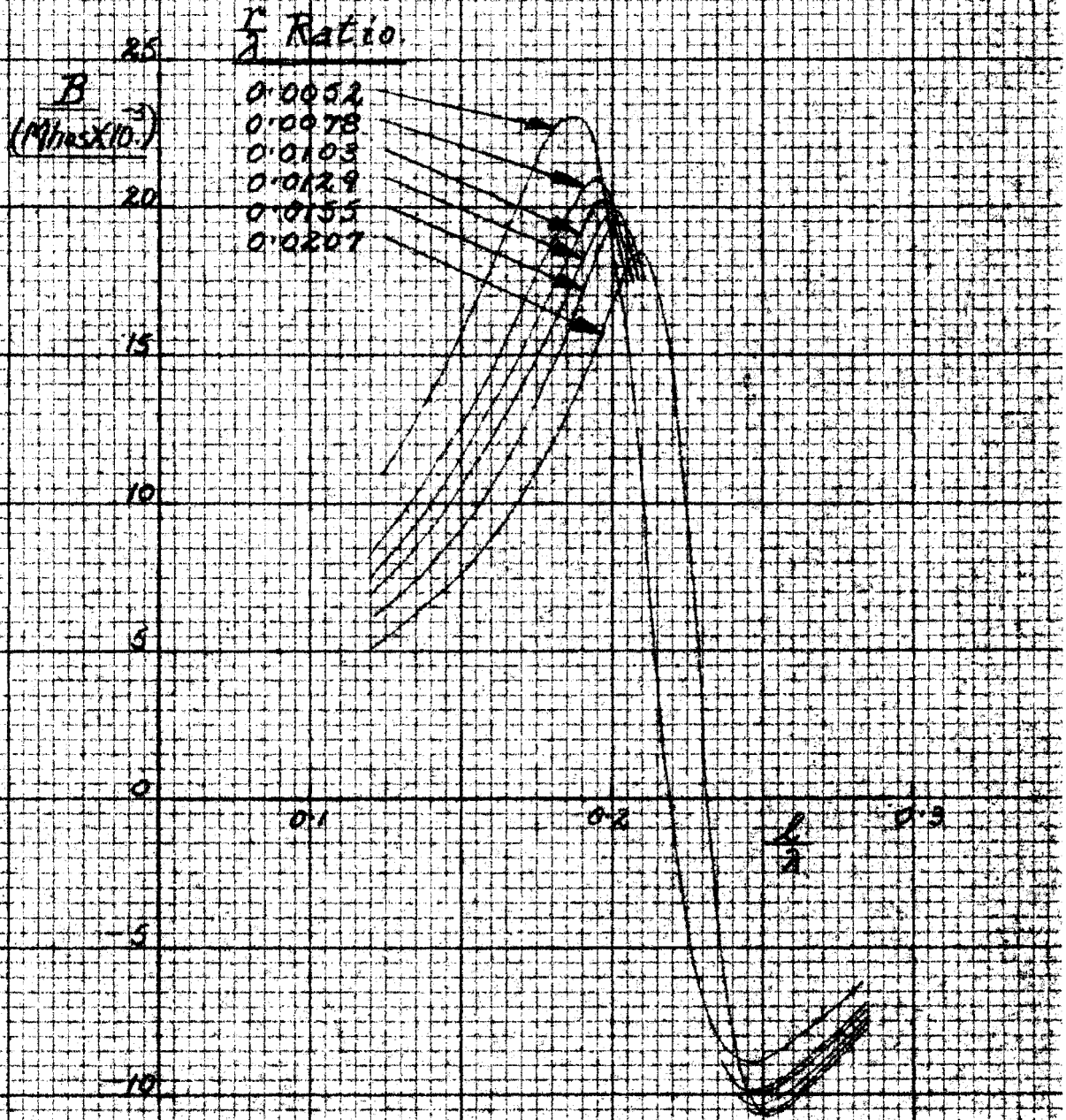

UNIPOLE INPUT CONDUCTANCE / $\frac{\ell}{\lambda}$ RATIO FOR A RANGE OF $\frac{r}{\lambda}$ RATIOS. INPUT CONE LENGTH $s = 0.0414\lambda$.

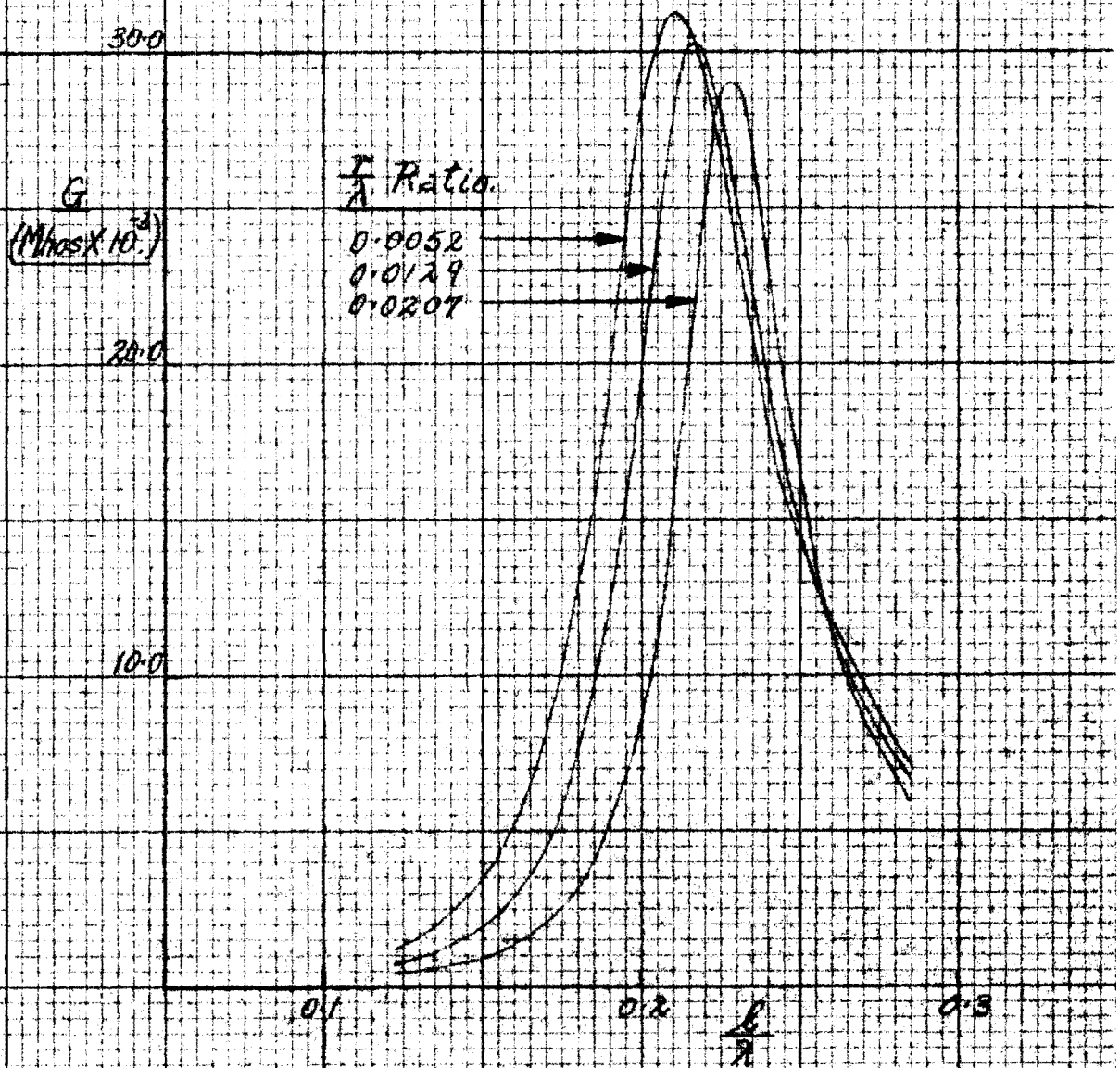

UNIPOLE INPUT SUSCEPTANCE/$\frac{\ell}{\lambda}$ RATIO FOR A RANGE OF r/λ RATIOS. INPUT CONE LENGTH $s = 0.0414\lambda$.

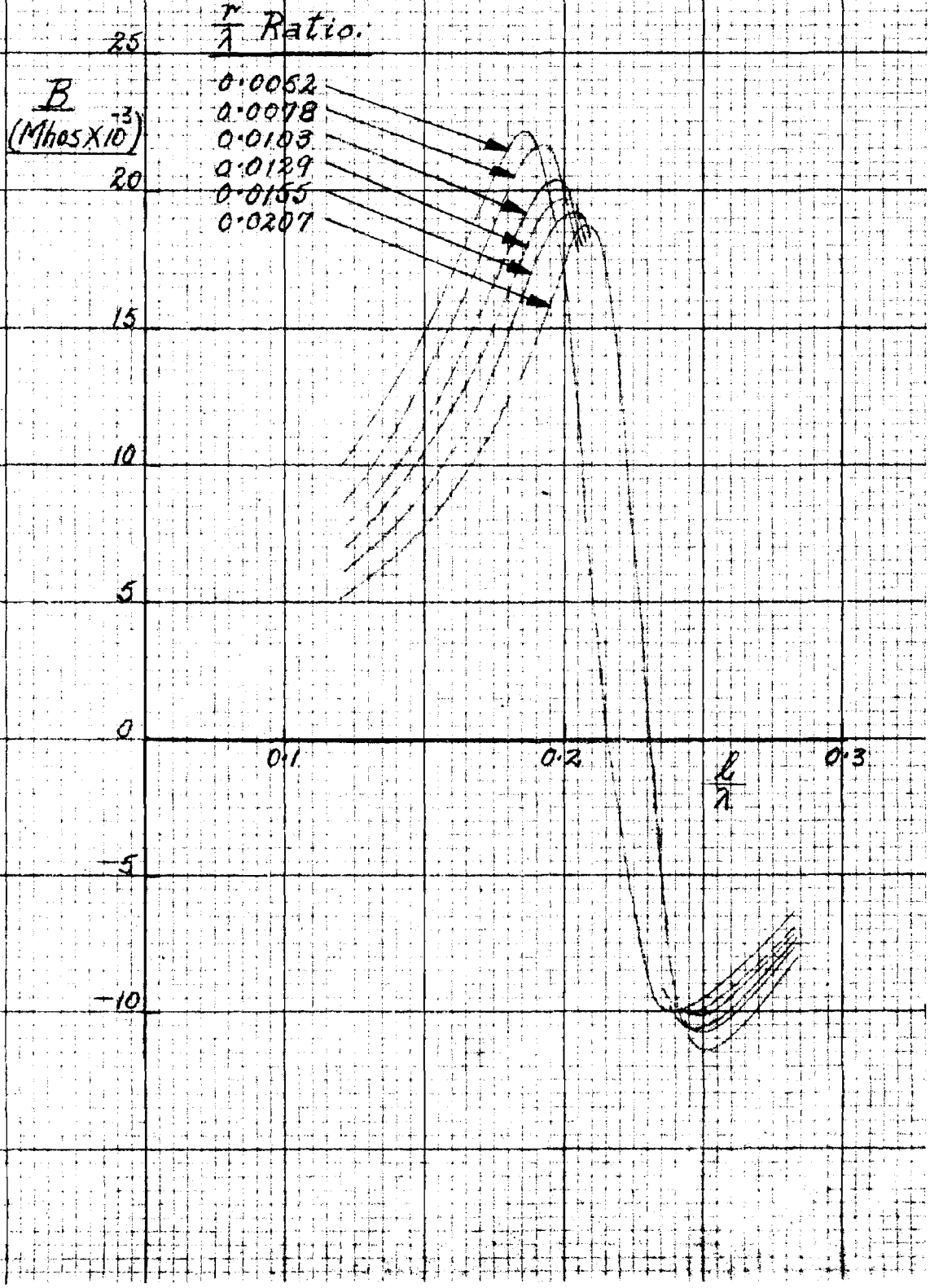

The following table of first resonant length and resistance as a function of r/l ratio has been deduced from the above experimental results. The first resonance results will be discussed in a later section.

Unipole First Resonance Results

	$\frac{r}{\lambda}$	0.00616	0.00775	0.0103	0.0129	0.0155	0.0207
S=0	$\frac{\ell}{\lambda}$	0.2336	0.2312	0.2305	0.2294	0.2290	0.2302
	$\frac{r}{\ell}$	0.0221	0.0335	0.0447	0.0562	0.0677	0.0900
	%Foreshort.	6.6	7.5	7.8	8.2	8.4	7.9
	$G_{res.}$	27.53	27.39	27.0	26.87	27.56	25.18
	$R_{res.}$(Dipole)	72.5	72.9	74.0	74.5	72.7	79.4
S=$\frac{1}{4}$"	$\frac{\ell}{\lambda}$	0.2335	0.2303	0.2290	0.2280	0.2264	0.2262
	$\frac{r}{\ell}$	0.0221	0.0337	0.0450	0.0566	0.0685	0.0915
	%Foreshort.	6.6	7.9	8.4	8.8	9.9	9.5
	$G_{res.}$	27.46	27.50	27.62	27.60	28.15	27.37
	$R_{res.}$(Dipole)	72.8	72.7	72.4	72.4	71.0	73.2
S=$\frac{1}{2}$"	$\frac{\ell}{\lambda}$	0.2330	0.2289	0.2270	0.2259	0.2246	0.2225
	$\frac{r}{\ell}$	0.0222	0.0339	0.0454	0.0571	0.0690	0.0930
	%Foreshort.	6.8	8.4	9.2	9.6	10.2	11.0
	$G_{res.}$	27.70	27.64	28.52	28.31	28.52	28.45
	$R_{res.}$(Dipole)	72.2	72.4	70.2	70.5	70.1	70.3
S=$\frac{3}{4}$"	$\frac{\ell}{\lambda}$	0.2319	0.2275	0.2257	0.2242	0.2226	0.2192
	$\frac{r}{\ell}$	0.0223	0.0341	0.0456	0.0576	0.0696	0.0945
	%Foreshort.	7.2	9.0	9.7	10.3	11.0	12.3
	$G_{res.}$	27.80	28.51	28.60	28.51	29.35	29.56
	$R_{res.}$(Dipole)	72.0	70.2	69.9	70.3	68.2	67.7
S=1"	$\frac{\ell}{\lambda}$	0.2318	0.2217	0.2245	0.2223	0.2202	0.2163
	$\frac{r}{\ell}$	0.0223	0.0350	0.0459	0.0580	0.0704	0.0957
	%Foreshort.	7.3	9.2	10.2	11.1	11.9	13.5
	$G_{res.}$	28.34	28.27	28.92	29.36	30.48	30.38
	$R_{res.}$(Dipole)	70.5	70.8	69.2	68.1	65.7	65.8

The following table of maximum conductance and $\frac{\ell}{\lambda}$ ratio as a function of r/l ratio has been deduced from the experimental results. The theoretical values included in the table have been calculated by the cylindrical aerial method. The results will be discussed in a later section.

Unipole Maximum Conductance Results

	$\frac{r}{\lambda}$	0.00516	0.00775	0.0103	0.0129	0.0155	0.0207
S=0	$\frac{\ell}{\lambda}$	0.2313	0.2280	0.2245	0.2225	0.2250	0.2215
	G	27.9	28.3	28.6	28.0	28.4	30.3
S=1/4"	$\frac{\ell}{\lambda}$	0.2295	0.2264	0.2243	0.2215	0.2210	0.2170
	G	28.2	28.5	28.8	28.9	29.2	29.1
S=1/2"	$\frac{\ell}{\lambda}$	0.2295	0.2260	0.2240	0.2210	0.2200	0.2155
	G	28.4	28.3	29.1	29.2	29.2	30.2
S=3/4"	$\frac{\ell}{\lambda}$	0.2295	0.2255	0.2224	0.2200	0.2156	0.2125
	G	28.4	28.9	29.5	29.0	30.1	30.9
S=1"	$\frac{\ell}{\lambda}$	0.2285	0.2245	0.2205	0.2170	0.2115	0.2110
	G	29.8	28.65	29.6	30.3	32.0	31.2
	G(Theory)	31.0	31.8	32.5	33.2	33.9	35.4

(ii) Dipole Aerial Admittance Experiments and Results.

The aerials used in the dipole admittance experiments were made of such a length that they were resonant at 477.5 Mcps. The resonant lengths were obtained from the results of the unipole admittance experiments. The measurements were made with the admittance meter by the method already described for dipole aerials of diameter 1/8", 3/16", 1/4", 5/16", 3/8" and 1/2" and conical input section slope length $S = 0, \frac{1}{4}", \frac{1}{2}", \frac{3}{4}"$ and 1". The gap length was 0.007 λ at 477.5 Mcps. The lengths of the dipole aerials were held constant throughout the measurements and the frequency altered from 450-500 Mcps. in eight steps. The admittances measured by the admittance

meter were subjected to the corrections given in subsection (f) of this section. The results of these calculations are shown below in tabular form and a typical result has been plotted. The results will be discussed later.

The above admittance measurements were then repeated for the dipole aerials with the compensating short circuit stub placed across the dipole aerials. The results of these measurements are shown below in tabulat form. These results will also be discussed later. All susceptance and conductance measurements are given in millimhos and resistances in ohms.

Dipole Aerial Admittance Results

The measurements were made at the following frequencies in Mcps.: 500.2, 494, 485.1, 478.6, 473, 465.2, 456.7, 449.9.

			d = 1/8"		s = 0			
ℓ/λ	0.246	0.242	0.237	0.234	0.231	0.228	0.224	0.220
G	8.6	9.3	10.7	11.9	12.6	13.4	13.2	12.9
B	-3.0	-3.1	-1.8	-1.4	-0.3	+1.9	+4.1	+7.6
					s = ¼"			
ℓ/λ	0.244	0.241	0.236	0.233	0.230	0.227	0.222	0.219
G	10.9	12.1	13.1	13.3	13.4	13.2	12.5	12.0
B	-3.5	-5.5	-1.5	-0.7	+1.6	+3.9	+6.3	+6.8
					s = ½"			
ℓ/λ	0.244	0.241	0.236	0.233	0.230	0.227	0.222	0.219
G	8.8	9.7	11.1	12.3	13.1	13.5	13.2	12.1
B	-3.1	-3.0	-1.9	-1.3	-0.3	+2.1	+4.8	+7.9
					s = ¾"			
ℓ/λ	0.244	0.240	0.235	0.232	0.229	0.226	0.221	0.218
G	8.8	9.9	11.2	12.5	13.4	13.6	13.3	11.9
B	-3.2	-3.0	-1.6	-1.2	-0.2	+2.0	+5.5	+8.0
					s = 1"			
ℓ/λ	0.244	0.240	0.235	0.232	0.229	0.226	0.221	0.218
G	8.6	9.8	11.2	12.4	13.3	14.6	13.9	12.0
B	-3.2	-3.1	-2.1	-1.5	-0.5	+2.3	+4.0	+7.7

d = 3/16"

s = 0								
ℓ/λ	0.242	0.238	0.233	0.231	0.228	0.224	0.220	0.217
G	10.2	10.4	11.5	12.2	13.8	13.9	13.4	11.8
B	-3.8	-3.7	-2.6	-2.2	+0.5	+2.9	+5.2	+6.2
s = 1/4"								
ℓ/λ	0.242	0.238	0.233	0.231	0.228	0.224	0.220	0.217
G	9.8	10.2	11.1	12.9	14.3	14.1	13.9	12.2
B	-3.9	-4.4	-2.8	-2.6	+0.9	+2.4	+5.1	+5.6
s = 1/2"								
ℓ/λ	0.240	0.237	0.232	0.229	0.226	0.223	0.219	0.215
G	10.0	10.3	11.2	13.3	14.1	14.1	13.8	13.8
B	-4.3	-4.0	-2.7	-2.5	+0.6	+2.4	+5.4	+8.2
s = 3/4"								
ℓ/λ	0.239	0.236	0.231	0.228	0.225	0.222	0.218	0.214
G	10.1	10.6	11.4	12.3	14.2	14.4	14.0	12.8
B	-4.3	-4.3	-2.8	-2.7	+0.6	+3.0	+5.4	+8.2
s = 1"								
ℓ/λ	0.238	0.234	0.229	0.226	0.224	0.220	0.216	0.213
G	10.1	10.7	11.6	12.7	14.2	14.2	13.8	12.9
B	-4.5	-4.3	-2.7	-2.5	+0.8	+3.0	+5.5	+8.0

d = 1/4"

s = 0								
ℓ/λ	0.242	0.238	0.233	0.231	0.228	0.224	0.220	0.217
G	9.6	10.2	10.8	11.8	13.7	13.7	14.0	13.8
B	-3.7	-3.7	-2.2	-1.7	+0.2	+2.1	+4.5	+6.9
s = 1/4"								
ℓ/λ	0.239	0.236	0.231	0.228	0.225	0.222	0.218	0.214
G	10.1	10.3	11.3	12.2	14.0	13.9	13.9	13.4
B	-3.9	-3.7	-2.3	-1.9	+0.6	+2.5	+5.1	+7.4
s = 1/2"								
ℓ/λ	0.238	0.234	0.229	0.226	0.224	0.220	0.216	0.213
G	10.2	10.4	11.6	12.2	14.4	14.3	14.0	13.9
B	-4.0	-3.8	-2.7	-2.5	+0.3	+2.3	+4.7	+7.2
s = 3/4"								
ℓ/λ	0.236	0.233	0.228	0.225	0.222	0.219	0.215	0.212
G	10.5	10.8	11.9	12.2	14.2	14.3	13.9	12.7
B	-4.3	-3.9	-2.8	-2.5	+0.6	+2.4	+5.0	+6.6
s = 1"								
ℓ/λ	0.235	0.232	0.227	0.224	0.221	0.218	0.214	0.210
G	9.8	10.7	11.8	12.7	14.5	14.8	14.3	13.1
B	-4.8	-4.2	-3.1	-2.3	-0.02	+2.1	+4.6	+6.5

d = 5/16"

s = 0								
ℓ/λ	0.240	0.237	0.232	0.229	0.226	0.223	0.219	0.215
G	10.1	10.2	11.1	11.7	13.6	14.0	13.9	13.2
B	-3.3	-2.7	-2.1	-1.8	+0.7	+2.1	+4.7	+5.9
s = ¼"								
ℓ/λ	0.239	0.236	0.231	0.228	0.225	0.222	0.218	0.214
G	10.0	10.4	11.4	11.8	13.9	14.7	14.3	13.8
B	-3.8	-3.2	-2.6	-2.3	-0.2	+1.4	+3.8	+5.7
s = ½"								
ℓ/λ	0.236	0.233	0.228	0.225	0.222	0.219	0.215	0.212
G	10.4	10.8	11.8	12.4	14.1	14.4	14.1	13.9
B	-4.0	-3.5	-2.6	-2.1	+0.2	+2.0	+4.6	+5.5
s = ¾"								
ℓ/λ	0.234	0.230	0.226	0.223	0.220	0.217	0.213	0.210
G	10.7	11.3	12.2	12.7	14.9	14.7	14.5	13.4
B	-4.0	-3.7	-2.5	-1.8	+0.6	+2.6	+5.3	+6.8
s = 1"								
ℓ/λ	0.232	0.230	0.224	0.221	0.219	0.216	0.212	0.208
G	10.7	11.3	12.4	12.7	14.9	15.0	14.8	14.2
B	-4.2	-3.9	-3.1	-2.2	+0.2	+2.1	+4.7	+3.6

d = 3/8"

s = 0								
ℓ/λ	0.240	0.237	0.232	0.229	0.226	0.223	0.219	0.215
G	9.6	10.2	11.0	11.2	13.4	13.7	14.1	13.2
B	-2.0	-2.0	-1.1	-1.0	+0.6	+2.4	+4.3	+5.5
s = ¼"								
ℓ/λ	0.236	0.233	0.228	0.225	0.222	0.219	0.215	0.212
G	10.6	10.9	11.8	12.1	14.3	14.3	14.4	13.5
B	-2.8	-2.5	-1.8	-1.5	+0.8	+2.5	+4.8	+6.0
s = ½"								
ℓ/λ	0.235	0.232	0.227	0.224	0.221	0.218	0.214	0.210
G	10.6	10.9	11.6	12.4	14.6	14.7	14.7	13.9
B	-3.6	-3.3	-2.5	-2.1	+0.1	+1.6	+4.2	+5.2
s = ¾"								
ℓ/λ	0.232	0.230	0.224	0.221	0.219	0.216	0.212	0.208
G	10.7	11.0	12.1	12.7	14.8	14.9	15.0	14.8
B	-3.8	-3.6	-2.7	-2.1	+0.8	+2.1	+4.6	+6.1
s = 1"								
ℓ/λ	0.230	0.227	0.222	0.219	0.216	0.213	0.209	0.206
G	11.2	11.6	12.6	13.2	15.0	15.1	14.8	14.7
B	-4.0	-3.8	-2.8	-2.2	+0.5	+2.5	+5.0	+6.3

$d = \frac{1}{2}''$

$s = \frac{1}{4}''$								
ℓ/λ	0.236	0.233	0.228	0.225	0.222	0.219	0.215	0.212
G	10.5	10.7	11.9	12.1	14.2	14.4	15.0	13.5
B	-1.1	-0.7	-0.4	-0.04	+1.7	+3.0	+5.4	+4.5
$s = \frac{1}{2}''$								
ℓ/λ	0.232	0.230	0.224	0.221	0.219	0.216	0.212	0.208
G	11.1	11.5	12.4	12.7	14.9	14.9	15.3	16.6
B	-2.6	-2.3	-1.8	-1.4	+0.7	+2.3	+4.8	+6.7
$s = \frac{3}{4}''$								
ℓ/λ	0.228	0.225	0.220	0.218	0.215	0.212	0.208	0.204
G	11.6	11.6	12.8	13.8	15.2	15.8	15.6	14.0
B	-3.1	-3.2	-2.3	-1.5	+0.6	+2.8	+5.2	+4.3
$s = 1''$								
ℓ/λ	0.226	0.223	0.218	0.215	0.212	0.209	0.206	0.202
G	11.8	12.2	13.2	13.5	15.4	15.6	15.8	14.7
B	-3.3	-3.0	-2.4	-1.6	+0.8	+2.7	+4.5	+6.8

TYPICAL MEASURED DIPOLE INPUT ADMITTANCE CURVES. CONDUCTANCE G/ ℓ/λ RATIO AND SUSCEPTANCE B/ ℓ/λ RATIO FOR A 1/8" DIAMETER DIPOLE AERIAL. INPUT CONE LENGTH s=1".

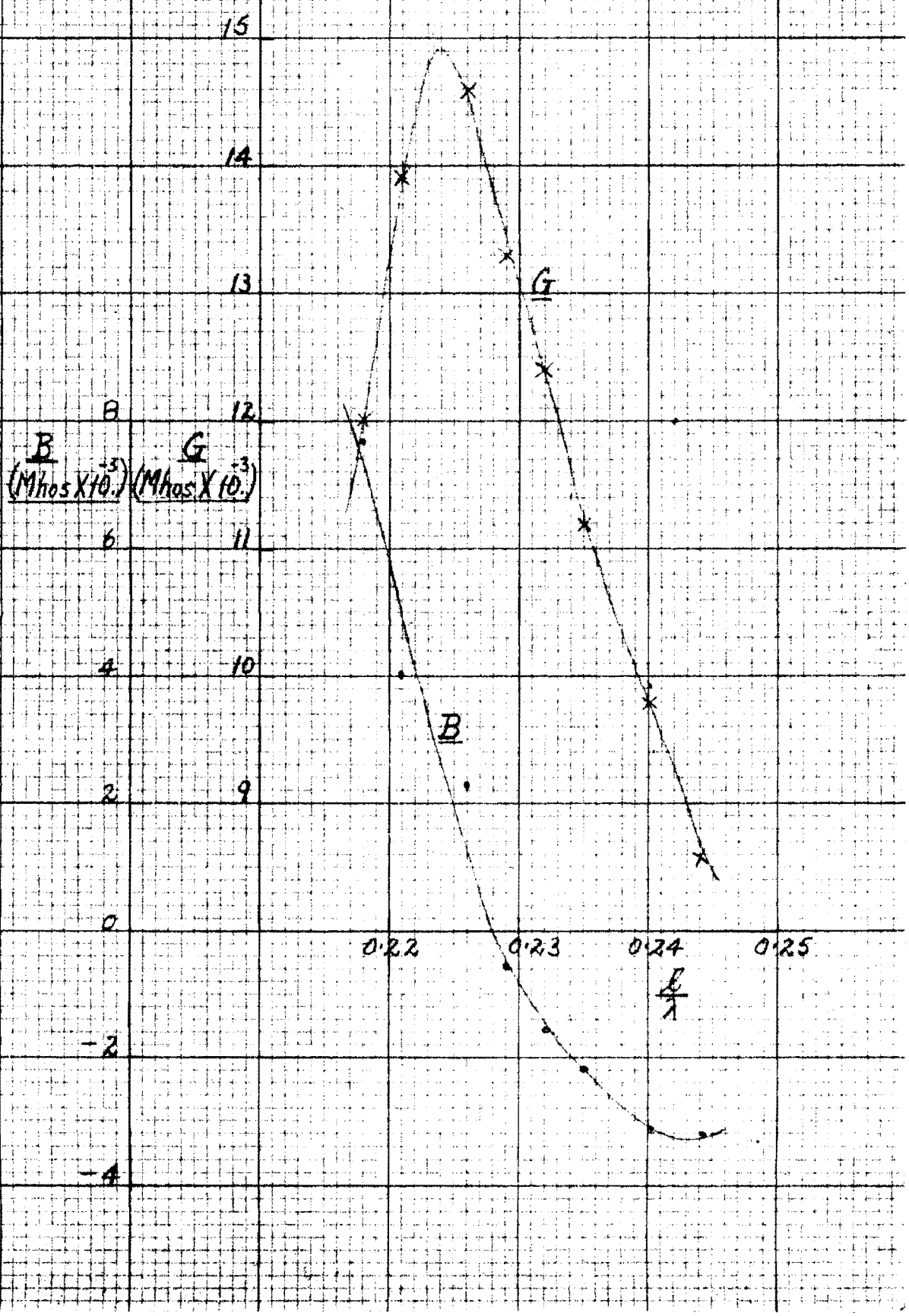

The following table of first resonant resistance and length as a function of r/l ratio has been deduced from the above experimental results. These results will be discussed in a later section.

Dipole First Resonance Results

	r(Inches.)	1/8	3/16	1/4	5/16	3/8	1/2
s=0	$\frac{\ell}{\lambda}$	0.2306	0.2285	0.2283	0.2268	0.2271	
	$\frac{r}{\ell}$	0.0221	0.0335	0.0447	0.0562	0.0677	
	% Foreshort.	7.8	8.6	8.7	9.3	9.2	
	$G_{res.}$	12.71	13.50	13.50	13.08	12.57	
	$R_{res.}$	78.7	74.1	74.1	76.5	79.6	
s=1/4"	$\frac{\ell}{\lambda}$	0.2321	0.2281	0.2257	0.2246	0.2230	0.2250
	$\frac{r}{\ell}$	0.0221	0.0337	0.0450	0.0566	0.0685	0.0915
	% Foreshort.	7.2	8.5	9.7	10.2	10.8	10.0
	$G_{res.}$	13.33	13.94	13.57	14.00	13.46	12.10
	$R_{res.}$	75.0	71.7	73.8	71.5	74.4	82.6
s=1/2"	$\frac{\ell}{\lambda}$	0.2296	0.2266	0.2242	0.2223	0.2211	0.2197
	$\frac{r}{\ell}$	0.0222	0.0339	0.0454	0.0571	0.0690	0.0930
	% Foreshort	8.2	9.4	10.3	11.1	11.6	12.1
	$G_{res.}$	13.15	13.96	14.16	13.96	14.50	14.17
	$R_{res.}$	76.0	71.7	70.7	71.7	69.0	70.7
s=3/4"	$\frac{\ell}{\lambda}$	0.2287	0.2255	0.2226	0.2208	0.2196	0.2159
	$\frac{r}{\ell}$	0.0223	0.0341	0.0456	0.0576	0.0696	0.0945
	% Foreshort.	8.5	9.8	11.0	11.7	12.2	13.6
	$G_{res.}$	13.42	13.85	13.81	14.35	14.22	14.80
	R_{res}	74.5	72.2	72.4	68.7	70.3	67.6
s=1"	$\frac{\ell}{\lambda}$	0.2285	0.2245	0.2210	0.2192	0.2166	0.2130
	$\frac{r}{\ell}$	0.0223	0.0350	0.0459	0.0580	0.0704	0.0957
	% Foreshort.	8.6	10.2	11.6	12.3	13.4	14.8
	$G_{res.}$	13.54	13.84	14.50	14.72	14.67	14.77
	$R_{res.}$	73.8	72.3	68.9	67.9	68.2	67.7

The following table of maximum conductance and $\frac{\ell}{\lambda}$ ratio as a function of r/l ratio has been deduced from the experimental results. The theoretical values included in the table have been calculated by the cylindrical aerial method. The results will be discussed in a later section.

Dipole Maximum Conductance Results

	r/l	1/8	3/16	1/4	5/16	3/8	1/2
s = 0	$\frac{\ell}{\lambda}$	0.2270	0.2250	0.2215	0.2216	0.2200	
	G	13.4	13.9	14.0	14.1	14.1	
s = $\frac{1}{4}$	$\frac{\ell}{\lambda}$	0.2310	0.2265	0.2220	0.2215	0.2184	0.2150
	G	13.4	14.3	14.1	14.7	14.4	15.0
s = $\frac{1}{2}$	$\frac{\ell}{\lambda}$	0.2254	0.2243	0.2230	0.2195	0.2165	0.2133
	G	13.6	14.1	14.4	14.4	14.8	15.3
s = $\frac{3}{4}$	$\frac{\ell}{\lambda}$	0.2245	0.2225	0.2200	0.2185	0.2138	0.2110
	G	13.7	14.4	14.4	15.0	15.0	15.8
s = 1	$\frac{\ell}{\lambda}$	0.2241	0.2220	0.2180	0.2165	0.2140	0.2065
	G	14.9	14.3	14.8	15.0	15.1	15.8
	G_{Theory}	15.5	15.9	16.2	16.6	16.9	17.7

(iii) Compensated Dipole Aerial Admittance Results.

d = 1/8" l = 13.9 cm.

s	0		¼"		½"		¾"		1"	
f	G	B	G	B	G	B	G	B	G	B
500.2	14.1	+0.7	14.1	+0.7	14.5	+0.7	14.7	+0.5	14.0	+0.6
494	14.8	-0.2	14.7	0	15.2	+0.1	15.2	+0.2	15.1	0
485.1	15.5	-0.5	15.9	-0.5	16.1	-0.4	16.2	+0.2	16.1	-0.3
478.6	16.1	-1.0	16.2	-0.6	16.8	-0.4	17.2	0	16.7	-0.7
473	17.1	-0.8	17.9	+0.1	17.3	-0.2	17.7	+0.3	17.4	0
465.2	17.2	+0.2	17.5	+0.4	17.4	+0.2	17.5	+1.5	17.5	+1.0
456.7	15.2	+1.1	15.4	+1.7	14.9	+1.2	15.0	+2.0	15.2	+1.8
449.9	14.4	+1.4	14.4	+1.6	14.1	+1.5	13.8	+2.2	14.2	+1.9

d = 3/16" l = 13.9 cm.

s	0		¼"		½"		¾"		1"	
f	G	B	G	B	G	B	G	B	G	B
500.2	14.9	+1.6	14.5	+1.6	14.8	+1.8	15.0	+1.3	15.0	+1.1
494	15.2	+1.3	15.3	+1.0	15.5	+1.0	15.6	+0.7	15.9	+1.0
485.1	15.9	+0.5	15.6	0	15.9	+0.2	16.4	+0.1	16.2	+0.1
478.6	16.8	+0.3	16.8	-0.2	16.8	-0.1	17.1	-0.2	17.3	+0.3
473	17.5	+0.2	17.2	-0.3	17.9	+0.3	18.3	+0.7	18.1	+0.5
465.2	17.6	+1.1	17.6	+0.8	17.9	+1.2	17.7	+1.3	17.8	+1.2
456.7	15.4	+1.7	15.7	+1.1	15.7	+1.7	15.7	+1.9	15.5	+1.7
449.9	14.6	+1.8	15.0	+1.9	15.0	+2.1	15.1	+1.9	14.6	+2.2

d = ¼" l = 13.9 cm.

s	0		¼"		½"		¾"		1"	
f	G	B	G	B	G	B	G	B	G	B
500.2	14.4	+2.8	15.1	+2.3	15.1	+1.9	15.2	+1.8	15.0	+1.6
494	15.1	+1.7	15.9	+1.8	15.5	+1.3	16.0	+1.3	16.4	+0.7
485.1	15.3	+0.6	16.1	+0.6	15.9	+0.3	16.4	+0.7	16.3	0
478.6	16.5	-0.1	17.4	+0.2	17.2	0	17.4	+0.1	17.7	-0.2
473	17.4	+0.1	17.6	+0.1	18.1	-0.1	17.8	+0.3	18.3	-0.1
465.2	17.7	+0.5	18.0	+1.2	18.5	+0.5	18.3	+1.0	18.7	+0.8
456.7	16.2	+1.3	16.1	+1.7	16.4	+1.6	16.4	+1.8	16.5	+1.7
449.9	15.7	+1.8	15.4	+2.1	15.9	+2.1	15.5	+2.1	15.9	+2.1

d = 5/16" l = 13.9 cm.

s	0		¼"		½"		¾"		1"	
f	G	B	G	B	G	B	G	B	G	B
500.2	14.4	+3.3	14.6	+2.5	15.2	+2.6	15.9	+2.7	15.6	+2.0
494.0	15.2	+2.4	15.5	+1.4	15.9	+1.7	16.4	+1.5	16.4	+1.2
485.1	15.5	+1.2	15.9	+0.5	16.1	+0.6	16.6	+0.8	16.9	+0.5
478.6	16.6	+0.4	16.9	0	17.4	+0.4	17.8	+0.5	17.6	-0.2
473.0	17.3	+0.2	17.9	0	18.4	+0.5	18.4	+0.2	18.6	0
465.2	17.9	+0.5	18.8	+0.6	18.6	+0.8	18.8	+1.0	18.7	+0.5
456.7	16.8	+1.5	17.5	+1.1	17.0	+1.8	17.0	+2.1	17.0	+1.7
449.9	16.3	+1.8	16.6	+1.5	16.1	+2.2	16.4	+2.0	16.5	+2.2

d = 3/8" l = 13.7 cm.

s	0		¼"		½"		¾"		1"	
f	G	B	G	B	G	B	G	B	G	B
500.2	14.5	+2.3	15.7	+2.1	15.6	+1.3	15.9	+1.0	16.6	+1.0
494.0	15.4	+2.2	16.1	+2.2	16.5	+1.1	16.6	+1.0	17.0	+1.0
485.1	15.6	+1.5	16.3	+1.5	16.4	+0.8	16.9	+0.9	17.0	+0.7
478.6	16.0	+0.6	16.6	+0.9	16.8	+0.1	17.0	0	17.5	+0.3
473.0	16.5	+0.1	17.0	+0.2	17.4	-0.5	17.8	+0.5	17.9	-0.2
465.2	17.0	-0.8	17.7	-0.3	18.3	-0.5	18.0	-0.4	18.5	-0.4
456.7	17.6	+0.2	17.7	+1.1	17.6	+0.4	17.6	+0.2	17.7	+0.8
449.9	16.9	+1.0	16.9	+1.1	17.4	+0.8	17.0	+0.8	16.6	+1.3

d = ½" l = 13.7 cm.

s	¼"		½"		¾"		1"	
f	G	B	G	B	G	B	G	B
500.2	15.8	+4.3	16.1	+2.0	16.9	+2.2	17.3	+2.0
494.0	16.4	+3.9	17.0	+2.8	17.7	+2.2	17.8	+2.3
485.1	16.1	+3.3	16.8	+2.0	17.5	+1.8	17.7	+1.9
478.6	16.5	+2.3	17.3	+1.1	17.8	+1.1	17.9	+1.4
473.0	17.6	+2.0	17.6	+0.8	18.2	+0.8	18.2	+0.9
465.2	17.8	+0.7	18.3	+0.7	18.3	+1.0	18.9	+0.1
456.7	17.9	+1.9	18.8	+1.3	18.3	+1.2	18.7	+2.0
449.9	17.6	+2.1	18.0	+1.5	17.6	+1.3	17.3	+2.0

(e) Dipole Aerial Polar Diagram Experiments and Results.

The dipole aerials used in the field strength experiments were made of such a length that they were resonant at 477.5 Mcps. The resonant lengths were obtained from the results of the unipole admittance experiments. The measurements were made in a field at Ilam Road by the method already described for dipole aerials of diameter 1/8", 3/16", 1/4", 5/16", 3/8" and $\frac{1}{2}$" and input section slope length $s = 0$, $\frac{1}{4}$", $\frac{1}{2}$", $\frac{3}{4}$", 1". The lengths of the dipole aerials were held constant throughout the measurements. The measurements were made at three frequencies, 457.5, 477.5 and 497.5 Mcps. corresponding to the carrier and upper and lower limits of an 8 Mcps. video signal on a 95.5 Mcps. carrier. The angular displacement between the transmitting and receiving aerial was altered from a position where the two aerials are parallel through 90° in 5° intervals and the U.H.F. Receiver voltmeter readings noted at each position. The appropriate field strength for each voltmeter reading was found from the calibration curves described in the preliminary experiments subsection. The resulting field strengths were normalized and are given below in tabular form. A typical polar diagram is shown plotted. The results will be discussed in a later section.

Normalized Field Strength E_θ d = 1/8"

s		0			¼"			½"			¾"			1"		
Position θ°	f	457.5	477.5	497.5	457.5	477.5	497.5	457.5	477.5	497.5	457.5	477.5	497.5	457.5	477.5	497.5
0		10.00	10.00	10.00	10.00	10.00	10.00	10.00	10.00	10.00	10.00	10.00	10.00	10.00	10.00	10.00
5		9.94	10.00	10.00	10.00	10.00	9.80	9.88	10.00	9.73	10.00	9.90	9.92	9.77	10.00	10.00
10		9.72	9.64	9.15	10.00	10.00	9.70	9.88	9.72	9.46	9.57	9.57	9.62	9.31	9.76	9.93
15		9.43	9.57	9.15	9.87	9.75	9.60	9.63	8.97	8.81	9.72	9.11	9.12	9.31	9.27	9.36
20		9.20	8.70	8.95	9.87	9.37	8.89	9.14	8.89	8.63	9.29	8.90	8.57	8.61	9.07	9.00
25		9.15	8.60	8.30	9.19	8.97	8.85	8.65	8.45	7.43	8.86	8.22	8.53	8.26	8.78	8.64
30		8.44	7.89	7.94	8.14	8.55	8.22	7.91	7.45	7.25	8.14	7.24	8.41	7.33	8.00	8.21
35		8.00	7.67	7.73	7.56	7.85	7.33	7.29	7.06	6.88	7.43	7.25	7.97	6.98	7.25	7.27
40		6.86	6.32	6.56	7.21	7.17	6.67	6.43	6.00	6.33	6.15	6.56	6.82	5.70	6.34	6.05
45		6.30	6.00	5.56	5.81	6.48	6.47	5.06	5.97	5.14	5.86	6.16	5.91	4.65	5.61	5.33
50		5.37	5.11	5.09	5.46	5.71	6.15	4.32	5.20	4.40	4.86	5.26	5.81	4.19	4.81	4.32
55		4.74	4.59	4.90	4.42	4.99	5.81	3.70	4.72	3.67	4.29	4.96	5.60	3.84	4.34	3.89
60		4.24	3.60	3.96	4.42	4.34	4.44	2.47	3.70	3.12	3.57	3.76	4.91	2.33	3.47	3.24
65		3.83	3.36	3.58	2.91	3.88	4.04	2.37	3.20	2.29	2.86	3.70	4.19	1.98	3.24	2.59
70		2.61	2.30	2.64	2.70	3.48	3.55	1.62	2.33	1.61	2.11	2.80	3.41	1.48	2.37	1.66
75		2.00	2.04	1.27	1.75	2.75	3.30	1.20	1.67	1.31	1.60	2.04	3.29	1.14	1.91	0.94
80		0.80	1.11	0.78	1.40	2.18	2.43	0.52	0.92	0.98	0.20	1.50	2.08	0.12	1.39	0.68
85		0.08	0.33	1.09	0.65	1.33	1.43	0.01	0.42	0.95	0.04	0.85	1.30	0.01	0.73	0.68
90		1.14	0.04	1.47	0.09	0.73	1.13	0.93	0.20	0.95	1.26	0.11	1.30	0.38	0.18	1.12

Normalized Field Strength E_θ d = 3/16"

s	0				$\frac{1}{4}$"			$\frac{1}{2}$"			$\frac{3}{4}$"			1"		
Position θ°	f	457.5	477.5	497.5	457.5	477.5	497.5	457.5	477.5	497.5	457.5	477.5	497.5	457.5	477.5	497.5
0		10.00	10.00	10.00	10.00	10.00	10.00	10.00	10.00	10.00	10.00	10.00	10.00	10.00	10.00	10.00
5		10.00	10.00	10.00	10.00	10.00	10.00	10.00	10.00	10.00	10.00	10.00	10.00	10.00	10.00	10.00
10		9.67	9.56	9.37	9.86	10.00	9.54	10.00	10.00	10.00	9.72	9.85	9.84	10.00	10.00	10.00
15		9.44	9.15	9.37	9.41	9.92	9.00	9.47	9.40	10.00	9.30	9.85	9.50	10.00	10.00	9.25
20		8.75	9.05	8.23	8.97	9.75	8.34	9.05	8.97	9.80	8.45	8.74	8.67	9.28	9.21	8.49
25		8.19	8.42	8.09	8.22	9.20	7.60	8.74	8.31	8.36	7.89	8.44	8.67	8.80	8.76	8.07
30		7.16	7.72	7.59	7.77	9.00	7.50	8.22	7.95	7.64	7.47	7.77	8.34	8.48	8.25	7.80
35		6.82	7.34	7.24	6.72	8.82	6.02	7.90	7.12	6.71	6.48	6.45	7.50	7.52	7.76	7.42
40		5.69	6.14	5.46	5.98	8.24	5.00	6.95	6.84	5.47	6.06	5.85	6.00	7.12	7.21	7.42
45		5.24	5.99	5.26	5.08	6.72	4.07	6.43	5.57	4.34	4.94	4.82	5.09	5.84	6.04	6.99
50		3.98	5.22	4.82	4.48	6.01	3.24	5.27	5.00	3.90	4.51	4.06	4.17	5.44	5.55	5.92
55		3.75	4.62	4.12	4.04	4.62	2.82	4.21	3.98	2.89	3.53	3.10	2.83	4.48	4.25	3.87
60		2.27	3.48	3.41	2.99	3.61	1.67	3.58	3.63	1.96	2.82	2.74	1.92	4.09	3.76	3.01
65		1.71	2.91	2.84	2.49	2.23	1.04	2.42	2.53	1.03	2.81	1.52	0.97	2.96	2.77	1.83
70		1.44	2.03	1.99	1.99	1.28	0.97	2.11	2.05	1.03	2.07	1.20	0.73	2.00	2.38	1.53
75		0.98	1.65	1.35	1.09	0.40	0.13	1.45	1.38	0.32	1.30	0.29	0.13	0.96	1.22	0.96
80		0.04	0.60	0.85	0.67	0.29	0.07	0.98	0.89	0.08	0.76	0.15	0.10	0.34	0.81	0.38
85		0.01	0.28	0.55	0.02	0.05	0	0.35	0.16	0.01	0.13	0.03	0.01	0.09	0.14	0.05
90		0.51	0.19	1.55	0.02	0.05	0	0.02	0.03	0	0.02	0	0	0	0.04	0

Normalized Field Strength E_θ d = $\frac{1}{4}$"

s		0			$\frac{1}{4}$"			$\frac{1}{2}$"			$\frac{3}{4}$"			1"		
Position θ°	f	457.5	477.5	497.5	457.5	477.5	497.5	457.5	477.5	497.5	457.5	477.5	497.5	457.5	477.5	497.5
0		10.00	10.00	10.00	10.00	10.00	10.00	10.00	10.00	10.00	10.00	10.00	10.00	10.00	10.00	10.00
5		10.00	10.00	10.00	10.00	10.00	10.00	10.00	10.00	10.00	10.00	10.00	10.00	10.00	10.00	10.00
10		10.00	10.00	10.00	10.00	10.00	10.00	10.00	10.00	9.50	10.00	10.00	9.94	10.00	9.85	10.00
15		9.90	9.96	9.77	9.77	9.77	9.53	10.00	9.86	9.20	9.89	9.85	9.83	9.76	9.61	9.34
20		9.35	9.76	8.90	9.65	9.47	9.17	9.89	9.21	8.80	9.66	9.83	9.59	9.41	9.46	8.86
25		8.92	9.47	8.25	9.06	9.13	9.13	9.32	8.61	8.50	9.09	9.04	9.41	9.06	9.06	8.79
30		8.59	9.22	7.90	8.83	8.55	8.22	8.86	8.31	8.22	8.98	8.54	9.01	8.71	8.75	8.69
35		7.94	8.54	6.63	8.47	8.12	8.18	8.39	7.62	7.80	8.41	7.68	8.50	8.24	8.06	8.17
40		7.61	8.15	6.26	7.89	7.35	7.83	7.93	7.07	6.54	7.96	7.02	8.00	7.65	7.70	6.56
45		7.07	7.22	5.73	6.59	6.48	5.61	6.90	6.02	6.00	7.05	6.21	7.00	6.47	6.75	5.41
50		5.99	6.35	5.59	6.36	5.94	5.22	6.33	5.57	5.60	6.25	5.66	5.25	5.89	6.00	4.46
55		5.00	5.56	5.36	5.06	5.07	4.79	5.17	4.73	5.53	5.23	4.70	5.50	4.94	5.25	4.09
60		4.46	4.78	3.88	4.47	4.59	4.09	4.60	4.23	3.93	4.77	4.29	5.00	4.47	4.80	3.82
65		3.26	3.61	2.97	3.29	3.53	3.48	3.33	3.23	3.32	3.53	3.13	4.00	3.18	3.40	3.54
70		2.72	3.08	2.36	2.83	3.04	3.39	3.11	2.83	2.68	2.95	2.63	3.45	2.83	2.85	3.02
75		1.96	2.05	1.83	2.59	1.06	2.52	2.07	0.91	2.43	2.05	0.67	3.00	2.12	0.84	2.22
80		1.87	0.88	1.05	2.05	0.87	2.13	1.92	0.61	1.82	1.83	0.51	2.50	1.97	0.69	1.61
85		0.87	0.47	1.00	0.94	0.44	2.09	1.08	0.24	1.78	0.94	0.24	2.05	0.97	0.22	1.20
90		0.65	0.54	0.90	0.74	0.44	1.00	0.74	0.38	0.82	0.63	0.56	1.28	0.69	0.45	1.01

Normalized Field Strength E_θ d = 5/16"

s		0			¼"			½"			¾"			1"		
Position θ°	f	457.5	477.5	497.5	457.5	477.5	497.5	457.5	477.5	497.5	457.5	477.5	497.5	457.5	477.5	497.5
0		10.00	10.00	10.00	10.00	10.00	10.00	10.00	10.00	10.00	10.00	10.00	10.00	10.00	10.00	10.00
5		10.00	10.00	10.00	10.00	10.00	10.00	10.00	10.00	10.00	10.00	10.00	10.00	10.00	10.00	9.77
10		10.00	10.00	9.60	10.00	10.00	10.00	10.00	10.00	10.00	10.00	10.00	9.75	10.00	10.00	9.52
15		9.80	9.42	9.57	9.67	9.89	10.00	9.78	10.00	10.00	9.88	9.45	9.31	9.89	9.73	9.47
20		9.50	9.15	9.37	9.57	9.73	9.61	9.68	9.63	9.15	9.66	9.45	9.03	9.67	9.67	9.25
25		9.00	8.88	9.29	9.14	8.92	9.09	9.35	9.47	8.86	9.43	8.94	8.90	9.35	9.29	9.15
30		8.70	8.67	9.00	8.82	8.86	8.65	9.24	9.04	8.30	9.20	8.44	8.70	8.91	8.69	9.03
35		8.20	7.55	8.38	8.07	8.05	7.95	8.59	7.76	7.58	8.62	7.53	8.18	8.57	7.80	8.05
40		7.90	6.59	8.11	7.96	7.57	7.65	8.26	7.11	6.61	8.39	7.23	7.36	8.25	7.53	7.37
45		7.20	5.59	7.44	6.99	6.27	6.47	7.83	5.99	6.15	7.36	6.36	7.04	7.48	6.81	6.79
50		6.70	5.11	7.11	6.56	5.95	6.31	7.07	5.51	5.11	6.90	5.66	6.38	7.04	6.54	6.45
55		5.50	4.36	5.78	5.49	5.13	5.21	5.87	4.87	4.89	5.75	4.80	5.32	5.72	4.78	5.44
60		4.90	3.83	5.22	4.85	4.59	4.36	4.89	3.42	3.61	5.17	4.19	4.97	4.95	4.45	3.78
65		3.90	2.92	4.21	3.55	3.46	3.57	3.81	3.15	3.08	4.02	3.23	4.56	3.74	3.24	3.66
70		3.40	2.45	3.89	3.01	2.76	3.14	3.59	2.46	2.53	3.45	2.12	3.80	3.30	2.47	3.23
75		2.40	0.80	3.39	2.26	0.90	2.65	2.39	0.96	2.48	2.53	0.88	3.11	2.31	0.86	2.58
80		2.20	0.63	2.74	1.91	0.72	2.31	2.17	0.63	1.61	2.35	0.61	2.56	2.18	0.67	2.27
85		1.14	0.26	2.11	1.04	0.42	1.49	1.41	0.09	1.26	1.38	0.26	1.76	1.38	0.39	1.27
90		0.70	0.56	1.40	0.60	0.33	1.06	0.79	0.04	1.01	0.93	0.34	1.14	0.86	0.38	0.83

Normalized Field Strength E_θ d = 3/8"

s		0			$\frac{1}{4}$"			$\frac{1}{2}$"			$\frac{3}{4}$"			1"		
Position θ°	f	457.5	477.5	497.5	457.5	477.5	497.5	457.5	477.5	497.5	457.5	477.5	497.5	457.5	477.5	497.5
0		10.00	10.00	10.00	10.00	10.00	10.00	10.00	10.00	10.00	10.00	10.00	10.00	10.00	10.00	10.00
5		10.00	10.00	10.00	10.00	10.00	10.00	10.00	10.00	10.00	10.00	10.00	10.00	10.00	10.00	10.00
10		10.00	10.00	10.00	10.00	10.00	10.00	10.00	10.00	9.83	10.00	10.00	10.00	10.00	9.90	9.62
15		9.14	9.57	9.73	10.00	9.83	9.67	9.75	9.95	9.53	9.76	10.00	10.00	9.82	9.86	9.42
20		9.09	9.43	9.70	9.71	9.62	9.52	9.64	9.67	9.49	9.37	9.22	9.35	9.52	9.42	9.18
25		8.38	8.68	9.43	9.14	9.20	9.35	9.00	9.29	9.34	8.70	9.21	8.86	9.17	8.84	8.16
30		8.12	8.59	9.01	8.71	9.07	9.23	8.93	8.85	9.24	8.66	8.95	7.37	8.84	8.54	7.58
35		7.62	7.94	8.39	7.86	8.34	9.03	8.16	8.31	8.79	8.12	8.00	6.90	8.24	8.15	7.41
40		7.21	7.67	7.54	7.29	8.12	8.61	7.90	7.60	8.14	7.56	7.21	6.16	7.75	7.27	6.36
45		6.14	5.86	6.20	6.43	7.14	7.81	6.79	6.77	7.21	6.92	6.42	5.31	6.99	6.50	6.15
50		5.74	5.69	5.77	5.86	6.75	7.57	6.37	6.01	6.00	6.54	5.90	5.47	6.61	5.71	6.01
55		4.47	4.85	4.25	5.00	5.94	6.30	5.56	4.97	5.17	5.79	5.00	5.07	5.81	4.00	5.79
60		4.31	4.41	3.43	4.71	5.17	5.76	5.19	4.26	4.91	5.15	4.42	3.95	5.66	3.27	4.57
65		2.79	3.70	1.92	3.43	3.72	4.25	4.07	3.33	4.58	3.83	3.21	3.38	4.54	2.83	4.00
70		2.44	3.70	1.36	3.15	3.51	3.61	3.33	2.79	3.99	3.19	3.00	2.70	3.97	2.34	3.09
75		1.47	2.60	1.08	2.60	2.09	2.39	2.00	0.96	2.98	2.31	0.95	2.50	2.34	0.67	2.87
80		1.12	0.59	0.78	2.22	0.97	1.44	0.89	0.84	2.58	1.60	0.75	2.10	2.04	0.51	2.02
85		0.05	0.33	0.45	1.10	0.33	0.78	0.40	0.34	1.36	1.24	0.32	1.59	1.21	0.19	1.29
90		0	0.22	0.71	0.51	0.38	0.51	0	0.40	1.03	1.14	0.34	0.88	1.21	0.28	0.87

Normalized Field Strength E_θ d = $\frac{1}{2}$"

s		$\frac{1}{4}$"			$\frac{1}{2}$"			$\frac{3}{4}$"			1"		
Position θ°	f	457.5	477.5	497.5	457.5	477.5	497.5	457.5	477.5	497.5	457.5	477.5	497.5
0		10.00	10.00	10.00	10.00	10.00	10.00	10.00	10.00	10.00	10.00	10.00	10.00
5		10.00	10.00	10.00	10.00	10.00	10.00	10.00	10.00	10.00	10.00	10.00	10.00
10		10.00	9.39	10.00	9.97	10.00	9.84	10.00	10.00	9.89	10.00	10.00	9.80
15		9.64	9.30	9.90	9.85	10.00	9.32	9.53	9.90	9.35	9.51	9.83	9.50
20		9.44	9.06	9.77	9.74	10.00	8.82	9.26	9.77	8.86	9.08	9.73	9.35
25		8.80	8.50	9.37	9.54	9.80	8.55	9.06	9.35	8.46	8.85	9.60	9.25
30		8.59	8.05	9.27	8.84	9.47	7.99	8.39	9.31	7.64	8.09	9.16	8.51
35		7.70	6.98	7.50	8.10	8.88	7.67	7.88	8.52	7.03	7.51	8.57	8.26
40		7.46	6.41	6.28	7.79	8.50	6.73	7.69	7.92	6.80	6.93	8.17	7.50
45		6.20	5.95	5.44	7.01	7.43	5.90	6.77	7.00	6.13	6.66	7.59	6.90
50		5.67	5.50	5.11	6.62	6.70	4.99	6.42	6.50	5.65	6.27	6.97	6.25
55		4.82	4.76	4.26	5.57	5.64	4.79	5.87	5.66	5.23	5.59	6.12	5.44
60		4.34	4.03	3.73	5.06	5.05	4.41	5.00	5.02	5.03	5.19	5.59	5.01
65		3.20	2.93	2.22	3.78	3.74	4.26	3.90	4.19	4.92	3.93	4.33	4.62
70		2.87	2.71	1.97	3.27	3.20	3.15	3.82	3.50	3.45	3.39	3.75	3.68
75		1.74	2.05	1.41	2.06	0.93	2.67	2.64	2.26	3.27	1.85	2.55	2.70
80		1.06	1.67	1.04	1.56	0.87	2.00	1.66	0.96	2.67	1.35	2.10	2.25
85		0.21	0.88	0.20	0.80	0.25	1.77	0.90	0.33	1.66	0.80	0.75	1.71
90		0.20	0.51	0.59	0	0.23	0.79	0	0.54	1.22	0	0.42	0.90

TYPICAL MEASURED DIPOLE POLAR DIAGRAM.
FIELD STRENGTH E_θ / ANGULAR DISPLACEMENT θ FOR A 1/8" DIAMETER DIPOLE AERIAL.
INPUT CONE LENGTH s = 1"

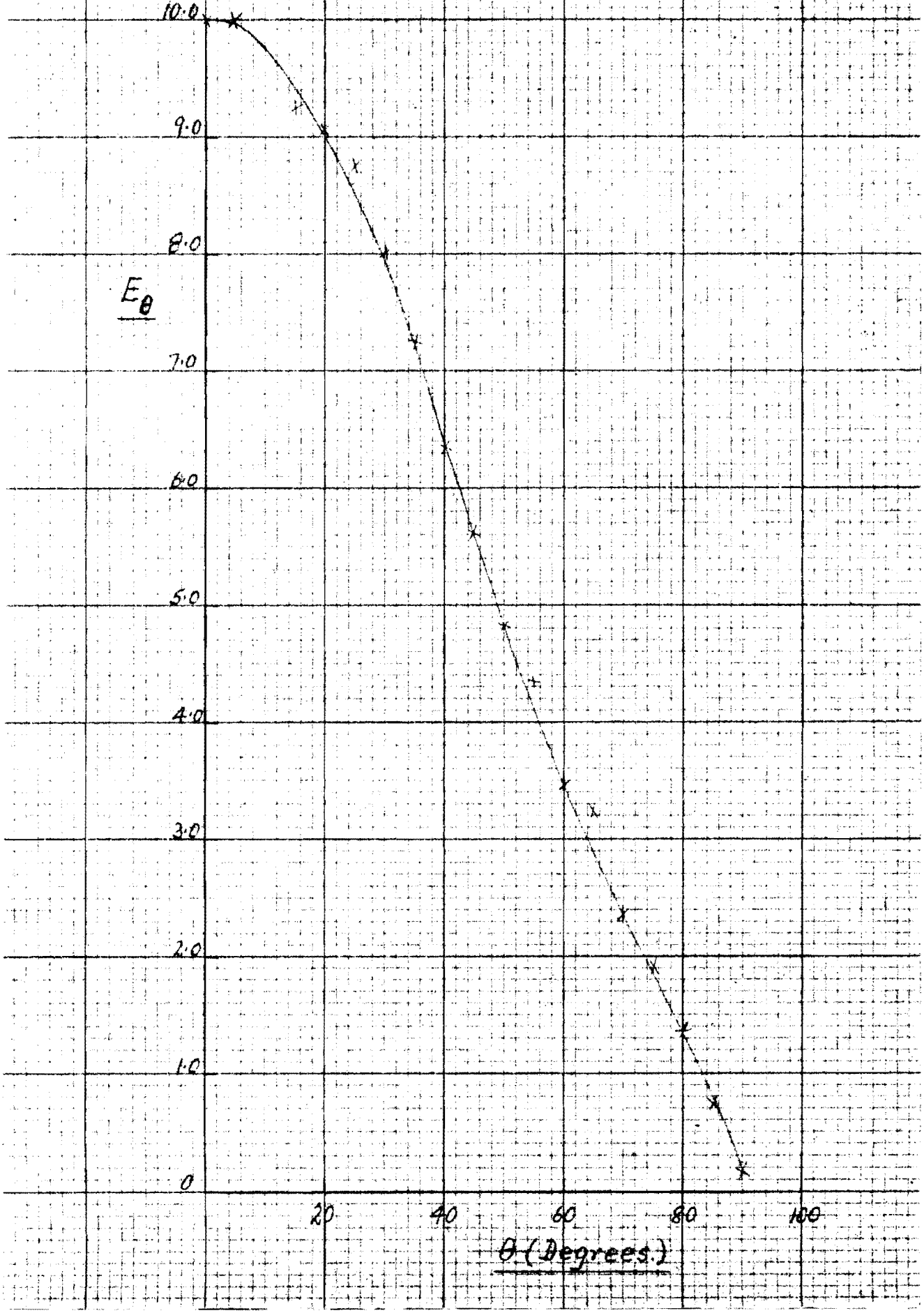

(f) Admittance Calculations.

The admittance of an aerial as registered by the admittance meter is not the true aerial admittance. The corrections which must be applied to the values of admittance as registered by the admittance meter to give the admittance of an aerial are given below. The admittances given in tabular form are those which were obtained after the following corrections had been applied.

(1) Cross Coupling Error Correction.[109]

The magnetic shielding of the junction box in the admittance meter is not perfect and small mutual couplings exist between each branch line and the loops associated with the other branches. The error produced by cross-couplings is a function of the measured admittance and of the sign of the standard susceptance. Corrections for the coupling are made using the following equations:

$$G_e = \frac{G_m - S \times 0.0085 B_m + 0.17}{D}$$

$$B_e = \frac{B_m + S(0.0085 G_m + 0.17)}{D}$$

$$D = 1 + 0.00042 G_m + S \times 0.00042 B_m$$

$S = -1$ for all the measurements.

G_m and B_m are the measured values of conductance and susceptance and G_e and B_e are the effective conductance and susceptance.

(2) Junction Inductance Error Correction.[109]

The inductance of the sections of line from the common junction point of the admittance meter to the centre of the coupling loops in the unknown and conductance standard branches causes an error which increases as the frequency increases. The inductance in the susceptance standard branch causes no error as it is compensated for when the stub is calibrated. The inductance in each branch is

approximately 1.19 millimicrohenries. The corrections for the junction inductance are made after corrections have been made for the cross-coupling error and the effective conductance and susceptance, G_e and B_e, have been obtained. The corrections for the junction inductance are made using the following equations:

$$G_x = \frac{G_e}{A}$$

$$B_x = \frac{B_e\left(1+\frac{B_e}{B_L}-\frac{2G_eY_o}{B_L^2}\right)+\frac{G_e}{Y_o}\left(G_e-Y_o\right)\frac{Y_o}{B_L}}{A}$$

$$A = \left(1+\frac{B_e}{B_L}\right)^2+\left(\frac{G_e}{B_L}\right)^2$$

$$B_L = \frac{10^3}{2\pi f L_j} = \frac{1}{2\pi f \times 1\cdot19\times10^{-12}}$$

where L_j is the junction inductance and G_x and B_x are the unknown conductance and susceptance.

(3) Frequency Change Correction.

The measurements were made for a line equal to three wavelengths in length at a frequency $f=f_o$. The admittance looking into a lossless line of length three wavelengths is $0+j0$. During the measurements the frequency of the U.H.F. Oscillator changed by an amount δf from the normal frequency of the measurements. This change in frequency is due to the increase in temperature of the U.H.F. Oscillator with time. Since the measurements were made at frequencies which differ slightly from the centre value the following corrections must be applied:

Let $f = f_o+\delta f$ $\qquad \lambda_o f_o = c = \lambda f$

Now $$\ell = 3\lambda_o = 3\lambda\frac{f}{f_o}$$

$$\frac{\ell}{\lambda} = 3\frac{f}{f_o} = 3\left(1+\frac{\delta f}{f_o}\right)$$

For the lossy line open circuited at frequency $f=f_o$

$$y_{oc} = g_{oc} \qquad b_{oc} = 0$$

$$\tan\beta\ell = 0$$

$$y_{oc} = \tanh\gamma\ell$$

Since $\tan\beta\ell = 0$

$$\therefore\ y_{oc} = \tanh\alpha\ell = g_{oc}$$

It is now possible to calculate the small change in susceptance of the open circuited line with change in frequency.

At $f = f_o + \delta f$

$$y_{oc} = \tanh\gamma\ell = \frac{\tanh\alpha\ell + j\tan\beta\ell}{1 + j\tanh\alpha\ell.\tan\beta\ell}$$

$$\tanh\alpha\ell = g_{oc}$$

$$\therefore\ y_{oc} = \frac{g_{oc}\sec^2\beta\ell}{1+g_{oc}^2\tan^2\beta\ell} + j\,\frac{\tan\beta\ell(1-g_{oc}^2)}{1+g_{oc}^2\tan^2\beta\ell}$$

$$\tan\beta\ell = \tan 2\pi\frac{\ell}{\lambda} = \tan\left(6\pi + 6\pi\frac{\delta f}{f_o}\right) = \tan 6\pi\frac{\delta f}{f_o} \doteq 6\pi\frac{\delta f}{f_o}$$

Now $g_{oc}^2\tan^2\beta\ell \ll 1$; $g_{oc}^2 \ll 1$; $\sec^2\beta\ell - 1 \to 0$

Using these approximations we have

$$y_{oc} = g_{oc} + j\tan\beta\ell$$

$$\therefore\ b_{oc} \doteq 6\pi\frac{\delta f}{f_o}$$

$$\therefore\ B_{oc} = 6\pi Y_o\frac{\delta f}{f_o}$$

This equation gives the open circuit susceptance of the line. The values of open circuit susceptance calculated from the above equation are used in applying the next correction.

(4) <u>Line Loss and Open Circuit Susceptance Variation Corrections</u>

For a line of length l and characteristic admittance Y_o, the admittance looking into the line open circuited at the far end is

$$Y_{oc} = Y_o\tanh\gamma\ell$$

If a load i.e. an aerial of admittance Y_L is connected across the far end of the line and the admittance looking into the line is Y_m then

$$Y_L = Y_o \frac{Y_o \tanh \gamma\ell - Y_m}{Y_m \tanh \gamma\ell - Y_o} = Y_o^2 \frac{Y_{oc} - Y_m}{Y_m Y_{oc} - Y_o^2}$$

Equating Real and Imaginary Parts

$$G_L = Y_o^2 \left\{ \frac{G_m Y_{oc}^2 - G_{oc} Y_m^2 + Y_o^2 (G_m - G_{oc})}{Y_{oc}^2 Y_m^2 + Y_o^2 (Y_o^2 + 2B_m B_{oc} - 2G_m G_{oc})} \right\}$$

$$B_L = Y_o^2 \left\{ \frac{B_{oc} Y_m^2 - B_m Y_{oc}^2 + Y_o^2 (B_m - B_{oc})}{Y_{oc}^2 Y_m^2 + Y_o^2 (Y_o^2 + 2B_m B_{oc} - 2G_m G_{oc})} \right\}$$

After this correction has been applied to the measured admittance the admittance Y_L obtained is that across the far end of the coaxial line.

(5) Discontinuity Correction.[116,117]

A correction was made for the discontinuity in the transmission line at the aerial in the case of the unipole admittance measurements. The method was based on the results of Whinnery for discontinuities in transmission lines.

(6) Capacitance Correction.

A correction was made to the admittance in the case of the dipole aerials for the capacitance of the short length of coaxial line protruding beyond the point where the dipole aerial was attached to the coaxial line.

The corrections given above were applied in the above order to the measured values of aerial admittance.

SECTION 5.

DISCUSSION AND CONCLUSION

(a) Introduction.

In this section the theoretical and experimental results of the foregoing sections will be discussed and compared.

(b) The Theoretical Impedance Results.

The results of theoretical analyses and calculations by the various methods are treated below.

(1) The Induced E.M.F. Method.

The theoretical analyses, calculations and graphs show the following properties:

(i) The loop reactance X is negative for small values of the $\frac{\ell}{\lambda}$ ratio. As the $\frac{\ell}{\lambda}$ ratio is increased the loop reactance curve follows a shape similar to a sine curve.

(ii) The value of $\frac{\ell}{\lambda}$ ratio for which the loop reactance is zero is less than 0.25 i.e. for the first resonant condition $\frac{\ell}{\lambda}$ is less than 0.25.

(iii) The amplitude of the loop reactance curve decreases as the r/l ratio increases. This means that the change in reactance about the resonant length for a given change in wavelength or frequency is smaller for fat aerials than it is for thin.

(iv) The value of the $\frac{\ell}{\lambda}$ ratio at which the loop reactance is zero decreases as the r/l ratio is increased. Hence, the foreshortening is greater for fat aerials than it is for thin aerials.

(v) The value of the input resistance at the first resonance is less than 73.2 ohms.

(vi) The value of input resistance at the first resonance decreases as the r/l ratio is increased.

(vii) The positive and negative slopes of the loop reactance - $\frac{\ell}{\lambda}$ ratio curves are approximately equal.

(viii) The first and second maximum values of the loop reactance curves are approximately equal.

With the exceptions of (vii) and (viii) all the above properties are true. The values obtained will be compared later.

(2) The Equivalent Transmission Line Method.

The theoretical analyses, calculations and graphs show the following properties:

(i) The input reactance X_{in} is negative for small values of the $\frac{\ell}{\lambda}$ ratio. As the $\frac{\ell}{\lambda}$ ratio is increased the input reactance follows a shape similar to a warped sine curve.

(ii) The value of $\frac{\ell}{\lambda}$ ratio for which the input reactance is zero is 0.25 for all r/l ratios. An attempt to modify the theory to correct this anomaly was not successful.

(iii) The amplitude of the input reactance curve decreases as the r/l ratio is increased.

(iv) The input resistance R_{in} is small for small values of the $\frac{\ell}{\lambda}$ ratio. As the $\frac{\ell}{\lambda}$ ratio is increased the input resistance follows a shape similar to a sine curve.

(v) The amplitude of the input resistance curve decreases as the r/l ratio is increased.

(vi) The values of $\frac{\ell}{\lambda}$ ratio at which the input resistance and reactance are a maximum decreases as the r/l ratio is increased.

(vii) The input resistance maxima occur at a greater value of $\frac{\ell}{\lambda}$ ratio than do the maxima for the input reactance.

(viii) The value of the input resistance at the first resonance is less than 73.2 ohms.

(ix) The value of input resistance at the first resonance decreases slightly as the r/l ratio is increased.

(x) The negative slope of the input reactance- $\frac{\ell}{\lambda}$ ratio curves is much greater than the positive slope.

(xi) The value of the second maximum for both the input resistance and input reactance curves is less than the first maximum.

With the exception of (iii) all the above properties are true. The values obtained will be compared later.

(3) The Biconical Aerial Method.

The theoretical analyses, calculations and graphs show the following properties:

(i) The input reactance X_{in} is negative for small values of the $\frac{\ell}{\lambda}$ ratio. As the $\frac{\ell}{\lambda}$ ratio is increased the input reactance follows a shape similar to a warped sine curve.

(ii) The value of $\frac{\ell}{\lambda}$ ratio for which the input reactance is zero is less than 0.25.

(iii) The value of the $\frac{\ell}{\lambda}$ ratio at which the loop reactance is zero decreases as the r/l ratio is increased.

(iv) The maximum of the input reactance curve decreases as the r/l ratio is increased.

(v) The input resistance R_{in} is small for small values of the $\frac{\ell}{\lambda}$ ratio. As the $\frac{\ell}{\lambda}$ ratio is increased the input resistance follows a shape similar to a sine curve.

(vi) The maximum value of the input resistance curve decreases as the r/l ratio is increased.

(vii) The value of $\frac{\ell}{\lambda}$ ratio at which the input resistance and reactance are a maximum decreases as the r/l ratio is increased.

(viii) The input resistance maxima occur at a greater value of $\frac{\ell}{\lambda}$ ratio than do the maxima for the input reactance.

(ix) The value of input resistance at the first resonance is less than 73.2 ohms.

(x) The value of input resistance at the first resonance decreases as the r/l ratio is increased.

(xi) The negative slope of the input reactance - $\frac{\ell}{\lambda}$ ratio curves is much greater than the positive slope.

(xii) The value of the second maximum for both the input resistance and input reactance curves is less than the first maximum.

The theory is based on the tacit assumption that $r/l < 0.030$. Hence, the odd shape of the input resistance and reactance curves for $r/l \geqslant 0.030$ shows that the

assumptions of the theory have been violated. The calculations for $r/l \geqslant 0.030$ were carried out so that an indication of the behaviour of fat dipole aerials could be obtained. The results for $r/l \geqslant 0.030$ are only qualitative and should not be considered in any quantitative manner. The values obtained will be compared later.

(4) The Cylindrical Aerial Method.

The properties which were obtained for the biconical aerial method apply to results obtained by both the cylindrical aerial method and the modified method. Further, the results obtained for $r/l \geqslant 0.030$ do not have any odd shapes. It is for this reason that the author feels that the method due to Hallen shows that the behaviour of the fat dipole may be treated by extrapolation from the results for the thin dipole.

Much of the above has been repeated intentionally so that the gradual improvement in the number of aerial properties covered by a particular theory could be emphasized.

The theoretical and experimental values will be compared in a later sub-section.

(c) The Aerial Input and Output Regions.

The effects of the physical arrangements of the aerial input on the properties of a cylindrical aerial will be discussed below.

(1) The Effect of the Distance δ Between the Ends of the Aerial on the Radiation Pattern.

The effect of δ on the radiation intensity is small. The directive pattern of a half wavelength aerial in free space, or of a quarter wavelength aerial above a perfect ground, does not differ appreciably from that of a simple current element. As mentioned previously the Radiation

Pattern is a distant field phenomenon and will not be affected by small changes at the input region.

(2) The Effect of the Distance δ Between the Ends of the Aerial on the Input Impedance of the Aerial.[118]

The theoretical analysis given above for the input impedance of a dipole aerial has been based on the assumption that the distance δ is vanishingly small. The above idealized aerial differs from the practical aerial used here in that there is present a small distance δ between the aerial ends at the input for the practical aerial. There is always some local capacitance between the terminals of any physical circuit. At low frequencies its effect on the performance of the circuit is negligible; but at high frequencies and particularly in the microwave region the effect may be substantial. In any practical case we are not concerned with aerial terminals as such. When the aerial is in operation, its terminals are connected either to a transmission line or to local circuits. Depending on the frequency, this transition region may, or may not, have much effect on the aerial performance. It is only in theory, when we wish to consider an aerial separately from the circuits connected to it, that it is essential to include the distance between the terminals in our calculations. Generally this distance cannot be made equal to zero without making the impedance equal to zero. But, if the wires are tapered to mere points, the impedance remains finite as the distance between the terminals vanishes. The admittance of the region in the vicinity of such terminals may be calculated and may be taken out of the aerial admittance and replaced by the admittance appropriate to a different input configuration. This enables a unique meaning to be applied to the aerial impedance for both theoretical and practical purposes. It is possible to carry out a theoretical analysis of a dipole aerial with gap by postulating a gap from $z=-\frac{\delta}{2}$

to $Z=+\frac{\delta}{2}$ and repeating the analysis as given by the Cylindrical Aerial Method.[119,120] The analysis is long and tedious and is not very useful because of a lack of knowledge of where the transmission line proper finishes and where the aerial starts. The aerial input region is a region of transition between the feed line and the aerial . Plane waves are guided down the coaxial line and emerge at some distance from the gap as spherical waves. If the gap is small compared to the wavelength then the region may be represented by a four terminal network $C_1C_2A_1A_2$. Aerial measurements are usually made at C_1C_2 whereas the theoretical results refer to the aerial proper i.e. across A_1A_2 . Certain discrepancies in measured and theoretical results are to be expected and also between one set of measurements and another set of measurements. The possible inaccuracy in the theoretical aerial current affects only the portion of the aerial in the immediate neighbourhood of the gap, and thus the points A_1A_2 are not accurately known. Hence it follows that a theoretical investigation which postulates a gap will only give an indication of the effect of the gap on the aerial impedance. The theoretical analysis shows that for small gap lengths the input impedance is not very sensitive to gap length so that impedances calculated for a zero gap are good approximations for that large class of aerials for which $\beta\delta < 0.02$. Also for $\beta\ell$ near $\frac{\pi}{2}$ i.e. a half wavelength dipole the input impedance corrected for the gap differs negligibly from the uncorrected input impedance if the actual conductor half length $\ell-\frac{\delta}{2}$ is used instead of ℓ .

An alternative method which is the usual engineering approach for gap lengths greater than $\beta\delta = 0.02$ is to investigate the four terminal network separately. A simple T low pass filter is found to be quite satisfactory

with ωL equal to a few ohms and a capacitance which is a few per cent. of the aerial capacitance. This method has been used in isolated cases to account for the divergence in input impedance from the theoretical value. The measured value of the input impedance with gap has been given as about 73 ohms. For large gaps the input impedance has been recorded as greater than 73 ohms as would be expected unless the length is taken as $\ell - \frac{\delta}{2}$. Since aerial gaps are of very different shape for various aerials, a single theory is of little use in determining the effect of the gap. Gap constants should, and may be, determined best experimentally for each particular aerial input arrangement .

(3) The Effect of Conical Input Sections.

It is desirable to use conical input sections for cylindrical aerials since these reduce the shunt capacitance at the input to the aerial caused by the abrupt change in section between the feed line and the aerial. This capacitance is included in the measured value of the aerial input impedance. Since the theoretical results neglect the impedance due to this capacitance the measured results with conical input sections will agree better with the theoretical results than will those for a straight cylindrical aerial. Also any abrupt change in section will deteriorate the broad band impedance properties of an aerial.

(4) The Effect of the Capacitance at the Ends of the Aerial.

In deriving the current distribution for dipole aerials it is assumed that the current at the ends vanishes. This is the true boundary condition in the limit, as the radius of the aerial vanishes. In dealing with dipole aerials for which the radius is finite an allowance should be made

for the charge on the ends of the conductors. Since these caps are small, the accumulated charge may be calculated from electrostatic equations. The capacitance of a disc of radius r is $8\epsilon r$, hence the capacitance of one face of the disc is equal to $4\epsilon r$. The current entering the cap at z = l is

$$I_{cap} = 4j\omega\epsilon r V(l) = j\omega C_{cap} V(l)$$

where V (l) is the potential at z = l.

The electric lines of force become crowded towards the ends of the aerial and bulge out causing a so-called "fringing effect." The concentration is due to a higher concentration of charge near the ends of the aerial, which implies a greater capacitance per unit length. To understand this we note that at any intermediate point a charged particle is subjected to forces exerted by the charged particles on both sides of it, while at the end it is acted upon only by the charge on one side. That is if we assume that the charge is distributed uniformly along the wire, the potential at the intermediate points is twice as large as the potential at the end. Now near the ends the potential must be substantially constant, since its gradient is proportional to the current and the current is small. Hence, more charge will be pushed toward the ends which is another way of saying that near the ends the capacitance per unit length is greater.

The sinusoidal form of potential and current distribution is characteristic of a uniform distribution of inductance and capacitance. Hence, we must expect a deviation from the sinusoidal form near the ends of the aerial. However, the end effect is large only in the immediate vicinity of the ends and may be represented, therefore, by a lumped capacitance at the ends, added to the cap capacitance. That is, the boundary condition at the ends, as far as our principal current component is concerned, is

$$I(\ell) = j\omega(C_t + C_{cap})V(\ell)$$

where C_t is the effective capacitance due to fringing and C_{cap} is the capacitance of the cap.

These end effects effectively lengthen the aerial. To obtain the effective extension δ in the length of each arm, we equate the end capacitance to the capacitance $C\delta$, where C is the average capacitance per unit length

$$C\delta = C_t + C_{cap}$$

Although δ is small, it has a direct effect on the position of the resonant and antiresonant lengths. For very thin aerials the effects of the cap capacitance become negligible, but the fringing effect remains noticeable even for small aerials.

(5) <u>The Effect of the Input Transmission Lines</u>.

The circuits supplying power to an aerial are designed so that the radiation from them is small. The small coupling that exists between the transmission line and the aerial may be evaluated if the current and charge distribution are known.

In free space, the two wire aerial feed system is perfectly balanced, the currents in the wires are equal and opposite, and there is little radiation from the transmission line; but, in the presence of the earth, the system is balanced only if it is horizontal. If the aerial is vertical the field reflected from the earth is impressed on the transmission line, and a parasitic aerial circuit is created. Since the field is impressed equally on both feed wires, the new circuit is composed of these wires in parallel with the earth, which acts as a return conductor.

If the aerial is fed by a coaxial transmission line, the inner conductor is connected to one arm of the aerial and the outer conductor to the other. In this case there exists a parasitic radiating circuit even if the aerial

system is in free space. The voltage transmitted along the coaxial line is impressed, not only between the arms of the aerial, but also between the outer surface of the outer conductor and the aerial arm connected to the inner conductor. The presence of a balance to unbalance transformer at the aerial input prevents this radiation. If the balun transformer is not included in the feed arrangements the impedance and radiation characteristics of the aerial system will be greatly affected.

The presence of the balance to unbalance transformer introduces a certain amount of capacitance which is reflected in the observed values of input impedance. This capacitance will have a deliterious effect on the bandwidth of a dipole aerial.

(d) The Effect of the Earth.

The effect of the earth on the radiation pattern and input impedance has been treated in a previous section. The effect of the earth is in general small if the aerial is at a height above the earth greater than a few wavelengths.

(e) The Aerial Bandwidth.

In television, frequency modulation and in other high frequency applications, a very wide band of frequencies must be transmitted; therefore aerials for these services must be designed to have a constant input impedance over a wide range of frequency. The necessary conditions for wide band properties are a small change in input resistance with frequency and a means of compensating for any residual reactance at any frequency in the band. The fat half wavelength dipole aerial has a small change in both input resistance and reactance with frequency, and the residual reactance may be compensated by the use of a quarter

wavelength stub. Abrupt changes in physical cross-section must be avoided, since the capacitance associated with these changes reduces the bandwidth. Consequently a dipole aerial with a conical input section will have a greater bandwidth than will a dipole aerial with no conical input section.

The experimental radiation diagrams and input admittance with stub show that it is possible to achieve reasonable wideband operation with a cylindrical dipole aerial. For example, the experiments on a 1/8" dipole aerial show that it has a small reactance variation, less than 10 ohms, and an input resistance variation of about 10% over a 50 Mcps. range of frequencies.

Details of the methods of wideband aerial design have been described in earlier sections.

The essential feature of a wideband aerial is a fat element with no discontinuities or lumped reactances in the feeding arrangements.

(f) The Experimental Input Admittance Results.

The properties of cylindrical aerials deduced from the experimental results will be summarized in the following paragraphs.

(1) Unipole Aerial Experimental Results.

The properties of unipole cylindrical aerials deduced from both the measurements and the graphs drawn from these measured values are as follows:

(i) The Input Susceptance is positive for small values of $\frac{\ell}{\lambda}$ ratio. As the $\frac{\ell}{\lambda}$ ratio is increased the input susceptance curve follows a shape similar to a warped sine curve.

(ii) The value of the $\frac{\ell}{\lambda}$ ratio for which the input susceptance is zero, is less than 0.25.

(iii) The value of the $\frac{\ell}{\lambda}$ ratio at which the input susceptance is zero decreases as the $\frac{r}{\lambda}$ ratio increases for a constant $\frac{s}{\lambda}$ ratio.

(iv) The value of the $\frac{\ell}{\lambda}$ ratio at which the input susceptance is zero decreases as the $\frac{s}{\lambda}$ ratio increases for a constant $\frac{r}{\lambda}$ ratio.

(v) The value of the first negative maximum of the input susceptance curve decreases as the $\frac{r}{\lambda}$ ratio is increased for a constant $\frac{s}{\lambda}$ ratio.

(vi) The value of the first negative maximum of the input susceptance curve increases as the $\frac{s}{\lambda}$ ratio is increased for a constant $\frac{r}{\lambda}$ ratio.

(vii) The input conductance is small for small values of the $\frac{\ell}{\lambda}$ ratio. As the $\frac{\ell}{\lambda}$ ratio is increased the input conductance follows a shape similar to a sine curve.

(viii) The maximum value of the input conductance curve in general increases as the $\frac{r}{\lambda}$ ratio is increased for a given $\frac{s}{\lambda}$ ratio.

(ix) The maximum value of the input conductance curve in general increases as the $\frac{s}{\lambda}$ ratio is increased for a given $\frac{r}{\lambda}$ ratio.

(x) The values of the $\frac{\ell}{\lambda}$ ratio at which the input conductance is a positive maximum and the input susceptance a negative maximum in general decrease as the $\frac{r}{\lambda}$ ratio is increased for a given $\frac{s}{\lambda}$ ratio.

(xi) The values of the $\frac{\ell}{\lambda}$ ratio at which the input conductance is a positive maximum and the input susceptance a negative maximum in general increase as the $\frac{s}{\lambda}$ ratio is increased for a given $\frac{r}{\lambda}$ ratio.

(xii) The input susceptance maxima occur at a greater value of $\frac{\ell}{\lambda}$ than do the maxima for the input conductance.

(xiii) The value of the input resistance at the first resonance is near 73.2 ohms.

(xiv) The value of the input resistance at the first resonance tends to decrease as the $\frac{r}{\lambda}$ ratio is increased for a given $\frac{s}{\lambda}$ ratio. The evidence is not conclusive.

(xv) The value of the input resistance at the first resonance tends to decrease as the $\frac{s}{\lambda}$ ratio is increased for a given $\frac{r}{\lambda}$ ratio. Again the evidence is not

conclusive.

(xvi) The negative slope of the input susceptance- $\frac{l}{\lambda}$ ratio curves is much greater than the positive slope.

The cylindrical aerial admittance curves for dipoles with r/l > 0.030 have the same general shape as the admittance curves for thinner dipoles. It follows that extrapolation techniques for fat dipoles will give a good approximation to the behaviour of fat dipoles. The first resonant lengths and impedances will be compared in a later section.

(2) Dipole Aerial Experimental Results.

The results of the cylindrical dipole aerial measurements are not as accurate as the unipole experimental results because a small amount of radiation was present and, also, the admittances measured are one half the value of the unipole admittances.

The measured values show that the properties given above for the unipole aerial in general apply equally well to the dipole aerial. The evidence in some cases is not conclusive and it is probably better to say that the results indicate that the properties which have been deduced for the unipole aerial apply also to the dipole aerial.

The dipole aerial resonant resistance is in some cases greater than 73.2 ohms. This anomaly is probably due to lack of accuracy in the measurements though values of resonant impedance greater than 73.2 ohms have been reported previously.

(3) Compensated Dipole Aerial Experimental Results.

In addition to the properties discussed above for the unipole and dipole aerials which apply also to the compensated dipole aerial, the experiments show that the following properties are applicable to the compensated dipole aerial.

(i) The presence of the quarter wavelength short circuit stub reduces the input susceptance variation considerably. If the stub had been expressly designed for one aerial and not a range of aerials it would have been possible to obtain greater input susceptance cancellation. The reduction in input susceptance means a greater bandwidth for the dipole aerial as has been previously discussed.

(ii) The input conductance for the same $\frac{r}{\lambda}$, $\frac{\ell}{\lambda}$ and $\frac{s}{\lambda}$ ratios is much higher for the compensated dipole than it is for either the dipole aerial or the unipole aerial. The input resistance for a resonant condition in one case is as low as 53.6 ohms. The additional input conductance is due to re-radiation from the outer surface of the outer conductor forming the stub. The measured values of resonant resistance below 60 ohms which have been reported are due to phenomena of this type.

The bandwidth of the compensated dipole aerials as given by the measurements is not very great as mentioned previously, but is probably adequate for most television services.

(g) Comparison of the Theoretical and Experimental Field Strength Results.

A study of the field strength results obtained for the cylindrical dipole aerial verifies the theoretical conclusions obtained earlier. The field strength pattern properties are:

(i) The points where $E_\theta = 0$ in the theoretical diagrams do not occur. The zeros are rounded off.

(ii) The change in pattern shape with change in the diameter of the aerial is not appreciable.

(iii) The change in pattern shape with change in the input cone slope lengths is not appreciable.

(iv) The change in pattern shape with a small change in frequency ±4% is not appreciable for a dipole aerial. This means that equal amounts of power will be propagated in a given direction for all frequencies within the range considered.

(v) The maximum value of the minor lobes in the theoretical diagram are generally increased.

(vi) The maximum value of the major lobes in the theoretical diagram are generally decreased.

(vii) The earth has negligible effect on the radiation diagram of a horizontal dipole provided the aerial is placed several wavelengths above the earth.

(viii) The change in pattern shape with change in the length of the aerial is appreciable.

The experimental results verify those of the above properties which are applicable to this study. The results show that the radiation pattern is a distant field phenomenon since physical changes near the input region to the aerial do not affect the radiation pattern. Further, it is evident that the simple theory will provide adequate information about the radiation pattern of a dipole aerial provided it is remembered that the zeros will be rounded off.

(h) Comparison of the Theoretical and Experimental Impedance Results.[10,104]

The impedance properties of the cylindrical dipole aerial will be treated under various sub-headings in this sub-section.

(1) The Input Impedance Characteristics.

The theoretical impedance - $\frac{\ell}{\lambda}$ curves discussed in sub-section (b) above, all show the same general characteristics. As mentioned previously, the cylindrical aerial method gives the best treatment of the fat cylindrical dipole aerial. The curves have been evaluated and plotted

for constant increments of r/l ratio. The experimental curves for input admittance have been plotted for constant increments of $\frac{r}{\lambda}$ ratio. The amount of calculation involved in calculating theoretical impedance curves for constant increments of $\frac{r}{\lambda}$ ratio would be extremely large. For this reason calculation of input impedance for constant increments of $\frac{r}{\lambda}$ ratio was not attempted. Because the theoretical curves are plotted for constant r/l ratio and the unipole experimental values were measured for constant $\frac{r}{\lambda}$ ratio it is not possible to compare the two sets of curves directly. However, if the impedance-admittance inversion properties are taken into account and the properties given in sub-sections (b) and (f) are examined it will be evident that the theoretical and experimental curves for the cylindrical dipole aerial show the same general properties.

(2) <u>The Maximum Input Resistance</u>.[10]

Considerable experimental data has been obtained by various experimenters verifying the value of maximum input resistance as determined by the theory. The values of r/l ratio vary from extremely thin aerials up to 0.035.

In 1934 C.B. Feldman measured the maximum resistance of a vertical unipole above the ground using a wavelength of 18 metres. The gap between the lower end of the aerial and the ground was 0.06 λ . In 1936 A.C. Beck made some measurements on squirrel cage aerials with tapered input sections. The wavelengths used were in the range 14 - 28 metres. Some measurements were made on balanced dipoles at a height of 60 feet above the ground. Other measurements were made on unbalanced unipoles. Measurements have also been made by Morrison and Smith for a unipole aerial of r/l ratio equal to 0.01. In April, 1945, Brown and Woodward carried out extensive measurements using a wavelength of 5 metres. In August, 1945, Ronold King and D.D. King made some measurements

on balanced dipole aerials. In October, 1946 D.D. King published some measurements on dipole aerial impedance. In 1949 C.F. Edwards and R.H. Brandt made some measurements using a wavelength of 3 inches.

All the values agree very well with the values of theoretical maximum input resistance obtained by the biconical aerial method.

The differences between the values of maximum input impedance as given by the biconical aerial method and the forms of the cylindrical aerial method are due to the choice of the expansion parameter used in solving the integral equation by successive approximations. This parameter corresponds to the average characteristic impedance K_a of the Schelkunoff Theory. A variety of series expansions for the aerial current may be obtained depending on the choice of the expansion parameter. Analytically they are identical; that is, one series can be transformed into another. But the numerical values of the maximum resistance obtained from the first few terms of the expansion are sensitive to the particular expansion parameter chosen. This accounts for the differences between the values of the maximum resistance which are given here.

In addition to the above experimental data other measurements have been made by Rösseler, Vilbig and Vogt,[121] Essen and Oliver,[114] Smith and Holt Smith[104] and by Cochrane.[104] The results of these measurements are in agreement with the theory.

(3) <u>The Maximum Input Conductance.</u>

The values of $G_{max.}$ as a function of r/l ratio show that the experimentally determined values of maximum conductance have approximately the same magnitude as the theory predicts. The theoretical values were determined by the cylindrical aerial method. The difference in

ordinates between the theoretical and experimental values represents a reduction in losses for the practical aerial over the theoretical aerial. The effect of the base and near base capacitance discussed below may account for the difference in the maximum input conductance due to these capacitances increasing the effective length of the aerial. If the aerial were made longer than its actual length by an amount dependent on these capacitances then the experimental values would move nearer to the theoretical values.

(4) The Effects of Base and Near Base Capacitance.

The effects of the base and near-base capacitance on the aerial impedance have been examined by Brown and Woodward.[112] Increase of the near base and base capacitances decreases the maximum input resistance and decreases the length of the aerial at which the maximum input resistance occurs. An increase in these capacitances has the same effect on the input reactance curves. Comparison of susceptance curves obtained by Brown and Woodward with those obtained by the author show a general agreement. The base and near base capacitances may be allowed for using the following formulae:

$$C_b = \frac{\epsilon \pi r^2}{h} \qquad Y_b = j\,\frac{\pi r^2}{60\lambda h}$$

$$C_{nb} = 4\epsilon r \log \frac{r}{h} \qquad Y_{nb} = j\,\frac{r}{15\lambda}\log\frac{r}{h}$$

where r is the aerial radius

h is the distance between the base of the cylinder and the ground plane.

Brown and Woodward's experiments confirm that the proximity of the aerial terminals produces a short circuiting effect. If there is no overlap between the coaxial line feeding the aerial and the aerial itself there is no base capacitance, but the near base capacitance is still present, particularly for cylinders of large

diameter. Theoretically this capacitance approaches infinity as the distance between the aerial terminals approaches zero, no matter how small the radius of the aerial as long as it is kept constant.

The effects described here are evident in the author's results. The tables of unipole and dipole resonant conductances show that there are large capacitances present for zero conical input slope lengths. The capacitance decreases as the conical input slope length increases. Also there is a capacitance between the balance to unbalance transformer and the aerial for the dipole aerial tests. This capacitance increases as the aerial diameter increases. The physical arrangement in the case of the dipole aerial makes it difficult to calculate the magnitude of these capacitances.

(5) The Resonant Resistance.

The theoretical curves show the resonant resistance as a function of r/l ratio. As the r/l ratio increases the resonant resistance decreases. The theoretical value of resonant impedance for r/l = 0 is 73.2 ohms. The resonant impedance obtained by Hallen's method agree reasonably with the Schelkunoff Theory. The values obtained are dependent on the choice of expansion parameter. All the theoretical calculations are based on the assumption that the aerial gap is very small but not so small that the base capacitance is significant.

Thus, there is some uncertainty about the theoretical values of the resonant impedance. Experiments are mutually conflicting; some reports give 73 ohms or even larger values whereas others give smaller values. R.A. Smith[104] presents experimental evidence which shows that, in the vicinity of resonance, the resistive part of the impedance increases with the length of the gap while the reactance remains the same. He gives curves for λ = 6 metres r = 0.625 ins. $\frac{\lambda}{4r}$ = 100, and for three different spacings between the

terminals of a balanced dipole, δ = 0.5, 4, 8 inches. For the longest gap, the resonant resistance is very nearly 73 ohms. For the shortest gap (which is comparable to the radius so that near base capacitance is still negligible), the resonant resistance is 61 ohms. This value compares well with the value obtained by the Schelkunoff Theory.

Edwards and Brandt[10] have measured consistently 36 ohms for unipoles backed by large metal sheets and fed by coaxial lines. The wavelength used was 3 inches. In proportion to the length of the unipole, the gaps have been larger than the 8 inch gap referred to in the above paragraph. Smith reports that, in the vicinity of resonance, the impedance depends not only on the spacing at the centre of the dipole but also on the method of connecting the transmission lines. It may then be expected that there will be some difference between the resistances of quarter-wave unipoles fed by coaxial lines and the half-values for the half-wave dipoles.

The experimental values of resonant resistance obtained by the author support the above remarks. The resonant resistance and resonant length are markedly affected by the capacitances present, the physical arrangement of the conductors and the feeding arrangements. The value of the resonant resistance for fat aerials is nearer to 73 ohms than theory indicates. Most authors contend that the resonant resistance for fat dipoles is between 50 - 70 ohms. The results show that this is not the case and that the resonant resistance for fat dipole aerials is of the order of 65 ohms. The reason for the lower values of resonant resistance reported is due to re-radiation from other parts of the aerial structure. The compensated dipole aerial admittance results support this contention.

(6) The Resonant Length.

The theoretical curves of resonant length show that the resonant length decreases as the diameter is increased. The theoretical curves of resonant length obtained by the modified cylindrical aerial method agree with those obtained by the biconical aerial theory and the experimental results obtained by the author.

Brown and Woodward[112] have obtained values of resonant length for $\frac{r}{\ell} \div$ 0.0053, 0.0025, 0.0010 which agree exactly with the theoretical values for the Schelkunoff Theory.

Experimental values of the resonant length have also been determined by Smith and Holt Smith,[104] Essen and Oliver,[114] Rösseler, Vilbig and Vogt[121] and Cochrane[104]. The values determined by these authors are in general agreement with the theoretical curves.

(i) Conclusion.

In the foregoing pages the theoretical properties of cylindrical aerials have been treated and some of the properties have been investigated experimentally.

The experiments show that the conclusions deduced from the theory are qualitatively true. The main quantitative divergence from the theory is the resonant resistance. The resonant resistance is much closer to 73 ohms even for fat dipole aerials than the theory predicts. As mentioned previously the lower value of measured resonant resistance reported by other authors is due to re-radiation from other parts of the aerial structure.

The experimental evidence is not entirely conclusive but indicates that a fat cylindrical dipole will give adequate bandwidth for services such as television.

SECTION 6.

References.

(I) Proc.I.R.E.April'34,p.457-480:G.H.Brown and R.King;High Frequency Models in Antenna Investigations.
(2) Proc.I.R.E.Nov.'48,p.I364-I370:George Sinclair;Theory of Models of Electromagnetic Systems.
(3) Antenna Theory and Design.Vol.I:H.P.Williams.
(4) Fields and Waves in Modern Radio:S.Ramo and J.R.Whinnery.
(5) Electromagnetic Waves:F.W.G.White.
(6) U.H.F.Radio Engineering:W.L.Emery.
(7) Short Wave Radiation Phenomena.Vol.I:A.Hund.
(8) E.M.Waves and Radiating Systems:E.C.Jordan.
(9) Proc.I.R.E.Dec'43,p.693-697:C.W.Harrison and R.King;The Radiation Field of a symmetrical centre driven antenna of finite cross-section.
(IO)Antennas:Theory and Practice;S.A.Schelkunoff and H.Friis.
(II)Advanced Antenna Theory:S.A.Schelkunoff.
(I2)Cruft Labs.Harvard Univ.Tech.Report No.46 June'48;E.Hallen; Admittance Diagrams for Antennas and RElations between Antenna Theories.
(I3)J.App.Phys.V.I@.p.230-248Mar'4I:J.A.Stratton and I.J.Chu.
(I4)Physics Review V.53.p.8I9-83I,I938:L.Page and N.I.Adams.
(I5)Elec.Comm.2I,4,257(I944)and 22,I,II(I944):Leon Brillouin; Antennae for U.H.F.
(I6)Ann.Physik66,435(I898)and Math.Ann.52,8I(I899):Max Abraham.
(I7)J.App.Phys.V.I3.p.327 (I942):Robert M.Ryder.
(I8)Proc.Acad.Science,2I,5I,(3I7)(I935):J.A.Stratton.
(I9)Proc.I.R.E.Dec'24,p.823:S.Ballantine;On the Radiation Resistance of a simple vertical antenna at wavelengths below the fundamental.
(20)Electric Oscillations and Electric Waves:G.W.Pierce.
(2I)Funktionentafeln mit Formeln und Kurven:E.Jahnke and F.Emde.
(22)Tables of Sine,Cosine and Exponential Integrals.
(23)Proc.I.R.E.June'32,p.I004-I04I:P.S.Carter;Circuit Relations in Radiating Systems and applications to Antenna Problems.
(24)Phil.Trans.Roy.Soc.(London)V.236p.38I-422,I937:L.King;On the Radiation Field of a perfectly conducting base insulated Cylindrical Antenna over a perfectly conducting earth, and the calculation of Radiation Resistance and Reactance.
(25)Proc.I.R.E.Mar'29,p.562:A.A.Pistolkors;The Radiation Resistance of beam antennas.
(26)Proc.I.R.E.Aug'3I,p.I47I:R.Bechmann;On the calculation of the Radiation Resistance of antennas and antenna combinations.
(27)Proc.I.R.E.Jan'37,p.78:G.H.Brown;Directional Antennas.
(28)Wireless Engineer April'44.p.I54:R.E.Burgess;Aerial Characteristics-relation between transmission and reception.
(29)Proc.I.R.E.Sept'4I,p.493:S.A.Schelkunoff;Theory of Antennas of Arbitrary Size and Shape.
(30)U.of Texas Pub.No,403I,Aug I5,I940:E.M.Siegel;Wavelength of Oscillations along Transmission Lines and Antennas.
(3I)Proc.I.R.E.Nov'42,p.5II-5I6:S.A.Schelkunoff and C.B.Feldman; On Radiation from Antennas.
(32)Bell Telephone System Monograph I922:S.A.Schelkunoff;General Theory of Symmetric Biconical Antennas.
(33)Jour.A.I.E.E.Oct'24,p.906:J.R.Carson:The guided and radiated energy in wire transmission.
(34)Electrician Mar'2I,p.272-273:J.R.Carson;Propagation of Periodic Currents over non-uniform lines.
(35)Nova Acta Upsal 4,I,I938:Erik Hallen;Theor. Investigations into the Trans. and Receiv. Qualities of Antennae.
(36)Arsskrift,Upsala 4 (I939):Erik Hallen;Further Investigations into the Receiving Qualities of Antennae;The Absorption of Transient Aperiodic Radiation.
(37)Trans Royal Inst.Tech.Stockholm I3(I947):E.Hallen; On Antenna Impedances.
(38)Trans Royal Inst.Tech.Stockholm I2(I947):E.Hallen; Iterated Sine and Cosine Integrals.
(39)Proc.I.R.E.July'42,p.335-349:Ronold King and F.G.Blake; The self-impedance of a symmetrical antenna.
(40)Proc.I.R.E.Nov'43,p.626-640:Ronold King;Coupled Antennas and Transmission Lines.

(4I)J.App.Phys.V.I5.p.I70 (I944):R.King and C.W.Harrison jr; The Impedance of Short,Long and Capacitively Loaded Antennas with a Critical Discussion of the Antenna Problem.
(42)J.App.Phys.V.I5.p.545 (I944):C.W.Harrison jr;An approximate representation of the electromagnetic field in the vicinity of a symmetrical radiator.
(43)Quart.App.Maths.Jan'48,V.5.No.4.p.395-402:C.J.Bouwkamp; Concerning a new transcendent,its tabulation and application in Antenna Theory.
(44)Bessel Functions for Engineers:N.W.McLachlan.
(45)Applied Mathematics for Engineers and Scientists;S.A.Schelkunoff.
(46)Quart.App.Maths.Jan'46.V.3.p.302-335:R.King and D.Middelton; The cylindrical antenna- current and impedance.
(47)J.App.Phys.June'44.V.I5.p.48I-495:R.King and C.W.Harrison; Mutual and Self Impedance of Coupled Antennas.
(48)Proc.I.R.E.April'48.p.487-500:C.Tai;Coupled Antennas.
(49)High Frequency Transmission Lines:Willis Jackson.
(50)Communications April'4I V.2I.p.I0-I4 and 24-26:N.E.Lindenblad; Antennas and Transmission Lines at Empire State T.V.Station.
(5I)R.C.A.Reveiw Oct'39 p.I68-I85:P.S.Carter; Simple T.V. Antennas.
(52)V.H.F.Techniques V.2:Radio Research Laboratory Staff.
(53)Proc.I.R.E.Oct'45,p.67I-700:F.D.Bennett,P.D.Coleman,A.S.Meier; The Design of Broadband Aircraft Antenna Systems.
(54)Wireless Engineer July'52 p.I74:B.Storm;Cylindrical Aerials- New Solution of Hallens Method for Current.
(55)Electromagnetic Waves:S.A.Schelkunoff.
(56)Proc.I.R.E.Oct'43,p.548-567:R.King and C.W.Harrison;The Distribution of Current along a Symmetrical Centre Driven Antenna.
(57)J.I.E.E.I952.V.99.No.I8:R.L.Smith-Rose;A Survey of British Research on Wave Propagation with particular reference to Television.
(58)Proc.I.R.E.I937,p.II92:K.A.Norton;The Physical Reality of Space and Surface Waves in the Radiation Field of Radio Antennas.
(59)Proc.I.R.E.Sept'36,p.I366:K.A.Norton;The Propagation of Radio Waves over the Surface of the Earth and in the Upper Atmosphere
(60)Ann.der Physik I930 p.273-294:B.van der Pol and K.F.Niessen.
(6I)Proc.London Maths.Soc.V.29.p.5I9-522 (I897-8):H.G.Dawson.
(62)J.I.E.E.Aug'40,p.I46:J.S.McPetrie and J.A.Saxton; An Experimental Investigation of the Propagation of Radiation having Wavelengths of 2 and 3 metres.
(63)Proc.I.R.E.Nov'4I,p.623:K.A.Norton;The calculation of ground wave field intensity over a finitely conducting spherical earth.
(64)Proc.I.R.E.Mar'33,p.427:J.C.Schelleng,C.R.Burrows and E.B.Ferrell;Ultra Short Wave Propagation.
(65)J.I.E.E.I928,V.66.p.204:R.H.Barfield;The Attenuation of Wireless Waves over Land.
(66)Proc.I.R.E.I937,p.2I9:Charles R.Burrows;The Surface Wave in Radio Propagation over Plane Earth.
(67)Wireless Engineer I940 V.I7.p.385:G.W.O.Howe;Wireless Waves at the Earths Surface.
(68)Proc.I.R.E.I935,p.470-480:C.R.Burrows;Radio Propagation over Spherical Earth.
(69)Proc.I.R.E.I933,p.765:C.B.Feldman;Optical Behaviour of the Ground.
(70)Phil.Mag.V.24.p.I4I-I76 and 825-864:Balth van der Pol and H.Bremmer;The diffraction of electromagnetic waves from an electrical point source round a finitely conducting sphere, with applications to radio-telegraphy and the theory of the rainbow.
(7I)N.D.R.C.Summary Technical Report C.P.V.3.I946:S.A.Attwood; The propagation of radio waves through the standard atmosphere.
(72)U.H.F.Techniques:J.G.Brainerd and others.
(73)Radar Engineering:D.G.Fink.

(74) U.H.F.Tubes for Communication and Measuring Equipment: Phillips.
(75) The Techniques of Radio Design:E.E.Zepler.
(76) G.R.Expter:Mar'50.
(77) G.R.Expter:Oct'44.
(78) G.R.Expter:Nov'44.
(79) G.R.Expter:Jan'53.
(80) Proc.I.R.E.July'45,p.426-44I:E.Karplus;Wide Range Tuned Circuits and Oscillators for High Frequencies.
(8I) Electronics Nov'46,p.I24-I29:E.Karplus;Components of U.H.F. Field Meters.
(82) G.R.Expter:Oct'48.
(83) G.R.Expter:Jan'50.
(84) G.R.Expter:May'50.
(85) G.R.Expter:Mar'49.
(86) G.R.Expter:Feb'50.
(87) G.R.Expter:Aug'53.
(88) G.R.Expter:Oct'53.
(89) Proc.I.R.E.July'40,p.3I0:D.B.Sinclair;The Twin Tee- A New Type of Null Instrument for Measuring Impedance at Frequencies up to 30 Mcps.
(90) Proc.I.R.E.Nov'40,p.497:D.B.Sinclair;A Radio Frequency Bridge for Impedance Measurements from 400 Kilocycles to 60 Megacycles per Second.
(9I) Electronics Jan'39:Philip H.Smith;Transmission Line Calculator.
(92) Electronics Jan'44:Philip H.Smith;An Improved Transmission Line Calculator.
(93) Radio Communication at U.H.F.:J.Thomson.
(94) Crystal Rectifiers:Radiation Laboratory Series;H.C.Torrey and C.A.Whitmer.
(95) Principles of Radar:M.I.T. Radar School Staff.
(96) J.I.E.E.Mar'43,p.28:F.M.Colebrook and A.C.Gordon-Smith;The design of Ultra Short Wave Field Strength Measuring Equipment.
(97) J.I.E.E.Mar'39,p.388:F.M.Colebrook and A.C.Gordon-Smith;The design and construction of a Short Wave Field Strength Measuring Set.
(98) Radio-Electronics July'5I,p.3I:T.V.Field Strength Meter.
(99) Electronics July'40,p.I4:C.E.Strong;The Inverted Amplifier.
(I00) Proc.I.R.E.July'44,p.423-429:M.C.Jones;Grounded Grid R.F. Voltage Amplifiers.
(I0I) Radio Receiver Design:K.R.Sturley.
(I02) G.R.Expter:Oct'52.
(I03) Electronics Sept'53:O.M.Woodward;Balance Measurements on Balun Transformers.
(I04) Aerials for Metre and Decimetre Wavelengths:R.A.Smith.
(I05) Antennas:J.D.Kraus.
(I06) The Theory and Practice of R.F.Measurements:E.B.Moullin.
(I07) R.C.A.Review Dec'52:G.H.Brown and O.M.Woodward;Experimentally Determined Radiation Characteristics of Conical and Triangular Antennas.
(I08) Proc.I.R.E.Dec'47,p.I462-I47I:C.C.Cutler,A.P.King and W.E. Kock;Microwave Antenna Measurements.
(I09) Operating Instructions for G.R.Type I602-A Admittance Meter.
(IIO) G.R.Expter:Nov'50.
(III) J.App.Phys.Aug'45,V.I6.p.435-453:Ronold King and D.D.King; Microwave impedance measurements with application to antennas.
(II2) Proc.I.R.E.April'45,p.257-262:G.H.Brown and O.M.Woodward; Experimentally Determined Impedance Characteristics of Cylindrical Antennas.
(II3) J.App.Phys.Oct'46.p.844-852:D.D.King;The measured impedance of cylindrical dipoles.
(II4) Wireless Engineer Dec'45.p.587-593:L.Essen and M.H.Oliver; Aerial Impedance Measurements.
(II5) Proc.I.R.E.June'49,p.609-6I6:A.S.Meier and W.P.Summers; Measured impedance of vertical antennas over finite ground planes.
(II6) Proc.I.R.E.Nov'44,p.695-709:J.R.Whinnery,H.W.Jameson and Theo Eloise Robbins;Coaxial Line Discontinuities.
(II7) Proc.I.R.E.Feb'44,p.98-II4:J.R.Whinnery and H.W.Jameson; Equivalent Circuits for Discontinuities in Transmission Lines.

(II8)J.App.Phys.Oct'50,p.945-956:J.R.Whinnery;The effect of input configuration on antenna impedance.
(II9)Quart.App.Maths.July'47 V.5.p.II3:L.Infield;The Influence of the width of the gap upon the theory of antennas.
(I20)Quart.App.Maths.Jan'48 V.5.p.403-4I6;R.King and T.W.Wintern-itz;The cylindrical antenna with gap.
(I2I)T.F.T.May'39.V.28.p.I70-I78:G.Röesseler,F.Vilbig and K.Vogt; Über das elektrische Verhalten von Vertikalantennen in Abhängigkeit von ihrem Durchmesser.